Universidade de Lisboa

Faculdade de Ciências

Departamento de Biologia Animal

FIBRONECTIN CUES DURING SOMITE FORMATION

Pedro Gonçalo Reis Rifes

Doutoramento em Biologia

(Biologia do Desenvolvimento)

2013

Universidade de Lisboa

Faculdade de Ciências

Departamento de Biologia Animal

FIBRONECTIN CUES DURING SOMITE FORMATION

Pedro Gonçalo Reis Rifes

Tese orientada pela Professora Doutora Sólveig Thorsteinsdóttir e Professora Doutora Isabel Palmeirim, especialmente elaborada para a obtenção do grau de doutor em Biologia (Biologia do Desenvolvimento)

2013

The work presented in this dissertation was developed with the support from the Fundação para a Ciência e Tecnologia, through a PhD Fellowship (SFRH/BD/37423/207), the Project Grants (PPCDT/BIA-BCM/59201/2004) and (PTDC/SAU-OBD/103771/2008), and from the European Union FP6 Network of Excellence 'Cells into Organs' (2004-2009).

Nota Prévia

Na elaboração da presente dissertação, e nos termos do nº1 do Artigo 45, do Regulamento de Estudos Pós-Graduados da Universidade de Lisboa, publicado no Diário da República, 2ª série, nº 65 de 30 de Março de 2012, foram usados integralmente artigos científicos publicados em revistas científicas internacionais indexadas. Uma vez que os trabalhos referidos foram efectuados em colaboração com outos investigadores, o autor desta dissertação esclarece que participou integralmente na concepção e execução do trabalho experimental, na análise, interpretação e discussão dos resultados, assim como na redação dos manuscritos. Uma descriminação geral da contribuição do autor desta dissertação nas referidas publicações prefacia cada um dos respectivos capítulos.

Contents

AGRADECIMENTOS V
RESUMO VII
ABSTRACT XIII
LIST OF ABBREVIATIONS AND ACRONYMS XV
CHAPTER 1: INTRODUCTION 1
I. STATE OF THE ART 3
1. PARAXIAL MESODERM AND SOMITES 3
1.1. Gastrulation and the origin of the three germ layers 3
1.1.1. General overview of cell movements during chick gastrulation 4
1.1.2. Epithelial to Mesenchymal Transition 6
1.2. Origin and development of the paraxial mesoderm. 7
1.2.1. Fate map of the origin of paraxial mesoderm cells 7
1.2.2. Plasticiy of the paraxial mesoderm 8
1.2.3. Mesoderm induction and commitment to paraxial mesoderm 9
1.2.4. Paraxial mesoderm or neural tube? 9
1.3. Maturation of the PSM 11
1.3.1. Entering the PSM 11
1.3.2. Establishing the PSM identity 12
1.3.3. Building gradients 14
1.3.4. Nomenclature 15
1.4. Time and space 17
1.4.1. Modeling somitogenesis periodicity 17
1.4.2. The segmentation clock 19
1.4.3. Notch signaling and the outcome of the clock and wavefront 21
1.5. "Sausages into meatballs" 24
1.5.1. Tissue interactions 25
1.5.2. Adhesion model 26
1.5.3. Somitogenesis from a cellular standpoint 27
1.5.4. The Paraxis gene 28
1.6. Rostral vs. caudal 29
1.7. Differentiation of somites 31
1.7.1. Axial specification and patterning of the somitic fate 33
1.7.2. The sclerotome 35
1.7.3. The dermomyotome 36
2. THE EXTRACELLULAR ENVIRONMENT 37
2.1. Fibronectin 38
2.1.1. Fibronectin structure 38
2.1.2. The 70kDa N-terminal fibronectin assembly domain 40

2.1.3. The RGD cell-binding site 42
2.1.4. Fibronectin matrix assembly 43
2.1.5. Fibronectin functions 45
2.2. Laminins 46
2.3. Other ECM molecules 49
2.4. Integrins 50
2.4.1. Integrin structure and signaling 50
2.4.2. Cytoplasmic molecules associated with integrins 52
2.4.3. Integrin-Fibronectin interactions 55
2.5. The third dimension of the ECM 56
2.6. Cell-cell adhesion 57
3. EXTRACELLULAR MATRIX AND EMBRYONIC DEVELOPMENT 59
3.1. Fibronectin and morphogenesis 60
3.2. Fibronectin matrix and somitogenesis 61
3.2.1. The chicken embryo (*Gallus gallus*) 61
3.2.2. The mouse embryo (*Mus musculus*) 63
3.2.3. The amphibian *Xenopus laevis* embryo 64
3.2.4. The Zebrafish embryo (*Danio rerio*) 64
II. AIMS AND OBJECTIVES 65
III. REFERENCES 68
CHAPTER 2: REDEFINING THE ROLE OF ECTODERM IN SOMITOGENESIS: A PLAYER IN THE FORMATION OF THE FIBRONECTIN MATRIX OF PRESOMITIC MESODERM 97
CHAPTER 3: DYNAMIC 3D CELL REARRANGEMENTS GUIDED BY A FIBRONECTIN MATRIX UNDERLIE SOMITOGENESIS 113
CHAPTER 4: EXTRACELLULAR MATRIX ASSEMBLY AND 3D ORGANIZATION DURING PARAXIAL MESODERM DEVELOPMENT IN THE CHICK EMBRYO 133
CHAPTER 5: EFFECT OF CELL TENSION INHIBITORS ON SOMITOGENESIS IN CHICKEN (*GALLUS GALLUS*) EMBRYOS 155
CHAPTER 6: DISCUSSION 193
Important note 195
DISCUSSION 199
6.1. ECM assembly and organization is part of the developmental program of the paraxial mesoderm 199
6.1.1. Fibronectin assembly in vivo 200
6.1.2. Laminin matrix assembly in vivo 203
6.1.3. Signaling from the matrix: what cells perceive from the ECM 205
6.2. A mature fibronectin matrix is an essential multi-task player during the morphogenesis of the somite segment 206

6.2.1. Fibronectin on the edge: the polarizing co-partner during somite cleft formation 207
6.2.2. Making a somite, putting the pieces together 208
6.3. Incresead ECM tension at the rostral PSM: tuning the tempo for determination?. 210
6.4. Final considerations 212
6.5. References 213

Agradecimentos

Em primeiríssimo lugar tenho de agradecer à Sólveig. Por me ter orientado, com saber, inteligência, muita amizade e uma enorme dose de humanidade (coisa rara nos dias de hoje!) durante estes anos, sem me conduzir em demasia. Pela paciência, pelo apoio sempre disponível, pelas discussões e conversas, científicas ou sobre mundo, pela visão contagiantemente positiva do mundo e dos resultados que obtinha! Tive e tenho o maior orgulho em ter-te como a minha mentora científica, mas ainda mais por ter conhecido melhor a enorme pessoa que és.

Agradeço também a Isabel, que me co-orientou sempre com um enorme sorriso estampado na cara, no telefone e nos e-mails! Pelo interesse e entusiasmo em discutir todo e qualquer assunto, por me receber de braços abertos, por me dar aquela palavra de apoio quando mais era necessário. Fui, sem dúvida, orientado por dois maravilhosos exemplos pessoais!

Um agradecimento especial à "chefe alternativa", Gabriela. Pela não-orientação, e pela eterna disponibilidade em ajudar no que fosse preciso; rever, ler, discutir, etc. Por todas a conversas sobre mil-e-um assuntos, sempre com uma jovialidade (e esta hem!) e alegria que tanta falta fazem a muita gente!

Um outro agradecimento especial ao Gabriel, o "criador do Monstro". Foi um privilégio aprender e ser ensinado pelo mais completo microscopista que já conheci, com ambos os pés bem assentes na vertente física e biológica, algo muito pouco comum! Obrigado pela sempre prestável ajuda, pelo humor, pelas conversas sobre tanta coisa, sempre espicaçadas pela incompatibilidade musical.

Agradeço também ao Prof.Crespo pelos pedaços de conversas pelos corredores ou gabinetes, sobre todos aqueles pequenos assuntos sobre ciência, o mundo, a vida ou o universo "em particular".

A todos os membros passados e presentes do Laboratório de BD na FCUL, pela ajuda, pela paciência, por me ouvirem e por não me ouvirem, por manterem sempre a boa disposição característica do laboratório: Sofia e Fernanda, Pedro Campinho, Catarina, Ana Gaspar, Ana Lina, Rita, Tomás e Raquel, e outros mais. E ainda os mais "novitos", Patrícia, Raquel "dois", Andreia e André; estou de olho em vocês… Um agradecimento particular ao meu companheiro nesta "luta", o Luís, por estar sempre disponível para ajudar a remediar todo e qualquer problema informático, por vezes muito para além do que queria originalmente. I must also thank Marianne, for all the help, either in discussions, text revisions, but also for the cool mood and all other conversations that aid to keep a sane mind in a crazy world.

A todos os companheiros da FCUL dos laboratórios em volta pela ajuda e boa disposição geral essential para uma sanidade mental mínima; Andreia e Marta, Carla, Maria Ana, Mónica, Ana Rita, Isa, Francisco, e tantos outros. Um agradecimento muito merecido à Irene pela ajuda com o RT-PCR, que correu demasiado bem! Um beijinho à Branquinha, pela boa disposição e por ser a adepta mais ferrenha do Glorioso! Um forte abraço e um grande obrigado ao Pedro Lima pela ajuda num momento chave e pela companhia nos almoços de negócios e afins!

A todos os que me acolheram em laboratórios alheios: Raquel, Susana e Tatiana (Braga) e também a Raquel e a Raquel (loura) no laboratório da Leonor. Um

agradecimento especial à Leonor por me acolher e ajudar, e pelo interesse que sempre demonstrou pelo meu trabalho.

Aos meus companheiros do Programa Doutoral do IGC, em particular às três Representantes com quem tive o prazer de partilhar o "tacho" e a organização de eventos derivados desse privilégio. Catarina, Tânia e Sara, um muito obrigado pela boa disposição, pelo apoio, e por partilharem a vossa "luta" comigo ao longo do doutoramento.

A big "thank you" is also in order for Arnoud. Your warm, generous welcome to the NKI laboratory was the stepping stone for an excellent experience in Amsterdam. Thank you also for all the help, particularly with all those eclectic "embryonic" questions, and for the lively, cheerful laboratory atmosphere you transmit, a balm in the chilled north. Many thanks to my laboratory partners, particularly Court, Norman, Sander and Saskia. A special thank you to my Lab/office/"Peninsular" mate, Pablo, for all the help, but also for all the other conversations and discussions, for your unending upward mood. More importantly, for being an example of a whole Man, at peace, and with a beautiful family. Another special thanks to my other "Southern" connection, Lab/office partners and fellow embryologist(s), Ruben and Sanne. For all the joy you brought me daily, with all the jokes and pranks, and the most cheerful lunches, "Aaaiiggght"! A big and special thank you to Mike, for being the most excellent friend, and a fantastic company exploring the life in Amsterdam; I wish you all the best in Seattle. I must also thank Susana in Leiden for all the enthusiastic support on those P-19 cells! I must also acknowledge Ana for introducing me to her warm-welcoming group of friends, including João, who instantly received me as a new flat mate, no-questions-asked.

A todos os meus amigos "fora da ciência", pela amizade, pelo companheirismo e tudo o mais que não se pode expressar por palavras escritas. Por todas as perguntas malucas que me fazem sobre "o meu trabalho", mesmo se apesar da minha explicação, continuarem-me a ver a navegar numa outra galáxia, tratando de galinhas e virando ovos.

Um agradecimento muito especial à minha família por acreditar em mim, e por tudo o que me deram. Especialmente aos meus pais pelo apoio incondicional a todos os níveis e pelo inesgotável interesse. Ao meu maninho, por todo o apoio e por ter uns filhos lindos.

E, finalmente (mas não por último), tenho que agradecer, e muito especialmente, à Ana, por me ter aturado, apoiado e puxado por mim nesta fase final tão crítica e tão ingrata para quem acompanha na proximidade. Um enorme, mas mesmo enorme obrigado!

Resumo

O esquema geral do desenvolvimento embrionário dos Vertebrados é marcado por duas conspícuas fileiras de elementos repetidos, situadas em ambos os lados do tubo neural, localizado numa posição axial. Estas estruturas repetidas, chamadas sómitos, vão originar os elementos ósseos que compõem o esqueleto axial, as vértebras, de onde deriva o nome deste sub-filo. Os sómitos dão também origem à musculatura esquelética do tronco e membros, assim como à derme das costas, entre outros tecidos. Os sómitos são originários de um tecido mesodérmico não-segmentado, de forma cilíndrica, situado em ambos os lados do tubo/placa neural, tecido esse que é denominado mesoderme pré-somítica (MPS). Em conjunto, os sómitos e as MPS compõem a mesoderme paraxial (i.e. a mesoderme imediatamente lateral ao eixo central). Cada par de sómitos destaca-se, de um modo temporal e espacialmente regulado, da extremidade mais rostral da MPS, originando um gradiente caudo-rostral de crescente maturação somítica. Ao mesmo tempo, o embrião continua a alongar-se no sentido caudal, e a gastrulação que decorre no botão caudal acrescenta celulas à MPS mesenquimatosa A formação de cada sómito epitelial é acompanhada por um processo de transição mesênquima epitélio, resultando na formação de uma esfera de células epiteliais rodeando um núcleo de células mesenquimatosas. A formação dos sómitos não só é importante para a formação das vértebras e outros tecidos que deles directamente derivam, mas também são responsáveis pela imposição do arranjo segmentado do sistema nervoso periférico.

Embora a formação dos sómitos intrigue observadores desde tempos longínquos, as mais recentes décadas foram fundamentais para elucidar alguns dos aspectos mais intrigantes deste fenómeno. Dada a importância estrutural dos sómitos em todo o desenvolvimento embrionário subsequente, a estrita regulação temporal e espacial da somitogénese foi alvo de um interesse superior, que culminou com a descoberta da primeira evidência da regulação temporal. Genes com um comportamento transcripcional cíclico, adequadamente denominados “genes cíclicos”, dos quais *Hairy1* foi o primeiro descrito, evidenciaram a existência de um mecanismo metrónomo (oscilador), essencial para a regulação temporal da somitogénese em embriões de galinha. Posteriormente foi descoberta a existência de um gradiente de maturação

caudo-rostral ao longo da MPS que balizava, a um nível hipotético do gradiente, a actividade do oscilador, transformando-a num localização espacial na MPS, coincidente com a formação de um segmento somítico. Estas evidências despoletaram toda uma nova compreensão do fenómeno, não só do ponto de vista conceptual como mecanístico, não obstante o mecanismo de oscilador-gradiente para a produção regular de segmentos já tivesse sido postulado anteriormente por modelos matemáticos. Embora nos dias de hoje já tenhamos uma ideia bastante robusta de como a somitogénese é regulada, ainda são numerosas as questões basilares cujas respostas ainda permanecem pouco claras.

Nesta tese pretendemos abordar o fenómeno da somitogénese num dos aspectos que tem sido mais negligenciado: a formação morfológica de estruturas epiteliais, individuais, discretas – os sómitos -, a partir de um tecido mesenquimatoso, uniforme e não-segmentado – a MPS. Durante a somitogénese as células da MPS rostral rearranjam-se de um modo rápido e dramático, formando uma fenda transversal, e destacando-se da MPS remanescente sob a forma de uma esfera epitelial. A formação de sómitos é um fenómeno extremamente robusto, ocorrendo mesmo quando genes envolvidos na regulação espácio-temporal são geneticamente removidos. Embora os mecanismos envolvidos na formação dos sómitos ainda sejam pouco claros, a investigação de outros fenómenos morfogenéticos embrionários têm revelado que o seu enquadramento extracelular é essencial na orquestração dos comportamentos celulares subjacentes à criação de novas formas. Nesta tese procurámos aprofundar a compreensão da formação dos sómitos no embrião de galinha, explorando a interacção entre as células das MPS e os componentes não-celulares presentes no espaço extracelular, conjuntamente denominados matriz extracelular (MEC). Em particular, investigámos o papel da fibronectina, uma glicoproteína da MEC, durante a formação do sómito epitelial.

De entre as várias moléculas que compõem a MEC, a fibronectina encontra-se presente de um modo ubíquo durante a embriogénese mas também em tecidos adultos. A fibronectina é polimerizada numa complexa rede de fibrilhas num processo totalmente dependente de uma acção celular. Décadas de investigação em células em

cultura revelaram que a fibronectina é secretada como um dímero numa conformação compacta, e a molécula é estendida através de ligações às células, expondo locais essenciais para a polimerização. A fibronectina é uma molécula de adesão por excelência, regularmente associada a fenómenos de fixação, num contexto de migração e dispersão celular. Assim como a fibronectina, outros componentes da MEC não só albergam passivamente as células, mas também desempenham um papel instrutivo na regulação do comportamento celular. A laminina, uma outra glicoproteína da MEC estudada nesta tese, é um componente essencial da membrana basal, uma MEC especializada, crítica para a formação e manutenção de tecidos epiteliais. As células obtêm a informação sobre a MEC circundante através de receptores transmembranares denominados integrinas. Estes receptores heterodiméricos são transductores de sinais importantíssimos, que, embora não sejam transmissores de sinais per se, interagem com inúmeras moléculas de variadas vias sinalizadoras. As integrinas servem também como o elo de ligação físico entre o cito-esqueleto das células e a MEC, participando assim não só na avaliação bioquímica da MEC, como também das suas propriedades mecânicas.

A interacção célula-MEC na regulação do comportamento celular tem sido alvo de investigação particularmente em células em cultura e num contexto patológico, sendo que o seu papel no desenvolvimento embrionário ainda não mereceu a devida atenção. Embora a deleção de vários genes para componentes da MEC tenham demonstrado claramente o seu papel fundamental nos estádios iniciais de desenvolvimento, os pormenores do papel da respectiva MEC em fenómenos mais particulares carecem de explicação. Notoriamente, a deleção do gene que codifica a fibronectina resulta numa letalidade embrionária precoce, e na completa ausência de sómitos embora a mesoderme paraxial seja formada normalmente, um fenótipo singular de entre as inúmeras deleções genéticas afectando a somitogénese. No entanto, e apesar de a fibronectina ter sido implicada na somitogénese noutros vertebrados-modelo, pouco se sabe do papel da matriz de fibronectina neste evento morfogenético.

Numa primeira fase, esta tese pretendeu resolver uma série de observações respeitantes à capacidade da MPS de formar sómitos na presença ou ausência de

tecidos circundantes, nomeadamente, a ectoderme, colocada dorsalmente à mesoderme paraxial. No **capítulo 2** desta tese evidenciamos que a somitogénese ocorria em MPS isoladas de todos os tecidos circundantes, ao contrário das numerosas observações anteriores, mas apenas se a matriz de fibronectina original for mantida. Neste capítulo demonstramos que a ectoderme serve a formação de sómitos como um parceiro na formação da matriz de fibronectina e não como uma fonte de factores parácrinos. Em combinação com o **capítulo 4**, esta tese revela que a ectoderme é uma importante fonte de produção de fibronectina, e que conformações globulares de fibronectina estão localizadas no seu lado basal. Este capítulo 2 não só clarifica a função da ectoderme, indicando como certas idiossincrasias metodológicas resultaram nas observações anteriores, como também reforça a noção da autonomia do programa genético na MPS mais rostral.

Dado a complexidade de um tecido embrionário que se estende em todas as direcções, no capítulo seguinte investigamos o fenómeno da formação da fenda intersomitica de um ponto de vista tridimensional. Aprimorando a visualização *in vivo* e em "time-lapse" da somitogénese, constatámos a complexidade dos movimentos celulares envolvidos na formação da fenda e no rearranjo de um novo sómito. Neste **capítulo 3** foi dado um enorme passo na compreensão da somitogénese numa perspectiva tri-dimensional de primeira linha. Esta nova perspectiva e a respectiva melhoria tecnológica e metodológica derivados deste trabalho possibilitaram e levaram a uma avaliação detalhada da ECM explanada no capítulo seguinte.

No **capítulo 4**, foi feito um extenso mapeamento da MEC ao longo do eixo caudal-rostral da mesoderme paraxial. Esta abordagem não só acompanhou as alterações da matriz de fibronectina e laminina durante o desenvolvimento deste tecido, como também evidenciou pela primeira vez, os passos iniciais na *formação in vivo* e em 3D destas matrizes. Uma vez que na sua extremidade caudal, a MPS mesenquimatosa é o resultado directo da gastrulação, onde a MEC original é degradada, o eixo caudal-rostral reflecte a formação *de novo* da matriz de fibronectina e laminina. Ao longo da mesoderme paraxial, a fibronectina torna-se crescentemente mais densa e fibrilar, mas após a formação do sómito a laminina passa a ocupar o espaço junto das células e a

matriz de fibronectina fica claramente exterior à membrana basal. Neste capítulo reforçamos a importância de uma matriz densa e fibrilar de fibronectina durante a formação do sómito epitelial, tal como demonstrado no capítulo 2, mas não da laminina, quase ausente. Adicionalmente, o acompanhamento da matriz de laminina revelou que a sua montagem ocorre de um modo fragmentado e disperso. Inesperadamente, observámos que os fragmentos de laminina crescem e coalescem, mas sem nunca formarem uma membrana basal contínua rodeando o sómito epitelial ou o seu derivado epitelial, o dermomiótomo.

No capítulo experimental final (**capítulo 5**) investigamos o papel da tensão celular na somitogénese, assumindo o princípio provável que a MEC rodeando a mesoderme paraxial serve como um suporte físico para as células da MPS e dos sómitos. Neste capítulo foram utilizados inibidores de tensão celular, prevenindo a capacidade das células não só de usarem mecanicamente a MEC, como de percepcionar as características mecânicas da MEC. Este trabalho revelou que o carácter epitelial dos sómitos normalmente surge imediatamente após o seu descolamento da MPS rostral, reforçando a integridade do segmento. Na presença de inibidores da tensão celular, o carácter epitelial em aquisição é perdido, mas os sómitos epiteliais mantêm pelo menos parcialmente a sua forma, demonstrando alguma robustez. A presença de inibidores de tensão, em particular, inibidores de vias próximas da sinalização mediada por integrinas, alteraram também o programa genético na MPS, revelando uma possível regulação mecanosensitiva da resposta aos gradientes subjacentes à determinação da MPS rostral.

Em conjunto, esta tese evidenciou que a contínua montagem de uma matriz de fibronectina, numa conjugação de esforços pela ectoderme e pela MPS, acompanha o desenvolvimento da mesoderme paraxial, levando ao estabelecimento de uma matriz madura, capaz de suportar a formação de sómitos e de manter os segmentos separados. Mostramos também que a complexa orquestração dos movimentos celulares durante a somitogénese requer um sinal polarizador da fibronectina (provavelmente com um valor mecânico), efectuador da epitelização do sómito e no processo separador da fenda intersomítica. São lançadas também hipóteses de como a matriz de fibronectina se integra noutros mecanismos durante a formação da fenda, e na regulação tenso-

mecânica da integração dos gradientes que definem espacialmente a MPS determinada mais rostral.

Palavras-chave: Somitogénese, sómito, mesoderme presomítica, matriz extracelular, fibronectina, mesenquimatoso, epitelial

Abstract

The formation of the string of individual somite segments is a hallmark morphogenetic event during embryonic development, establishing the basic foundations of the vertebrate body. Somites pinch off from the mesenchymal presomitic mesoderm on either side of the neural tube, as epithelial blocks of cells, with a strict chronological sequence in a rostral to caudal fashion. In recent decades, the intense scrutiny and investigation on the temporal and spatial regulation of somitogenesis has produced a fascinating picture on the mechanisms underlying vertebrate embryo segmentation. However, our knowledge regarding the cellular performance involved in the detachment and individualization of the somitic segment remains quite obscure. The extracellular matrix molecule fibronectin has been implicated in somitogenesis since its discovery and its role was reinforced with the genetic deletion in the mouse embryo, but how fibronectin participates in the formation of the epithelial somite is still unclear.

The aim of this thesis is to investigate how the interaction between the presomitic mesoderm cells and the fibronectin matrix contributes to the detachment of the somite sphere of epithelial cells, using the chicken embryo as a model. In **Chapter 2** we first resolve the disputed role of the ectoderm overlying the presomitic mesoderm, showing that is serves as a source of fibronectin, which becomes assembled as a fibrillar matrix around the presomitic mesoderm, supporting somite formation. Through microsurgical explant collection and culture we show for the first time that a presomitic mesoderm isolated from all surrounding tissues can undergo somitogenesis provided that the original fibrillar fibronectin sleeve is preserved.

In **Chapter 3** and **4** we adopt a three-dimensional view of somite formation, evaluating in detail the cellular rearrangements underlying somitogenesis (Chapter 3) and the architecture of the fibronectin matrix along the full extent of the presomitic mesoderm and somites (Chapter 4). The combination of time-lapsed movies and explant culture analysis presented in **Chapter 3** revealed that intersomitic cleft formation is mostly driven by the cells in the rostral border and that mesenchymal cells from the central locations contribute to the outer epithelial layer of somites. The high-resolution analysis of the extracellular matrix displayed in **Chapter 4** revealed that an increased

fibrillar complexity of the fibronectin matrix accompanies presomitic mesoderm maturation, preluding somite formation. We co-analyzed the distribution of the epithelium-associated extracellular molecule laminin and found, together with our observations in Chapter 2 that it does not contribute to the epithelialization of the somite. The thorough analysis in this Chapter is also one of the few detailed evaluations of extracellular matrix component assembly in a complex three-dimensional *in vivo* tissue.

In the final chapter, **Chapter 5**, we investigate the role of cell tension, elicited by the cell attachment to its milieu, in the epithelialization and detachment of somites. The epithelialization process is abrogated by specific cell tension inhibitors, but already formed somites can partially maintain their epithelial organization. Remarkably, these inhibitors also interfere with the spatial regulation of *Meso1* expression, a key gene underlying both the location of the future somite boundary and the establishment of the rostral-caudal polarity of the somite segment. In combination with the previous chapters, these results indicate that the assembly of a fibronectin matrix along the caudal-rostral axis of the presomitic maturation is a part of the maturation process: the increased fibrillar complexity provides the tensional support for both the cell rearrangements essential for somite detachment, epithelialization of the peripheral cells and apparently also as a spatial cue influencing the developmental programs of the presomitic mesoderm.

Overall, this thesis demonstrates the prominent role of the fibronectin extracellular matrix during somitogenesis in the chicken embryo. The results obtained highlight that the extracellular matrix dimension is a worthy player during embryonic development.

Keywords: Somitogenesis, somite, presomitic mesoderm, extracellular matrix, fibronectin, mesenchymal, epithelial

List of abbreviations and acronyms

3D ..... Three-dimensions, three-dimensional

AKT/PKB... (Ak) Thymoma viral proto-oncogene, also called PKB, Protein Kinase B

bHLH..... basic Helix-Loop-Helix

BMP..... Bone Morphogenetic Protein

Cdc42..... Cell Division Cycle 42

DOC ..... Deoxycholate detergent

ECM ..... Extracellular Matrix

EMT ..... Epithelial-Mesenchymal Transition

FAK ..... Focal Adhesion Kinase

FGF ..... Fibroblast Growth Factor

GAG ..... Glycosaminoglycan

GTPases .... Guanosine Triphosphatases

ILK..... Integrin-linked Kinase

IPP ..... ILK-PINCH-Parvin protein complex

IQGAP..... IQ motif containing GTPase activating protein

JNK ..... c-Jun N-terminal Kinase

LRP ..... Low-density-lipoprotein-related Protein

MET ..... Mesenchymal-Epithelial Transition

NICD ..... Notch Intracellular Domain

Pax..... Paired-box

PINCH ..... Particularly interesting Cys-His-rich protein

PSM ..... Presomitic Mesoderm

RA..... Retinoic Acid

Rac1..... Ras-related C3 botulinum substrate 1

RhoA..... Ras homolog A

Src..... Cellular homolog of transforming gene of Rous sarcoma virus

TGF ..... Transforming Growth Factor

VASP..... Vasodilator-stimulated phosphoprotein

Wnt ..... Wingless-type Mouse Mammary Tumor Virus (MMTV) Integration Site

Chapter 1

Introduction

I. State of the art

1. Paraxial mesoderm and somites

The foundations for the characteristic segmented body plan of vertebrates are laid down early in embryonic development as repeated individual blocks of mesodermal cells on each side of the neural tube. These conspicuous structures, called somites, are not only the anlagen of segmented tissues but also impose a segmented pattern onto neighboring tissues. Somites generate the distinctly metamerized vertebral column, i.e., composed of similar, repeated elements, and contribute to its intervertebral discs. Somites also give rise to all the skeletal muscles of trunk and limbs, the dermis of the back, and contribute to several other tissues (for reviews, see Brent and Tabin, 2002; Christ et al., 2004; Christ et al., 2007; Hirsinger et al., 2000; Scaal and Christ, 2004). Furthermore, the repeated pattern of the string of somites also imposes a repeated arrangement onto the peripheral nervous system and early embryonic vasculature (see Keynes and Stern, 1984; Keynes and Stern, 1988; Krull, 2001; Kuan et al., 2004). In this chapter I will focus on the paraxial mesoderm, from its origin through its first stages of differentiation, focusing mainly on chick and mouse embryogenesis, but also referring to other model systems when appropriate.

1.1. Gastrulation and the origin of the three germ layers

The presomitic mesoderm (PSM), from which somites arise, is originated early in development, during gastrulation. In amniotes (i.e. reptiles, birds and mammals), gastrulation leads to the formation of the three germ layers from the original, single cell layered epiblast: the ectoderm, covering the dorsal side of the embryo, the endoderm, lining the ventral side, and the mesoderm, sandwiched between these two layers. The epiblast of amniote embryos forms a characteristic thickening at its midline, the primitive streak, and a regional thickening at the anterior end of the streak, termed Hensen's node (or simply node in mammalian embryos). As gastrulation starts, some epiblast cells ingress, i.e., sink in and move through the primitive streak or Hensen's node, and migrate to their destined location to originate the endoderm and mesoderm, while the remaining epiblast becomes the embryonic ectoderm (Figure 1).

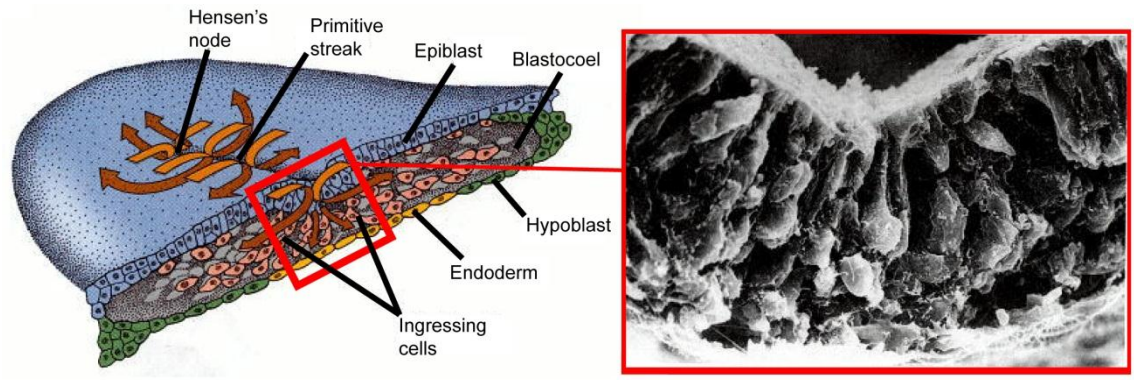

Figure 1. Ingression and migration of epiblast cells through the primitive streak. On the left: Illustrative depiction of gastrulation in the chicken embryo, showing the various migration routes of the ingressing cells. Note the single layered epiblast, and the two new germ layers formed through gastrulation, the endoderm and mesoderm. On the right: Scanning electron microscopy of chicken embryo through the primitive streak. Adapted from Gilbert, 2006

1.1.1. General overview of cell movements during chick gastrulation

Thanks to the easy accessibility and flatness of avian embryos, they, most commonly chicken (Gallus gallus) embryos, have been the subject of extensive fate mapping studies with different techniques, which provided a detailed blueprint of early embryogenesis as gastrulation takes place (Catala et al., 1996; Freitas et al., 2001; Hatada and Stern, 1994; Iimura et al., 2007; Psychoyos and Stern, 1996; Sawada and Aoyama, 1999; Schoenwolf et al., 1992; Selleck and Stern, 1992). In the chicken embryo, the first ingressing cells migrate rostrally beneath the epiblast and give rise to the pharyngeal endoderm and foregut, while the cells which ingress slightly later, migrate rostrally, but a shorter distance, and contribute to the cephalic mesodermal tissues (Psychoyos and Stern, 1996). Once the primitive streak is fully extended rostrally, Hensen's node begins to regress caudally along the primitive streak, elongating the tridermic embryo as it leaves in its wake the endoderm and the precursors of the four mesodermal tissues of the trunk (see Figure 2). The embryo's midline is occupied by the axial mesoderm, the notochord, and above it, the neural plate of ectodermal origin, which folds inwards to form the neural tube. The remaining three mesodermal tissues are named according to their position respective to the midline. Immediately next to the axis we find the paraxial mesoderm, flanking both sides of the medial structures. The paraxial mesoderm is composed of the PSM, in the form of two strips or rods of

mesenchymal cells, and the somites which it originates. Immediately lateral to the paraxial mesoderm is the intermediate mesoderm, the precursor of the urogenital system, while the lateral-most region is designated the lateral plate mesoderm. This lateral plate mesoderm then slits horizontally into two portions, and associates with the ectoderm and endoderm, resulting in the dorsal somatopleure and the ventral splanchnopleure, respectively. These two pleura originate or contribute to a variety of embryonic tissues, such as the visceral organs and the circulatory system, but also to the extra-embryonic membranes.

Fate maps generated for the chick embryo showed that the proximity of epiblast cells to Hensen's node before ingression reflects their medial-lateral position after gastrulation; i.e. cells closest to the node originate more medial tissues (such as notochord or the medial portion of the paraxial mesoderm), while cells positioned progressively further posterior in the streak give rise to the lateral portion of the paraxial mesoderm, the intermediate and lateral mesoderm, respectively (see Figure 3) (Freitas et al., 2001; Psychoyos and Stern, 1996; Schoenwolf et al., 1992). Gastrulation in chick

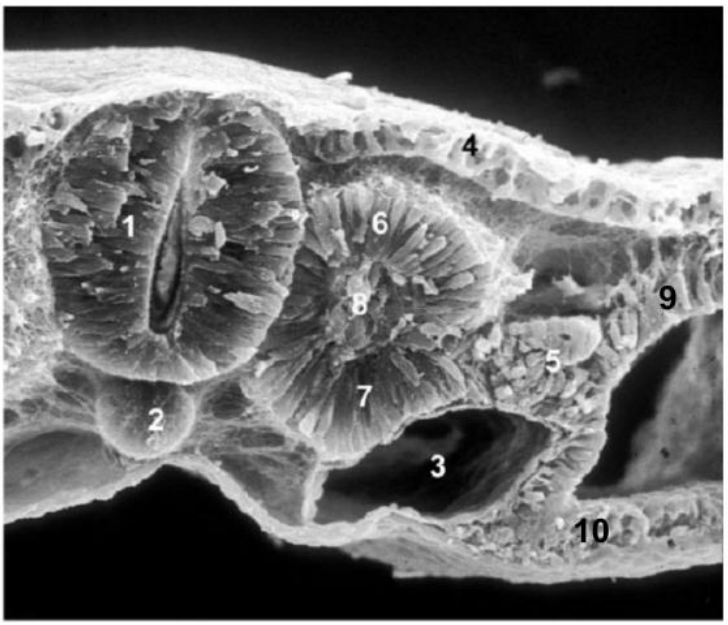

Figure 2: The tridermic vertebrate embryo. Scanning electron microscopy of a transverse fracture through an epithelial somite of a 2 day-old chicken embryo. 1. Neural tube, 2. Notochord (axial mesoderm), 3. Dorsal Aorta, 4. Ectoderm, 5. Intermediate mesoderm, 6. Somite (dorsal epithelium), 7. Somite (ventral epithelium), 8. Somite (mesenchymal somitocoel), 9. Lateral plate mesoderm (somatopleure), 10. Lateral plate mesoderm (splanchnopleure). The thin endoderm is visible lining the bottom. Adapted from Christ et al., 2007

embryos continues through the primitive streak until stage 15 (Hamburger and Hamilton, 1992, see "Nomenclature") concomitantly with embryo elongation. From this stage onwards, caudal elongation proceeds in the tail bud, with the process of secondary gastrulation (Christ et al., 2000). The tail bud originates the caudal tissues, and shares a fate map that parallels the primitive streak at earlier stages, although in a more compact form (Catala et al., 1996). I will address the origin of the paraxial mesoderm in more detail in the section 1.2., *Origin and development of the paraxial mesoderm*.

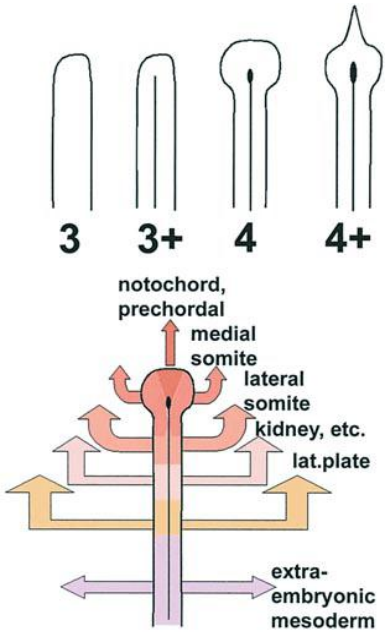

Figure 3. Fate map of gastrulation through the primitive streak (stage HH3 and HH4 chicken embryos). Rostral to the top. Note the relation between rostral-caudal axis of the primitive streak and the medio-lateral fate of the resulting ingressing cells. Adapted from Stern, 2004.

1.1.2. Epithelial to Mesenchymal Transition

Gastrulation through the primitive streak involves the first embryonic epithelial-mesenchymal transition (EMT), where cells from the epiblast de-epithelialize and displace ventrally, forming the mesenchymal mesoderm (Nakaya and Sheng, 2008). Before gastrulating, the epiblast cells are aligned on top of a rich extracellular matrix (ECM) (Harrisson et al., 1984; Nakaya et al., 2008; Sanders, 1982; Sanders, 1984). They adhere strongly to each other through tight junctions and E-cadherin-containing *adherens* junctions (Nakaya et al., 2008; Wakely and Badley, 1982), E-cadherin being a membrane protein involved in cell-cell adhesion (see section 2.6., *Cell-cell adhesion*, for

more details). Breakdown of the basal ECM by the primitive streak cells is a land-mark event for the initiation of gastrulation (Sanders and Prasad, 1986), and requires the rearrangement of the cytoskeletal regulators of the cells in the primitive streak (Nakaya et al., 2008). At the same time, the tight cell-cell contacts typical of the epithelial epiblast are lost, and E-cadherin is replaced by N-cadherin at the new *adherens* junctions of the mesenchymal tissue (Hatta and Takeichi, 1986; Nakaya et al., 2008).

Numerous events in embryonic development and in pathological conditions can be categorized into an EMT (Kalluri and Weinberg, 2009). Also, several signaling pathways can pour in to initiate and regulate such complex cellular behavior, and gastrulation is no exception (for reviews on EMT in development, see Acloque et al., 2009; Baum et al., 2008; Ferrer-Vaquer et al., 2010; Nieto, 2011; Thiery et al., 2009; Thiery and Sleeman, 2006). In mouse and chicken embryos, Wnt signaling is essential to prepare the prospective primitive streak region that undergoes the EMT in the epiblast (Liu et al., 1999; Voiculescu et al., 2007, reviewed in Robb and Tam, 2004; Stern, 2006; Yamaguchi, 2001). The Fibroblast-Growth-Factor (FGF) signaling pathway is required to regulate the EMT process (Sun et al., 1999) and does so by inducing the expression of Snail (Ciruna and Rossant, 2001), an EMT-promoting zinc-finger transcription factor (Barrallo-Gimeno and Nieto, 2005; Nieto, 2002). In parallel, Nodal, a member of the Transforming Growth Factor (TGF) -β superfamily pathway (Shen, 2007), though apparently not directly involved in the EMT, is pivotal for the establishment and maintenance of the primitive streak (Conlon et al., 1994; Zhou et al., 1993). At the same time, these signaling pathways also contribute to determine cell commitment towards a mesodermal fate (Arnold and Robertson, 2009; Robb and Tam, 2004; Stern, 2005). In the next section I will overview the molecular events that lead to a mesodermal fate, and focus on the formation and specification of the paraxial mesoderm.

1.2. Origin and development of the paraxial mesoderm.

1.2.1. Fate map of the origin of paraxial mesoderm cells

In the chicken embryo, the first paraxial mesoderm precursors are located in the lateral sides of the rostral primitive streak and ingress while the streak is still extending

(Hatada and Stern, 1994; Psychoyos and Stern, 1996; Schoenwolf et al., 1992). Once Hensen's node starts regressing, the presumptive territory of the paraxial mesoderm remains in the primitive streak caudal to the node (Psychoyos and Stern, 1996) and also in the node itself (Selleck and Stern, 1991). In fact, these two regions give rise to medial paraxial mesoderm (closest to the axis), while the precursors of the lateral portion are located further caudally in the primitive streak (Psychoyos and Stern, 1996; Selleck and Stern, 1991). Throughout the remaining primary gastrulation, the prospective paraxial territory remains just caudal to Hensen's node, and the separation between the prospective medial and lateral territories of the PSM is maintained (Catala et al., 1996; Freitas et al., 2001; Iimura et al., 2007; Sawada and Aoyama, 1999). The remaining caudal primitive streak originates intermediate and lateral plate mesoderm (Ooi et al., 1986). Interestingly, only the prospective region of the medial PSM behaves as a stem cell niche providing cells for the paraxial mesoderm at all axial levels (Iimura et al., 2007; Selleck and Stern, 1991). Once the tail bud is formed, the territory of the future paraxial mesoderm is located in a broader domain, encompassing the caudal and latero-caudal tip of the bud (Catala et al., 1995).

1.2.2. Plasticiy of the paraxial mesoderm

The embryonic tissues that form as gastrulation initiates and propagates are meticulously arranged, laying the adequate foundations of the following embryonic events. Nevertheless, these tissues are not ultimately committed towards a given fate. In the chick embryo and also in the mouse embryo, paraxial mesoderm precursor cells can re-specify to a new fate when transplanted to a different territory. Portions of prospective paraxial mesoderm from the epiblast adopt a new fate when ectopically grafted into a prospective neural territory (Garcia-Martinez et al., 1997). The primitive streak territory from which the PSM arises is also labile to adopt a new fate when grafted to more caudal regions of the streak (Beddington, 1982; Garcia-Martinez and Schoenwolf, 1992) or to the area of prospective neuro-ectoderm in the epiblast (Garcia-Martinez et al., 1997). The PSM also shows some degree of plasticity, as cells from orthotropic grafts colonize lateral plate mesoderm and even embryonic blood vessels (Tam, 1988). Moreover, even recently formed somites grafted under the ectoderm of primitive streak stage embryo, were able to adopt a non-paraxial mesoderm fate,

although to a lesser extent (Veini and Bellairs, 1991). Moreover, medio-lateral mesoderm specification is influenced by Bone-Morphogenetic-Protein (BMP) signaling (Pourquié et al., 1996), the BMPs being members of the TGF-β super-family. In fact, treatment with the protein BMP4 can convert PSM into lateral mesoderm (Tonegawa et al., 1997; Tonegawa and Takahashi, 1998). Thus, despite the rather precise discrimination of prospective regions for the tissues generated during gastrulation, several signaling events contribute, in a stepwise manner, to initiate, adopt and reinforce cell fate.

1.2.3. Mesoderm induction and commitment to paraxial mesoderm

The signaling pathways that regulate EMT during gastrulation, TGF-β (Nodal), FGF and Wnt, all target the expression of the transcription factor *Brachyury* (Ciruna and Rossant, 2001; Sheng et al., 2003; Yamaguchi et al., 1999). *Brachyury*, also known just as *T* (from Tail), is the most studied gene of the T-box transcription factor family (reviewed in Naiche et al., 2005; Showell et al., 2004; Wardle and Papaioannou, 2008). *Brachyury* is expressed in the primitive streak and its deficiency leads to the absence of trunk mesoderm (Wilkinson et al., 1990; Wilson et al., 1995). While considered as a *bona fide* marker for mesoderm precursors across vertebrates (Showell et al., 2004; Wardle and Papaioannou, 2008), *Brachyury* is continuously expressed in the notochord, but is only transiently expressed in the primitive streak and caudal mesoderm (Wilson et al., 1995). Thus the mesoderm becomes committed to a paraxial fate through the concurrent activation of another transcription factor of the T-box family, *Tbx6*, specific for paraxial mesoderm (Chapman et al., 1996). The onset of *Tbx6* expression occurs normally in the earliest stages of *Brachyury*-null mouse embryos, but is rapidly lost, indicating that the expression of Tbx6 requires *Brachyury* for its maintenance but not for its initiation (Chapman et al., 1996).

1.2.4. Paraxial mesoderm or neural tube?

Remarkably, the genetic deletion of either *Brachyury* or *Tbx6* results in the loss of paraxial mesoderm, which is converted into ectopic neural tube structures in early mutant mouse embryos (Chapman and Papaioannou, 1998; Yamaguchi et al., 1999). This

observation indicates that both T-box genes are determinants in the suppression of the neural fate in favor of the (paraxial) mesoderm fate. Moreover, the same loss of paraxial mesoderm and replacement for neural tissue resulted from the deletion of *Wnt3* (Takada et al., 1994; Yoshikawa et al., 1997) and *Fgfr1* (Ciruna et al., 1997; Deng et al., 1997). Despite the early separation into three germ layers, the trunk paraxial mesoderm and neural cells share a common axial bipotential progenitor (Tzouanacou et al., 2009). In the tissues posterior to the node, the Wnt and FGF signaling pathways promote a neural fate, while a contextual BMP signal suppresses, at the same time and using the same enhancer, the activation of the neural progenitor marker *Sox2* (Takemoto et al., 2006). As the node moves caudally, the suppressing influence of the BMP signal is released thus allowing the neural fate, except in the mesoderm cells, where *Tbx6* maintains the neural suppression (Takemoto et al., 2011). Interestingly, *Tbx6* acts not only as an inhibitor of the neural fate, but also as the promoter of paraxial mesoderm development (Takemoto et al., 2011), discussed in (Kondoh and Takemoto, 2012; Li and Storey, 2011). Apparently, the aforementioned mesoderm replacement following the genetic deletion of *Wnt3a* and *Fgfr1*, results from a paucity of *Tbx6* activation.

Wnt3a is expressed in the primitive streak and early mesoderm, in both mouse (Takada et al., 1994; Yoshikawa et al., 1997) and chicken embryos (Baranski et al., 2000; Chapman et al., 2004), but its expression starts later than *Brachyury* or *Tbx6* (Takada et al., 1994; Wilkinson et al., 1990; Wilson et al., 1995). Thus, *Wnt3a*-/- embryos show severe axial truncation visible from embryonic (E) day 9.5 onwards, where, beyond the level of the 7th somite, mesoderm is absent and is instead replaced by ectopic neural tissue (Takada et al., 1994; Yoshikawa et al., 1997). In accordance, expression of *Brachyury* and *Tbx6* wanes rapidly in the mesoderm precursors after the first formed somites (Yamaguchi et al., 1999).

On the other hand, *Fgfr1*, which encodes for the main receptor for FGF signaling, is expressed throughout the epiblast, prior to gastrulation (Orr-Urtreger et al., 1991; Yamaguchi et al., 1992). Therefore, *Fgfr1*-null embryos show severely impaired gastrulation (Yamaguchi et al., 1994). Chimeric (*Fgfr1*-/- ; *Fgfr1*-/+) mouse embryos are able to gastrulate and develop further, but have ectopic neural tubes composed of

Fgfr1-/- cells (Ciruna et al., 1997; Deng et al., 1997). These chimeric embryo allowed to ascertain that *Fgfr1*-/- primitive streak cells are not only unable to ingress and migrate adequately, but also fail to express *Brachyury* and *Tbx6* (Ciruna and Rossant, 2001). Apparently, *Fgf8* and also *Fgf4*, which encode for FGFR1 ligands, are required for the activation of *Brachyury* and *Tbx6* in the primitive streak precursors of the paraxial mesoderm (Sun et al., 1999). Likewise, double knock-out mouse embryos for *Lrp5* and *Lrp6* (low-density-lipoprotein-related proteins), do not express *Tbx6*, although *Brachyury* is present in the primitive streak (Kelly et al., 2004). LRP5 and LRP6 are partially redundant co-receptors essential for the transduction of canonical Wnt signaling (see Cadigan and Liu, 2006; He et al., 2004; Nusse, 2012), thus indicating that some other Wnt ligand may support the early activation of *Tbx6* observed in *Wnt3a*-/- embryos.

Although still not completely elucidated, a mechanism involving FGF and canonical Wnt signaling initiates the expression of *Tbx6* and *Brachyury* in the mesoderm precursors during gastrulation, and maintains *Tbx6* expression in the paraxial precursors. It is relevant to note that the mouse *Tbx6* gene and the chicken "equivalent" *Tbx6L* (short for *Tbx6*-like) are not true homologs. Despite their analogous embryonic domains of expression (Chapman et al., 1996; Knezevic et al., 1997), *Tbx6* and *Tbx6L* share little nucleotide similarity outside the T-box sequence (Knezevic et al., 1997). Nevertheless, the chicken *Tbx6L* participates in the mesoderm versus neural fate decisions (Sheng et al., 2003) in an almost identical fashion as *Tbx6* in the mouse embryo (discussed in (Kondoh and Takemoto, 2012), thus supporting their validity as functionally comparable markers of paraxial mesoderm in both systems, specifically, the PSM (see ahead).

1.3. Maturation of the PSM

1.3.1. Entering the PSM

As gastrulation takes place at the caudal end of the embryo, new cells are supplied to the PSM, while at the same time, blocks of cells exit the rostral PSM, as somites periodically pinch off. Thus, as long as new PSM tissue is created, somite formation endures until no PSM remains. The rate at which new PSM is generated varies throughout chick embryo development (Gomez et al., 2008), peaking at around 48 hours

of incubation (stage HH 13 and 14, see section 1.3.4, *Nomenclature*) when the PSM is the longest (Stockdale et al., 2000), and decreases as development proceeds. Eventually somitogenesis catches up with gastrulation at the tail bud (Gomez et al., 2008), and completes the species specific number of somites in the individual (Richardson et al., 1998). The regulation of the ratio between the rate of somite formation versus the generation rate of new PSM allows for the species specific length and number of somites in vertebrates (Gomez et al., 2008). While it remains unclear how the balance between these two rates is regulated, it has been reported that somite formation abruptly stops before all PSM tissue is used up (Tenin et al., 2010).

Once paraxial mesoderm cells enter the caudal PSM in the chicken embryo, they can spend up to 18 hours and undergo one or two rounds of mitosis as mesenchymal cells, before being incorporated into a somite (Packard and Jacobson, 1976; Stern et al., 1988). Throughout this time, the PSM cells undergo a maturation process, preparing for somite formation. In its caudal portion (roughly two thirds), the PSM cells are committed to a paraxial mesoderm fate but are maintained in an undifferentiated state. In the rostral third, or region II (Saga and Takeda, 2001), of the PSM, cells are committed to a somitic fate, undergoing alterations in gene expression patterns which establish the foundations for somitogenesis: the regular temporal and spatial interval between segments; the rostro-caudal polarity of somites; the individualization into discrete morphological units and the initiation of differentiation programs. In this section I will introduce the events occurring in the caudal region of the PSM, although some are intricately related to the events occurring in the rostral region (region II). I will then dedicate sections 1.4 to 1.7 to the events occurring in the rostral PSM.

1.3.2. Establishing the PSM identity

Cells in the caudal PSM territories can still contribute to intermediate or lateral plate mesoderm (Stern et al., 1988), although *Tbx6* expression commits them to a paraxial mesoderm fate (Chapman et al., 1996; Chapman and Papaioannou, 1998; Knezevic et al., 1997). The influence of BMP signaling may explain such switches in fate (Tonegawa et al., 1997), however, several genes are expressed specifically in the PSM, reinforcing the PSM identity and laying the foundations for somitogenesis.

Mesogenin (*Msgn1*) is expressed early in development, in the caudal PSM in both mouse (Yoon et al., 2000) and chicken embryos (Buchberger et al., 2000), called *cMespo* at the time). Although this gene does not seem to participate in the neural versus mesodermal fate as *Tbx6* does (Kondoh and Takemoto, 2012), it establishes the paraxial mesoderm identify together with *Tbx6* (Yoon and Wold, 2000). *Msgn1* expression in the PSM is controlled in synergy by Wnt signaling and *Tbx6* (Wittler et al., 2007), and its genetic deletion results in severe paraxial mesoderm defects caudal to the level of the forelimb at E9.0 and later on (Yoon and Wold, 2000). Despite the activation of *Tbx6* in *Msgn1*-null embryos, expression of several genes of the Notch/Delta family is missing in the paraxial mesoderm (Yoon and Wold, 2000). Thus, *Msgn1* is important to reinforce the PSM identity, although little is known of other functions of *Msgn1*.

Delta-like 1 (*Dll1*) is specifically expressed throughout the PSM of mouse (Bettenhausen et al., 1995) and chicken embryos (Henrique et al., 1995; Palmeirim et al., 1998). *Tbx6* and *Dll1* genetically interact, making *Dll1* a possible target for *Tbx6* (Beckers et al., 2000; White and Chapman, 2005), which acts in synergy with Wnt signaling to activate *Dll1* (Galceran et al., 2004; Hofmann et al., 2004). *Dll1* encodes for a ligand for Notch receptors, namely *Notch1*, which is also expressed throughout the entire PSM (mouse - (Reaume et al., 1992), chicken – (Henrique et al., 1995; Palmeirim et al., 1998). These two transmembrane proteins are major players in the Notch/Delta juxtacrine signaling pathway (see Katsube and Sakamoto, 2005). *Notch1* and *Dll1* are two of the Notch signaling pathway genes expressed in the PSM (see Freitas et al., 2005; Rida et al., 2004 and references therein). Genetic deletion of either *Notch1* (Conlon et al., 1995) or *Dll1* (Hrabě de Angelis et al., 1997) leads to deficient and uncoordinated somitogenesis. Thus, Notch signaling in the PSM is of particular importance to ensure the correct synchronization of PSM cells to form somites. I will focus on this issue in section 1.4., *Time and space*. Moreover, the *Dll1* gene is particularly interesting as it is also a major player and benchmark in the establishment of the rostro-caudal polarity in the somite, which I will expand on in section 1.6, *Rostral vs. caudal*.

1.3.3. Building gradients

Once cells enter the PSM, their movements become quite restricted, never moving freely along the PSM. This was demonstrated by dextran-labeling of single PSM cells, whose progeny was limited to small clusters of cells, never encompassing more than two adjacent somites (Stern et al., 1988). Therefore, the PSM does not act as a static conveyor belt, where new cells are loaded at one end with gastrulation and are put out at the other end as somitic packages of cells. Rather, the PSM grows caudally while its cells remain fairly still, much like a farmer's baler going through the field and producing bales of hay in its trail. During their static journey (sic), PSM cells go from an undifferentiated state at the caudal end into the initiation of differentiation at the rostral end. This effect is achieved with a gradient of morphogens.

The first morphogen gradient to be described was that of *Fgf8* mRNA found in the chick embryo (Dubrulle et al., 2001), in zebrafish (Sawada et al., 2001) and later also reported in mouse embryos (Dubrulle and Pourquié, 2004a). Rather than a gradient of transcription of mRNA, it turned out to be a gradient of mRNA decay, as *de novo* transcription is restricted to the progenitor areas at the caudal end (Dubrulle and Pourquié, 2004a). This gradient is characterized by a strong FGF signal at the caudal end of the PSM that maintains the cells in an undifferentiated state (Dubrulle et al., 2001; Dubrulle and Pourquié, 2004a; Sawada et al., 2001). High levels of FGF8 protein in the caudal region (Dubrulle and Pourquié, 2004a) resulted in a graded activation of pathways downstream of FGF (Delfini et al., 2005; Dubrulle and Pourquié, 2004a; Sawada et al., 2001). A parallel gradient of *Wnt3a* mRNA has also been described (Aulehla et al., 2003) although neither a gradient of mRNA decay or WNT3a protein have been reported. Nevertheless, high levels of WNT3a protein in the caudal region reinforce the undifferentiated state of the PSM (Aulehla et al., 2003) and activate the Notch/Delta signaling pathway (Nakaya et al., 2005). Once PSM cells escape the influence of FGF and Wnt signaling, they become part of the rostral region, committed to form somites. Moreover, these two parallel gradients are opposed by an inverse gradient of retinoic acid (RA). RA is a small molecule that results from vitamin A metabolism (Rhinn and Dolle, 2012) and cannot be visualized directly. A retinoic acid signaling responsive element (termed RARE) driving *LacZ* expression, showed a clear

gradient of RA signaling throughout the embryo, strongest in rostral areas, including somites and anterior PSM (Rossant et al., 1991). The existence of this gradient is further supported by the localization of *Raldh2* mRNA in somites and rostral PSM, an enzyme involved in RA synthesis (Niederreither et al., 1997) and the caudal expression of *Cyp26*, codifying an enzyme involved in RA degradation (Fujii et al., 1997; Sakai et al., 2001). In the chick embryo, these two enzymes are expressed in the same locations (Swindell et al., 1999), reinforcing the notion that the RA gradient functions as a source and sink gradient. Apparently, RA signaling can directly counteract FGF signaling in chick (Diez del Corral et al., 2003) and Xenopus (Moreno and Kintner, 2004) embryos, promoting differentiation. Thus, these opposing gradients sharpen the interface that separates the caudal undifferentiated region under the influence of FGFs and Wnts, from the RA dominated rostral portion (Diez del Corral and Storey, 2004; Dubrulle and Pourquié, 2004b). As the embryo elongates, both opposing gradients are displaced caudally. Therefore, PSM cells remain undifferentiated until a particular threshold level of FGF/Wnt versus RA signal passes through their location, switching them into a somitic fate. This hypothetical, continuously moving, threshold line, which separates the two regions, is termed determination front (Dubrulle et al., 2001; Dubrulle and Pourquié, 2002 and Figure 4). In the chicken embryo the determination front is located 4 to 5 somite lengths caudal to the PSM's rostral end (Dubrulle et al., 2001), therefore explaining the commitment of PSM portions rostral to this position, but not of PSM portions from the caudal region (Dubrulle et al., 2001; Dubrulle and Pourquié, 2004a; discussed in Dubrulle and Pourquié, 2004b). I will further expand on the implications of these gradients and the determination front in section 1.4., *Time and space*.

1.3.4. Nomenclature

The staging of chicken embryos has been meticulously performed by (Hamburger and Hamilton, 1992), using several landmark features in the embryos, including the number of somites. For example, a stage Hamburger and Hamilton 10 (HH10) embryo contains 10 somites, while a stage HH11 embryo has 13 somites, a stage HH12 embryo, 16 somites, and so forth. As somites are formed periodically, the presence of an increasing number of somites faithfully represents a linearly older embryo.

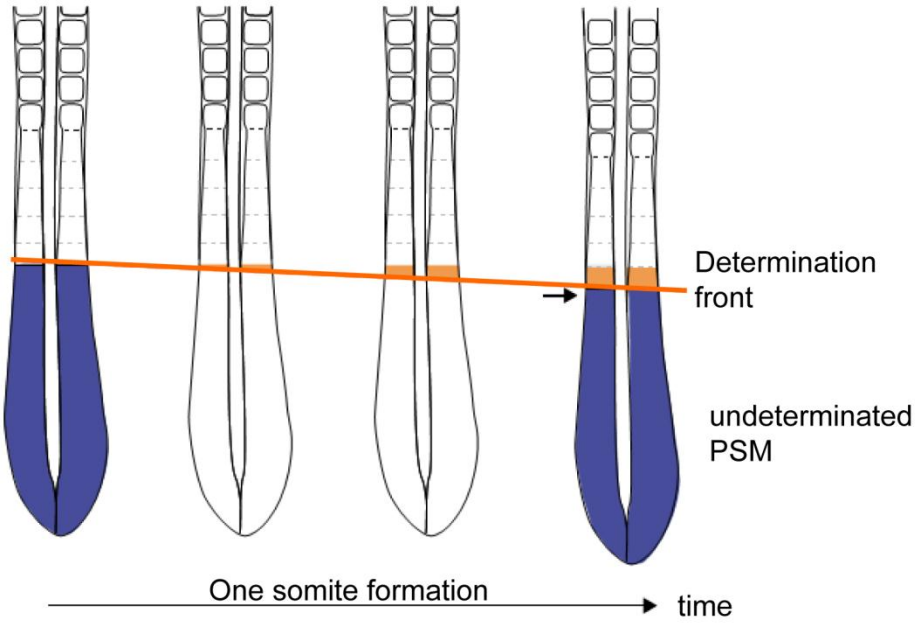

Figure 4. The positioning of the determination front (orange line), relative to the ongoing embryonic development and somitogenesis. At the same time the embryo grows caudally, producing new undetermined PSM (in blue), the determination front recedes caudally, and new determined PSM is generated (in orange). Adapted from Dubrulle and Pourquié, 2002.

However, this system does not give any information regarding the "age" of a given somite in a developing embryo, as each embryo comprises numerous somites of different "ages" (see Christ and Ordahl, 1995). Therefore, based on previous staging systems (see Christ and Ordahl, 1995), a comprehensive nomenclature system of somite development was devised (Pourquié and Tam, 2001, see Figure 5). The somite number, indicating its location respective to the embryos rostral end, is attributed in Arabic numerals. For example, in both mouse and chicken, somites 1 to 5 give rise to the occipital bone in the skull (Christ and Ordahl, 1995). On the other hand, the somites "age" since it was formed is represented as a somite stage in roman numerals, where the rostral end of the PSM, i.e. the forming somite, is termed somite 0 (zero, or S0 for short). Somites rostral to S0 are numbered in positive roman numerals; SI, SII, SIII (one, two, three) and so forth; while somite-length portions of PSM caudal to S0 are numbered in negative roman numerals; S-I, S-II, S-III (minus one, minus two, minus three) and so forth. As the PSM has no signs of overt segmentation, the somite-length portions are a somewhat subjective, but are unquestionably useful to describe the events in the PSM, mainly in the rostral PSM. For example, the determination front is

roughly located 4 to 5 somite lengths caudal to the PSMs rostral end, i.e. at the S-III to S-IV region in the PSM (3 to 4 prospective somites, plus the forming somite, S0) (Dubrulle et al., 2001).

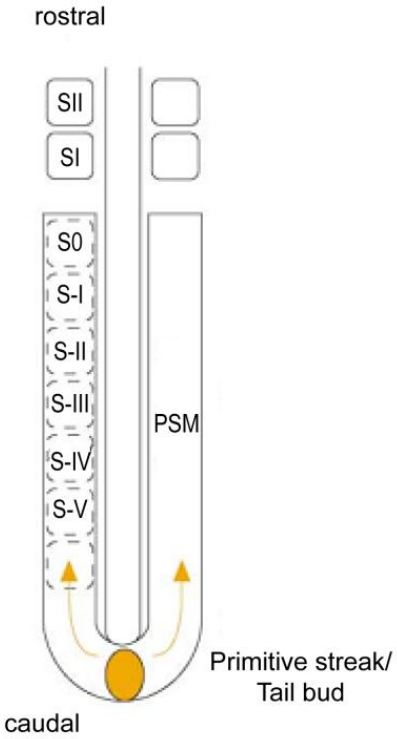

Figure 5. Somite staging nomenclature of the vertebrate embryo. Adapted from Pourquié and Tam, 2001.

1.4. Time and space

The segmentation of the vertebrate embryo occurs sequentially, one pair of somites after another pair. Thus, the temporal control of the formation of a new pair of somites impinges on the spatial organization of the somitic border, hence, the regularity of the metameric pattern. In other words, somitogenesis is an excellent example where tight temporal control is directly reflected on the spatial organization of the embryonic pattern.

1.4.1. Modeling somitogenesis periodicity

Somites are formed in a rhythmic pace, originating an orderly string of individualized segments along the embryonic axis. The pace of somite formation is

characteristic for a given species, at a given temperature: 90 minutes in the chicken, 120 minutes in the mouse (at 37ºC), and 20 minutes in zebra fish (at 25 º C). Although the first observations of somites in the chick embryo date back to the seventeenth century (see Wolpert, 2004), the mechanism that supports such a robust feature in vertebrate embryo were only envisioned by scientists in the last decades (see Lash and Ostrovsky, 1986).

Several mathematical models of somitogenesis were proposed in 1970's and 80's, but only two contained fundamental features that persisted with the advent of modern molecular biology (see Aulehla and Herrmann, 2004; Dale and Pourquié, 2000; Kulesa et al., 2007; Schnell and Maini, 2000). First, the "Clock and Wavefront" model proposed by (Cooke and Zeeman, 1976) postulates the existence of an intrinsic oscillatory mechanism (the clock) that gates cell behavior between two states, a receptive and a non-receptive state, and an interface between the mature and non-mature tissue that progresses along the rostro-caudal axis (the wavefront). As the travelling wavefront assigns the mature state to a cohort of PSM cells, the coordinated oscillation into the receptive state stamps them as a discrete unit, the prospective somite. Another model, suggested by (Meinhardt, 1982; Meinhardt, 1986) also proposes an internal oscillator, between an Anterior (A) and a Posterior (P) state, and the conjugation of the doublet AP consigns the somitic segment, separated from the neighboring doublet at the P-A interface. Although this model accounts for the establishment of the two somitic domains, which have been extensively demonstrated (see section 1.6, *Rostral vs Caudal*), it suffered from the lack of explanation on why the somite border was established at the P-A interface but not at the A-P interface within the somite, hence, forming half-somites. The proposed third intermediate state at the somite border solved this aspect of the model, though no biological equivalent of such a state has been described. A third model, the cell cycle model, based on numerous heat-shock experiments, still lingers on to the present day (Collier et al., 2000; Keynes and Stern, 1988; Primmett et al., 1989), but no new data has supported or clarified it further. Curiously, the refractory abnormalities observed after heat-shock treatments in amphibian (Cooke and Elsdale, 1980; Elsdale et al., 1976; Pearson and Elsdale, 1979) and chicken embryos (Primmett et al., 1988) were initially considered to favor the "Clock and Wavefront" model (Cooke, 1998; Cooke and Elsdale,

1980; Elsdale et al., 1976; Primmett et al., 1988). Studies on the mitotic activity along the PSM (Stern and Bellairs, 1984) and the uniqueness of the repeated abnormalities observed after a single heat-shock in the chicken embryo lead to the proposal of the cell cycle model (Keynes and Stern, 1988; Primmett et al., 1989). It must be noted that there is still no theory explaining these heat-shock observations, other than the cell-cycle model.

1.4.2. The segmentation clock

The molecular evidence for the oscillatory behavior in PSM cells was discovered a few decades after theoretical models postulated its existence (see Cooke, 1998). The basic helix-loop-helix (bHLH) transcriptional repressor *Hairy1*, the avian homolog of the *D. melanogaster* pair-rule gene *hairy*, was the first of the to-be-called cycling genes to be discovered, because of its oscillatory transcriptional behavior in chicken embryos (Palmeirim et al., 1997). The mRNA expression pattern of *Hairy1* in the PSM varied consistently throughout batches of stage-matched chicken embryos. This observation was interpreted as a dynamic, cyclic expression of *Hairy1*, reiterated every 90 minutes, concomitantly with the formation of a new pair of somites. Thus, the variety of expression patterns observed among same stage embryos consisted of “freeze-frames” of this oscillatory behavior along the PSM (Palmeirim et al., 1997, see Dale et al., 2003). The patterns could be grouped into three general topographic descriptions, or phases, repeated every 90 minutes: a broad domain encompassing the posterior two thirds of the PSM, a narrower band roughly in the middle of the PSM and a thin stripe located in the rostral PSM (see Figure 6). Further modeling of the observed patterns revealed that the intrinsic cellular oscillatory mechanism was slightly out-of-phase throughout the PSM, creating this wave of expression, apparently propagating from caudal to rostral, and finally settling as a stripe at the rostral PSM where the oscillation arrested (Palmeirim et al., 1997). This seminal set of observations sparked the discovery of numerous genes with oscillatory transcriptional behavior –the cycling genes - in all vertebrate model systems (see Andrade et al., 2007; Bessho and Kageyama, 2003; Rida et al., 2004). For example, it originated the discovery of cycling behavior of the *Lunatic fringe* (*Lfng*) gene (Aulehla and Johnson, 1999; Forsberg et al., 1998; McGrew et al., 1998), which was previously described to have a dynamic (but not identified as periodic)

expression pattern (Johnston et al., 1997). The list of cycling genes increased steadily (see Andrade et al., 2007), and recently an elegant microarray approach added a few hundred more to the list (Dequeant et al., 2006). In the meantime the wave of expression was visualized *in vivo*, through time-lapsed live imaging of transgenic mouse embryos expressing a fluorescent luciferase reporter driven by the promoter of the cycling gene *Hes1* (Masamizu et al., 2006).

Most of the reported cycling genes appear, however, to be outputs of the oscillatory mechanism rather than parts of the mechanism itself. Although the oscillatory patterns of expression seem to involve self-inhibitory feedback loops (Bessho et al., 2003; Dale et al., 2003; Hirata et al., 2002; Jen et al., 1999) and short-lived mRNA and proteins (Hirata et al., 2004; Hirata et al., 2002), the core pacemaker mechanism of the segmentation clock remains elusive (discussed in Dequeant and Pourquié, 2008; Giudicelli and Lewis, 2004; Ozbudak and Pourquié, 2008; Pourquié, 2011). Beyond the initially reported Notch-related cycling genes (reviewed in Giudicelli and Lewis, 2004; Kageyama et al., 2007; Rida et al., 2004), genes of the Wnt (Aulehla et al., 2003) and of the FGF family (Dequeant et al., 2006) also cycle, independently and out-of-phase of the Notch-related genes, adding complexity to the system. Moreover, synchronous somite

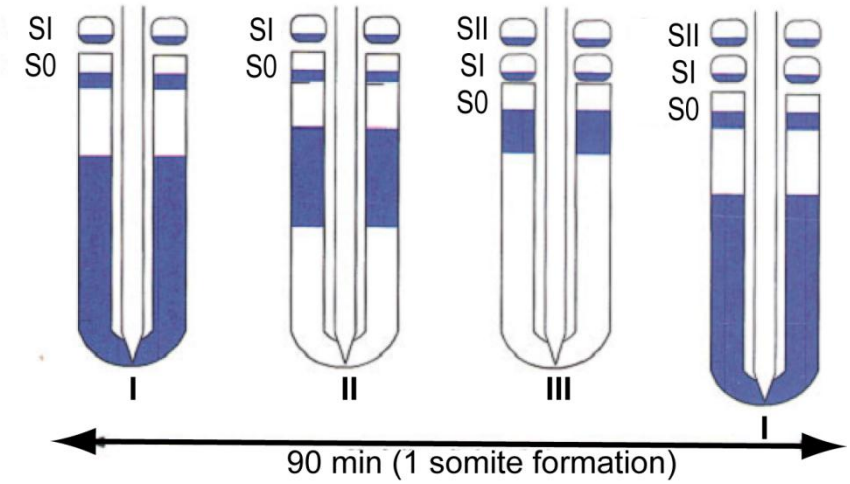

Figure 6. Representation of the dynamic expression pattern of the chicken *Hairy1* gene during somite formation. The wave of *Hairy1* expression sweeps through the PSM during one somite formation cycle, and repeats itself every 90 minutes long somite cycle. The various patterns of expression observed in individual, stage-matched embryos, can be catalogued into the 3 anatomical descriptions: **I**. broad caudal band, **II**. Wide band in the middle of the PSM, **III**. Short band at the rostral PSM. Adapted from Palmeirim et al., 1997.

formation on both sides of the neural tube is under the control of RA (Vermot et al., 2005; Vermot and Pourquié, 2005). Thus, no single gene, gene interactions or signaling pathway can account for all the oscillatory behavior (Ozbudak and Pourquié, 2008), and most likely the complex inter-cellular genetic network confers robustness and noise resistance to the system (Horikawa et al., 2006; Ishimatsu et al., 2007). Dramatically, although it is unquestionable that the segmentation clock and somite formation are linked, there is no experimental causal relation between the oscillatory behavior and the morphogenetic process (see Oates et al., 2012). Most of the cycling genes have unknown functions and many display redundancy. However, the Notch signaling pathway has been repeatedly implicated in both the synchronization of the clock in the caudal PSM and the establishment of the molecular segmentation of the rostral PSM.

1.4.3. Notch signaling and the outcome of the clock and wavefront

Notch signaling starts with the interaction of the Notch transmembrane receptor in one cell with the transmembrane ligand in the neighboring cell. As a consequence of this binding, the intra-cellular cleavage of the Notch protein is induced, releasing the Notch-intra-cellular-domain (NICD), which is translocated to the nucleus (see Borggrefe and Oswald, 2009; Bray, 2006, and Figure 7). The Notch signaling pathway became implicated in somitogenesis, as null-mutant mouse embryos for various elements of this pathway showed a somitic phenotype, such as: the receptor *Notch1* (Conlon et al., 1995); the ligands *Dll1* (Hrabě de Angelis et al., 1997) and *Dll3* (Kusumi et al., 1998); the Notch-cleaving molecule *Presenilin1* (*Psen1*, Wong et al., 1997); the Notch modulator *Lfng* (Evrard et al., 1998; Zhang and Gridley, 1998) or the Notch transcriptional partner *RBPjκ* (Oka et al., 1995). These disruptions of the Notch pathway lead to abnormal somitogenesis, with deregulated, unsynchronized or otherwise perturbed formation of somitic boundaries. Hence, these phenotypes evidenced that, rather than being responsible for the metameric pattern itself, Notch signaling is crucial to coordinate and synchronize somite formation. Interestingly, null-mutants for cycling genes downstream of Notch signaling, such as the *Hairy/Enhancer of Split* homologs *Her1* and *Her5*, but not *Her7* (Bessho et al., 2001), show no somitogenesis defects (Ishibashi et al., 1995; Ohtsuka et al., 1999) or alterations in other cycling genes (Jouve et al., 2000). Thus, it seems that the Notch signaling pathway ensures that whole cohorts of PSM cells

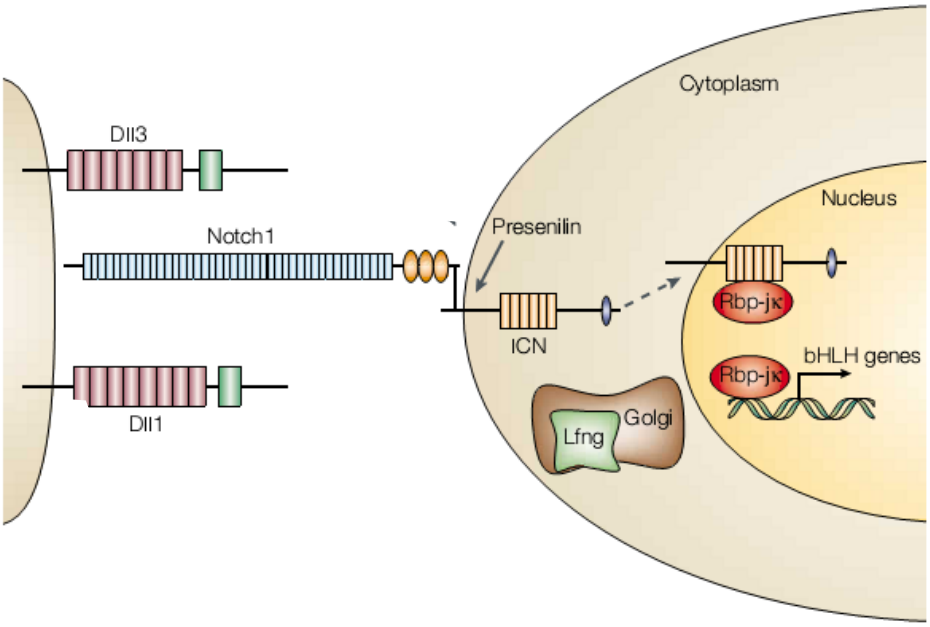

Figure 7. Simplified version of the Notch signaling pathway involved in somitogenesis. The interaction of Delta-like (Dll) ligand with the Notch receptor induces its intracellular cleavage by the presenilin-dependent γ-secretase enzymatic complex. The resulting Notch intracellular domain (ICN) is transported to the nucleus where it acts in conjunction with the *RBPjκ* co-factor as a transcription factor, upregulating target genes such as those of the bHLH family. The Lunatic fring (Lfng) glycosyltransferase acts in the Golgi complex as a Notch modifier, diminishing its activity. Adapted from Saga and Takeda, 2001

oscillate their Notch-downstream cycling genes synchronously. In fact, cyclic mRNA expression can be achieved in individual cells through serum treatment (Hirata et al., 2002), whereas dispersed PSM cells lose their synchronous oscillations, emphasizing the requirement of close cell-cell contact for synchronized waves of transcription in the PSM (Maroto et al., 2005). The importance of Notch signaling in the segmentation clock has also been reported and extensively studied in zebrafish embryos (Giudicelli et al., 2007; Holley and Takeda, 2002; Jiang et al., 2000; Ozbudak and Lewis, 2008; Rida et al., 2004).

Mathematical modeling shows that reciprocal Notch based activation/repression feedback loops between neighboring PSM cells support coherent oscillations at the tissue level (see Lewis et al., 2009). As noted above, the pacemaker mechanism seems far more complex, beyond the "simplicity" of reciprocal Notch signaling, since, for example, the oscillatory behavior of murine *Wnt*-related genes is Notch independent (Aulehla et al., 2003; Feller et al., 2008), and the FGF pathway may act upstream of Wnt and Notch to control the segmentation clock (Niwa et al., 2007; Wahl et al., 2007).

Nevertheless, Notch signaling, particularly the cleaved NICD, remain as a crucial output of the segmentation clock in mouse embryos (Huppert et al., 2005; Morimoto et al., 2005; Saga, 2007). Although *Notch1* mRNA expression extends throughout the PSM, the processed form of the NOTCH protein, NICD, which acts as a transcription factor in the nucleus, exhibits a dynamic pattern in the caudal PSM (Huppert et al., 2005; Morimoto et al., 2005). The oscillations of the cleaved NICD are dependent on the Notch ligand Dll1 and the Notch modifier Lfng (Morimoto et al., 2005; Takahashi et al., 2003), but how the oscillations are arrested into a defined band at the rostral PSM remains unknown. Nevertheless, it is known that Notch signaling controls the expression of *Mesp2* in a defined band in the rostral PSM (Takahashi et al., 2003; Takahashi et al., 2000).

Mesp2 (mesoderm posterior 2) is a bHLH transcription factor crucial for somitogenesis and is dynamically expressed at the S-I and/or at the S-II position in mouse (Saga et al., 1996; Saga et al., 1997), chicken (*cMeso1*, Buchberger et al., 1998), zebrafish (*mesp-a/b*, Sawada et al., 2000) and even at the S-III position in amphibian embryos (*Thylacine1*, Sparrow et al., 1998). Neither *Mesp2* knock-out mouse embryos, nor zebrafish embryos injected with *mesp-a/b* translation-blocking morpholinos have somites (Saga et al., 1997; Sawada et al., 2000, respectively). Through genetic analysis in mouse embryos and *in vitro* genetic screens, Tbx6 was identified as an essential promoter of *Mesp2* expression, and its effect is enhanced by Notch signaling (Yasuhiko et al., 2006; Yasuhiko et al., 2008). Since both *Tbx6* and Notch signaling are present throughout the PSM, it still unclear how *Mesp2* is restricted to the rostral PSM; in chicken embryos FGF signaling seems to repress *Mesp2* (Delfini et al., 2005) while in *Xenopus* RA, directly activates *Thylacine1*, the Mesp2 homolog (Moreno and Kintner, 2004). Regardless of this, in mouse embryos, Mesp2 promotes the expression of its own repressor *Ripply2* (Morimoto et al., 2007), and suppresses Notch signaling (Morimoto et al., 2005) thus confining *Mesp2* expression to a stripe underlining somite formation (Takahashi et al., 2007b, Figure 8).

How the *Mesp2* stripe first encompasses the whole prospective somite –II and then becomes restricted to the rostral portion of somite –I, remains a crucial, but unanswered question (see Saga, 2012). Nevertheless, the activation of *Mesp2* in the

rostral portion suppresses the expression of *Dll1* in the rostral somite half and *Dll1* expression becomes restricted to the caudal portion (Takahashi et al., 2000). This differential Notch signaling suppression/activation in the rostral/caudal somitic compartment is the cornerstone for the establishment of rostro-caudal polarity within the somitic compartment (Saga, 2007), as I will discuss in section 1.6, *Rostral vs. Caudal*. Moreover, visualization of fluorescently-tagged Mesp2 in mouse embryos showed that the anterior border of *Mesp2* expression at the S-I position reflects the prospective somitic border (Morimoto et al., 2005) as I will expand on in the next section, section 1.5, *Sausages into meatballs*.

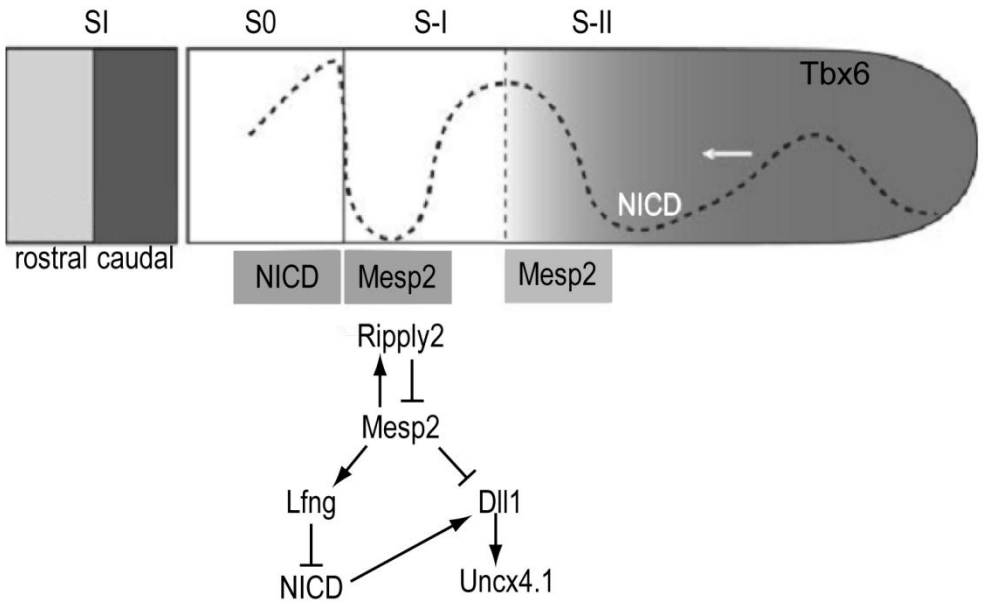

Figure 8. Present model for Mesp2 upregulation and the establishment of the rostro-caudal polarity during mouse embrogenesis. The oscillating waves of Notch signaling (interrupted wavy line of NICD) aid the *Tbx6*-dependent upregulation of *Mesp2* at the S-II position. Mesp2 expression at the rostral half of the presumptive S-I upregulates *Ripply2*, *Mesp2* own repressor, and *Lfng,* a negative modulator of Notch activity, and downregulates *Dll1* expression. As a result *Mesp2* is only transiently expressed and *Dll1* expression is restricted to the caudal somite half, where Notch signaling remains active. Adapted from Saga, 2007

1.5. "Sausages into meatballs"

The overt segmentation of the paraxial mesoderm into somites and their relation with the vertebral column has been a subject of investigation for the last 150 years, initiated by Remak and von Ebner (see Christ et al., 2000; Lash and Ostrovsky, 1986). The initial studies included detailed descriptions and exquisite drawings of somites, in whole views or sections of chicken embryos, such as those portrayed by (Williams, 1910).

1.5.1. Tissue interactions

Experimentation, mostly by extirpation of particular tissues, began in the second half of the twentieth century, with particular interest in the tissues that controlled or originated somite formation. The axial structures, notochord and neural tube, where extensively studied, in both avian and amphibian embryos, but the initial lack of a systematic approach between laboratories frequently generated conflicting results and opposing theories (see Bellairs, 1963; Lipton and Jacobson, 1974), for reviews see Christ et al., 2000; Gossler and Hrabě de Angelis, 1998; Pourquié, 2004). The systematization of the embryonic manipulation eventually reduced one by one the list of surrounding tissues essential for somite formation. The absence of the notochord or neural tube (Packard, 1980; Packard and Jacobson, 1976), the lateral plate mesoderm (Packard and Jacobson, 1976), the endoderm (Bellairs and Veini, 1980) and even of the formed somites and rostral PSM (Packard, 1978) did not influence somite formation (for a review, see Gossler and Hrabě de Angelis, 1998). Some doubt still remained regarding the overlying ectoderm and also the underlying endoderm (Packard and Jacobson, 1976) as the reposition of the ectodermal flap after microsurgical windowing of avian embryos improved somite formation (Packard et al., 1993). More recently, the importance of the ectoderm to support somite formation was clearly reinstated (Borycki et al., 2000; Borycki et al., 1998; Correia and Conlon, 2000; Palmeirim et al., 1998; Sosic et al., 1997), and a role for the endoderm was ruled out (Palmeirim et al., 1998).

The extensive microsurgical experimentations performed until the late 1990's clearly evidenced that PSMs isolated from all surrounding tissues did not form somites (Borycki et al., 2000; Borycki et al., 1998; Correia and Conlon, 2000; Lash and Ostrovsky, 1986; Lash et al., 1984; Lash and Yamada, 1986; Linker et al., 2003; Packard, 1980; Packard and Jacobson, 1976; Palmeirim et al., 1998). Interestingly, although unable to form somites, cultured isolated PSMs show a normal pattern of segmentally expressed genes (Borycki et al., 2000; Linker et al., 2003), notably *Dll1* and *Hairy1* (Palmeirim et al., 1998; Palmeirim et al., 1997) indicating that the segmentation clock is an intrinsic property of the PSM.

1.5.2. Adhesion model

Alongside tissue extirpations, experiments addressing the cellular properties of the paraxial mesoderm and other embryonic tissues were also performed. The initial work by Ruth Bellairs and colleagues (1978) tested the adhesiveness of the somites and PSM, but also other surrounding tissues, paving the way for the cell-adhesion model of somite formation (Bellairs et al., 1978). Scanning and transmission electron microscopy images of the loose PSM mesenchyme versus the densely packed somites further supported the hypothesis of increasing adhesiveness (Bellairs, 1979; Chernoff, 1985; Lipton and Jacobson, 1974). Further testing of the adhesiveness of somitic cells soon followed (Bellairs et al., 1981; Bellairs et al., 1980; Cheney and Lash, 1984; Sanders et al., 1986), and a fibrous material in the intercellular space was discovered (Bellairs, 1979; Lipton and Jacobson, 1974). This extracellular material was localized around the paraxial mesoderm (Duband et al., 1987; Kosher and Solursh, 1989; Ostrovsky et al., 1983; Solursh et al., 1979; Thiery et al., 1982). Additional testing on the components of the extracellular materials further contributed to relating the cell adhesiveness to this material (Bellairs and Veini, 1980; Lash et al., 1987; Lash et al., 1984), the increase in cell-cell adhesion between cells (Bellairs et al., 1978; Cheney and Lash, 1984; Duband et al., 1987) and the formation of somites. Thus, although other mechanisms were recognized to be involved in somitogenesis, it was hypothesized that somite formation culminates from an increase in cell adhesiveness throughout the PSM (Lash and Ostrovsky, 1986; Tam and Trainor, 1994).

Despite the contemporary surge in the interest in and knowledge about these extracellularly deposited proteins and their role in influencing cell behavior (Ruoslahti, 2003, see ahead), the adhesion model was soon overrun by the genetic and molecular studies on somitogenesis. An avalanche of data from knock-out mice with somitic defects, some of which are mentioned above, shifted the interest in somitogenesis away from the particularities of the cells, their behavior and their interactions with each other and their surroundings. Moreover, neither the alterations in the adhesive properties of the paraxial cells nor the adhesion model could incorporate or explain the new genetic observations. Inactivation of a few genes encoding adhesion-related molecules confirmed the proposed importance of cell-cell adhesion and the surrounding

extracellular material in somitogenesis (e.g. (George et al., 1993; Radice et al., 1997; Yang et al., 1993), but again fell short in contributing or integrating the framework which was being raised around the role of transcription factors and small paracrine factors. I will focus on the extracellular material and how it affects somitogenesis in sections 2, *Extracellular Environment* and 3, *ECM and embryogenesis*.

1.5.3. Somitogenesis from a cellular standpoint

In the aftermath of the intense focus on the regulation of gene expression patterns in the context of embryo development, interest in the cellular aspects of embryonic morphogenesis reemerged (see Solnica-Krezel and Eaton, 2003). Soon, somitogenesis was scrutinized within a cellular framework, and the first live imaging analysis of somite formation was produced, using the almost transparent zebrafish embryo (Wood and Thorogood, 1994). The zebrafish embryo, with its advantages and recent systematization of developmental stages (Kimmel et al., 1995), provided several cues of the mechanisms of somitogenesis at a cellular level. Cell movements during the formation of the somitic clefts could be observed and analyzed in several different mutant lines (Henry et al., 2000). These movies revealed a complex orchestration into segregated populations of cells constituting somites (Henry et al., 2000). Nevertheless, the intricacy observed during the formation of the zebrafish somite, composed of a few, large cells, was nothing short of what was observed for an amniote embryo. The live imaging of fluorescently labeled chicken embryos, revealed extensive displacements of PSM cells during their aggregation into a somite (Kulesa and Fraser, 2002). These “simple” time-lapsed movies, focused on a single plane, showed that the establishment of the gap between the newly formed somite and the remaining PSM involved exquisitely choreographed movements of cells including cell displacements across the presumptive somitic boundaries (Kulesa and Fraser, 2002). Thus, the formation of the somitic boundaries was revealed to be much more complex than the simple orthogonal slicing of the cylindrical PSM, detaching the spheroid somite. The range of these movements was in accordance with what was previously reported (Stern et al., 1988) but violated the well-ordered striped expression of genes (such as the cycling genes) in the rostral PSM, which hypothetically underlies somitogenesis (Iulianella et al., 2003; Kulesa and Fraser, 2002). Notably, the limits of *EphA4* expression were crossed,

indicating that the orchestration of cell behavior into a somite must involve rapid local changes in gene expression (Iulianella et al., 2003; Kulesa and Fraser, 2002).

Eph proteins are a family of tyrosine kinase transmembrane receptors which bind to ephrin ligands on neighboring cells. They play a role in cell sorting during the segmentation of the cranial neural tube (Cooke and Moens, 2002; Holder and Klein, 1999; Xu et al., 1999) and numerous other cellular events (see Pasquale, 2005; Pasquale, 2008; Pasquale, 2010). Out of the dozens of Eph and ephrins described, the expression of *EphA4* and *ephrinB2* as a stripe in the rostral PSM and somites in both mouse (Bergemann et al., 1995; Nieto et al., 1992) and chicken embryos (Baker and Antin, 2003; Irving et al., 1996), made them putative players is somite formation. However, the deletion of either gene resulted in unscathed somite formation (Adams et al., 1999; Dottori et al., 1998; Helmbacher et al., 2000; Wang et al., 1998).

In zebrafish, the injection of mRNA for dominant negative forms of *EphA4* into wild-type embryos disrupted somite formation (Durbin et al., 1998). On the other hand, injecting *EphA4* over-expressing cells into *fused somites* mutant embryos, which lack somites (*fss*, van Eeden et al., 1996) generated ectopic boundaries at the interface with the host paraxial mesoderm cells (Barrios et al., 2003; Durbin et al., 2000). Unfortunately, the gene targeted in the *fss* mutant was identified as *Tbx24*, a T-box transcription factor involved in PSM maturation with no homology in mammals, birds or amphibians (Nikaido et al., 2002). Although *EphA4* appears to be a direct target for *Mesp2* (Nakajima et al., 2006), the complexity of the extensive bidirectional signaling involved, and the functional redundancy between the numerous Eph-ephrin proteins, have undermined any attempts to clarify their role in somitogenesis so far.

1.5.4. The Paraxis *gene*

Out of the numerous mutants with disrupted somitogenesis, *Paraxis*-null mouse embryos (Burgess et al., 1996) depicted a defect in the epithelialization of somites, and the demarcation of the somite boundaries. This phenotype is clearly different from those of the Notch-related mutants referred to above, which have perturbations in the coordination of segmentation. *Paraxis* (*Tcf15*) is a bHLH gene expressed in somites and

in the rostral PSM (S0 to S –III), in mouse (Burgess et al., 1995), chicken (Barnes et al., 1997), zebrafish (Shanmugalingam and Wilson, 1998) and *Xenopus* (Carpio et al., 2004; Tseng and Jamrich, 2004). Mouse mutants have no somites, as no epithelial blocks of cells are visible in the paraxial mesoderm, though the intersomitic clefts were still perceptible (Burgess et al., 1996). The absence of *Paraxis* does not influence the expression of Notch-related genes or the somitic differentiation program, but rostro-caudal somite polarity was diffuse (Burgess et al., 1996; Johnson et al., 2001). Thus, *Paraxis* seemed particularly involved in endowing the epithelial character to the paraxial mesoderm cells, necessary for their neat rearrangement into an individualized segment (Burgess et al., 1996; Johnson et al., 2001). Hence, *Paraxis* in somites was proposed to control the formation of the characteristic columnar epithelium of somites, identified decades earlier through transmission electron microscopy in chicken embryos (see Bellairs, 1979; Christ et al., 2004; Christ et al., 2000; Solursh et al., 1979; Tajbakhsh and Sporle, 1998). As a consequence of the analysis of the *Paraxis* mutant, the epithelialization of the rostral PMS, observed much earlier (Duband et al., 1987) was foreshadowed as a crucial reinforcement step of the segmentation program, characteristic of the determined PSM, i.e. rostral to the determination front (Dubrulle and Pourquié, 2004b; Pourquié, 2003). Unfortunately, no epithelium-related targets of the *Paraxis* transcription factor have been identified to date.

1.6. Rostral vs. caudal

The generation of the regular array of the nerves of the peripheral nervous system, emanating from the spinal cord, is not intrinsic to the developing neural tube, but is imposed by the adjacent somites (Keynes and Stern, 1988). Both sensory and motor neurons, emerging from the neural tube, invade the ventral portion of the somite, called sclerotome (see section 1.7, *Differentiation of somites*), but only migrate through the rostral half, avoiding the caudal half (Keynes and Stern, 1984; Keynes et al., 1987). The establishment of the rostral/caudal compartments occurs before overt segmentation because PSM portions, rotated 180º and then grafted into recipient embryos impose their original rostro-caudal polarity on the peripheral nervous system (Aoyama and Asamoto, 1988; Keynes and Stern, 1984). In addition to the evidence

provided by tissue grafting, identification of genes which are differentially expressed in the prospective rostral and caudal regions of the somite robustly support the existence of the two compartments. The spinal ganglia defects observed in the *Dll1* mutant embryo (Hrabě de Angelis et al., 1997), clearly pointed to the Notch pathway as a critical player. The expression pattern of *Dll1* is also a particularly good *bona fide* indicator of rostro-caudal somite polarity, as the continuous expression along the PSM becomes restricted to the caudal somite half in S0 (Bettenhausen et al., 1995; Henrique et al., 1995; Palmeirim et al., 1998). In agreement with the early grafting experiments, the establishment of *Dll1* expression solely in the caudal half occurs before overt segmentation of the PSM (Dubrulle et al., 2001; Palmeirim et al., 1998), though there is some dispute about whether the formation of the intersomitic border can readjust the pre-established polarity (Sato et al., 2002).

Restriction of *Dll1* expression to the caudal half is induced by *Mesp2*, since *Mesp2*-null mutants show caudalized somites with even expression of *Dll1* (Saga et al., 1997; Takahashi et al., 2000). An unknown mechanism restricts *Mesp2* expression to the rostral half at the somite –I level, which represses *Dll1* in this somitic domain (Takahashi et al., 2000). *Mesp2* also induces the expression of *Lfng*, the Notch signaling modulator, which further inhibits Notch signaling (Morimoto et al., 2005), and consequently reinforces *Dll1* repression in this domain. Interestingly, whereas activation of *Dll1* expression in the PSM is *Psen1*-independent, the maintenance of *Dll1* expression in the somite's caudal half requires a *Psen1*-dependent Notch signal (Takahashi et al., 2000). In the caudal half, the activation of *Dll1*, and consequently, Notch signaling, is the stepping-stone for the caudal identity, marked by the expression of downstream target genes such as *Uncx4.1* (Feller et al., 2008; Takahashi et al., 2003; Takahashi et al., 2000; see Figure 8). *Uncx4.1* is a paired homeobox gene expressed in the caudal half of mouse (Mansouri et al., 1997) and avian somites (Schragle et al., 2004) and is required for the specification of the pedicles and proximal ribs (Leitges et al., 2000; Mansouri et al., 2000). On the other hand, in the rostral half, the total repression of Notch signaling by *Mesp2*, not only downregulates *Dll1*, but allows for the upregulation of rostral specific genes, such as *Tbx18* (Feller et al., 2008). *Tbx18*, a member of the T-box transcription factor family, is expressed as two stripes in the rostral PSM, and in the rostral half of

somites in mouse (Kraus et al., 2001) and chicken embryos (Haenig and Kispert, 2004; Tanaka and Tickle, 2004). Neither *Uncx4.1* nor *Tbx18* are involved in establishing the somitic polarity, but rather participate in specifying the characteristics of their respective half (Bussen et al., 2004; Leitges et al., 2000; Mansouri et al., 2000). Interestingly, in the chick embryo, somitic *Tbx18* expression is restricted to the first two somites and appears to have a role in the maintenance of the somitic border (Tanaka and Tickle, 2004). Once the rostro-caudal polarity is established, other determinants reinforce the two distinct moieties which together create the correct environment for the segmented guidance of neural projections (see Kuan et al., 2004) and Figure 9).

1.7. Differentiation of somites

Only a few hours after the formation of the epithelial somite, it undergoes the first compartmentalization, representing the first divergence between distinct paraxial mesoderm fates. However, even before the overt segmentation of the PSM, a few genes are expressed in anticipation of the differentiation programs ahead. *Pax3*, a member of

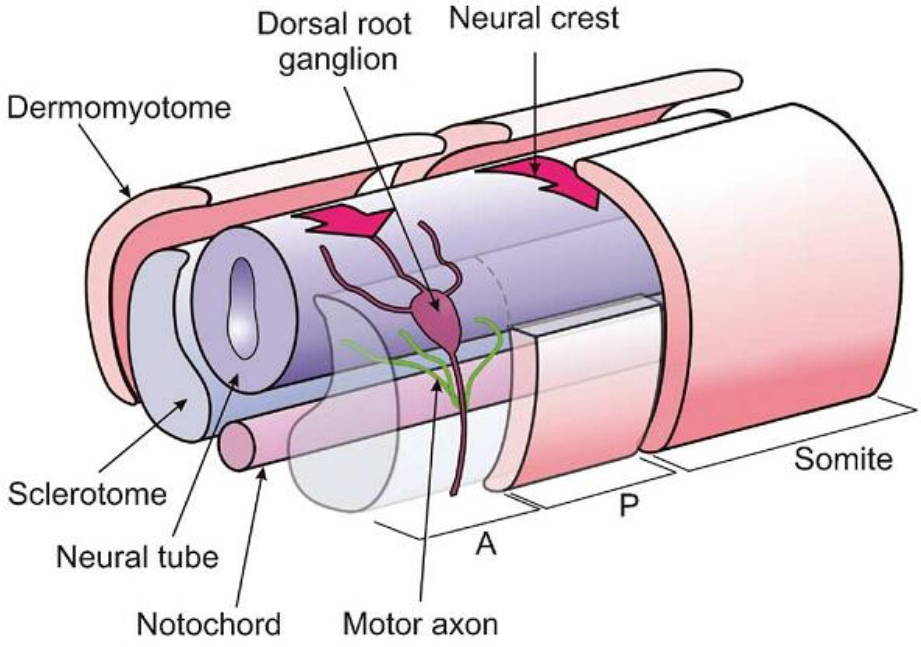

Figure 9. Representation of spinal nerve segmentation imposed by the somitic rostro-caudal polarity. The neural extensions arising from the neural tube, that will originate the peripheral nervous system, migrate through the rostral portion of the sclerotomal space. Note that the rostral or anterior (A) and caudal or posterior (P) moieties of the somitic segment are visible in the sclerotome and not in the dermomyotome. The dermomyotome closer to the viewer was partially excluded for clarity From Kuan et al., 2004.

the Paired box family (Pax) transcription factors, is expressed during the early development of mouse and chicken embryos (Goulding et al., 1994; Goulding et al., 1991; Goulding et al., 1993). *Pax3* is expressed in the rostral PSM in both mouse (Goulding et al., 1991; Horikawa et al., 1999) and chicken embryos (Otto et al., 2006; Schubert et al., 2001). In combination with *Pax7*, which is expressed slightly later in epithelial somites in the mouse, *Pax3* regulates the commitment of paraxial mesoderm cells towards a myogenic fate (see Buckingham, 2006; Buckingham and Relaix, 2007). Additionally, the expression of *Paraxis* in the rostral PSM and somites also contributes to the development of the somitic derivatives (see above). Unlike the situation during somite formation, where gene expression seems rather intrinsic to the PSM, with the maturation process, the somite becomes susceptible to the influence of the surrounding tissues, which act as sources of paracrine signaling molecules (Bothe et al., 2007), see below).

The epithelial somite remains a sphere for a few hours, until the two main compartments become evident: the dorsal portion maintains the epithelial form, originating the dermomyotome, while the ventral portion disaggregates, and, together

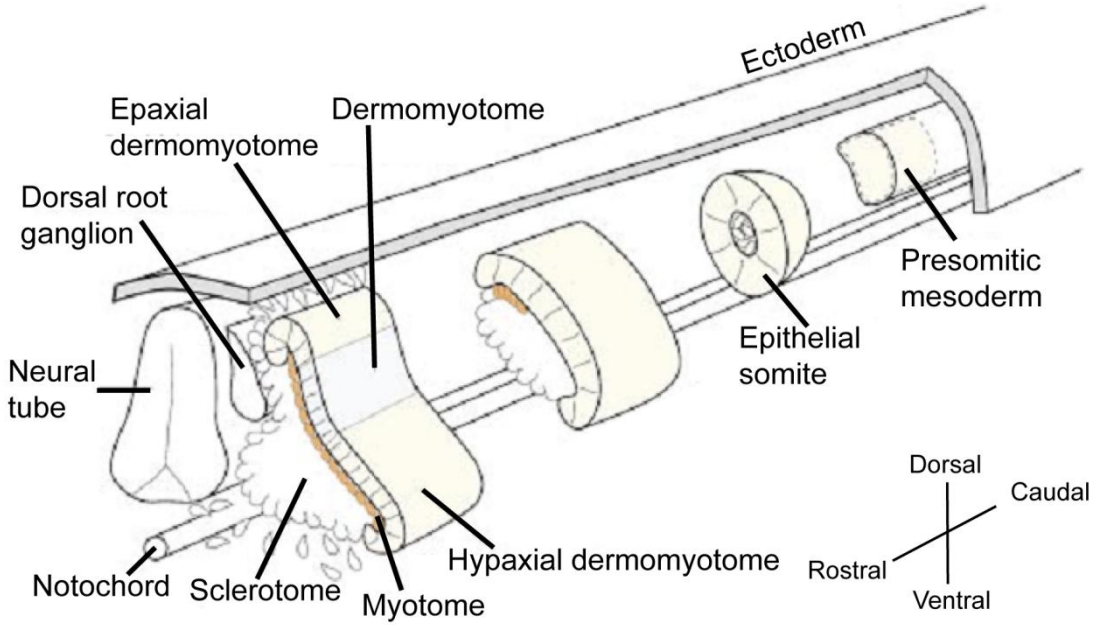

Figure 10. Schematic representation of paraxial mesoderm development. The "sausage-shape" presomitic mesoderm segments into epithelial somite spheres. In the initial stages of differentiation, the somitic segment portrays the sclerotome, the hypaxial and epaxial dermomyotome and the first myogenic tissue, the myotome. Adapted from Buckingham et al., 2003.

with the mesenchymal somitocoel, forms the sclerotome (see Brand-Saberi et al., 1996; Christ et al., 2007; Hirsinger et al., 2000; Stockdale et al., 2000), and Figure 10). As the embryo grows, it closes ventrally which imposes an increased body curvature, the whole somitic segment rotates and extends more ventrally; the dermomyotome spreads laterally, while the sclerotome maintains its proximity to the medial structures (see Brand-Saberi et al., 1996; Stockdale et al., 2000). In this section, I will focus on these two compartments, one of which will originate the cartilage and bone of the axial skeleton and ribs (the sclerotome), and the other gives rise to the dermis in the back and all the skeletal muscles in the trunk and limbs (dermomyotome) (Brent and Tabin, 2002; Christ et al., 2007; Stockdale et al., 2000).

1.7.1. Axial specification and patterning of the somitic fate

The linear array of somites extending along the embryonic rostro-caudal axis implies that their derivatives will acquire distinct anatomical configurations along the vertebrate body, e.g. the sclerotomal derivatives will give rise to the distinct cervical, thoracic, lumbar, sacral and caudal vertebrae. Remarkably, somite cells are endowed with their axial specification, i.e. their position along the rostro-caudal axis, prior to somite compartmentalization. Numerous paraxial mesoderm transplantation experiments in avian embryos showed that this positional information is acquired very early (reviewed in Gossler and Hrabě de Angelis, 1998; Stockdale et al., 2000). For example, somites or PSM portions from a prospective thoracic region grafted to a cervical level, give rise to rib-containing vertebrae, characteristic of their original location (Kieny et al., 1972). Remarkably, this early axial patterning does not apply to the myogenic descendants of the PSM, which adequate their morphology and innervation according to their new location (Chevallier et al., 1977; Keynes et al., 1987).

The molecular control of the axial positioning is achieved by the collinear activation of the genes encoding the Hox transcription factors (see Mallo et al., 2010; Wellik, 2009 for reviews). The positional information provided by the Hox code is exerted in the PSM, although the translation into an axial position only occurs later in the somites (Carapuço et al., 2005; Mallo et al., 2009). There have also been indications that the transcription of the *Hox* genes is linked to somitogenesis (Dubrulle et al., 2001;

Zakany et al., 2001). Interestingly, a provocative report indicates that the axial positioning may occur even earlier, during gastrulation, as the ingression itself is controlled by the expression of the *Hox* gene axial code (Iimura and Pourquié, 2006). Since the 1970s, an enormous wealth of information has been gathered on the collinear activation of *Hox* genes, their axial expression and consequent translation into positional information (see Kmita and Duboule, 2003), though a complete comprehension of the mechanisms involved are still under intense debate and scrutiny (see Alexander et al., 2009; Aulehla and Pourquié, 2009; Aulehla and Pourquié, 2010; Durston et al., 2010; Iimura and Pourquié, 2007; Mallo et al., 2010; Soshnikova and Duboule, 2009).

In addition to their axial specification, each somite is individually patterned in all the three anatomical axes. Unlike the rostro-caudal patterning, established prior to overt segmentation (discussed in section 1.6, *Rostral vs. caudal*), the patterning along the dorso-ventral and the medio-lateral axes, is achieved only after somites are formed (Aoyama and Asamoto, 1988; Dietrich et al., 1997). The medio-lateral patterning establishes the epaxial and hypaxial territories, which encompass both the dermomyotome and sclerotome (Brand-Saberi et al., 1996, Figure 10, see below). However, it is the dorso-ventral patterning that imposes the most visible alteration, resulting in the formation of the first two somitic compartments, the dermomyotome and the sclerotome. These initial compartments result from a “tug-of war” between the influence of dorsalizing and ventralizing cues. Further compartmentalization and differentiation involves a complex interaction of several players of at least three signaling pathways which are activated by paracrine factors released from the surrounding tissues (see Bothe et al., 2007; Christ et al., 2007; Yusuf and Brand-Saberi, 2006). Wnt signaling proteins are secreted by the ectoderm and dorsal neural tube, BMP cues emanate from the lateral plate mesoderm and the neural roof plate, while Sonic hedgehog protein is produced by the notochord and the floor plate of the neural tube. In general, signals from notochord and floor plate induce somite ventralization and promote the ventral cell fates, while the neural roof plate and the ectoderm provide dorsalizing signals (Hirsinger et al., 2000).

1.7.2. The sclerotome

In a striking contrast with the preceding spherical epithelial somite, the sclerotome presents itself as a dispersed mass of cells on the ventral side of each segment. Cells from the ventral somite lose their strong cell-cell contacts and the intercellular space increases (Duband et al., 1987; Solursh et al., 1979) as in an EMT. The signal that initiates cell dispersal remains unclear, since cell dispersal occurs in the absence of the axial structures, but can be imposed on the dorsal somite compartment with ectopic notochord grafts (see Christ et al., 2007). *Pax1* is an essential gene for the development of the axial skeleton (Wallin et al., 1994), and is already expressed in somite II (Deutsch et al., 1988; Ebensperger et al., 1995), indicating that cell dispersal is not essential for sclerotome development. The combination of *Pax1* and *Pax9*, another sclerotome specific gene expressed slightly later, is essential for the formation of the future vertebrae (Peters et al., 1999). Sonic hedgehog secreted from the notochord and floor plate and *Noggin* from the notochord are involved not only in the activation of *Pax1* gene, but also in the subsequent chondrogenic and osteogenic sclerotomal programs (see Brand-Saberi et al., 1996; Christ et al., 2004; Monsoro-Burq, 2005). The BMP-inhibitor *Noggin* and Hedgehog signals, as well as BMP4 from the lateral plate mesoderm participate in the further compartmentalization of the sclerotome into several subdomains (reviewed in Christ et al., 2004; Monsoro-Burq, 2005).

Particularly, the sclerotome (but not the dermomyotome) undergoes an important physical partition in the rostro-caudal axis. This process was observed in the nineteenth century by Remak and von Ebner (see Christ et al., 2004; Christ et al., 2007; Christ et al., 2000; Christ et al., 1998 for an historic perspective). Fate-mapping experiments grafting a quail somite into a chick embryo host showed that the descendants of a single quail somite encompassed both the rostral half of a vertebra and the caudal half of the immediately preceding vertebra (Bagnall et al., 1988; Huang et al., 2000). The physical division of the sclerotome in an anterior and posterior compartment is a hallmark event for vertebrae formation in amniotes, and is a consequence of the rostro-caudal somite polarity established earlier (Saga and Takeda, 2001, see Figure 11). Accordingly, null mutants for either *Uncx4.1* or *Tbx18*, markers for the caudal or rostral somite half, respectively, show defects in elements on the rostral or caudal portion of the vertebrae,

respectively (Bussen et al., 2004; Leitges et al., 2000; Mansouri et al., 2000). The final physical separation of the two somitic moieties can be foreseen during sclerotome maturation, when, among other observable sub-domains, the caudal and rostral compartments are separated by the von Ebner fissure (see Christ et al., 2004). Other compartments, such as the syndetome, from which tendons arise (Brent et al., 2003) or the arthrotome, which contributes to the intervertebral discs (see Christ et al., 2004) are also visible during sclerotome maturation.

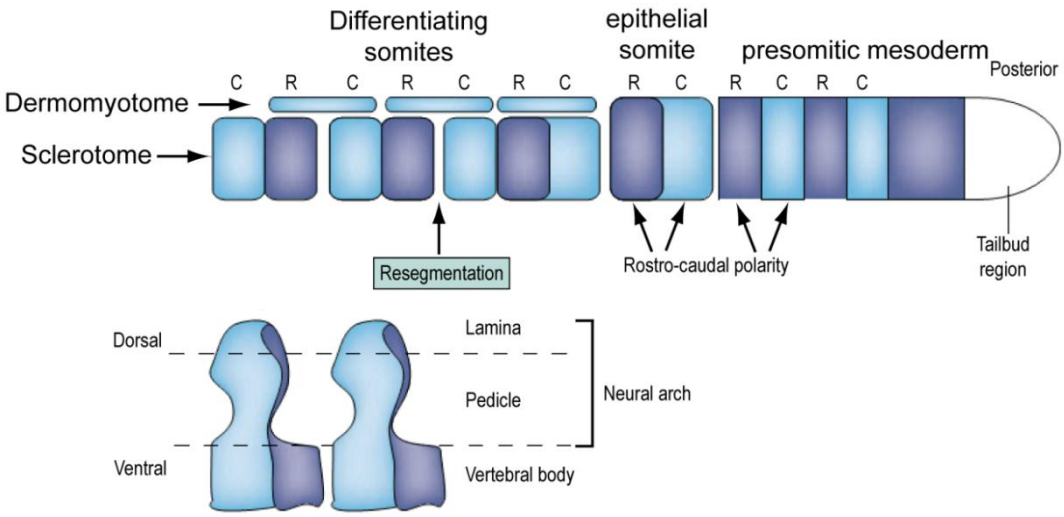

Figure 11. Illustration summarizing the rostro-caudal segmentation and resegmentation of the paraxial mesoderm in the mouse embryo, on top. Caudal to the right. Below: Representation of the final location of the somitic rostral and caudal portions in the resulting vertebral body. Adapted from Saga and Takeda, 2001.

1.7.3. The dermomyotome

The regionalization of the epithelial dermomyotome is primarily achieved through a canonical Wnt signal emanating from the overlying ectoderm, which drives the expression of *Paraxis*, preserving the epithelial character of the dermomyotome (Linker et al., 2005). In parallel with the ectoderm, the neural roof plate also provides a dorsalizing signal and only the ablation of both tissues abolishes the expression of *Pax3*, the dermomyotomal marker (Dietrich et al., 1997). Cell proliferation in the dermomyotome leads to its lateral expansion, adopting an elongated rectangular form, like a sheet lining the interior of the ectoderm. At each of the four margins, dermyomotomal cells extend towards the sclerotome, forming lip-like structures which originate the first myogenic precursor cells which give rise to the myotome, the first

differentiated skeletal muscle tissue. The myotome, which becomes located just beneath the dermomyotome, is unequivocally of dermomyotomal origin, although there is still some debate about the exact mechanism of its formation (Brent and Tabin, 2002; Buckingham and Relaix, 2007; Scaal and Christ, 2004). Later in development, the cells of the central part of the dermomyotome undergo an asymmetrical division, the basal cell originating the precursors for the dermis in the back, while apical cells invade the myotome as myogenic progenitor cells which participate in muscle growth (Ben-Yair and Kalcheim, 2005; Gros et al., 2005; Kassar-Duchossoy et al., 2005; Relaix et al., 2005). This population of myogenic precursors expresses *Pax3* and *Pax7*, and they contribute to myogenesis not only throughout embryonic development, but also in post-natal myogenesis and muscle regeneration (Buckingham and Relaix, 2007).

2. The Extracellular Environment

In multicellular organisms, cells are seldom isolated, suspended in a fluid. Rather, cells adhere to their surrounding extracellular environment, either to other cells via cell-cell adhesion molecules or to the non-cellular components of the extracellular space, the extracellular matrix (ECM), through membrane-bound ECM receptors. The ECM components can be divided into proteoglycans (with major polysaccharide composition and a minor protein core) and fibrous proteins (many of which are glycosylated). Proteoglycans are mostly found in the intercellular space, such as the large Hyalectans (e.g. versican), but also associated to the cell membrane, such as syndecan (Schaefer and Schaefer, 2010). The fibrous ECM components include, among others, collagens, fibronectin, laminins and tenascins. In this section I will focus on the ECM, giving emphasis to two major constituents, fibronectin and laminin, which closely interact with cells both during development and in adult tissues. I will also briefly address other ECM constituents, the ECM receptors (section 2.4, *Integrins*), and the molecules involved in

cell-cell adhesion. The information regarding the functions and properties of these molecules has been overwhelmingly obtained through studies of cultured cells, which will be reflected on the contents of this chapter. I will refer to *in vivo* observations sporadically, and address in more detail the main molecules in an *in vivo*, embryological context in section 3, *Extracellular matrix and embryonic development*.

2.1. Fibronectin

Fibronectin is a multifunctional ECM glycoprotein, initially reported as a cell surface protein on cultured fibroblast cells, and later also identified as soluble constituent of circulating plasma (see Hynes, 1981; Ruoslahti, 1988; Ruoslahti, 2003). Fibronectin is a ubiquitous component of the ECM in vertebrates, forming a fibrillar matrix which associates with cells in several tissues. Fibronectin proteins fall into two major groups according to their solubility: the relatively insoluble cellular fibronectin in tissues and the soluble plasma fibronectin. Nevertheless, around 20 variants of human fibronectin have been reported, due to alternative splicing of the single fibronectin gene (see ffrench-Constant, 1995). Interestingly, matching the various alternative splice variants to the numerous roles of fibronectin has not been successful (ffrench-Constant, 1995; Singh et al., 2010). Despite several decades of intensive research (mostly in *in vitro* systems) since its discovery, (Hynes, 1985; Mao and Schwarzbauer, 2005a; McDonald et al., 1987; Pankov and Yamada, 2002; Ruoslahti, 1988; Singh et al., 2010; Wierzbicka-Patynowski and Schwarzbauer, 2003; Yamada and Olden, 1978), many intricacies of the biological role of fibronectin remain elusive, particularly in an *in vivo* context.

2.1.1. Fibronectin structure

Fibronectin is modular polypeptide composed of three different types of repeating modules; type I, type II and type III. Although all three types of fibronectin repeats have been reported in other proteins, their combination into a single fibronectin gene (*Fn1*) seems to be a vertebrate novelty (Hynes and Zhao, 2000). Fibronectin is secreted as a large dimeric glycoprotein, with each subunit ranging in size between 230 and 270kDa. Each subunit is composed of a string of 12 type I repeats, 2 type II repeats and 15-17 type III repeats, depending on the splicing alternative (Hynes, 1985; Pankov and Yamada,

2002; Potts and Campbell, 1994; Singh et al., 2010, see Figure 12). The two subunits are bound to each other at their carboxyl-terminal end by two disulfide bonds essential for the multimerization of fibronectin molecules (Schwarzbauer, 1991). Two type III fibronectin repeats, termed EIIIA and EIIIB, can be either included or skipped by alternative splicing, generating fibronectin variants of unclear function. A third region of alternative splicing, termed V region, can be either included, totally or partially, or even completely excluded during alternative splicing. The V region has been implicated in fibronectin dimer secretion and cell adhesion through specific cell receptors (Hynes, 1985; Schwarzbauer and DeSimone, 2011; Singh et al., 2010, see section 2.3.4., *Integrins-Fibronectin interactions*).

While the sequence of fibronectin repeats was being elucidated, extensive studies using proteolytic cleavage of the fibronectin molecule into numerous portions, revealed several domains of interaction with other molecules. Treatment with specific proteases isolated unique protease-resistant domains in the fibronectin molecule, which are either specific to particular repeats or span through several different types of repeats (Hynes and Yamada, 1982; Singh et al., 2010, Figure 12). Binding assays using these fibronectin domains showed that fibronectin can bind to itself at several locations, and also binds to other to ECM molecules such, as collagens, tenascin, heparin or fibrin (Hynes and Yamada, 1982; Ruoslahti, 1988; Singh et al., 2010). This approach also revealed that fibronectin has several attachment sites for cell surface receptors (discussed in section 2.4., *Integrins*). An extensive list of functional domains, proteolytic cleavage sites and binding interactions has been described elsewhere (Figure 13, Pankov and Yamada, 2002). I will focus on the amino-terminal 70kDa fragment containing a fibronectin-fibronectin binding site, and the RGD (Arg-Gly-Asp) sequence located in the central cell binding domain of fibronectin.

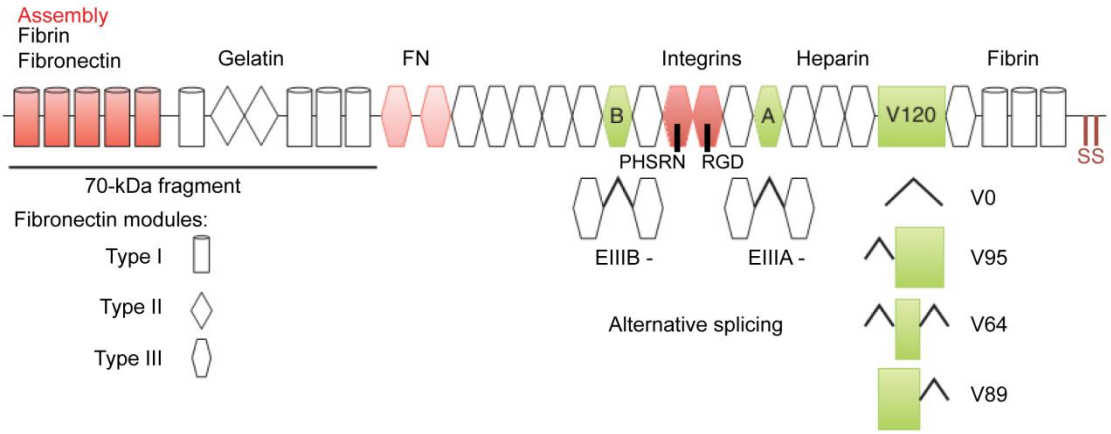

Figure 12. Structure of the fibronectin monomer. The modular organization of the fibronectin molecule (lower left), the main interaction sites (on top) and the alternative splicing isoforms (lower right). The main fibronectin-fibronectin interaction site, essential for fibronectin matrix assembly is located on the amino terminal end, towards the left. The carboxy-terminal end, on the right, contains two disulfide bonds that link to another fibronectin molecule, forming the fibronectin dimer. Cells adhere to fibronectin through their integrin receptors, mainly interacting with the 9th and 10th type III fibronectin module (red hexagons). These modules contain the synergy site (PHSRN) and the RGD sequence, respectively, which compose the critical binding site for the canonical integrin receptor. Adapted from Schwarzbauer and DeSimone, 2011.

2.1.2. The 70kDa N-terminal fibronectin assembly domain

There are several fibronectin-fibronectin binding sites throughout the fibronectin polypeptide, but only the one present in the amino-terminal 70 kDa portion is essential for the assembly of a fibrillar fibronectin matrix (Schwarzbauer, 1991, see Figure 12). The remaining fibronectin interaction sites are dispensable for the initiation of fibronectin matrix assembly, although they all interact with the amino-terminal fibronectin binding site (Singh et al., 2010). These other fibronectin interaction domains, composed of type III repeats, have a more regulatory role in fibronectin assembly, involving the exposure of specific cryptic sites, but despite their extensive study in recent years, their precise biological function(s) remain(s) unclear (see Mao and Schwarzbauer, 2005a; Singh et al., 2010; Wierzbicka-Patynowski and Schwarzbauer, 2003).

The 70kDa amino-terminal fragment binds to cells at the fibronectin matrix assembly initiation sites (McKeown-Longo and Mosher, 1985) and both the excess presence of this fragment (McKeown-Longo and Mosher, 1985) and antibodies against

this region (McDonald et al., 1987) abolish fibronectin matrix assembly. Moreover, cells expressing recombinant fibronectin lacking this region are unable to assemble fibronectin fibrils (Schwarzbauer, 1991). This fibronectin binding site was further narrowed down to the 27 kDa fragment containing the first five amino-terminal type I repeats (III1-5) (McDonald et al., 1987; McKeown-Longo and Mosher, 1985; Schwarzbauer, 1991). Interestingly, although the remaining 40kDa domain, which binds to collagen, is dispensable for fibronectin assembly, the excess presence of the 27 kDa fragment has a less inhibitory effect on fibronectin matrix assembly than the presence of the whole 70 kDa portion (McKeown-Longo and Mosher, 1985). Nevertheless it can be concluded that the presence of excess 70 kDa fragment acts as a dominant negative,

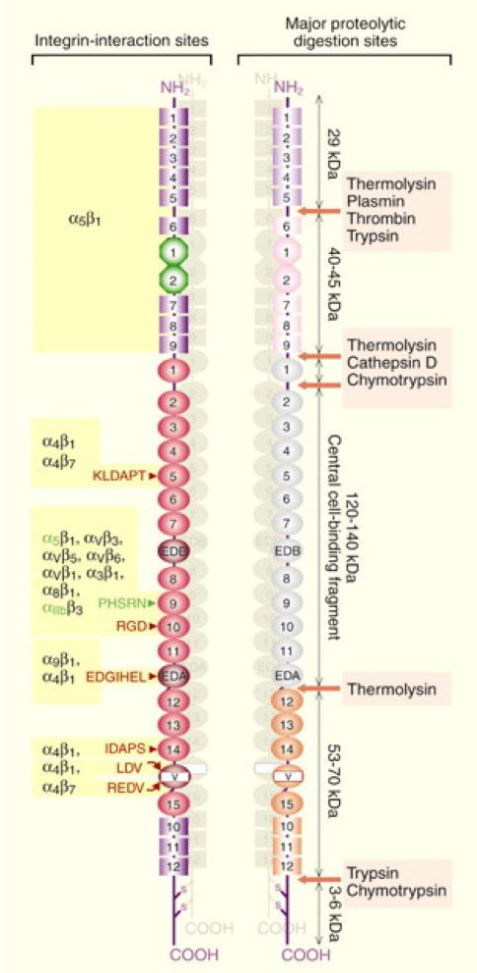

Figure 13. Fibronectin proteolytic digestion and integrin-interaction sites. On the left, detailed map on the integrin interaction sites and respective recognition sequences on the fibronectin molecule. On the right, the main proteolytic digestion sites and resulting functional fragments, with size. Adapted from Pankov and Yamada, 2002.

competing for the fibronectin binding sites essential for multimerization of fibronectin, but not the cell binding sites. Thus, the 70 kDa fragment not only inhibits *de novo* fibronectin assembly (McKeown-Longo and Mosher, 1985) but also destabilizes existing fibronectin matrices (Sottile and Hocking, 2002).

2.1.3. The RGD cell-binding site

Fibronectin assembly into an insoluble ECM is a cell-dependent event. This is a particularly important property for an abundant plasma constituent (300μg/ml), as it avoids the formation of circulating aggregates or thrombuses. Although the fibronectin molecule displays numerous binding sites to other ECM molecules, it does not become prone to form a matrix until it binds to its preferential cell surface receptor, integrin $\alpha5\beta1$ (see section 2.4., *Integrins*). The two long polypeptide chains that compose the fibronectin molecule are secreted in a folded compact form (Potts and Campbell, 1994; Ruoslahti, 1988). Thus, an initial attachment to the cell surface receptor, via the central cell-binding domain of the fibronectin molecule, is essential to unfold it and allow the initiation of matrix assembly. The main cell binding site on fibronectin is the RGD (Arg-Gly-Asp) sequence located on the tenth type III repeat (Pierschbacher and Ruoslahti, 1984) which is neighbored by a synergy site located on the ninth type III repeat (Aota et al., 1994; Dufour et al., 1988, see Figure 12 and 13). The recognition of both sites by the $\alpha5\beta1$integrin is essential for strong binding (Friedland et al., 2009) and proper fibronectin assembly (Sechler et al., 1997). Other integrin receptors can also attach through the RGD sequence or other sequences on the fibronectin molecule (Hynes, 2002; Pankov and Yamada, 2002), and even partially compensate fibronectin matrix assembly (detailed in section 2.4., *Integrins*). Nevertheless, the RGD-$\alpha5\beta1$ integrin interaction remains essential for embryonic development (Takahashi et al., 2007a). The presence of excess RGD inhibits fibronectin matrix assembly, although not by inhibiting fibronectin-fibronectin binding as the case for the 70 kDa fragment, but by occupying all the available RGD-recognition pockets on the integrin receptors (Pierschbacher and Ruoslahti, 1984). Unlike the 70 kDa fragment, excess RGD can also prevent the

attachment of cells to their substrate and even lead to their detachment (Ruoslahti, 1996).

2.1.4. Fibronectin matrix assembly

The initial electron microscopy images of fibronectin molecules sprayed onto surfaces depicted fibronectin as an elongated chain. However, under physiological conditions, in solution, the string of fibronectin modules adopts a compact form (Potts and Campbell, 1994). The first steps of fibronectin assembly in cultured cells consist of the appearance of dots or clusters of fibronectin on the cell surface (Peters and Mosher, 1987). Once fibronectin binds to cells, it acquires an elongated conformation, first as 5-10nm long fibrils (Chen et al., 1978) linking the cells to their neighbors or substrate (McDonald et al., 1987). This initial multimerization occurs as end-to-end association of fibronectin dimers and proceeds by the stacking of more and more fibronectin molecules (Dzamba and Peters, 1991). At this point, fibronectin lacking the RGD cell-binding site can be incorporated together with native fibronectin, indicating that the RGD sequence is only essential for cell-fibronectin binding and not for fibronectin matrix growth (Sechler et al., 1996). Assembly continues through the clustering of fibrils into thicker fibers that compose the typical mesh-like fibronectin matrix (Mao and Schwarzbauer, 2005a; Singh et al., 2010, see assembly model in Figure 14). In a typical cell culture monolayer, the initial radial fibrils remain immotile at their peripheral end and extend in their proximal end, indicating that the addition of the new fibronectin molecules occurs near the cell surface (Ohashi et al., 2002).

Immunolabeling of the exogenous fibronectin supplied to cells cultured in their own matrix showed that newly assembled fibrils can align and coalesce with existing fibrils, but can also originate new fibrils (Mao and Schwarzbauer, 2005b; Peters et al., 1990). Thus, how can one know when a state of a fully mature fibronectin matrix is reached? Almost 30 years ago, Dean Mosher and colleagues described a solubility property of the fibronectin matrix that has become the established benchmark for fibronectin matrix maturity (Mao and Schwarzbauer, 2005a; McKeown-Longo and Mosher, 1983; Singh et al., 2010; Wierzbicka-Patynowski and Schwarzbauer, 2003). Cell culture extracts from recently plated cells, i.e., in their initial stages of fibronectin matrix

assembly, are soluble in solutions containing the detergent deoxycholate (DOC). On the other hand, extracts of "older" cultures, reveal that the fibronectin matrix present includes a DOC-insoluble fraction (McKeown-Longo and Mosher, 1983). This biochemical

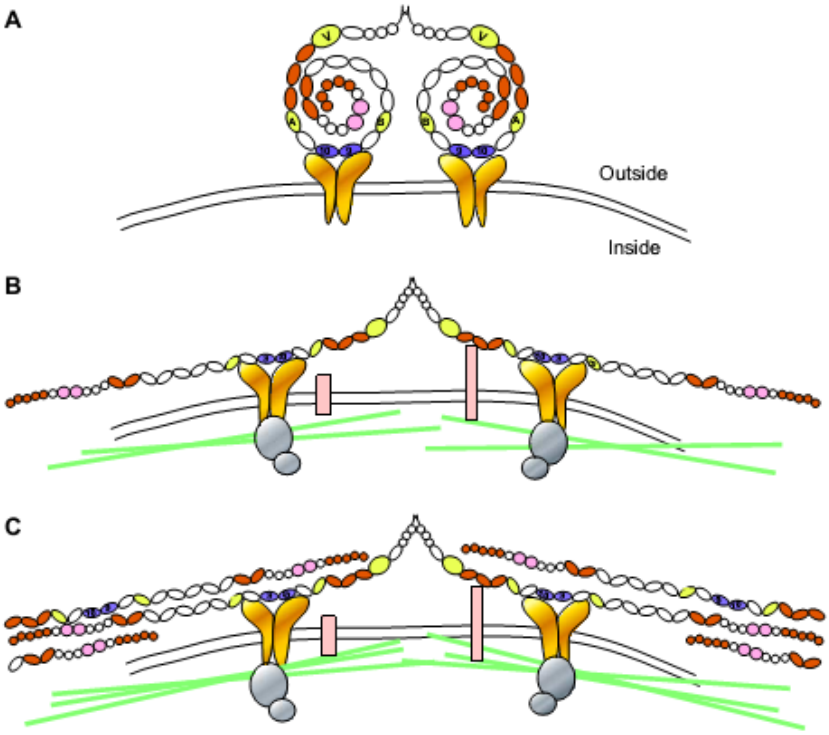

Figure 14. Current model for the initial stages of fibronectin matrix assembly. A: The secreted folded form of the fibronectin dimer attaches to the integrin cell receptor through the RGD binding sites. **B**: Cytoplasmic molecules (gray circles) attach to the short integrin cytoplasmic tails abridging the actin cytoskeleton (green lines). The tensioned integrins unfold and stretch the fibronectin molecules, exposing cryptic fibronectin binding sites **C**: The exposed sites allow for fibronectin-fibronectin interaction with new fibronectin molecules, forming the fibronectin matrix composed of numerous, stretched and bonded fibronectin molecules. Adapted from Wierzbicka-Patynowski and Schwarzbauer, 2003.

property identified the successful assembly of fibronectin into a more mature and resistant matrix, irreversibly insoluble under physiological conditions. Nevertheless, this matrix still requires a basal level of continuous assembly to be maintained: the fibrillar matrix initially assembled by fibronectin-null cells supplied with exogenous fibronectin is lost in the presence of excess 70 kDa fibronectin fragment (abolishing assembly) or when transferred into fibronectin-depleted medium (Sottile and Hocking, 2002). Interestingly, the biochemical properties of the fibronectin fibrils that lead to their DOC-insolubility are still under much debate (Singh et al., 2010) although it seems that it involves non-covalent binding which supports fibronectin dimer cross-linking (Ohashi and Erickson, 2009). Unfortunately, so far, this clearly identifiable characteristic has

failed to be correlated with any particular biological significance (Schwarzbauer and DeSimone, 2011).

2.1.5. Fibronectin functions

The original discovery and identification of fibronectin, by multiple and independent observations, found a correlation between the decrease in fibronectin levels and malignant transformation of cells (Gahmberg and Hakomori, 1973; Hynes, 1973; Ruoslahti et al., 1973; Yamada and Weston, 1974). Although the importance of these initial observations became less preponderant, due to the pleiotropic effect of malignant transformation recognized years later (Hynes and Yamada, 1982), numerous contemporary reports identified other no less important functions of fibronectin. Many of these roles involved adhesion phenomena, such as cell-substrate adhesion, cell attachment and spreading, migration and binding of fibronectin to other ECM molecules, while other studies demonstrated that fibronectin regulates cell growth and differentiation (see Hynes, 1981; Hynes and Yamada, 1982; Ruoslahti, 1988; Yamada and Olden, 1978). Thus, new data regarding the function of fibronectin is continuously coming forth, and by now, no single review can compile the tremendous variety of biological events where fibronectin plays a role. In particular cases, where fibronectin can be implicated in pathological conditions, such as cardio-vascular morphogenesis and thrombus formation (Astrof and Hynes, 2009; Cho and Mosher, 2006; Magnusson and Mosher, 1998; Maurer et al., 2010), fibronectin remains as a preponderant player, worthy of dedicated reviews.

The complexity of the role of fibronectin increases exponentially as the various integrin receptors and other cell surface receptors use a myriad of associated signaling molecules to transduce the signals from the fibronectin extracellular environment to the cell cytoplasm (see section 2.4., *Integrins*). Thus, the cellular interpretation of the ECM environment funnels into the cell-ECM adhesion, rather than to the fibronectin component itself. I will refer some of the signaling events attributed to the main fibronectin $\alpha 5\beta 1$ integrin receptor in section 2.4., *Integrins*, and address the role of fibronectin in embryogenesis in section 3 of this Introduction.

2.2. Laminins

The laminins comprise a family of heterotrimeric glycoproteins originated from the combination of 3 types of laminin chains, α, β and γ (Colognato and Yurchenco, 2000; Timpl and Brown, 1996). The laminin molecule is composed of one central α chain with one β and one γ chains partially wrapped around it via their coiled-coil domains, forming a cross-shaped molecule (see Figure 15, Durbeej, 2010). In vertebrates, five α, three β and three γ chains have been identified, each codified by distinct genes, which combine to form at least 16 different forms of laminin (Durbeej, 2010; Thorsteinsdóttir et al., 2011). Each laminin isoform is named in a three number sequence corresponding to its combination of chains (Aumailley et al., 2005), e.g. laminin 511, one of the earliest laminins expressed in mammalian embryos (Copp et al., 2011), is composed of an α5, a β1 and a γ1 chain (see Table 1).

Laminins are the major components of basement membranes, sheet-like ECMs that underlie epithelial and endothelial cells and surround muscle, neural and fat cells. Basement membranes also contain other ECM molecules such as collagen type IV,

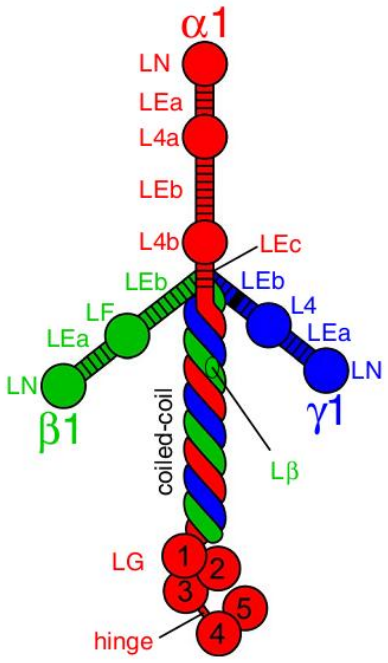

Figure 15: Illustrative depiction of laminin 111, as a general representation of the laminin structure. The three laminins chains are united at the common coiled coil domain, while the three free arms compose the remaining laminin crux figure. The several laminin domains are also depicted. Adapted from Durbeej, 2010.

nidogen and perlecan (Yurchenco and Patton, 2009; Yurchenco and Wadsworth, 2004). Interestingly, in a cell-free environment, both laminin and collagen type IV can self-assemble in solution (Yurchenco et al., 1992). However, in cultured embryonic stem cells, basement membranes fail to assemble in the absence of laminins, despite the presence of the remaining components (Li et al., 2002). Similarly in mammalian embryos, the absence of laminin abolished the assembly of a basement membrane (Miner et al., 2004; Smyth et al., 1999). Thus, the polymerization of laminin into a matrix is vital for the integration of the remaining components into a basement membrane (Sasaki et al., 2004; Yurchenco and Patton, 2009; Yurchenco and Wadsworth, 2004).

Laminin name	Chain composition	Gene products	Old nomenclature
Laminin 111	α1β1γ1	*Lama1 Lamb1 Lamc1*	Laminin-1
Laminin 121	α1β2γ1	*Lama1 Lamb2 Lamc1*	Laminin-3
Laminin 211	α2β1γ1	*Lama2 Lamb1 Lamc1*	Laminin-2
Laminin 221	α2β2γ1	*Lama2 Lamb2 Lamc1*	Laminin-4
Laminin 213	α2β1γ3	*Lama2 Lamb1 Lamc3*	Laminin-12
Laminin 212 [§]	α2β1γ2	*Lama2 Lamb1 Lamc2*	-
Laminin 222 [§]	α2β2γ2	*Lama2 Lamb2 Lamc2*	-
Laminin 311	α3Aβ1γ1	*Lama3A* Lamb1 Lamc1*	Laminin-6
Laminin 321	α3Aβ2γ1	*Lama3A* Lamb2 Lamc1*	Laminin-7
Laminin 332	α3Aβ3γ2	*Lama3A* Lamb3 Lamc2*	Laminin-5
Laminin 3B32	α3Bβ3γ2	*Lama3B* Lamb3 Lamc2*	Laminin-5B
Laminin 333	α3Aβ3γ3	*Lama3A* Lamb3 Lamc3*	-
Laminin 411	α4β1γ1	*Lama4 Lamb1 Lamc1*	Laminin-8
Laminin 421	α4β2γ1	*Lama4 Lamb2 Lamc1*	Laminin-9
Laminin 423	α4β2γ3	*Lama4 Lamb2 Lamc3*	Laminin-14
Laminin 511	α5β1γ1	*Lama5 Lamb1 Lamc1*	Laminin-10
Laminin 521	α5β2γ1	*Lama5 Lamb2 Lamc1*	Laminin-11
Laminin 522	α5β2γ2	*Lama5 Lamb2 Lamc2*	-
Laminin 523	α5β2γ3	*Lama3 Lamb2 Lamc3*	Laminin-15

Table1. The Laminins. Current and old nomenclature for the various trimeric laminin forms, and the respective gene products that generate them. [§] Existence proposed. ***** The *Lama3* gene can generate two splicing alternative isoforms, the truncated A isoform and the B isoform. Adapted from Thorsteinsdóttir et al., 2011.

Laminin is secreted in its trimeric form and polymerized at the cell surface, tethered by membrane receptors, such as integrins and dystroglycan (Yurchenco and Patton, 2009). Laminin polymerization is essential for basement membrane formation, but the linkage to the cell surface receptors is dispensable at initial stages of development (Li et al., 2002), although it may regulate the initiation sites for laminin nucleation (Yurchenco and Patton, 2009). Cell anchorage to the basement membrane is provided by receptors specific to laminin (or other components), and do not overlap with the fibronectin receptors (Hynes, 2002). Cell-laminin adhesions, much like fibronectin adhesions, also comprehend numerous signaling and tethering-reinforcement molecules associated with the laminin receptors (Li et al., 2003; Yurchenco and Patton, 2009).

The basement membrane is a specialized ECM (Kruegel and Miosge, 2010), and the attachment of cells to their basement membrane provides a mechanical anchorage point, particularly important for tissues subjected to physical stress, such as the epithelial epidermis or muscle. Beyond the physical anchorage, the basement membrane of epithelia also provides polarizing cues essential for the establishment of the epithelial cell phenotype (Bryant and Mostov, 2008; Li et al., 2003). Laminins (and other basement membrane components) also elicit differentiation and anti-apoptotic cues, frequently in cooperation with or through regulation of other signaling pathways (Domogatskaya et al., 2012; Li et al., 2002; Miner and Yurchenco, 2004).

Given its cardinal importance for basement membrane assembly, laminin functions largely overlap basement membrane functions. The deletion of any of the laminin isoforms present at early stages of development, results in the absence of basement membrane and blocks embryonic development even before the establishment of the germ layers (laminin γ1, *Lamc1*, (Smyth et al., 1999), reviewed in (Domogatskaya et al., 2012; Miner et al., 2004; Miner and Yurchenco, 2004). Deletions or mutations in other laminin isoforms result in defects in specific tissues, such as epidermis blistering (laminin α3, *Lama3*), or severe muscular dystrophy and peripheral neuropathies (laminin α2, *Lama2*) (reviewed in Domogatskaya et al., 2012; Yurchenco et al., 2004).

Several cell surface receptors can bind to different laminins isoforms, at different domains. Some are proteoglycans, such as syndecan (see section 2.3., *Other ECM molecules)*, but most laminin receptors are of the integrin family. Certain integrins, such as integrin $\alpha1\beta1$ and $\alpha2\beta1$ can also bind to collagens, while others, $\alpha3\beta1$, $\alpha6\beta1$, $\alpha7\beta1$ and $\alpha6\beta4$ are laminin specific (Durbeej, 2010; Thorsteinsdóttir et al., 2011). Nevertheless, the integrin that bind to laminins are non-overlapping with the fibronectin-binding receptors.

2.3. Other ECM molecules

A distinguishable fraction of the ECM is made up of proteoglycans, which are for the most part composed of carbohydrates (up to 95% in dry weight), mostly in the form of long, branched chains of glycosaminoglycans (GAGs). The remaining ECM components are glycoproteins with much lower carbohydrate content (0-65%). The GAG disaccharide molecules fall into four categories: chondroitin sulfate and dermatan sulfate, heparan sulfate, keratan sulfate and the non-sulfated hyaluronan (or hyaluronic acid) (Alberts et al., 2002). The numerous free sulfate and carboxyl groups present in the GAGs result in negatively-charged proteoglycans, with high hydrophilic properties, which gives them important space-filling, lubrication and ion binding properties. Although proteoglycans do not contain hyaluronic acid in their GAG chains, numerous proteoglycans can non-covalently bind to a hyaluronic acid chain, thus combining into larger molecules. Most proteoglycans are associated with other ECM molecules in the interstitial ECM, but also in more specialized ECMs, such as in the basement membrane (e.g. perlecan), and can also be found associated with the cell membrane (e.g. syndecan) (see Iozzo and Murdoch, 1996; Schaefer and Schaefer, 2010). Despite their rather passive space-filling function, proteoglycans can also bind to growth factors, regulating their distribution and/or release (Lin, 2004).

Collagens are, by far, the most abundant proteinaceous group of the ECM (roughly 30% of the protein mass in an adult human body). They provide structural strength to all kinds of extracellular matrices, such as the resilient tendons and ligaments, bones and cartilage, the vitreous humor in the eye or the interstitial matrix of the dermis. Collagens are formed by long, stiff, triple-stranded helical chains of polypeptides, mainly

containing proline and glycine (Gordon and Hahn, 2010). Collagen synthesis involves numerous post-translational modifications, both before and after the secretion as a triple helix procollagen (Myllyharju and Kivirikko, 2004). The majority of the collagen superfamily form fibrils or networks, but can also participate in specific ECMs such as the basement membrane (Gordon and Hahn, 2010; Myllyharju and Kivirikko, 2004; Ricard-Blum and Ruggiero, 2005).

Numerous other ECM glycoproteins have been described, having various, more or less tissue-specific functions (see Hynes and Naba, 2012). Some are regularly associated with more common ECM molecules, such as fibrillin associated to collagen fibers, or tenascin and fibrillin to fibronectin. Some of these molecules are associated to specific disorders, such as the Marfan's syndrome (mutation in fibrillin 1) (see Jarvelainen et al., 2009), though their embryonic relevance has not been as thoroughly investigated as other glycoproteins.

2.4. Integrins

2.4.1. Integrin structure and signaling

The discovery of integrins dates back to the mid 1980's, even though the existence of a receptor for ECM proteins responsible for cell adhesion was postulated earlier (see Barczyk et al., 2010; Hynes, 2004; Miranti and Brugge, 2002). All integrins are transmembrane heterodimeric glycoproteins, composed of one α chain and one β chain (see Figure 16, on top). The two non-covalently associated subunits can be combined into 24 distinct cell surface receptors, assembled out of 18 α- and 8 β-subunits described so far (Barczyk et al., 2010; Hynes, 2002). Specific binding pockets in the large extracellular portion of each integrin subunit bind to particular domains or peptide sequences in the ECM components (Humphries et al., 2006). The generally short integrin cytoplasmic tail is responsible for bridging the cell cytoskeleton to the external ECM, ensuring the transmission of signals and cell anchorage (Damsky and Ilic, 2002; Harburger and Calderwood, 2009; Hynes, 2002; Wiesner et al., 2005).

Integrins transduce signals across the membrane, providing the cell with information about its local environment. Such information is crucial for the cellular responses, such as migration, survival, differentiation and also to contextualize other

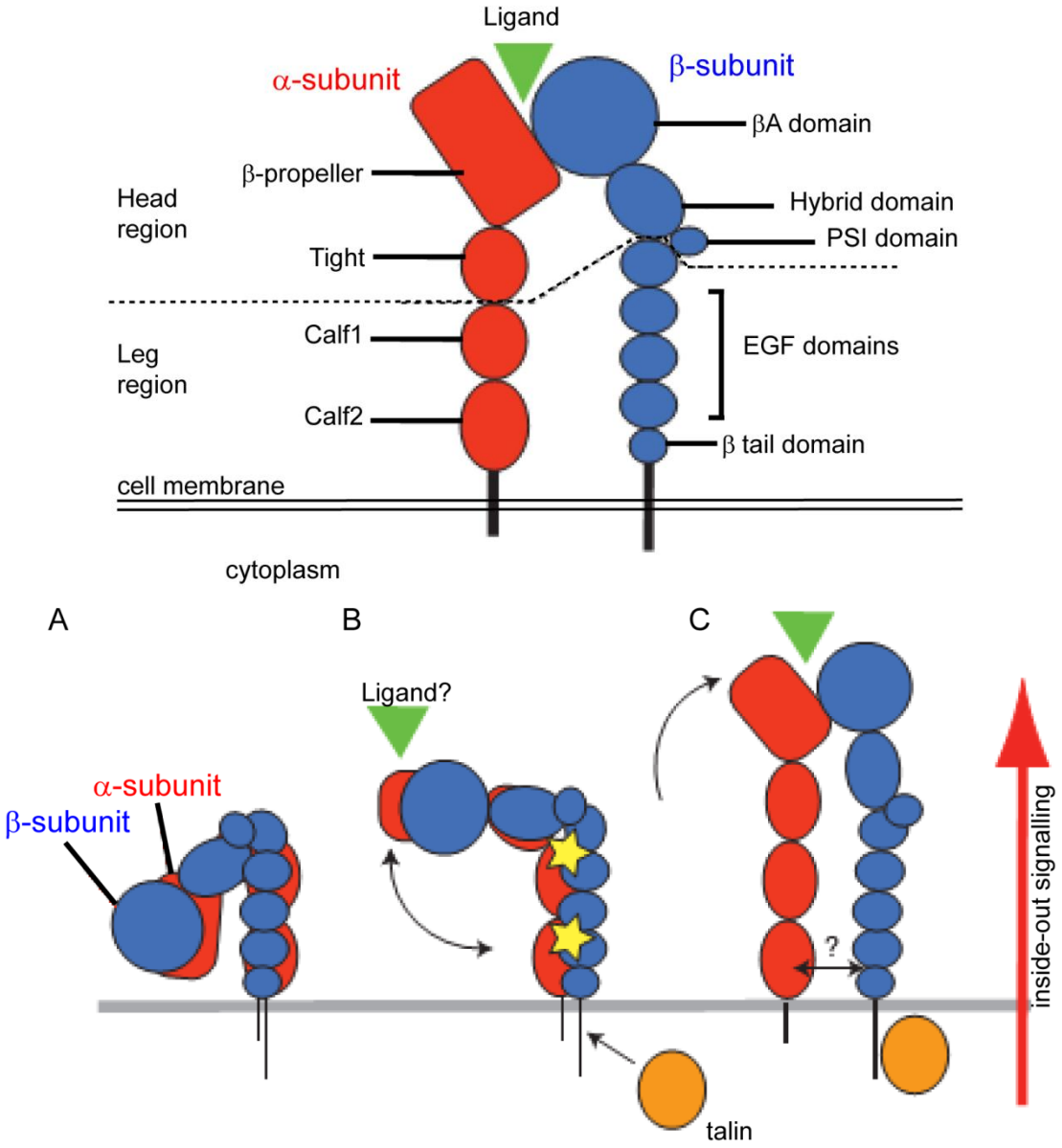

Figure 16. Structure of the integrin heterodimer and its conformational changes. On top: The schematic diagram of the integrin receptor, composed of the two subunits, α (in red) and β (in blue).The general binding ligand as green triangle. Note the extent of the extracellular portion and respective domains of either subunit in comparison with the small cytoplasmic tails. On the bottom: The current model for the integrin conformational changes during inside-out signaling. **A**: the folded, inactive form, with the cytoplasmic tails of both subunits closely associated ; **B**: the inherent flexibility of the integrin molecule allows for the intermediate, semi raised form, primed for ligand binding. Although cytoplasmic interaction with talin (orange oval) can further release the closed conformation, exposing epitopes in the leg regions (yellow stars), ligand binding is still unclear. **C**: the fully extended, ligand-bound integrin form, spreads apart the cytoplasmic tails, enough to allow the binding to talin and other integrin associated molecules. Adapted from Askari et al., 2009.

received signals (e.g. paracrine signaling pathways) (Damsky and Ilic, 2002; Geiger et al., 2001; Miranti and Brugge, 2002). Remarkably, integrins are also capable of signaling inside-out, particularly, by regulating the activation state of the integrins themselves (see Askari et al., 2009; Qin et al., 2004). This inside-out regulation of the integrin adhesiveness is of paramount importance for the circulating immune cells (see Abram and Lowell, 2009). Paradoxically, despite being an important signal transducing element, the integrin tail has no enzymatic activity of its own, which encouraged the extensive and exhaustive research on the molecular structure of integrins. Signal transduction, either inside-out or outside-in, is accomplished by major alterations in the structural conformation of both heterodimers; extending the ectodomains and exposing ECM binding pockets (inside-out) or by separating the α and β cytoplasmic tails, releasing them for the interaction with other molecules (outside in) (reviewed in Anthis and Campbell, 2011; Campbell and Humphries, 2011; Ginsberg et al., 2005; Kim et al., 2011; Luo et al., 2007; Mould and Humphries, 2004). The initial binding to an ECM component leads to an increased proximity and availability of integrin ligands, inducing the clustering of the receptors and associated molecules into large cell-ECM adhesion structures (Geiger et al., 2001; Miyamoto et al., 1995; Miyamoto et al., 1998). The structure and composition of these distinct integrin-based adhesion structures, formed by adherent cells in culture, has also been subject of intense research in the last decades.

2.4.2. Cytoplasmic molecules associated with integrins

The decade following the discovery of integrins, it became noticeable that integrins were cytoplasmically associated to several tyrosine phophorylated molecules, probably eliciting integrin signals (see Hynes, 1992). Since then, many integrin partners and other molecules have been located to the cell-ECM adhesion plaque. For reference, the number of molecules associated to cell-ECM adhesions has increased, from over 50 reported roughly 10 years ago (Miranti and Brugge, 2002; Zamir and Geiger, 2001a; Zamir and Geiger, 2001b) to a staggering 156 elements with 690 connections mapped in an “adhesome network” (Zaidel-Bar et al., 2007), recently updated to 180 elements (Zaidel-Bar and Geiger, 2010). Thus, it is beyond the scope of any review to describe the molecular interactions and signaling events that occur at the cell-ECM adhesion in detail

(see Figure 17). Here, I will provide a glimpse of a few of the most conspicuous molecules associated with cell-ECM adhesion structures, particularly, molecules proximal to the β cytoplasmic tail (see Harburger and Calderwood, 2009; Legate and Fassler, 2009).

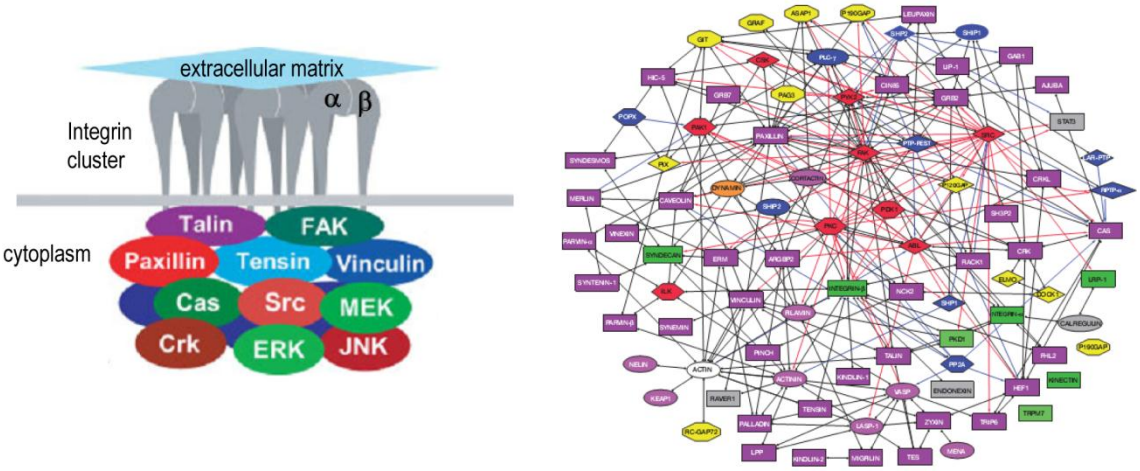

Figure 17: Molecules associated to the integrin-based cell-ECM adhesion site. On the left: Simplified view of integrin-proximal molecules and some associated signaling molecules. Adapted from Berrier and Yamada, 2007. On the right: The complex "adhesome" network of the intrinsic component of the integrin adhesion plaque, obtained through *in silico* analysis of reported protein interaction. For details, see Zaidel-Bar et al., 2007.

Talin, a component of the cell-ECM adhesion structures, exists in the cytoplasm in a closed head-tail autoinhibitory form. Talin can bind directly to the NPxY motif on the β cytoplasmic tail through its head domain. This binding releases the long tail which has numerous binding sites for the actin cytoskeleton and other structural molecules such as vinculin (Critchley and Gingras, 2008). Although little is known on the regulation of the talin-integrin interaction, talin is considered to be the final common step for integrin activation (Tadokoro et al., 2003), and therefore, essential for subsequent signaling (Critchley and Gingras, 2008; Moser et al., 2009).

Focal Adhesion Kinase (FAK) is a non-receptor tyrosine kinase signaling scaffold protein that also interacts directly with β integrins, and it is frequently associated with other tyrosine kinases of the Src family. This ubiquitously expressed molecule is a key regulator of the cytoskeleton, essential for the formation and turnover of cell-ECM adhesions, particularly during cell migration (Mitra et al., 2005; Schaller, 2010).

The Integrin Linked Kinase (ILK) is an ubiquitous multidomain signaling scaffold protein that directly interacts with β integrins and with other cytoplasmic molecules, (see Wu, 2001). Despite its name, ILK has no kinase activity of its own, but is the central molecule of the integrin-associated ILK-PINCH-Parvin (IPP) complex, implicated in the phosphorylation of numerous signaling pathway elements (see Wickstrom et al., 2010). Though closely associated to cell-ECM adhesion structures, this complex interacts with several, spatially more distant molecules, such as receptor tyrosine kinases, key players in the Wnt, AKT/PKB and JNK signaling pathways, and regulators of the actin cytoskeleton, thus influencing most aspects of cell behavior (see Legate et al., 2006; Wickstrom et al., 2010).

Paxillin is also an essential multi-domain scaffold protein, already present during the initial steps of the formation of cell-ECM adhesion structures. Its multiple protein-binding domains are regulated by phosphorylation and serve as multiple docking sites on the cytoplasmic side of the cell-adhesion site, engaging components such as FAK, ILK, vinculin and regulators of the actin cytoskeleton ((Deakin and Turner, 2008; Turner, 2000). Therefore, the main function of paxillin is to serve as a nexus between the numerous molecules involved in cell-ECM adhesion, ensuring proper signaling (see Brown and Turner, 2004; Deakin and Turner, 2008).

Vinculin is a cytoskeleton-associated molecule that interacts with the cell-ECM adhesion structure mainly through talin, but also through paxillin. Though talin binds directly to the integrin β tail and to actin, vinculin is required to strengthen the bond to the actin cytoskeleton (Critchley and Gingras, 2008). It is believed that, the closed head-tail inactivated form of vinculin is opened upon ECM attachment, releasing the talin-binding head domain and the tail domain for vinculin dimerization and further actin cross-linking (Ziegler et al., 2006). Interestingly, vinculin can also be found associated with cell-cell adhesions, also mediating the binding to the cytoskeleton (Yonemura, 2011; Ziegler et al., 2006).

2.4.3. Integrin-Fibronectin interactions

Several integrins recognize and bind to fibronectin, most by recognizing the RGD sequence, but other sites on the fibronectin molecule can also be used (Pankov and Yamada, 2002). Different cell types can adhere and even migrate using a variety of fibronectin receptors but only a few integrins beyond the canonical $\alpha5\beta1$ have been implicated in fibronectin assembly. For example, the $\alpha4\beta1$ integrin, interacts with the V (variable) alternatively spliced region of fibronectin, and can, when exogenously stimulated, assemble a fibronectin matrix *in vitro* (Sechler et al., 2000). Notably, integrins composed of the αv subunit ($\alpha v\beta1$ and $\alpha v\beta3$), can adhere to fibronectin through the RGD site, and are thus able to partially compensate for the absence of $\alpha5\beta1$ (Wennerberg et al., 1996; Yang and Hynes, 1996; Zhang et al., 1993). Although the efficiency of fibronectin assembly by αv-containing integrins remains controversial (Danen et al., 2002; Wennerberg et al., 1996; Zhang et al., 1993), it is clear that the resulting fibronectin matrix is composed of shorter, less profuse fibrils (Danen et al., 2002; Takahashi et al., 2007a; Wennerberg et al., 1996).

In spite of these findings, the $\alpha5\beta1$ integrin remains as the primary fibronectin receptor, signal transducer and responsible for fibronectin assembly. Unlike the above mentioned integrins, the $\alpha5\beta1$ integrin binds both to the RGD and to the neighboring synergy site on the fibronectin molecule (Aota et al., 1991; Aota et al., 1994; Nagai et al., 1991; Pierschbacher et al., 1982). The key RGD site ensures integrin activation and proper alignment of the integrin-fibronectin interface, while the synergy site provides a strong binding (Friedland et al., 2009; Garcia et al., 2002). The extra binding to the synergy site leads to downstream activation of FAK (Friedland et al., 2009), which is also essential for fibronectin assembly (Ilic et al., 2004). Though $\alpha5\beta1$ integrin can bind to fibronectin lacking a functional synergy domain (Danen et al., 1995), the assembly of this recombinant fibronectin into a matrix is drastically reduced (Sechler et al., 1997). Moreover, the $\alpha5\beta1$ integrin, but not the other RGD-binding receptors, can bind plasma fibronectin in an efficient manner due to its greater affinity for the RGD site (Huveneers et al., 2008).

The strong binding of the α5β1 integrin to a fibronectin substrate also transduces different signals than αv-containing integrins, thus influencing cell behavior. The initial attachment to a fibronectin substrate results in divergent activity of RhoA, Rac1 and Cdc42, members of the small Rho GTPases family, key regulators of actin cytoskeleton dynamics (Hall, 1998; Heasman and Ridley, 2008). Upon attachment, the activity of RhoA decreases (Ren 1999) while Rac1 and Cdc42 increases (Price et al., 1998) allowing cell spreading. Moreover, the fibronectin concentration on the attaching substrate also influences the spreading dynamics through the small Rho GTPases (Cox et al., 2001). However, once cells are spread out, fibronectin-α5β1 mediated (but not αvβ3-mediated) signaling supports the surge in RhoA activation and the concomitant formation of stress fibers and mature cell-ECM attachment sites essential for fibronectin assembly (Danen et al., 2002). Also, α5β1 integrins, but not other integrins, support the formation of dynamic cell-matrix adhesions leading to random cell migration (Danen et al., 2005) apparently by differentially regulating the integrin recycling pathways (White et al., 2007). These dynamic α5β1-based adhesions to fibronectin can translocate along actin cables (Pankov et al., 2000), extending fibronectin fibrils towards the center of the cell, further promoting fibronectin-fibronectin interactions and, hence, matrix assembly (Clark et al., 2005; Ohashi et al., 2002). Moreover, blocking integrin-substrate interaction with excess RGD abolishes activation of Cdc42 and consequently, polarized cell migration (Etienne-Manneville and Hall, 2001).

2.5. The third dimension of the ECM

"Snatched from a life of obscurity and installed in contemporary glass and plastic palaces, cells are in danger of becoming Pygmalion's protégés. Housed in more traditional residences constructed of water and collagen instead of plastic or glass, do cells lead primitive, less cultured lives?" These famous introductory words by (Elsdale and Bard, 1972) clearly state the disquieting bias underlying conventional cell biology: isolated cells, plated on bi-dimensional glass/plastic substrates are poor reproductions of the cellular three dimensional (3D) environment *in vivo*. Despite the decades passed since these stated concerns, the study of cell-ECM adhesion in a 3D context is still in its infancy (see Harunaga and Yamada, 2011). The initial observations from Elsdale and

Bard spurred, with moderation, the field of 3D cell migration in collagen gels (see Grinnell and Petroll, 2010). The unusual cell shape, motility and growth observed in cells embedded in 3D gels clearly indicated that cell interactions with the surrounding medium must have its own 3D particularities. These suspicions were confirmed by the Yamada group, with their pivotal observations of fibroblasts embedded in 3D fibronectin rich matrix. Remarkably, cell elongation, attachment, motility and proliferation were enhanced in 3D compare to the 2D fibronectin matrix substrate, in a $\alpha5\beta1$ (but not αv-containing) integrin dependent manner (Cukierman et al., 2001). The panoply of molecules and the respective phosphorylation state associated to 3D ECM-cell attachment sites differed from the cell adhesions observed in a 2D environment (Cukierman et al., 2001). These observations preluded new dynamics in the cell-fibronectin matrix interactions (see Cukierman et al., 2002), such as the selective usage of fibronectin receptors during cell migration in 3D (Mao and Schwarzbauer, 2006), and the stimulatory effect of a 3D matrix in the assembly of new fibronectin matrix (Mao and Schwarzbauer, 2005b). Therefore, the transposition of the wealth of knowledge obtained from 2D systems into a 3D environment is starting to be abridged, shedding some light into the cell-ECM interactions in *in vivo* conditions (Nelson and Bissell, 2006; Rozario and DeSimone, 2010; Yamada and Cukierman, 2007).

2.6. Cell-cell adhesion

In multicellular organisms, cells make specialized contacts with their neighbors, providing a coherent structure to the tissues. Through these cell-cell adhesion contacts, cells can anchor, communicate or create with their neighbors a separating barrier. These three general types of cell-cell contacts (anchoring, communicating and occluding junctions) are particularly common and abundant in adult epithelial tissues (Alberts et al., 2002). The anchoring junctions are the general cell-cell adhesion tool, while the latter two are more restricted to specific tissues. Here I will review a particular type of anchoring junction, the *adherens* junction, which connects to the actin filament cytoskeleton of cells and is considered the universal adhesion machinery in metazoans (Oda and Takeichi, 2011).

Adherens junctions are mainly mediated by single-pass transmembrane molecules of the cadherin family. Cadherins establish the link between the actin cytoskeleton of neighboring cells, through extracellular, Ca^{+2} dependent non-exclusive homodimerization (Pokutta and Weis, 2007). E-cadherin is the most prominently known cadherin, and belongs to the classical cadherin family, which also includes N- and P-cadherin. Though these cadherins are named after the tissues they were originally located in, epithelial tissues (E), the neural tube (N) and placenta (P) (Alberts et al., 2002), they can be found in other locations. While E-cadherin is present in most epithelial tissues, N-cadherin can be found in mesodermal tissues (Duband et al., 1987; Hatta and Takeichi, 1986; Radice et al., 1997), and is involved in the development of mesodermal derivatives, such as in myogenesis (George-Weinstein et al., 1997). Intracellularly, cadherins interact with coupling molecules that connect to the actin cytoskeleton, such as α- and β-catenin, α-actinin or vinculin, and with several regulators of actin dynamics (Yonemura, 2011). β-catenin binds directly to the cytoplasmic tails of cadherins in a phospho-regulated manner, and also binds to actin-interacting proteins, such as IQGAP, filamin or α-catenin (Hartsock and Nelson, 2008). The latter, in turn, can interact either as a monomer with β-catenin or as a dimer promoting the formation of actin-filament bundles (Drees et al., 2005; Yamada et al., 2005). Although this dual role impedes α-catenin of being the strong link between the cadherins and the actin cytoskeleton, filamentous actin is closely associated with *adherens* junctions, through other bridging molecules, such as vinculin or α-actinin (Harris and Tepass, 2010).

The formation of *adherens* junctions has been mostly studied in isolated epithelial cells in culture. Migrating cells extend exploratory actin rich protrusions until two neighboring cell membranes meet. Upon contact, punctate cadherin adhesions are formed and recruit actin filaments which become radial to the cell instead of circumferential. The proximity of the two cell membranes leads to new cadherin punctae that coalesce into a cadherin adhesion belt which is associated with actin filaments (Cavey and Lecuit, 2009; Green et al., 2010; Harris and Tepass, 2010). Thus, the formation of *adherens* junctions between cells involves an intensive interaction with regulators of actin dynamics as extensively studied during epithelial morphogenesis

during *Drosophila melanogaster* development (see Baum and Georgiou, 2011; Halbleib and Nelson, 2006; Harris and Tepass, 2010).

The cadherin-catenin complex of stable *adherens* junctions is also fundamental player in the establishment of epithelial cell polarity. *Adherens* junction proteins are closely associated with the small RhoGTPases, which are not only regulators of actin dynamics but also major players in the establishment of epithelial apico-basal polarity ((Baum and Georgiou, 2011; Iden and Collard, 2008). Moreover, *adherens* junctions provide structural support for the formation of more specialized epithelial cell-cell contact such as tight junctions (Eckert and Fleming, 2008; Niessen, 2007). The formation of an epithelial tissue requires an initial cue from the surrounding ECM, providing the basal signal, while cell-cell adhesions provides the lateral cue, thus discriminating the baso-lateral portion from the apical side (Bryant and Mostov, 2008; Nelson, 2009).

3. Extracellular matrix and embryonic development

Until the tremendous expansion in the field of cell and molecular biology in the late 1970's, the extracellular material, mostly collagenous fibrils in connective tissue, was perceived as an important, yet passive dwelling for cells (see Piez, 1997, for an historical perspective). Concomitantly with the discovery of the fibronectin and laminin ECM glycoproteins, the advances in the comprehension of cell behavior started to show that this "packaging material" for cells was much more influential. The discovery of integrins in the mid 1980's provided the mechanistic link between the ECM and the cells' cytoplasm (see Rozario and DeSimone, 2010). Not only the ECM and its receptors proved to be basic, instrumental regulators of all aspects of cell behavior in culture, but also the respective gene knock-out mouse embryos generated, many of which were embryonic lethal, demonstrated their importance for embryonic development (see Goody and

Henry, 2010; Rozario and DeSimone, 2010). In spite of these initial advances, the ECM remained relegated to a semi-passive player in embryonic development, dependent of the cells' genetic program, even though the reciprocal influence between the two was postulated early on (Bissell et al., 1982).

3.1. Fibronectin and morphogenesis

The *Xenopus* embryo was one of the earliest models in which the role of the ECM, particularly fibronectin was explored. The injection of antibodies blocking cell-fibronectin interaction impedes gastrulation (Boucaut et al., 1984; Boucaut et al., 1985) and mesendoderm cell migration as a coherent tissue along the fibronectin-lined blastocoel is blocked (see Winklbauer et al., 1996). Moreover, the fibronectin matrix serves as a polarizing substrate for the choreographed morphogenetic movements during early development (Davidson et al., 2002; Marsden and DeSimone, 2001; Marsden and DeSimone, 2003; Nagel and Winklbauer, 1999). The adhesive properties of fibronectin (as well as other ECM glycoproteins) were also implicated in other embryonic migration events, such as neural crest cell migration (see Perris and Perissinotto, 2000) or migration of cardiac precursors towards the embryonic midline (see Linask et al., 2005). For example, the timely deposition of fibronectin is essential, not for the migration process itself, but rather for the organized, coherent migration and integrity of the epithelium of cardiac precursors in the zebrafish embryo (Trinh and Stainier, 2004).

Branching morphogenesis is also a field where the importance of the ECM environment has been explored extensively. Thanks to the visionary work by Mina Bissel and colleagues, the post-natal development of the mouse mammary gland is an established model where the branching morphogenesis and the differentiation program are interdependent on ECM components, the 3D architecture and local microenvironment (Bissell et al., 2003; Fata et al., 2004; Nelson and Bissell, 2006). A laminin-rich basement membrane is essential for the formation of the mammary acinus and to promote the production of milk proteins such as casein (Klinowska et al., 1999; Li et al., 1987), while fibronectin participates in the branching event (Fata et al., 2007). In fact, fibronectin is a common ECM molecule during the branching of several organs such

as the lung (De Langhe et al., 2005), and most notoriously, the salivary gland (Sakai et al., 2003). Local accumulation of fibronectin induces a decrease in cell-cell adhesion, allowing for cleft initiation (Sakai et al., 2003), while the continuous deposition of fibronectin further supports the separation of the two new branches (Larsen et al., 2006).

3.2. Fibronectin matrix and somitogenesis

The association between ECM components, cell adhesion and somitogenesis dates back to the initial experimentation on somitogenesis (briefly overviewed in section 1.5., "*Sausages into meatballs"*). However, several other observations have been composing, though timidly, the picture on how cell-ECM (and cell-cell) adhesion participate in somitogenesis. Here, I provide the observations made in some detail, and divide them into the four different vertebrate model systems used.

*3.2.1. The chicken embryo (*Gallus gallus*)*

The flurry of research on the increasing list of new ECM molecules in the late 1970's, early 80's gave a new push to research on the mechanism of somite formation, also fueled by the adhesiveness experiments performed by Ruth Bellairs and other contemporary researchers (Bellairs et al., 1978; Bellairs et al., 1980). At the time, a myriad of observations and theories subsisted, from the somite-inducing properties of neighboring tissues, to pre-existing "whorls of cells" in the PSM, along with the clock and wavefront theoretical model, all enrolled as mechanisms of somite formation (see Lash and Ostrovsky, 1986). With the advent of the new knowledge about the ECM, experimentation and theory testing was now feasible (see Lash and Ostrovsky, 1986). Initially, the fibers observed surrounding somites, presumed to be collagen (Lipton and Jacobson, 1974) were proposed to have a regulatory role in somite formation (Bellairs, 1979). The inhibition of cytoskeletal actin polymerization by cytochalasin D also abrogated somite formation (Chernoff and Lash, 1981), indicating that contractility of the cell cytoskeleton was an important factor (Chernoff, 1985; Lash et al., 1985; Ostrovsky et al., 1983). Though the actin cytoskeleton and the extracellular fibers were clearly located in non-interacting locations (Lash et al., 1985), the postulated cell surface

ECM receptors were being discovered, providing the missing link (Lash et al., 1985 see Hynes, 2004 and section 2.4, *Integrins*). Additionally, more precise studies on the adhesiveness of PSM and somite cells in suspension further hinted to the importance of cell-cell or cell-fibronectin interactions as external anchorage points for the aggregation of cells (Cheney and Lash, 1984). At the same time, immunolabeling for fibronectin in chick embryos (Critchley et al., 1979) allowed for the distinction of an extensive fibrillar fibronectin matrix around the PSM (Duband et al., 1987; Krotoski et al., 1986; Lash et al., 1985; Newgreen and Thiery, 1980; Ostrovsky et al., 1983; Thiery et al., 1982). These observations, together with the contemporary reports of fibronectin playing a role in amphibian gastrulation (Boucaut et al., 1984), lead to the proposition of fibronectin as a somite aggregator agent (Lash and Ostrovsky, 1986; Lash et al., 1984). Isolated PSMs and PSM cells supplemented with fibronectin (Lash et al., 1984) or even RGD-containing peptides (Lash and Yamada, 1986) could be rescued to form somite-like structures or cell aggregates, respectively. In the meantime, the putative fibronectin receptor was also reported to localize in the basal cell membranes at the somite's periphery (Duband et al., 1986; Krotoski et al., 1986), providing the adhesive link between PSM cells and the extracellular material.

Other ECM molecules were also reported to be present in the PSM, but most of the focus was placed on fibronectin (Duband et al., 1987; Duband and Thiery, 1987; Lash et al., 1985). Attention was also paid to the potential role of cell-cell adhesion molecules in somite aggregation (Duband et al., 1987; Duband et al., 1988; Linask et al., 1998; Thiery et al., 1982). Cell-cell adhesion interference using function-blocking N-cadherin antibodies resulted in slight somitic abnormalities, particularly in early stage chick embryos (Linask et al., 1998). The same antibodies or calcium depletion (affecting cadherin function) prevented the re-aggregation of PSM/somite cells and lead to cell dissociation in cultured isolated PSMs (Duband et al., 1987).

*3.2.2. The mouse embryo (*Mus musculus*)*

The advent of the mouse gene knock-out technology reinforced the importance of fibronectin in somitogenesis. The deletion of the *Fn1* gene (George et al., 1993) induced early embryonic lethality from E9.5 onwards, and although the paraxial mesoderm formed, it did not originate any somites (George et al., 1993; Georges-Labouesse et al., 1996). The overall phenotype of the complete lack of somites, was also shared by FAK (*Ptk2*, (Furuta et al., 1995; Ilic et al., 1995) and Paxillin knock-out mouse embryos (*Pxn*, Hagel et al., 2002 see section 2.4., *Integrins*). The deletion of the α5 integrin subunit (*Itgα5*), also embryonic lethal, from E10 onwards, resulted in impaired somitogenesis, but only from the seventh somite onwards (Goh et al., 1997; Yang et al., 1993). Unexpectedly, despite the severe mesodermal defects of the *Itgα5*-/- embryos, they still had a fibronectin matrix (Yang et al., 1993). Fibronectin was also detected in αv-null (*Itgav*) embryos (Bader et al., 1998) but not in the α5-/-:αv -/-compound mutant (Yang et al., 1999) indicating a compensatory effect in matrix assembly between these two integrin subunits.

On the other hand, deletion of the main cell-cell adhesion molecule in the paraxial mesoderm, N-cadherin (*Cdh2*) did not result in a strong somitic phenotype (Radice et al., 1997). Beyond the embryonic lethality by E10, and general neural and mesodermal defects, *Cdh2*-/- embryos still displayed irregular, but epithelial somites (Horikawa et al., 1999; Radice et al., 1997). The combined deletion of N-cadherin and cadherin 11 (*Cdh11*) lead to massively disorganized embryos with hardly any distinguishable somite segments, although the paraxial rostral-caudal segmentation persisted (Horikawa et al., 1999). Genetic deletion of *Cdh11*, expressed in somites (Kimura et al., 1995), resulted in viable, apparently normal embryos, with no discernible somitogenesis defects (Horikawa et al., 1999; Manabe et al., 2000). The pleiotropic effects and embryonic lethality of the fibronectin and other related mutants embryos diminished the interest in these molecules as players in mouse somitogenesis, as other more relevant somitic phenotypes were being generated (discussed above in section 1.5., *Sausages into meatballs*). Other vertebrate models provided further evidence of the importance of cell-fibronectin interaction during somitogenesis.

3.2.3. The amphibian Xenopus laevis *embryo*

In *Xenopus* embryos, fibronectin accumulates at the intersomitic borders (Davidson et al., 2004; Wedlich et al., 1989) and accurately reflects the boundary defects after heat shock treatment (Danker et al., 1992) described much earlier (Elsdale et al., 1976; Pearson and Elsdale, 1979). However, fibronectin is also crucial for the massive cellular movements that occur during *Xenopus* gastrulation, thus underlying essential embryonic events previous to paraxial mesoderm formation (Boucaut et al., 1984; Davidson et al., 2002; Davidson et al., 2006; Winklbauer et al., 1996). Nevertheless, injection of a dominant-negative form of integrin β1 (Marsden and DeSimone, 2003) or integrin α5 translation-blocking morpholinos (Kragtorp and Miller, 2007) disrupts somite formation. Interestingly, inhibition of FAK or downstream actin regulatory proteins Ena/VASP also disturbs somite cell rearrangement, concomitant with defective fibronectin and β1-integrin accumulation at the intersomitic boundaries (Kragtorp and Miller, 2006).

*3.2.4. The Zebrafish embryo (*Danio rerio*)*

The initial genetic screens in zebrafish (Haffter and Nusslein-Volhard, 1996) generated a list of genes affecting somite formation (van Eeden et al., 1996), most of which were, or turned out to encode for important Notch signaling related proteins (see Rida et al., 2004). Years later, phophorylated FAK, Paxillin, fibronectin (and laminin) were reported to accumulate at the intersomitic boundaries (Crawford et al., 2003; Henry et al., 2001). At the same time, a mutation from the original screen, called *natter*, was identified as encoding for fibronectin (fn, Trinh and Stainier, 2004). Originally grouped in the mutations affecting the cardiovascular system (Chen et al., 1996) and neurogenesis (Chen et al., 1996), *natter* embryos showed no obvious somitic defects (Trinh and Stainier, 2004). More or less simultaneously, a mutation in the *integrinα5* (*itga5*) gene was also identified in a separate screen for head alterations, and again, no somitic defect was reported (Crump et al., 2004).

However, two new independent genetic screens identified mutations with strong somitic phenotype, in the genes encoding for fibronectin (Koshida et al., 2005) and the

α5 integrin subunit (Koshida et al., 2005) *before eight - bfe*, (Jülich et al., 2005). The somitic defects resulting from the deletion or morpholino knock-down of *itga5* in zebrafish were restricted to the rostral 5 to 7 somites, and did not affect more caudal ones (Jülich et al., 2005; Koshida et al., 2005). This observation is in clear contrast to the *Itga5* mouse mutants, and to most Notch-related mouse and zebrafish mutants, with have somitic defects visible only beyond somite 7-10 (Goh et al., 1997; van Eeden et al., 1996; Yang et al., 1993, see Pourquié, 2001).

A similar phenotypic difference in the rostral versus caudal somites was also observed for the *fn1*/*natter* mutants and morphants (Jülich et al., 2005; Koshida et al., 2005). However, the knock-down of the second, zebrafish-specific, fibronectin gene (*fn1b*, also called *fn3*, see Sun et al., 2005) resulted in a full axial penetrance of the somitic defects (Jülich et al., 2005). Although a genetic interaction between Notch signaling and Fibronectin/Integrin signaling was proposed (Jülich et al., 2005), it was noted that the stability and sharpness of the intersegmental border was diminished with the knock-down of fibronectin (Jülich et al., 2005; Koshida et al., 2005).

II. Aims and objectives

The preceding introduction unveiled only a portion of the transverse scope of the questions posed by developmental biology. Several disciplines, such as regulation of gene expression (spatial and temporal), molecular interaction within and outside the cell, cell behavior, either with relation to its neighbors or with the surrounding medium, the construction of overall tissue morphology as well as tissue interactions, just to name a few, cross over and are intricately entangled in the comprehension of a single phenomenon such as somitogenesis (or any morphogenetic event, for that matter). As presented above, the comprehension of the exquisite temporal and spatial regulation of somitogenesis has been the major driving force of the field. Particularly, the quantum-

leap resulting from the discovery of the cycling genes (Palmeirim et al., 1997) fueled the interest in the genetic regulation of the phenomenon. And while extensive work on the genetic regulation of somitogenesis is being carried out in numerous laboratories (many of which I do not refer to as I often only relegate to the numerous key reviews), many basic questions remain unanswered (see Oates et al., 2012; Saga, 2012). Rather than joining in on this flurried interest in genetic regulation, this thesis is focused on, and aimed to clarify, the generation of a new supracellular architecture, the somite. This is of course, ultimately, one of the major goals of somitogenesis: to produce numerous regular, discrete units of cells from a single homogeneous mass of cells.

One of the main drivers for this work on somitogenesis was to reduce the blatant contrast between the vast amount of information available on cell-ECM interaction and cell behavior in *in vitro* culture systems, and the scant information on the intricate regulation of cell behavior, essential for this conspicuous morphogenetic event. It was particularly disturbing that, despite the available information on fibronectins' crucial involvement in somite formation, particularly the unique phenotype of the total absence of somites in the fibronectin KO mouse (George et al., 1993; Georges-Labouesse et al., 1996) and classical immunohistological localization of fibronectin in and around the PSM (Duband et al., 1987; Ostrovsky et al., 1983), there was hardly any interest in this molecule in mainstream somitogenesis research. Thus, the following chapters address somitogenesis in the chick embryo in the morphological sense, from a cellular point of view, particularly regarding the interaction between cells and the fibronectin matrix.

In **Chapter 2** we re-address an issue raised in the first days of experimentation on somitogenesis; the importance of surrounding tissues. As classic extirpation experiments rendered the surrounding tissues redundant for somite formation, the remaining doubts over the ectoderm and endoderm were cleared with a few more recent papers. Although three different labs demonstrated the paramount importance of the ectoderm (Correia and Conlon, 2000; Palmeirim et al., 1998; Sosic et al., 1997), there was no agreement on the mechanism involved, as these studies obtained different results on the expression of the *Paraxis* gene, thought to be the major player in somite epithelialization, both between and within the reports. In this first experimental chapter

(Chapter 2) we clarify the relevance of the ectoderm in chick somite formation and in the expression of *Paraxis*. We particularly put into evidence the importance of the experimental procedure used during microsurgery. We show that the enzymatic treatment used to facilitate microsurgery lead to a misinterpretation of the prominence of the surrounding tissues during somite formation. The research presented in this chapter was published in co-authorship in *Development* (2007) 134, 3155-65.

In the next chapter, **Chapter 3**, we initiate the study of somitogenesis in a 3D perspective, and follow the cell movements that accompany and underline the formation of the epithelial somite. In the wake of the seminal, single-plane, live-imaging of a single somite being formed (Kulesa and Fraser, 2002), our lab obtained a full 3D imaging view of somite formation during several hours. This work provided the first evidence of the complexity of the cell behavior during somitogenesis seen in a 3D perspective. We also explore the relevance of the continuous assembly of a fibronectin matrix as somitogenesis proceeds, with regard to the formation of the somite outer epithelial layer, versus the inner mesenchymal somitocoel. Part of the work presented in this chapter was performed by other laboratory members, and was published in co-authorship in *PLoS One* (2009) 4, e7429.

The 3D perspective of somite formation initiated in chapter 3, is taken into a full 3D analysis in **Chapter 4**. Here, we perform an extensive 3D analysis of the ECM components, fibronectin and laminin, throughout the development of the paraxial mesoderm. This analysis, taking advantage of the technical knowledge acquired during the work in Chapter 3, revealed with unprecedented cellular detail, the ECM architecture in the paraxial mesoderm while still retaining the whole 3D tissue perspective. We show the qualitative alterations in the fibronectin and laminin matrices that accompany several events in paraxial mesoderm development. The work described in this chapter was published in *Developmental Biology* (2012) 368, 370-81.

Chapter 5 is oriented to investigate the acquisition of the epithelial phenotype by the peripheral cells in the paraxial mesoderm. Somitogenesis provides a particularly interesting and useful landscape for the analysis of a mesenchymal to epithelial

transition (MET), as the MET repeats itself every time a new somite is formed. We set out to investigate the formation of mature forms of cell-cell contacts during paraxial mesoderm development, with particular focus on somite formation. Moreover, based on the observations from the previous chapters, we hypothesized that the extracellular fibronectin matrix could serve as an anchoring point for the peripheral PSM cells to rearrange themselves into the outer epithelial layer. Using inhibitors of cell-derived force, we investigated whether cell tension is required for somitogenesis, addressing both the morphogenetic process and the simultaneous regulation of gene expression. The results presented in this chapter are part of a manuscript still in preparation.

In the final chapter (**Chapter 6**) the main observations from the chapters presented in this thesis are summarized and viewed in a wider perspective. This chapter contains an overall discussion of the results, integrating them with the main advancements in the somitogenesis field and boundary formation in general, as well as in ECM assembly in an *in vivo* context.

III. References

Abram, C. L. and Lowell, C. A. (2009). The ins and outs of leukocyte integrin signaling. *Annual Review of Immunology* 27, 339-62.

Acloque, H., Adams, M. S., Fishwick, K., Bronner-Fraser, M. and Nieto, M. A. (2009). Epithelial-mesenchymal transitions: the importance of changing cell state in development and disease. *Journal of Clinical Investigation* **119**, 1438-49.

Adams, R. H., Wilkinson, G. A., Weiss, C., Diella, F., Gale, N. W., Deutsch, U., Risau, W. and Klein, R. (1999). Roles of ephrinB ligands and EphB receptors in cardiovascular development: demarcation of arterial/venous domains, vascular morphogenesis, and sprouting angiogenesis. *Genes & Development* **13**, 295-306.

Alberts, B., Bray, D., Lewis, J., Raff, M., Roberts, K. and Walter, P. (2002). Molecular Biology of the Cell. New York: Garland Science.

Alexander, T., Nolte, C. and Krumlauf, R. (2009). Hox genes and segmentation of the hindbrain and axial skeleton. *Annual Review of Cell and Developmental Biology* **25**, 431-56.

Andrade, R. P., Palmeirim, I. and Bajanca, F. (2007). Molecular clocks underlying vertebrate embryo segmentation: A 10-year-old hairy-go-round. *Birth Defects Research Part C: Embryo Today: Reviews* **81**, 65-83.

Anthis, N. J. and Campbell, I. D. (2011). The tail of integrin activation. *Trends in Biochemical Sciences* **36**, 191-8.

Aota, S., Nagai, T. and Yamada, K. M. (1991). Characterization of regions of fibronectin besides the arginine-glycine-aspartic acid sequence required for adhesive function of the cell-binding domain using site-directed mutagenesis. *Journal of Biological Chemistry* **266**, 15938-43.

Aota, S., Nomizu, M. and Yamada, K. M. (1994). The short amino acid sequence Pro-His-Ser-Arg-Asn in human fibronectin enhances cell-adhesive function. *Journal of Biological Chemistry* **269**, 24756-61.

Aoyama, H. and Asamoto, K. (1988). Determination of somite cells: independence of cell differentiation and morphogenesis. *Development* **104**, 15-28.

Arnold, S. J. and Robertson, E. J. (2009). Making a commitment: cell lineage allocation and axis patterning in the early mouse embryo. *Nature Reviews: Molecular Cell Biology* **10**, 91-103.

Askari, J. A., Buckley, P. A., Mould, A. P. and Humphries, M. J. (2009). Linking integrin conformation to function. *Journal of Cell Science* **122**, 165-70.

Astrof, S. and Hynes, R. O. (2009). Fibronectins in vascular morphogenesis. *Angiogenesis* **12**, 165-75.

Aulehla, A. and Herrmann, B. G. (2004). Segmentation in vertebrates: clock and gradient finally joined. *Genes & Development* **18**, 2060-7.

Aulehla, A. and Johnson, R. L. (1999). Dynamic expression of lunatic fringe suggests a link between notch signaling and an autonomous cellular oscillator driving somite segmentation. *Developmental Biology* **207**, 49-61.

Aulehla, A. and Pourquié, O. (2009). More than patterning--Hox genes and the control of posterior axial elongation. *Developmental Cell* **17**, 439-40.

Aulehla, A. and Pourquié, O. (2010). Signaling gradients during paraxial mesoderm development. *Cold Spring Harbor Perspectives in Biology* **2**, a000869.

Aulehla, A., Wehrle, C., Brand-Saberi, B., Kemler, R., Gossler, A., Kanzler, B. and Herrmann, B. G. (2003). Wnt3a plays a major role in the segmentation clock controlling somitogenesis. *Developmental Cell* **4**, 395-406.

Aumailley, M., Bruckner-Tuderman, L., Carter, W. G., Deutzmann, R., Edgar, D., Ekblom, P., Engel, J., Engvall, E., Hohenester, E., Jones, J. C. et al. (2005). A simplified laminin nomenclature. *Matrix Biology* **24**, 326-32.

Bader, B. L., Rayburn, H., Crowley, D. and Hynes, R. O. (1998). Extensive vasculogenesis, angiogenesis, and organogenesis precede lethality in mice lacking all alpha v integrins. *Cell* **95**, 507-19.

Bagnall, K. M., Higgins, S. J. and Sanders, E. J. (1988). The contribution made by a single somite to the vertebral column: experimental evidence in support of resegmentation using the chick-quail chimaera model. *Development* **103**, 69-85.

Baker, R. K. and Antin, P. B. (2003). Ephs and ephrins during early stages of chick embryogenesis. *Developmental Dynamics* **228**, 128-42.

Baranski, M., Berdougo, E., Sandler, J. S., Darnell, D. K. and Burrus, L. W. (2000). The dynamic expression pattern of frzb-1 suggests multiple roles in chick development. *Developmental Biology* **217**, 25-41.

Barczyk, M., Carracedo, S. and Gullberg, D. (2010). Integrins. *Cell and Tissue Research* **339**, 269-80.

Barnes, G. L., Alexander, P. G., Hsu, C. W., Mariani, B. D. and Tuan, R. S. (1997). Cloning and characterization of chicken Paraxis: a regulator of paraxial mesoderm development and somite formation. *Developmental Biology* **189**, 95-111.

Barrallo-Gimeno, A. and Nieto, M. A. (2005). The Snail genes as inducers of cell movement and survival: implications in development and cancer. *Development* **132**, 3151-61.

Barrios, A., Poole, R. J., Durbin, L., Brennan, C., Holder, N. and Wilson, S. W. (2003). Eph/Ephrin signaling regulates the mesenchymal-to-epithelial transition of the paraxial mesoderm during somite morphogenesis. *Current Biology* **13**, 1571-82.

Baum, B. and Georgiou, M. (2011). Dynamics of adherens junctions in epithelial establishment, maintenance, and remodeling. *Journal of Cell Biology* **192**, 907-17.

Baum, B., Settleman, J. and Quinlan, M. P. (2008). Transitions between epithelial and mesenchymal states in development and disease. *Seminars in Cell & Developmental Biology* **19**, 294-308.

Beckers, J., Schlautmann, N. and Gossler, A. (2000). The mouse rib-vertebrae mutation disrupts anterior-posterior somite patterning and genetically interacts with a Delta1 null allele. *Mechanisms of Development* **95**, 35-46.

Beddington, R. S. (1982). An autoradiographic analysis of tissue potency in different regions of the embryonic ectoderm during gastrulation in the mouse. *Journal of Embryology and Experimental Morphology* **69**, 265-85.

Bellairs, R. (1963). The Development of Somites in the Chick Embryo. *Journal of Embryology and Experimental Morphology* **11**, 697-714.

Bellairs, R. (1979). The mechanism of somite segmentation in the chick embryo. *Journal of Embryology and Experimental Morphology* **51**, 227-43.

Bellairs, R., Curtis, A. S. and Sanders, E. J. (1978). Cell adhesiveness and embryonic differentiation. *Journal of Embryology and Experimental Morphology* **46**, 207-13.

Bellairs, R., Ireland, G. W., Sanders, E. J. and Stern, C. D. (1981). The behaviour of embryonic chick and quail tissues in culture. *Journal of Embryology and Experimental Morphology* **61**, 15-33.

Bellairs, R., Sanders, E. J. and Portch, P. A. (1980). Behavioural properties of chick somitic mesoderm and lateral plate when explanted in vitro. *Journal of Embryology and Experimental Morphology* **56**, 41-58.

Bellairs, R. and Veini, M. (1980). An experimental analysis of somite segmentation in the chick embryo. *Journal of Embryology and Experimental Morphology* **55**, 93-108.

Ben-Yair, R. and Kalcheim, C. (2005). Lineage analysis of the avian dermomyotome sheet reveals the existence of single cells with both dermal and muscle progenitor fates. *Development* **132**, 689-701.

Bergemann, A. D., Cheng, H. J., Brambilla, R., Klein, R. and Flanagan, J. G. (1995). ELF-2, a new member of the Eph ligand family, is segmentally expressed in mouse embryos in the region of the hindbrain and newly forming somites. *Molecular and Cellular Biology* **15**, 4921-9.

Berrier, A. L. and Yamada, K. M. (2007). Cell-matrix adhesion. *Journal of Cellular Physiology* **213**, 565-73.

Bessho, Y., Hirata, H., Masamizu, Y. and Kageyama, R. (2003). Periodic repression by the bHLH factor Hes7 is an essential mechanism for the somite segmentation clock. *Genes & Development* **17**, 1451-6.

Bessho, Y. and Kageyama, R. (2003). Oscillations, clocks and segmentation. *Current Opinion in Genetics and Development* **13**, 379-84.

Bessho, Y., Sakata, R., Komatsu, S., Shiota, K., Yamada, S. and Kageyama, R. (2001). Dynamic expression and essential functions of Hes7 in somite segmentation. *Genes & Development* **15**, 2642-7.

Bettenhausen, B., Hrabě de Angelis, M., Simon, D., Guenet, J. L. and Gossler, A. (1995). Transient and restricted expression during mouse embryogenesis of Dll1, a murine gene closely related to Drosophila Delta. *Development* **121**, 2407-18.

Bissell, M. J., Hall, H. G. and Parry, G. (1982). How does the extracellular matrix direct gene expression? *Journal of Theoretical Biology* **99**, 31-68.

Bissell, M. J., Rizki, A. and Mian, I. S. (2003). Tissue architecture: the ultimate regulator of breast epithelial function. *Current Opinion in Cell Biology* **15**, 753-62.

Borggrefe, T. and Oswald, F. (2009). The Notch signaling pathway: transcriptional regulation at Notch target genes. *Cellular and Molecular Life Sciences* **66**, 1631-46.

Borycki, A., Brown, A. M. and Emerson, C. P., Jr. (2000). Shh and Wnt signaling pathways converge to control Gli gene activation in avian somites. *Development* **127**, 2075-87.

Borycki, A. G., Mendham, L. and Emerson, C. P., Jr. (1998). Control of somite patterning by Sonic hedgehog and its downstream signal response genes. *Development* **125**, 777-90.

Bothe, I., Ahmed, M. U., Winterbottom, F. L., von Scheven, G. and Dietrich, S. (2007). Extrinsic versus intrinsic cues in avian paraxial mesoderm patterning and differentiation. *Developmental Dynamics* **236**, 2397-409.

Boucaut, J. C., Darribere, T., Boulekbache, H. and Thiery, J. P. (1984). Prevention of gastrulation but not neurulation by antibodies to fibronectin in amphibian embryos. *Nature* **307**, 364-7.

Boucaut, J. C., Darribere, T., Li, S. D., Boulekbache, H., Yamada, K. M. and Thiery, J. P. (1985). Evidence for the role of fibronectin in amphibian gastrulation. *Journal of Embryology and Experimental Morphology* **89 Suppl**, 211-27.

Brand-Saberi, B., Wilting, J., Ebensperger, C. and Christ, B. (1996). The formation of somite compartments in the avian embryo. *International Journal of Developmental Biology* **40**, 411-20.

Bray, S. J. (2006). Notch signalling: a simple pathway becomes complex. *Nature Reviews: Molecular Cell Biology* **7**, 678-89.

Brent, A. E., Schweitzer, R. and Tabin, C. J. (2003). A somitic compartment of tendon progenitors. *Cell* **113**, 235-48.

Brent, A. E. and Tabin, C. J. (2002). Developmental regulation of somite derivatives: muscle, cartilage and tendon. *Current Opinion in Genetics and Development* **12**, 548-57.

Brown, M. C. and Turner, C. E. (2004). Paxillin: adapting to change. *Physiological Reviews* **84**, 1315-39.

Bryant, D. M. and Mostov, K. E. (2008). From cells to organs: building polarized tissue. *Nature Reviews: Molecular Cell Biology* **9**, 887-901.

Buchberger, A., Bonneick, S. and Arnold, H. (2000). Expression of the novel basic-helix-loop-helix transcription factor cMespo in presomitic mesoderm of chicken embryos. *Mechanisms of Development* **97**, 223-6.

Buchberger, A., Seidl, K., Klein, C., Eberhardt, H. and Arnold, H. H. (1998). cMeso-1, a novel bHLH transcription factor, is involved in somite formation in chicken embryos. *Developmental Biology* **199**, 201-15.

Buckingham, M. (2006). Myogenic progenitor cells and skeletal myogenesis in vertebrates. *Current Opinion in Genetics and Development* **16**, 525-32.

Buckingham, M., Bajard, L., Chang, T., Daubas, P., Hadchouel, J., Meilhac, S., Montarras, D., Rocancourt, D. and Relaix, F. (2003). The formation of skeletal muscle: from somite to limb. *Journal of Anatomy* **202**, 59-68.

Buckingham, M. and Relaix, F. (2007). The role of Pax genes in the development of tissues and organs: Pax3 and Pax7 regulate muscle progenitor cell functions. *Annual Review of Cell and Developmental Biology* **23**, 645-73.

Burgess, R., Cserjesi, P., Ligon, K. L. and Olson, E. N. (1995). Paraxis: a basic helix-loop-helix protein expressed in paraxial mesoderm and developing somites. *Developmental Biology* **168**, 296-306.

Burgess, R., Rawls, A., Brown, D., Bradley, A. and Olson, E. N. (1996). Requirement of the paraxis gene for somite formation and musculoskeletal patterning. *Nature* **384**, 570-3.

Bussen, M., Petry, M., Schuster-Gossler, K., Leitges, M., Gossler, A. and Kispert, A. (2004). The T-box transcription factor Tbx18 maintains the separation of anterior and posterior somite compartments. *Genes & Development* **18**, 1209-21.

Cadigan, K. M. and Liu, Y. I. (2006). Wnt signaling: complexity at the surface. *Journal of Cell Science* **119**, 395-402.

Campbell, I. D. and Humphries, M. J. (2011). Integrin structure, activation, and interactions. *Cold Spring Harbor Perspectives in Biology* **3**.

Carapuço, M., Novoa, A., Bobola, N. and Mallo, M. (2005). Hox genes specify vertebral types in the presomitic mesoderm. *Genes & Development* **19**, 2116-21.

Carpio, R., Honore, S. M., Araya, C. and Mayor, R. (2004). Xenopus paraxis homologue shows novel domains of expression. *Developmental Dynamics* **231**, 609-13.

Catala, M., Teillet, M. A., De Robertis, E. M. and Le Douarin, M. L. (1996). A spinal cord fate map in the avian embryo: while regressing, Hensen's node lays down the notochord and floor plate thus joining the spinal cord lateral walls. *Development* **122**, 2599-610.

Catala, M., Teillet, M. A. and Le Douarin, N. M. (1995). Organization and development of the tail bud analyzed with the quail-chick chimaera system. *Mechanisms of Development* **51**, 51-65.

Cavey, M. and Lecuit, T. (2009). Molecular bases of cell-cell junctions stability and dynamics. *Cold Spring Harbor Perspectives in Biology* **1**, a002998.

Chapman, D. L., Agulnik, I., Hancock, S., Silver, L. M. and Papaioannou, V. E. (1996). Tbx6, a mouse T-Box gene implicated in paraxial mesoderm formation at gastrulation. *Developmental Biology* **180**, 534-42.

Chapman, D. L. and Papaioannou, V. E. (1998). Three neural tubes in mouse embryos with mutations in the T-box gene Tbx6. *Nature* **391**, 695-7.

Chapman, S. C., Brown, R., Lees, L., Schoenwolf, G. C. and Lumsden, A. (2004). Expression analysis of chick Wnt and frizzled genes and selected inhibitors in early chick patterning. *Developmental Dynamics* **229**, 668-76.

Chen, J. N., Haffter, P., Odenthal, J., Vogelsang, E., Brand, M., van Eeden, F. J., Furutani-Seiki, M., Granato, M., Hammerschmidt, M., Heisenberg, C. P. et al. (1996). Mutations affecting the cardiovascular system and other internal organs in zebrafish. *Development* **123**, 293-302.

Chen, L. B., Murray, A., Segal, R. A., Bushnell, A. and Walsh, M. L. (1978). Studies on intercellular LETS glycoprotein matrices. *Cell* **14**, 377-91.

Cheney, C. M. and Lash, J. W. (1984). An increase in cell-cell adhesion in the chick segmental plate results in a meristic pattern. *Journal of Embryology and Experimental Morphology* **79**, 1-10.

Chernoff, E. A. (1985). Cell movement and contraction in somite development. *Scanning Electron Microscopy*, 257-67.

Chernoff, E. A. and Lash, J. W. (1981). Cell movement in somite formation and development in the chick: inhibition of segmentation. *Developmental Biology* **87**, 212-9.

Chevallier, A., Kieny, M. and Mauger, A. (1977). Limb-somite relationship: origin of the limb musculature. *Journal of Embryology and Experimental Morphology* **41**, 245-58.

Cho, J. and Mosher, D. F. (2006). Role of fibronectin assembly in platelet thrombus formation. *Journal of Thrombosis and Haemostasis* **4**, 1461-9.

Christ, B., Huang, R. and Scaal, M. (2004). Formation and differentiation of the avian sclerotome. *Anatomy and Embryology (Berl)* **208**, 333-50.

Christ, B., Huang, R. and Scaal, M. (2007). Amniote somite derivatives. *Developmental Dynamics* **236**, 2382-96.

Christ, B., Huang, R. and Wilting, J. (2000). The development of the avian vertebral column. *Anatomy and Embryology (Berl)* **202**, 179-94.

Christ, B. and Ordahl, C. P. (1995). Early stages of chick somite development. *Anatomy and Embryology (Berl)* **191**, 381-96.

Christ, B., Schmidt, C., Huang, R., Wilting, J. and Brand-Saberi, B. (1998). Segmentation of the vertebrate body. *Anatomy and Embryology (Berl)* **197**, 1-8.

Ciruna, B. and Rossant, J. (2001). FGF signaling regulates mesoderm cell fate specification and morphogenetic movement at the primitive streak. *Developmental Cell* **1**, 37-49.

Ciruna, B. G., Schwartz, L., Harpal, K., Yamaguchi, T. P. and Rossant, J. (1997). Chimeric analysis of fibroblast growth factor receptor-1 (Fgfr1) function: a role for FGFR1 in morphogenetic movement through the primitive streak. *Development* **124**, 2829-41.

Clark, K., Pankov, R., Travis, M. A., Askari, J. A., Mould, A. P., Craig, S. E., Newham, P., Yamada, K. M. and Humphries, M. J. (2005). A specific alpha5beta1-integrin conformation promotes directional integrin translocation and fibronectin matrix formation. *Journal of Cell Science* **118**, 291-300.

Collier, J. R., McInerney, D., Schnell, S., Maini, P. K., Gavaghan, D. J., Houston, P. and Stern, C. D. (2000). A cell cycle model for somitogenesis: mathematical formulation and numerical simulation. *Journal of Theoretical Biology* **207**, 305-16.

Colognato, H. and Yurchenco, P. D. (2000). Form and function: the laminin family of heterotrimers. *Developmental Dynamics* **218**, 213-34.

Conlon, F. L., Lyons, K. M., Takaesu, N., Barth, K. S., Kispert, A., Herrmann, B. and Robertson, E. J. (1994). A primary requirement for nodal in the formation and maintenance of the primitive streak in the mouse. *Development* **120**, 1919-28.

Conlon, R. A., Reaume, A. G. and Rossant, J. (1995). Notch1 is required for the coordinate segmentation of somites. *Development* **121**, 1533-45.

Cooke, J. (1998). A gene that resuscitates a theory--somitogenesis and a molecular oscillator. *Trends in Genetics* **14**, 85-8.

Cooke, J. and Elsdale, T. (1980). Somitogenesis in amphibian embryos. III. Effects of ambient temperature and of developmental stage upon pattern abnormalities that follow short temperature shocks. *Journal of Embryology and Experimental Morphology* **58**, 107-18.

Cooke, J. and Zeeman, E. C. (1976). A clock and wavefront model for control of the number of repeated structures during animal morphogenesis. *Journal of Theoretical Biology* **58**, 455-76.

Cooke, J. E. and Moens, C. B. (2002). Boundary formation in the hindbrain: Eph only it were simple. *Trends in Neurosciences* **25**, 260-7.

Copp, A. J., Carvalho, R., Wallace, A., Sorokin, L., Sasaki, T., Greene, N. D. and Ybot-Gonzalez, P. (2011). Regional differences in the expression of laminin isoforms during mouse neural tube development. *Matrix Biology* **30**, 301-9.

Correia, K. M. and Conlon, R. A. (2000). Surface ectoderm is necessary for the morphogenesis of somites. *Mechanisms of Development* **91**, 19-30.

Cox, E. A., Sastry, S. K. and Huttenlocher, A. (2001). Integrin-mediated adhesion regulates cell polarity and membrane protrusion through the Rho family of GTPases. *Molecular Biology of the Cell* **12**, 265-77.

Crawford, B. D., Henry, C. A., Clason, T. A., Becker, A. L. and Hille, M. B. (2003). Activity and distribution of paxillin, focal adhesion kinase, and cadherin indicate cooperative roles during zebrafish morphogenesis. *Molecular Biology of the Cell* **14**, 3065-81.

Critchley, D. R., England, M. A., Wakely, J. and Hynes, R. O. (1979). Distribution of fibronectin in the ectoderm of gastrulating chick embryos. *Nature* **280**, 498-500.

Critchley, D. R. and Gingras, A. R. (2008). Talin at a glance. *Journal of Cell Science* **121**, 1345-7.

Crump, J. G., Swartz, M. E. and Kimmel, C. B. (2004). An integrin-dependent role of pouch endoderm in hyoid cartilage development. *PLoS Biology* **2**, E244.

Cukierman, E., Pankov, R., Stevens, D. R. and Yamada, K. M. (2001). Taking cell-matrix adhesions to the third dimension. *Science* **294**, 1708-12.

Cukierman, E., Pankov, R. and Yamada, K. M. (2002). Cell interactions with three-dimensional matrices. *Current Opinion in Cell Biology* **14**, 633-9.

Dale, J. K., Maroto, M., Dequeant, M. L., Malapert, P., McGrew, M. and Pourquié, O. (2003). Periodic notch inhibition by lunatic fringe underlies the chick segmentation clock. *Nature* **421**, 275-8.

Dale, K. J. and Pourquié, O. (2000). A clock-work somite. *Bioessays* **22**, 72-83.

Damsky, C. H. and Ilic, D. (2002). Integrin signaling: it's where the action is. *Current Opinion in Cell Biology* **14**, 594-602.

Danen, E. H., Aota, S., van Kraats, A. A., Yamada, K. M., Ruiter, D. J. and van Muijen, G. N. (1995). Requirement for the synergy site for cell adhesion to fibronectin depends on the activation state of integrin alpha 5 beta 1. *Journal of Biological Chemistry* **270**, 21612-8.

Danen, E. H., Sonneveld, P., Brakebusch, C., Fassler, R. and Sonnenberg, A. (2002). The fibronectin-binding integrins alpha5beta1 and alphavbeta3 differentially modulate RhoA-GTP loading, organization of cell matrix adhesions, and fibronectin fibrillogenesis. *Journal of Cell Biology* **159**, 1071-86.

Danen, E. H., van Rheenen, J., Franken, W., Huveneers, S., Sonneveld, P., Jalink, K. and Sonnenberg, A. (2005). Integrins control motile strategy through a Rho-cofilin pathway. *Journal of Cell Biology* **169**, 515-26.

Danker, K., Hacke, H. and Wedlich, D. (1992). Effects of heat shock on the pattern of fibronectin and laminin during somitogenesis in Xenopus laevis. *Developmental Dynamics* **193**, 136-44.

Davidson, L. A., Hoffstrom, B. G., Keller, R. and DeSimone, D. W. (2002). Mesendoderm extension and mantle closure in Xenopus laevis gastrulation: combined roles for integrin alpha(5)beta(1), fibronectin, and tissue geometry. *Developmental Biology* **242**, 109-29.

Davidson, L. A., Keller, R. and DeSimone, D. W. (2004). Assembly and remodeling of the fibrillar fibronectin extracellular matrix during gastrulation and neurulation in Xenopus laevis. *Developmental Dynamics* **231**, 888-95.

Davidson, L. A., Marsden, M., Keller, R. and Desimone, D. W. (2006). Integrin alpha5beta1 and fibronectin regulate polarized cell protrusions required for Xenopus convergence and extension. *Current Biology* **16**, 833-44.

De Langhe, S. P., Sala, F. G., Del Moral, P. M., Fairbanks, T. J., Yamada, K. M., Warburton, D., Burns, R. C. and Bellusci, S. (2005). Dickkopf-1 (DKK1) reveals that fibronectin is a major target of Wnt signaling in branching morphogenesis of the mouse embryonic lung. *Developmental Biology* **277**, 316-31.

Deakin, N. O. and Turner, C. E. (2008). Paxillin comes of age. *Journal of Cell Science* **121**, 2435-44.

Delfini, M. C., Dubrulle, J., Malapert, P., Chal, J. and Pourquié, O. (2005). Control of the segmentation process by graded MAPK/ERK activation in the chick embryo. *Proceedings of the National Academy of Sciences of the United States of America* **102**, 11343-8.

Deng, C., Bedford, M., Li, C., Xu, X., Yang, X., Dunmore, J. and Leder, P. (1997). Fibroblast growth factor receptor-1 (FGFR-1) is essential for normal neural tube and limb development. *Developmental Biology* **185**, 42-54.

Dequeant, M. L., Glynn, E., Gaudenz, K., Wahl, M., Chen, J., Mushegian, A. and Pourquié, O. (2006). A complex oscillating network of signaling genes underlies the mouse segmentation clock. *Science* **314**, 1595-8.

Dequeant, M. L. and Pourquié, O. (2008). Segmental patterning of the vertebrate embryonic axis. *Nature Reviews: Genetics* **9**, 370-82.

Deutsch, U., Dressler, G. R. and Gruss, P. (1988). Pax 1, a member of a paired box homologous murine gene family, is expressed in segmented structures during development. *Cell* **53**, 617-25.

Dietrich, S., Schubert, F. R. and Lumsden, A. (1997). Control of dorsoventral pattern in the chick paraxial mesoderm. *Development* **124**, 3895-908.

Diez del Corral, R., Olivera-Martinez, I., Goriely, A., Gale, E., Maden, M. and Storey, K. (2003). Opposing FGF and retinoid pathways control ventral neural pattern, neuronal differentiation, and segmentation during body axis extension. *Neuron* **40**, 65-79.

Diez del Corral, R. and Storey, K. G. (2004). Opposing FGF and retinoid pathways: a signalling switch that controls differentiation and patterning onset in the extending vertebrate body axis. *Bioessays* **26**, 857-69.

Domogatskaya, A., Rodin, S. and Tryggvason, K. (2012). Functional diversity of laminins. *Annual Review of Cell and Developmental Biology* **28**, 523-53.

Dottori, M., Hartley, L., Galea, M., Paxinos, G., Polizzotto, M., Kilpatrick, T., Bartlett, P. F., Murphy, M., Kontgen, F. and Boyd, A. W. (1998). EphA4 (Sek1) receptor tyrosine kinase is required for the development of the corticospinal tract. *Proceedings of the National Academy of Sciences of the United States of America* **95**, 13248-53.

Drees, F., Pokutta, S., Yamada, S., Nelson, W. J. and Weis, W. I. (2005). Alpha-catenin is a molecular switch that binds E-cadherin-beta-catenin and regulates actin-filament assembly. *Cell* **123**, 903-15.

Duband, J. L., Dufour, S., Hatta, K., Takeichi, M., Edelman, G. M. and Thiery, J. P. (1987). Adhesion molecules during somitogenesis in the avian embryo. *Journal of Cell Biology* **104**, 1361-74.

Duband, J. L., Rocher, S., Chen, W. T., Yamada, K. M. and Thiery, J. P. (1986). Cell adhesion and migration in the early vertebrate embryo: location and possible role of the putative fibronectin receptor complex. *Journal of Cell Biology* **102**, 160-78.

Duband, J. L. and Thiery, J. P. (1987). Distribution of laminin and collagens during avian neural crest development. *Development* **101**, 461-78.

Duband, J. L., Volberg, T., Sabanay, I., Thiery, J. P. and Geiger, B. (1988). Spatial and temporal distribution of the adherens-junction-associated adhesion molecule A-CAM during avian embryogenesis. *Development* **103**, 325-44.

Dubrulle, J., McGrew, M. J. and Pourquié, O. (2001). FGF signaling controls somite boundary position and regulates segmentation clock control of spatiotemporal Hox gene activation. *Cell* **106**, 219-32.

Dubrulle, J. and Pourquié, O. (2002). From head to tail: links between the segmentation clock and antero-posterior patterning of the embryo. *Current Opinion in Genetics and Development* **12**, 519-23.

Dubrulle, J. and Pourquié, O. (2004). fgf8 mRNA decay establishes a gradient that couples axial elongation to patterning in the vertebrate embryo. *Nature* **427**, 419-22.

Dubrulle, J. and Pourquié, O. (2004b). Coupling segmentation to axis formation. *Development* **131**, 5783-93.

Dufour, S., Duband, J. L., Humphries, M. J., Obara, M., Yamada, K. M. and Thiery, J. P. (1988). Attachment, spreading and locomotion of avian neural crest cells are mediated by multiple adhesion sites on fibronectin molecules. *EMBO Journal* **7**, 2661-71.

Durbeej, M. (2010). Laminins. *Cell and Tissue Research* **339**, 259-68.

Durbin, L., Brennan, C., Shiomi, K., Cooke, J., Barrios, A., Shanmugalingam, S., Guthrie, B., Lindberg, R. and Holder, N. (1998). Eph signaling is required for segmentation and differentiation of the somites. *Genes & Development* **12**, 3096-109.

Durbin, L., Sordino, P., Barrios, A., Gering, M., Thisse, C., Thisse, B., Brennan, C., Green, A., Wilson, S. and Holder, N. (2000). Anteroposterior patterning is required within segments for somite boundary formation in developing zebrafish. *Development* **127**, 1703-13.

Durston, A. J., Jansen, H. J. and Wacker, S. A. (2010). Review: Time-space translation regulates trunk axial patterning in the early vertebrate embryo. *Genomics* **95**, 250-5.

Dzamba, B. J. and Peters, D. M. (1991). Arrangement of cellular fibronectin in noncollagenous fibrils in human fibroblast cultures. *Journal of Cell Science* **100 (Pt 3)**, 605-12.

Ebensperger, C., Wilting, J., Brand-Saberi, B., Mizutani, Y., Christ, B., Balling, R. and Koseki, H. (1995). Pax-1, a regulator of sclerotome development is induced by notochord and floor plate signals in avian embryos. *Anatomy and Embryology (Berl)* **191**, 297-310.

Eckert, J. J. and Fleming, T. P. (2008). Tight junction biogenesis during early development. *Biochimica et Biophysica Acta* **1778**, 717-28.

Elsdale, T. and Bard, J. (1972). Collagen substrata for studies on cell behavior. *Journal of Cell Biology* **54**, 626-37.

Elsdale, T., Pearson, M. and Whitehead, M. (1976). Abnormalities in somite segmentation following heat shock to Xenopus embryos. *Journal of Embryology and Experimental Morphology* **35**, 625-35.

Etienne-Manneville, S. and Hall, A. (2001). Integrin-mediated activation of Cdc42 controls cell polarity in migrating astrocytes through PKCzeta. *Cell* **106**, 489-98.

Evrard, Y. A., Lun, Y., Aulehla, A., Gan, L. and Johnson, R. L. (1998). lunatic fringe is an essential mediator of somite segmentation and patterning. *Nature* **394**, 377-81.

Fata, J. E., Mori, H., Ewald, A. J., Zhang, H., Yao, E., Werb, Z. and Bissell, M. J. (2007). The MAPK(ERK-1,2) pathway integrates distinct and antagonistic signals from TGFalpha and FGF7 in morphogenesis of mouse mammary epithelium. *Developmental Biology* **306**, 193-207.

Fata, J. E., Werb, Z. and Bissell, M. J. (2004). Regulation of mammary gland branching morphogenesis by the extracellular matrix and its remodeling enzymes. *Breast Cancer Research* **6**, 1-11.

Feller, J., Schneider, A., Schuster-Gossler, K. and Gossler, A. (2008). Noncyclic Notch activity in the presomitic mesoderm demonstrates uncoupling of somite compartmentalization and boundary formation. *Genes & Development* **22**, 2166-71.

Ferrer-Vaquer, A., Viotti, M. and Hadjantonakis, A. K. (2010). Transitions between epithelial and mesenchymal states and the morphogenesis of the early mouse embryo. *Cell Adhesion & Migration* **4**, 447-57.

ffrench-Constant, C. (1995). Alternative splicing of fibronectin--many different proteins but few different functions. *Experimental Cell Research* **221**, 261-71.

Forsberg, H., Crozet, F. and Brown, N. A. (1998). Waves of mouse Lunatic fringe expression, in four-hour cycles at two-hour intervals, precede somite boundary formation. *Current Biology* **8**, 1027-30.

Freitas, C., Rodrigues, S., Charrier, J. B., Teillet, M. A. and Palmeirim, I. (2001). Evidence for medial/lateral specification and positional information within the presomitic mesoderm. *Development* **128**, 5139-47.

Freitas, C., Rodrigues, S., Saúde, L. and Palmeirim, I. (2005). Running after the clock. *International Journal of Developmental Biology* **49**, 317-24.

Friedland, J. C., Lee, M. H. and Boettiger, D. (2009). Mechanically activated integrin switch controls alpha5beta1 function. *Science* **323**, 642-4.

Fujii, H., Sato, T., Kaneko, S., Gotoh, O., Fujii-Kuriyama, Y., Osawa, K., Kato, S. and Hamada, H. (1997). Metabolic inactivation of retinoic acid by a novel P450 differentially expressed in developing mouse embryos. *EMBO Journal* **16**, 4163-73.

Furuta, Y., Ilic, D., Kanazawa, S., Takeda, N., Yamamoto, T. and Aizawa, S. (1995). Mesodermal defect in late phase of gastrulation by a targeted mutation of focal adhesion kinase, FAK. *Oncogene* **11**, 1989-95.

Gahmberg, C. G. and Hakomori, S. I. (1973). Altered growth behavior of malignant cells associated with changes in externally labeled glycoprotein and glycolipid. *Proceedings of the National Academy of Sciences of the United States of America* **70**, 3329-33.

Galceran, J., Sustmann, C., Hsu, S. C., Folberth, S. and Grosschedl, R. (2004). LEF1-mediated regulation of Delta-like1 links Wnt and Notch signaling in somitogenesis. *Genes & Development* **18**, 2718-23.

Garcia-Martinez, V., Darnell, D. K., Lopez-Sanchez, C., Sosic, D., Olson, E. N. and Schoenwolf, G. C. (1997). State of commitment of prospective neural plate and prospective mesoderm in late gastrula/early neurula stages of avian embryos. *Developmental Biology* **181**, 102-15.

Garcia-Martinez, V. and Schoenwolf, G. C. (1992). Positional control of mesoderm movement and fate during avian gastrulation and neurulation. *Developmental Dynamics* **193**, 249-56.

Garcia, A. J., Schwarzbauer, J. E. and Boettiger, D. (2002). Distinct activation states of alpha5beta1 integrin show differential binding to RGD and synergy domains of fibronectin. *Biochemistry* **41**, 9063-9.

Geiger, B., Bershadsky, A., Pankov, R. and Yamada, K. M. (2001). Transmembrane crosstalk between the extracellular matrix--cytoskeleton crosstalk. *Nature Reviews: Molecular Cell Biology* **2**, 793-805.

George-Weinstein, M., Gerhart, J., Blitz, J., Simak, E. and Knudsen, K. A. (1997). N-cadherin promotes the commitment and differentiation of skeletal muscle precursor cells. *Developmental Biology* **185**, 14-24.

George, E. L., Georges-Labouesse, E. N., Patel-King, R. S., Rayburn, H. and Hynes, R. O. (1993). Defects in mesoderm, neural tube and vascular development in mouse embryos lacking fibronectin. *Development* **119**, 1079-91.

Georges-Labouesse, E. N., George, E. L., Rayburn, H. and Hynes, R. O. (1996). Mesodermal development in mouse embryos mutant for fibronectin. *Developmental Dynamics* **207**, 145-56.

Gilbert, S. F. (2006). Developmental Biology. Sunderland (MA): Sinauer Associates.

Ginsberg, M. H., Partridge, A. and Shattil, S. J. (2005). Integrin regulation. *Current Opinion in Cell Biology* **17**, 509-16.

Giudicelli, F. and Lewis, J. (2004). The vertebrate segmentation clock. *Current Opinion in Genetics and Development* **14**, 407-14.

Giudicelli, F., Ozbudak, E. M., Wright, G. J. and Lewis, J. (2007). Setting the tempo in development: an investigation of the zebrafish somite clock mechanism. *PLoS Biology* **5**, e150.

Goh, K. L., Yang, J. T. and Hynes, R. O. (1997). Mesodermal defects and cranial neural crest apoptosis in alpha5 integrin-null embryos. *Development* **124**, 4309-19.

Gomez, C., Ozbudak, E. M., Wunderlich, J., Baumann, D., Lewis, J. and Pourquié, O. (2008). Control of segment number in vertebrate embryos. *Nature* 454, 335-9.

Goody, M. F. and Henry, C. A. (2010). Dynamic interactions between cells and their extracellular matrix mediate embryonic development. *Molecular Reproduction and Development* **77**, 475-88.

Gordon, M. K. and Hahn, R. A. (2010). Collagens. *Cell and Tissue Research* **339**, 247-57.

Gossler, A. and Hrabě de Angelis, M. (1998). Somitogenesis. *Current Topics in Developmental Biology* **38**, 225-87.

Goulding, M., Lumsden, A. and Paquette, A. J. (1994). Regulation of Pax-3 expression in the dermomyotome and its role in muscle development. *Development* **120**, 957-71.

Goulding, M. D., Chalepakis, G., Deutsch, U., Erselius, J. R. and Gruss, P. (1991). Pax-3, a novel murine DNA binding protein expressed during early neurogenesis. *EMBO Journal* **10**, 1135-47.

Goulding, M. D., Lumsden, A. and Gruss, P. (1993). Signals from the notochord and floor plate regulate the region-specific expression of two Pax genes in the developing spinal cord. *Development* **117**, 1001-16.

Green, K. J., Getsios, S., Troyanovsky, S. and Godsel, L. M. (2010). Intercellular junction assembly, dynamics, and homeostasis. *Cold Spring Harbor Perspectives in Biology* **2**, a000125.

Grinnell, F. and Petroll, W. M. (2010). Cell motility and mechanics in three-dimensional collagen matrices. *Annual Review of Cell and Developmental Biology* **26**, 335-61.

Gros, J., Manceau, M., Thome, V. and Marcelle, C. (2005). A common somitic origin for embryonic muscle progenitors and satellite cells. *Nature* **435**, 954-8.

Haenig, B. and Kispert, A. (2004). Analysis of TBX18 expression in chick embryos. *Development Genes and Evolution* **214**, 407-11.

Haffter, P. and Nusslein-Volhard, C. (1996). Large scale genetics in a small vertebrate, the zebrafish. *International Journal of Developmental Biology* **40**, 221-7.

Hagel, M., George, E. L., Kim, A., Tamimi, R., Opitz, S. L., Turner, C. E., Imamoto, A. and Thomas, S. M. (2002). The adaptor protein paxillin is essential for normal development in the mouse and is a critical transducer of fibronectin signaling. *Molecular Biology of the Cell* **22**, 901-15.

Halbleib, J. M. and Nelson, W. J. (2006). Cadherins in development: cell adhesion, sorting, and tissue morphogenesis. *Genes & Development* **20**, 3199-214.

Hall, A. (1998). Rho GTPases and the actin cytoskeleton. *Science* **279**, 509-14.

Hamburger, V. and Hamilton, H. L. (1992). A series of normal stages in the development of the chick embryo. 1951. *Developmental Dynamics* **195**, 231-72.

Harburger, D. S. and Calderwood, D. A. (2009). Integrin signalling at a glance. *Journal of Cell Science* **122**, 159-63.

Harris, T. J. and Tepass, U. (2010). Adherens junctions: from molecules to morphogenesis. *Nature Reviews: Molecular Cell Biology* **11**, 502-14.

Harrisson, F., Vanroelen, C., Foidart, J. M. and Vakaet, L. (1984). Expression of different regional patterns of fibronectin immunoreactivity during mesoblast formation in the chick blastoderm. *Developmental Biology* **101**, 373-81.

Hartsock, A. and Nelson, W. J. (2008). Adherens and tight junctions: structure, function and connections to the actin cytoskeleton. *Biochimica et Biophysica Acta* **1778**, 660-9.

Harunaga, J. S. and Yamada, K. M. (2011). Cell-matrix adhesions in 3D. *Matrix Biology* **30**, 363-8.

Hatada, Y. and Stern, C. D. (1994). A fate map of the epiblast of the early chick embryo. *Development* **120**, 2879-89.

Hatta, K. and Takeichi, M. (1986). Expression of N-cadherin adhesion molecules associated with early morphogenetic events in chick development. *Nature* **320**, 447-9.

He, X., Semenov, M., Tamai, K. and Zeng, X. (2004). LDL receptor-related proteins 5 and 6 in Wnt/beta-catenin signaling: arrows point the way. *Development* **131**, 1663-77.

Heasman, S. J. and Ridley, A. J. (2008). Mammalian Rho GTPases: new insights into their functions from in vivo studies. *Nature Reviews: Molecular Cell Biology* **9**, 690-701.

Helmbacher, F., Schneider-Maunoury, S., Topilko, P., Tiret, L. and Charnay, P. (2000). Targeting of the EphA4 tyrosine kinase receptor affects dorsal/ventral pathfinding of limb motor axons. *Development* **127**, 3313-24.

Henrique, D., Adam, J., Myat, A., Chitnis, A., Lewis, J. and Ish-Horowicz, D. (1995). Expression of a Delta homologue in prospective neurons in the chick. *Nature* **375**, 787-90.

Henry, C. A., Crawford, B. D., Yan, Y. L., Postlethwait, J., Cooper, M. S. and Hille, M. B. (2001). Roles for zebrafish focal adhesion kinase in notochord and somite morphogenesis. *Developmental Biology* **240**, 474-87.

Henry, C. A., Hall, L. A., Burr Hille, M., Solnica-Krezel, L. and Cooper, M. S. (2000). Somites in zebrafish doubly mutant for knypek and trilobite form without internal mesenchymal cells or compaction. *Current Biology* **10**, 1063-6.

Hirata, H., Bessho, Y., Kokubu, H., Masamizu, Y., Yamada, S., Lewis, J. and Kageyama, R. (2004). Instability of Hes7 protein is crucial for the somite segmentation clock. *Nature Genetics* **36**, 750-4.

Hirata, H., Yoshiura, S., Ohtsuka, T., Bessho, Y., Harada, T., Yoshikawa, K. and Kageyama, R. (2002). Oscillatory expression of the bHLH factor Hes1 regulated by a negative feedback loop. *Science* **298**, 840-3.

Hirsinger, E., Jouve, C., Dubrulle, J. and Pourquié, O. (2000). Somite formation and patterning. *International Review of Cytology* **198**, 1-65.

Hofmann, M., Schuster-Gossler, K., Watabe-Rudolph, M., Aulehla, A., Herrmann, B. G. and Gossler, A. (2004). WNT signaling, in synergy with T/TBX6, controls Notch signaling by regulating Dll1 expression in the presomitic mesoderm of mouse embryos. *Genes & Development* **18**, 2712-7.

Holder, N. and Klein, R. (1999). Eph receptors and ephrins: effectors of morphogenesis. *Development* **126**, 2033-44.

Holley, S. A. and Takeda, H. (2002). Catching a wave: the oscillator and wavefront that create the zebrafish somite. *Seminars in Cell & Developmental Biology* **13**, 481-8.

Horikawa, K., Ishimatsu, K., Yoshimoto, E., Kondo, S. and Takeda, H. (2006). Noise-resistant and synchronized oscillation of the segmentation clock. *Nature* **441**, 719-23.

Horikawa, K., Radice, G., Takeichi, M. and Chisaka, O. (1999). Adhesive subdivisions intrinsic to the epithelial somites. *Developmental Biology* **215**, 182-9.

Hrabě de Angelis, M., McIntyre, J., 2nd and Gossler, A. (1997). Maintenance of somite borders in mice requires the Delta homologue Dll1. *Nature* **386**, 717-21.

Huang, R., Zhi, Q., Brand-Saberi, B. and Christ, B. (2000). New experimental evidence for somite resegmentation. *Anatomy and Embryology (Berl)* **202**, 195-200.

Humphries, J. D., Byron, A. and Humphries, M. J. (2006). Integrin ligands at a glance. *Journal of Cell Science* **119**, 3901-3.

Huppert, S. S., Ilagan, M. X., De Strooper, B. and Kopan, R. (2005). Analysis of Notch function in presomitic mesoderm suggests a gamma-secretase-independent role for presenilins in somite differentiation. *Developmental Cell* **8**, 677-88.

Huveneers, S., Truong, H., Fassler, R., Sonnenberg, A. and Danen, E. H. (2008). Binding of soluble fibronectin to integrin alpha5 beta1 - link to focal adhesion redistribution and contractile shape. *Journal of Cell Science* **121**, 2452-62.

Hynes, R. (1985). Molecular biology of fibronectin. *Annual Review of Cell and Developmental Biology* **1**, 67-90.

Hynes, R. O. (1973). Alteration of cell-surface proteins by viral transformation and by proteolysis. *Proceedings of the National Academy of Sciences of the United States of America* **70**, 3170-4.

Hynes, R. O. (1981). Fibronectin and Its Relation to Cellular Structure and Behaviour. In *The Cell Biology of the Extracellular Matrix*, (ed. E. Hay), pp. 295-333. New York: Plenum Press.

Hynes, R. O. (1992). Integrins: versatility, modulation, and signaling in cell adhesion. *Cell* **69**, 11-25.

Hynes, R. O. (2002). Integrins: bidirectional, allosteric signaling machines. *Cell* **110**, 673-87.

Hynes, R. O. (2004). The emergence of integrins: a personal and historical perspective. *Matrix Biology* **23**, 333-40.

Hynes, R. O. and Naba, A. (2012). Overview of the matrisome--an inventory of extracellular matrix constituents and functions. *Cold Spring Harbor Perspectives in Biology* **4**, a004903.

Hynes, R. O. and Yamada, K. M. (1982). Fibronectins: multifunctional modular glycoproteins. *Journal of Cell Biology* **95**, 369-77.

Hynes, R. O. and Zhao, Q. (2000). The evolution of cell adhesion. *Journal of Cell Biology* **150**, F89-96.

Iden, S. and Collard, J. G. (2008). Crosstalk between small GTPases and polarity proteins in cell polarization. *Nature Reviews: Molecular Cell Biology* **9**, 846-59.

Iimura, T. and Pourquié, O. (2006). Collinear activation of Hoxb genes during gastrulation is linked to mesoderm cell ingression. *Nature* **442**, 568-71.

Iimura, T. and Pourquié, O. (2007). Hox genes in time and space during vertebrate body formation. *Development Growth & Differentiation* **49**, 265-75.

Iimura, T., Yang, X., Weijer, C. J. and Pourquié, O. (2007). Dual mode of paraxial mesoderm formation during chick gastrulation. *Proceedings of the National Academy of Sciences of the United States of America* **104**, 2744-9.

Ilic, D., Furuta, Y., Kanazawa, S., Takeda, N., Sobue, K., Nakatsuji, N., Nomura, S., Fujimoto, J., Okada, M. and Yamamoto, T. (1995). Reduced cell motility and enhanced focal adhesion contact formation in cells from FAK-deficient mice. *Nature* **377**, 539-44.

Ilic, D., Kovacic, B., Johkura, K., Schlaepfer, D. D., Tomasevic, N., Han, Q., Kim, J. B., Howerton, K., Baumbusch, C., Ogiwara, N. et al. (2004). FAK promotes organization of fibronectin matrix and fibrillar adhesions. *Journal of Cell Science* **117**, 177-87.

Iozzo, R. V. and Murdoch, A. D. (1996). Proteoglycans of the extracellular environment: clues from the gene and protein side offer novel perspectives in molecular diversity and function. *FASEB Journal* **10**, 598-614.

Irving, C., Nieto, M. A., DasGupta, R., Charnay, P. and Wilkinson, D. G. (1996). Progressive spatial restriction of Sek-1 and Krox-20 gene expression during hindbrain segmentation. *Developmental Biology* **173**, 26-38.

Ishibashi, M., Ang, S. L., Shiota, K., Nakanishi, S., Kageyama, R. and Guillemot, F. (1995). Targeted disruption of mammalian hairy and Enhancer of split homolog-1 (HES-1) leads to up-regulation of neural helix-loop-helix factors, premature neurogenesis, and severe neural tube defects. *Genes & Development* **9**, 3136-48.

Ishimatsu, K., Horikawa, K. and Takeda, H. (2007). Coupling cellular oscillators: a mechanism that maintains synchrony against developmental noise in the segmentation clock. *Developmental Dynamics* **236**, 1416-21.

Iulianella, A., Melton, K. R. and Trainor, P. A. (2003). Somitogenesis: breaking new boundaries. *Neuron* **40**, 11-4.

Jarvelainen, H., Sainio, A., Koulu, M., Wight, T. N. and Penttinen, R. (2009). Extracellular matrix molecules: potential targets in pharmacotherapy. *Pharmacological Reviews* **61**, 198-223.

Jen, W. C., Gawantka, V., Pollet, N., Niehrs, C. and Kintner, C. (1999). Periodic repression of Notch pathway genes governs the segmentation of Xenopus embryos. *Genes & Development* **13**, 1486-99.

Jiang, Y. J., Aerne, B. L., Smithers, L., Haddon, C., Ish-Horowicz, D. and Lewis, J. (2000). Notch signalling and the synchronization of the somite segmentation clock. *Nature* **408**, 475-9.

Johnson, J., Rhee, J., Parsons, S. M., Brown, D., Olson, E. N. and Rawls, A. (2001). The anterior/posterior polarity of somites is disrupted in paraxis-deficient mice. *Developmental Biology* **229**, 176-87.

Johnston, S. H., Rauskolb, C., Wilson, R., Prabhakaran, B., Irvine, K. D. and Vogt, T. F. (1997). A family of mammalian Fringe genes implicated in boundary determination and the Notch pathway. *Development* **124**, 2245-54.

Jouve, C., Palmeirim, I., Henrique, D., Beckers, J., Gossler, A., Ish-Horowicz, D. and Pourquié, O. (2000). Notch signalling is required for cyclic expression of the hairy-like gene HES1 in the presomitic mesoderm. *Development* **127**, 1421-9.

Jülich, D., Geisler, R., Consortium, T. S. and Holley, S. A. (2005). Integrinalpha5 and delta/notch signaling have complementary spatiotemporal requirements during zebrafish somitogenesis. *Developmental Cell* **8**, 575-86.

Kageyama, R., Masamizu, Y. and Niwa, Y. (2007). Oscillator mechanism of Notch pathway in the segmentation clock. *Developmental Dynamics* **236**, 1403-9.

Kalluri, R. and Weinberg, R. A. (2009). The basics of epithelial-mesenchymal transition. *Journal of Clinical Investigation* **119**, 1420-8.

Kassar-Duchossoy, L., Giacone, E., Gayraud-Morel, B., Jory, A., Gomes, D. and Tajbakhsh, S. (2005). Pax3/Pax7 mark a novel population of primitive myogenic cells during development. *Genes & Development* **19**, 1426-31.

Katsube, K. and Sakamoto, K. (2005). Notch in vertebrates--molecular aspects of the signal. *International Journal of Developmental Biology* **49**, 369-74.

Kelly, O. G., Pinson, K. I. and Skarnes, W. C. (2004). The Wnt co-receptors Lrp5 and Lrp6 are essential for gastrulation in mice. *Development* **131**, 2803-15.

Keynes, R. J. and Stern, C. D. (1984). Segmentation in the vertebrate nervous system. *Nature* **310**, 786-9.

Keynes, R. J. and Stern, C. D. (1988). Mechanisms of vertebrate segmentation. *Development* **103**, 413-29.

Keynes, R. J., Stirling, R. V., Stern, C. D. and Summerbell, D. (1987). The specificity of motor innervation of the chick wing does not depend upon the segmental origin of muscles. *Development* **99**, 565-75.

Kieny, M., Mauger, A. and Sengel, P. (1972). Early regionalization of somitic mesoderm as studied by the development of axial skeleton of the chick embryo. *Developmental Biology* **28**, 142-61.

Kim, C., Ye, F. and Ginsberg, M. H. (2011). Regulation of integrin activation. *Annual Review of Cell and Developmental Biology* **27**, 321-45.

Kimmel, C. B., Ballard, W. W., Kimmel, S. R., Ullmann, B. and Schilling, T. F. (1995). Stages of embryonic development of the zebrafish. *Developmental Dynamics* **203**, 253-310.

Kimura, Y., Matsunami, H., Inoue, T., Shimamura, K., Uchida, N., Ueno, T., Miyazaki, T. and Takeichi, M. (1995). Cadherin-11 expressed in association with mesenchymal morphogenesis in the head, somite, and limb bud of early mouse embryos. *Developmental Biology* **169**, 347-58.

Klinowska, T. C., Soriano, J. V., Edwards, G. M., Oliver, J. M., Valentijn, A. J., Montesano, R. and Streuli, C. H. (1999). Laminin and beta1 integrins are crucial for normal mammary gland development in the mouse. *Developmental Biology* **215**, 13-32.

Kmita, M. and Duboule, D. (2003). Organizing axes in time and space; 25 years of colinear tinkering. *Science* **301**, 331-3.

Knezevic, V., De Santo, R. and Mackem, S. (1997). Two novel chick T-box genes related to mouse Brachyury are expressed in different, non-overlapping mesodermal domains during gastrulation. *Development* **124**, 411-9.

Kondoh, H. and Takemoto, T. (2012). Axial stem cells deriving both posterior neural and mesodermal tissues during gastrulation. *Current Opinion in Genetics and Development* **22**, 374-80.

Kosher, R. A. and Solursh, M. (1989). Widespread distribution of type II collagen during embryonic chick development. *Developmental Biology* **131**, 558-66.

Koshida, S., Kishimoto, Y., Ustumi, H., Shimizu, T., Furutani-Seiki, M., Kondoh, H. and Takada, S. (2005). Integrinalpha5-dependent fibronectin accumulation for maintenance of somite boundaries in zebrafish embryos. *Developmental Cell* **8**, 587-98.

Kragtorp, K. A. and Miller, J. R. (2006). Regulation of somitogenesis by Ena/VASP proteins and FAK during Xenopus development. *Development* **133**, 685-95.

Kragtorp, K. A. and Miller, J. R. (2007). Integrin alpha5 is required for somite rotation and boundary formation in Xenopus. *Developmental Dynamics* **236**, 2713-20.

Kraus, F., Haenig, B. and Kispert, A. (2001). Cloning and expression analysis of the mouse T-box gene Tbx18. *Mechanisms of Development* **100**, 83-6.

Krotoski, D. M., Domingo, C. and Bronner-Fraser, M. (1986). Distribution of a putative cell surface receptor for fibronectin and laminin in the avian embryo. *Journal of Cell Biology* **103**, 1061-71.

Kruegel, J. and Miosge, N. (2010). Basement membrane components are key players in specialized extracellular matrices. *Cellular and Molecular Life Sciences* **67**, 2879-95.

Krull, C. E. (2001). Segmental organization of neural crest migration. *Mechanisms of Development* **105**, 37-45.

Kuan, C. Y., Tannahill, D., Cook, G. M. and Keynes, R. J. (2004). Somite polarity and segmental patterning of the peripheral nervous system. *Mechanisms of Development* **121**, 1055-68.

Kulesa, P. M. and Fraser, S. E. (2002). Cell dynamics during somite boundary formation revealed by time-lapse analysis. *Science* **298**, 991-5.

Kulesa, P. M., Schnell, S., Rudloff, S., Baker, R. E. and Maini, P. K. (2007). From segment to somite: segmentation to epithelialization analyzed within quantitative frameworks. *Developmental Dynamics* **236**, 1392-402.

Kusumi, K., Sun, E. S., Kerrebrock, A. W., Bronson, R. T., Chi, D. C., Bulotsky, M. S., Spencer, J. B., Birren, B. W., Frankel, W. N. and Lander, E. S. (1998). The mouse pudgy mutation disrupts Delta homologue Dll3 and initiation of early somite boundaries. *Nature Genetics* **19**, 274-8.

Larsen, M., Wei, C. and Yamada, K. M. (2006). Cell and fibronectin dynamics during branching morphogenesis. *Journal of Cell Science* **119**, 3376-84.

Lash, J. W., Linask, K. K. and Yamada, K. M. (1987). Synthetic peptides that mimic the adhesive recognition signal of fibronectin: differential effects on cell-cell and cell-substratum adhesion in embryonic chick cells. *Developmental Biology* **123**, 411-20.

Lash, J. W. and Ostrovsky, D. (1986). On the formation of somites. In *Developmental Biology (N.Y.)*, vol. 2 (ed. L. Browder), pp. 547-563. New York: Plenum Press.

Lash, J. W., Ostrovsky, D., Mittal, B. and Sanger, J. W. (1985). Alpha actinin distribution and extracellular matrix products during somitogenesis and neurulation in the chick embryo. *Cell Motility* **5**, 491-506.

Lash, J. W., Seitz, A. W., Cheney, C. M. and Ostrovsky, D. (1984). On the role of fibronectin during the compaction stage of somitogenesis in the chick embryo. *Journal of Experimental Zoology* **232**, 197-206.

Lash, J. W. and Yamada, K. M. (1986). The adhesion recognition signal of fibronectin: a possible trigger mechanism for compaction during somitogenesis. In *Somites in Developing Embryos*, (ed. R. Bellairs D. A. Ede and J. W. Lash), pp. 201-208. New York: Plenum Press.

Legate, K. R. and Fassler, R. (2009). Mechanisms that regulate adaptor binding to beta-integrin cytoplasmic tails. *Journal of Cell Science* **122**, 187-98.

Legate, K. R., Montanez, E., Kudlacek, O. and Fassler, R. (2006). ILK, PINCH and parvin: the tIPP of integrin signalling. *Nature Reviews: Molecular Cell Biology* **7**, 20-31.

Leitges, M., Neidhardt, L., Haenig, B., Herrmann, B. G. and Kispert, A. (2000). The paired homeobox gene Uncx4.1 specifies pedicles, transverse processes and proximal ribs of the vertebral column. *Development* **127**, 2259-67.

Lewis, J., Hanisch, A. and Holder, M. (2009). Notch signaling, the segmentation clock, and the patterning of vertebrate somites. *Journal of Biology* **8**, 44.

Li, M. L., Aggeler, J., Farson, D. A., Hatier, C., Hassell, J. and Bissell, M. J. (1987). Influence of a reconstituted basement membrane and its components on casein gene expression and secretion in mouse mammary epithelial cells. *Proceedings of the National Academy of Sciences of the United States of America* **84**, 136-40.

Li, R. A. and Storey, K. G. (2011). An emerging molecular mechanism for the neural vs mesodermal cell fate decision. *Cell Research* **21**, 708-10.

Li, S., Edgar, D., Fassler, R., Wadsworth, W. and Yurchenco, P. D. (2003). The role of laminin in embryonic cell polarization and tissue organization. *Developmental Cell* **4**, 613-24.

Li, S., Harrison, D., Carbonetto, S., Fassler, R., Smyth, N., Edgar, D. and Yurchenco, P. D. (2002). Matrix assembly, regulation, and survival functions of laminin and its receptors in embryonic stem cell differentiation. *Journal of Cell Biology* **157**, 1279-90.

Lin, X. (2004). Functions of heparan sulfate proteoglycans in cell signaling during development. *Development* **131**, 6009-21.

Linask, K. K., Ludwig, C., Han, M. D., Liu, X., Radice, G. L. and Knudsen, K. A. (1998). N-cadherin/catenin-mediated morphoregulation of somite formation. *Developmental Biology* **202**, 85-102.

Linask, K. K., Manisastry, S. and Han, M. (2005). Cross talk between cell-cell and cell-matrix adhesion signaling pathways during heart organogenesis: implications for cardiac birth defects. *Microscopy and Microanalysis* **11**, 200-8.

Linker, C., Lesbros, C., Gros, J., Burrus, L. W., Rawls, A. and Marcelle, C. (2005). beta-Catenin-dependent Wnt signalling controls the epithelial organisation of somites through the activation of paraxis. *Development* **132**, 3895-905.

Linker, C., Lesbros, C., Stark, M. R. and Marcelle, C. (2003). Intrinsic signals regulate the initial steps of myogenesis in vertebrates. *Development* **130**, 4797-807.

Lipton, B. H. and Jacobson, A. G. (1974). Analysis of normal somite development. *Developmental Biology* **38**, 73-90.

Liu, P., Wakamiya, M., Shea, M. J., Albrecht, U., Behringer, R. R. and Bradley, A. (1999). Requirement for Wnt3 in vertebrate axis formation. *Nature Genetics* **22**, 361-5.

Luo, B. H., Carman, C. V. and Springer, T. A. (2007). Structural basis of integrin regulation and signaling. *Annual Review of Immunology* **25**, 619-47.

Magnusson, M. K. and Mosher, D. F. (1998). Fibronectin: structure, assembly, and cardiovascular implications. *Arteriosclerosis, Thrombosis, and Vascular Biology* **18**, 1363-70.

Mallo, M., Vinagre, T. and Carapuço, M. (2009). The road to the vertebral formula. *International Journal of Developmental Biology* **53**, 1469-81.

Mallo, M., Wellik, D. M. and Deschamps, J. (2010). Hox genes and regional patterning of the vertebrate body plan. *Developmental Biology* **344**, 7-15.

Manabe, T., Togashi, H., Uchida, N., Suzuki, S. C., Hayakawa, Y., Yamamoto, M., Yoda, H., Miyakawa, T., Takeichi, M. and Chisaka, O. (2000). Loss of cadherin-11 adhesion receptor enhances plastic changes in hippocampal synapses and modifies behavioral responses. *Molecular and Cellular Neuroscience* **15**, 534-46.

Mansouri, A., Voss, A. K., Thomas, T., Yokota, Y. and Gruss, P. (2000). Uncx4.1 is required for the formation of the pedicles and proximal ribs and acts upstream of Pax9. *Development* **127**, 2251-8.

Mansouri, A., Yokota, Y., Wehr, R., Copeland, N. G., Jenkins, N. A. and Gruss, P. (1997). Paired-related murine homeobox gene expressed in the developing sclerotome, kidney, and nervous system. *Developmental Dynamics* **210**, 53-65.

Mao, Y. and Schwarzbauer, J. E. (2005a). Fibronectin fibrillogenesis, a cell-mediated matrix assembly process. *Matrix Biology* **24**, 389-99.

Mao, Y. and Schwarzbauer, J. E. (2005b). Stimulatory effects of a three-dimensional microenvironment on cell-mediated fibronectin fibrillogenesis. *Journal of Cell Science* **118**, 4427-36.

Mao, Y. and Schwarzbauer, J. E. (2006). Accessibility to the fibronectin synergy site in a 3D matrix regulates engagement of alpha5beta1 versus alphavbeta3 integrin receptors. *Cell Communication & Adhesion* **13**, 267-77.

Maroto, M., Dale, J. K., Dequeant, M. L., Petit, A. C. and Pourquié, O. (2005). Synchronised cycling gene oscillations in presomitic mesoderm cells require cell-cell contact. *International Journal of Developmental Biology* **49**, 309-15.

Marsden, M. and DeSimone, D. W. (2001). Regulation of cell polarity, radial intercalation and epiboly in Xenopus: novel roles for integrin and fibronectin. *Development* **128**, 3635-47.

Marsden, M. and DeSimone, D. W. (2003). Integrin-ECM interactions regulate cadherin-dependent cell adhesion and are required for convergent extension in Xenopus. *Current Biology* **13**, 1182-91.

Masamizu, Y., Ohtsuka, T., Takashima, Y., Nagahara, H., Takenaka, Y., Yoshikawa, K., Okamura, H. and Kageyama, R. (2006). Real-time imaging of the somite segmentation clock: revelation of unstable oscillators in the individual presomitic mesoderm cells. *Proceedings of the National Academy of Sciences of the United States of America* **103**, 1313-8.

Maurer, L. M., Tomasini-Johansson, B. R. and Mosher, D. F. (2010). Emerging roles of fibronectin in thrombosis. *Thrombosis Research* **125**, 287-91.

McDonald, J. A., Quade, B. J., Broekelmann, T. J., LaChance, R., Forsman, K., Hasegawa, E. and Akiyama, S. (1987). Fibronectin's cell-adhesive domain and an amino-terminal matrix assembly domain participate in its assembly into fibroblast pericellular matrix. *Journal of Biological Chemistry* **262**, 2957-67.

McGrew, M. J., Dale, J. K., Fraboulet, S. and Pourquié, O. (1998). The lunatic fringe gene is a target of the molecular clock linked to somite segmentation in avian embryos. *Current Biology* **8**, 979-82.

McKeown-Longo, P. J. and Mosher, D. F. (1983). Binding of plasma fibronectin to cell layers of human skin fibroblasts. *Journal of Cell Biology* **97**, 466-72.

McKeown-Longo, P. J. and Mosher, D. F. (1985). Interaction of the 70,000-mol-wt amino-terminal fragment of fibronectin with the matrix-assembly receptor of fibroblasts. *Journal of Cell Biology* **100**, 364-74.

Meinhardt, H. (1982). Digits, segments, somites: the superposition of periodic and sequential structures. In *Models of biological pattern formation*, pp. 152-171: London Academic Press.

Meinhardt, H. (1986). Models of segmentation. In *Somites in Developing Embryos*, (ed. R. Bellairs D. A. Ede and J. W. Lash), pp. 179-189. New York: Plenum Press.

Miner, J. H., Li, C., Mudd, J. L., Go, G. and Sutherland, A. E. (2004). Compositional and structural requirements for laminin and basement membranes during mouse embryo implantation and gastrulation. *Development* **131**, 2247-56.

Miner, J. H. and Yurchenco, P. D. (2004). Laminin functions in tissue morphogenesis. *Annual Review of Cell and Developmental Biology* **20**, 255-84.

Miranti, C. K. and Brugge, J. S. (2002). Sensing the environment: a historical perspective on integrin signal transduction. *Nature Cell Biology* **4**, E83-90.

Mitra, S. K., Hanson, D. A. and Schlaepfer, D. D. (2005). Focal adhesion kinase: in command and control of cell motility. *Nature Reviews: Molecular Cell Biology* **6**, 56-68.

Miyamoto, S., Akiyama, S. K. and Yamada, K. M. (1995). Synergistic roles for receptor occupancy and aggregation in integrin transmembrane function. *Science* **267**, 883-5.

Miyamoto, S., Katz, B. Z., Lafrenie, R. M. and Yamada, K. M. (1998). Fibronectin and integrins in cell adhesion, signaling, and morphogenesis. *Annals of the New York Academy of Sciences* **857**, 119-29.

Monsoro-Burq, A. H. (2005). Sclerotome development and morphogenesis: when experimental embryology meets genetics. *International Journal of Developmental Biology* **49**, 301-8.

Moreno, T. A. and Kintner, C. (2004). Regulation of segmental patterning by retinoic acid signaling during Xenopus somitogenesis. *Developmental Cell* **6**, 205-18.

Morimoto, M., Sasaki, N., Oginuma, M., Kiso, M., Igarashi, K., Aizaki, K., Kanno, J. and Saga, Y. (2007). The negative regulation of Mesp2 by mouse Ripply2 is required to establish the rostro-caudal patterning within a somite. *Development* **134**, 1561-9.

Morimoto, M., Takahashi, Y., Endo, M. and Saga, Y. (2005). The Mesp2 transcription factor establishes segmental borders by suppressing Notch activity. *Nature* **435**, 354-9.

Moser, M., Legate, K. R., Zent, R. and Fassler, R. (2009). The tail of integrins, talin, and kindlins. *Science* **324**, 895-9.

Mould, A. P. and Humphries, M. J. (2004). Regulation of integrin function through conformational complexity: not simply a knee-jerk reaction? *Current Opinion in Cell Biology* **16**, 544-51.

Myllyharju, J. and Kivirikko, K. I. (2004). Collagens, modifying enzymes and their mutations in humans, flies and worms. *Trends in Genetics* **20**, 33-43.

Nagai, T., Yamakawa, N., Aota, S., Yamada, S. S., Akiyama, S. K., Olden, K. and Yamada, K. M. (1991). Monoclonal antibody characterization of two distant sites required for function of the central cell-binding domain of fibronectin in cell adhesion, cell migration, and matrix assembly. *Journal of Cell Biology* **114**, 1295-305.

Nagel, M. and Winklbauer, R. (1999). Establishment of substratum polarity in the blastocoel roof of the Xenopus embryo. *Development* **126**, 1975-84.

Naiche, L. A., Harrelson, Z., Kelly, R. G. and Papaioannou, V. E. (2005). T-box genes in vertebrate development. *Annual Review of Genetics* **39**, 219-39.

Nakajima, Y., Morimoto, M., Takahashi, Y., Koseki, H. and Saga, Y. (2006). Identification of Epha4 enhancer required for segmental expression and the regulation by Mesp2. *Development* **133**, 2517-25.

Nakaya, M. A., Biris, K., Tsukiyama, T., Jaime, S., Rawls, J. A. and Yamaguchi, T. P. (2005). Wnt3a links left-right determination with segmentation and anteroposterior axis elongation. *Development* **132**, 5425-36.

Nakaya, Y. and Sheng, G. (2008). Epithelial to mesenchymal transition during gastrulation: an embryological view. *Development Growth & Differentiation* **50**, 755-66.

Nakaya, Y., Sukowati, E. W., Wu, Y. and Sheng, G. (2008). RhoA and microtubule dynamics control cell-basement membrane interaction in EMT during gastrulation. *Nature Cell Biology* **10**, 765-75.

Nelson, C. M. and Bissell, M. J. (2006). Of extracellular matrix, scaffolds, and signaling: tissue architecture regulates development, homeostasis, and cancer. *Annual Review of Cell and Developmental Biology* **22**, 287-309.

Nelson, W. J. (2009). Remodeling epithelial cell organization: transitions between front-rear and apical-basal polarity. *Cold Spring Harbor Perspectives in Biology* **1**, a000513.

Newgreen, D. and Thiery, J. P. (1980). Fibronectin in early avian embryos: synthesis and distribution along the migration pathways of neural crest cells. *Cell and Tissue Research* **211**, 269-91.

Niederreither, K., McCaffery, P., Drager, U. C., Chambon, P. and Dolle, P. (1997). Restricted expression and retinoic acid-induced downregulation of the retinaldehyde dehydrogenase type 2 (RALDH-2) gene during mouse development. *Mechanisms of Development* **62**, 67-78.

Niessen, C. M. (2007). Tight junctions/adherens junctions: basic structure and function. *The Journal of Investigative Dermatology* **127**, 2525-32.

Nieto, M. A. (2002). The snail superfamily of zinc-finger transcription factors. *Nature Reviews: Molecular Cell Biology* **3**, 155-66.

Nieto, M. A. (2011). The ins and outs of the epithelial to mesenchymal transition in health and disease. *Annual Review of Cell and Developmental Biology* **27**, 347-76.

Nieto, M. A., Gilardi-Hebenstreit, P., Charnay, P. and Wilkinson, D. G. (1992). A receptor protein tyrosine kinase implicated in the segmental patterning of the hindbrain and mesoderm. *Development* **116**, 1137-50.

Nikaido, M., Kawakami, A., Sawada, A., Furutani-Seiki, M., Takeda, H. and Araki, K. (2002). Tbx24, encoding a T-box protein, is mutated in the zebrafish somite-segmentation mutant fused somites. *Nature Genetics* **31**, 195-9.

Niwa, Y., Masamizu, Y., Liu, T., Nakayama, R., Deng, C. X. and Kageyama, R. (2007). The initiation and propagation of Hes7 oscillation are cooperatively regulated by Fgf and notch signaling in the somite segmentation clock. *Developmental Cell* **13**, 298-304.

Nusse, R. (2012). Wnt signaling. Cold Spring Harbor Perspectives in Biology **4**.

Oates, A. C., Morelli, L. G. and Ares, S. (2012). Patterning embryos with oscillations: structure, function and dynamics of the vertebrate segmentation clock. *Development* **139**, 625-39.

Oda, H. and Takeichi, M. (2011). Evolution: structural and functional diversity of cadherin at the adherens junction. *Journal of Cell Biology* **193**, 1137-46.

Ohashi, T. and Erickson, H. P. (2009). Revisiting the mystery of fibronectin multimers: the fibronectin matrix is composed of fibronectin dimers cross-linked by non-covalent bonds. *Matrix Biology* **28**, 170-5.

Ohashi, T., Kiehart, D. P. and Erickson, H. P. (2002). Dual labeling of the fibronectin matrix and actin cytoskeleton with green fluorescent protein variants. *Journal of Cell Science* **115**, 1221-9.

Ohtsuka, T., Ishibashi, M., Gradwohl, G., Nakanishi, S., Guillemot, F. and Kageyama, R. (1999). Hes1 and Hes5 as notch effectors in mammalian neuronal differentiation. *EMBO Journal* **18**, 2196-207.

Oka, C., Nakano, T., Wakeham, A., de la Pompa, J. L., Mori, C., Sakai, T., Okazaki, S., Kawaichi, M., Shiota, K., Mak, T. W. et al. (1995). Disruption of the mouse RBP-J kappa gene results in early embryonic death. *Development* **121**, 3291-301.

Ooi, V. E., Sanders, E. J. and Bellairs, R. (1986). The contribution of the primitive streak to the somites in the avian embryo. *Journal of Embryology and Experimental Morphology* **92**, 193-206.

Orr-Urtreger, A., Givol, D., Yayon, A., Yarden, Y. and Lonai, P. (1991). Developmental expression of two murine fibroblast growth factor receptors, flg and bek. *Development* **113**, 1419-34.

Ostrovsky, D., Cheney, C. M., Seitz, A. W. and Lash, J. W. (1983). Fibronectin distribution during somitogenesis in the chick embryo. *Cell Differentiation* **13**, 217-23.

Otto, A., Schmidt, C. and Patel, K. (2006). Pax3 and Pax7 expression and regulation in the avian embryo. *Anatomy and Embryology (Berl)* **211**, 293-310.

Ozbudak, E. M. and Lewis, J. (2008). Notch signalling synchronizes the zebrafish segmentation clock but is not needed to create somite boundaries. *PLoS Genetics* **4**, e15.

Ozbudak, E. M. and Pourquié, O. (2008). The vertebrate segmentation clock: the tip of the iceberg. *Current Opinion in Genetics and Development* **18**, 317-23.

Packard, D. S., Jr. (1978). Chick somite determination: the role of factors in young somites and the segmental plate. *Journal of Experimental Zoology* **203**, 295-306.

Packard, D. S., Jr. (1980). Somitogenesis in cultured embryos of the Japanese quail, Coturnix coturnix japonica. *American Journal of Anatomy* **158**, 83-91.

Packard, D. S., Jr. and Jacobson, A. G. (1976). The influence of axial structures on chick somite formation. *Developmental Biology* **53**, 36-48.

Packard, D. S., Jr., Zheng, R. Z. and Turner, D. C. (1993). Somite pattern regulation in the avian segmental plate mesoderm. *Development* **117**, 779-91.

Palmeirim, I., Dubrulle, J., Henrique, D., Ish-Horowicz, D. and Pourquié, O. (1998). Uncoupling segmentation and somitogenesis in the chick presomitic mesoderm. *Developmental Genetics* **23**, 77-85.

Palmeirim, I., Henrique, D., Ish-Horowicz, D. and Pourquié, O. (1997). Avian hairy gene expression identifies a molecular clock linked to vertebrate segmentation and somitogenesis. *Cell* **91**, 639-48.

Pankov, R., Cukierman, E., Katz, B. Z., Matsumoto, K., Lin, D. C., Lin, S., Hahn, C. and Yamada, K. M. (2000). Integrin dynamics and matrix assembly: tensin-dependent translocation of alpha(5)beta(1) integrins promotes early fibronectin fibrillogenesis. *Journal of Cell Biology* **148**, 1075-90.

Pankov, R. and Yamada, K. M. (2002). Fibronectin at a glance. *Journal of Cell Science* **115**, 3861-3.

Pasquale, E. B. (2005). Eph receptor signalling casts a wide net on cell behaviour. *Nature Reviews: Molecular Cell Biology* **6**, 462-75.

Pasquale, E. B. (2008). Eph-ephrin bidirectional signaling in physiology and disease. *Cell* **133**, 38-52.

Pasquale, E. B. (2010). Eph receptors and ephrins in cancer: bidirectional signalling and beyond. *Nature Reviews: Cancer* **10**, 165-80.

Pearson, M. and Elsdale, T. (1979). Somitogenesis in amphibian embryos. I. Experimental evidence for an interaction between two temporal factors in the specification of somite pattern. *Journal of Embryology and Experimental Morphology* **51**, 27-50.

Perris, R. and Perissinotto, D. (2000). Role of the extracellular matrix during neural crest cell migration. *Mechanisms of Development* **95**, 3-21.

Peters, D. M. and Mosher, D. F. (1987). Localization of cell surface sites involved in fibronectin fibrillogenesis. *Journal of Cell Biology* **104**, 121-30.

Peters, D. M., Portz, L. M., Fullenwider, J. and Mosher, D. F. (1990). Co-assembly of plasma and cellular fibronectins into fibrils in human fibroblast cultures. *Journal of Cell Biology* **111**, 249-56.

Peters, H., Wilm, B., Sakai, N., Imai, K., Maas, R. and Balling, R. (1999). Pax1 and Pax9 synergistically regulate vertebral column development. *Development* **126**, 5399-408.

Pierschbacher, M. D. and Ruoslahti, E. (1984). Cell attachment activity of fibronectin can be duplicated by small synthetic fragments of the molecule. *Nature* **309**, 30-3.

Pierschbacher, M. D., Ruoslahti, E., Sundelin, J., Lind, P. and Peterson, P. A. (1982). The cell attachment domain of fibronectin. Determination of the primary structure. *Journal of Biological Chemistry* **257**, 9593-7.

Piez, K. A. (1997). History of extracellular matrix: a personal view. *Matrix Biology* **16**, 85-92.

Pokutta, S. and Weis, W. I. (2007). Structure and mechanism of cadherins and catenins in cell-cell contacts. *Annual Review of Cell and Developmental Biology* **23**, 237-61.

Potts, J. R. and Campbell, I. D. (1994). Fibronectin structure and assembly. *Current Opinion in Cell Biology* **6**, 648-55.

Pourquié, O. (2003). Vertebrate somitogenesis: a novel paradigm for animal segmentation? *International Journal of Developmental Biology* **47**, 597-603.

Pourquié, O. (2004). The chick embryo: a leading model in somitogenesis studies. *Mechanisms of Development* **121**, 1069-79.

Pourquié, O. (2011). Vertebrate segmentation: from cyclic gene networks to scoliosis. *Cell* **145**, 650-63.

Pourquié, O. (2001). Vertebrate somitogenesis. *Annual Review of Cell and Developmental Biology* **17**, 311-50.

Pourquié, O., Fan, C. M., Coltey, M., Hirsinger, E., Watanabe, Y., Breant, C., Francis-West, P., Brickell, P., Tessier-Lavigne, M. and Le Douarin, N. M. (1996). Lateral and axial signals involved in avian somite patterning: a role for BMP4. *Cell* **84**, 461-71.

Pourquié, O. and Tam, P. P. (2001). A nomenclature for prospective somites and phases of cyclic gene expression in the presomitic mesoderm. *Developmental Cell* **1**, 619-20.

Price, L. S., Leng, J., Schwartz, M. A. and Bokoch, G. M. (1998). Activation of Rac and Cdc42 by integrins mediates cell spreading. *Molecular Biology of the Cell* **9**, 1863-71.

Primmett, D. R., Norris, W. E., Carlson, G. J., Keynes, R. J. and Stern, C. D. (1989). Periodic segmental anomalies induced by heat shock in the chick embryo are associated with the cell cycle. *Development* **105**, 119-30.

Primmett, D. R., Stern, C. D. and Keynes, R. J. (1988). Heat shock causes repeated segmental anomalies in the chick embryo. *Development* **104**, 331-9.

Psychoyos, D. and Stern, C. D. (1996). Fates and migratory routes of primitive streak cells in the chick embryo. *Development* **122**, 1523-34.

Qin, J., Vinogradova, O. and Plow, E. F. (2004). Integrin bidirectional signaling: a molecular view. *PLoS Biology* **2**, e169.

Radice, G. L., Rayburn, H., Matsunami, H., Knudsen, K. A., Takeichi, M. and Hynes, R. O. (1997). Developmental defects in mouse embryos lacking N-cadherin. *Developmental Biology* **181**, 64-78.

Reaume, A. G., Conlon, R. A., Zirngibl, R., Yamaguchi, T. P. and Rossant, J. (1992). Expression analysis of a Notch homologue in the mouse embryo. *Developmental Biology* **154**, 377-87.

Relaix, F., Rocancourt, D., Mansouri, A. and Buckingham, M. (2005). A Pax3/Pax7-dependent population of skeletal muscle progenitor cells. *Nature* **435**, 948-53.

Rhinn, M. and Dolle, P. (2012). Retinoic acid signalling during development. *Development* **139**, 843-58.

Ricard-Blum, S. and Ruggiero, F. (2005). The collagen superfamily: from the extracellular matrix to the cell membrane. *Pathologie Biologie* **53**, 430-42.

Richardson, M. K., Allen, S. P., Wright, G. M., Raynaud, A. and Hanken, J. (1998). Somite number and vertebrate evolution. *Development* **125**, 151-60.

Rida, P. C., Le Minh, N. and Jiang, Y. J. (2004). A Notch feeling of somite segmentation and beyond. *Developmental Biology* **265**, 2-22.

Robb, L. and Tam, P. P. (2004). Gastrula organiser and embryonic patterning in the mouse. *Seminars in Cell & Developmental Biology* **15**, 543-54.

Rossant, J., Zirngibl, R., Cado, D., Shago, M. and Giguere, V. (1991). Expression of a retinoic acid response element-hsplacZ transgene defines specific domains of transcriptional activity during mouse embryogenesis. *Genes & Development* **5**, 1333-44.

Rozario, T. and DeSimone, D. W. (2010). The extracellular matrix in development and morphogenesis: a dynamic view. *Developmental Biology* **341**, 126-40.

Ruoslahti, E. (1988). Fibronectin and its receptors. *Annual Review of Biochemistry* **57**, 375-413.

Ruoslahti, E. (1996). RGD and other recognition sequences for integrins. *Annual Review of Cell and Developmental Biology* **12**, 697-715.

Ruoslahti, E. (2003). The RGD story: a personal account. *Matrix Biology* **22**, 459-65.

Ruoslahti, E., Vaheri, A., Kuusela, P. and Linder, E. (1973). Fibroblast surface antigen: a new serum protein. *Biochimica et Biophysica Acta* **322**, 352-8.

Saga, Y. (2007). Segmental border is defined by the key transcription factor Mesp2, by means of the suppression of Notch activity. *Developmental Dynamics* **236**, 1450-5.

Saga, Y. (2012). The mechanism of somite formation in mice. *Current Opinion in Genetics and Development* **22**, 331-8.

Saga, Y., Hata, N., Kobayashi, S., Magnuson, T., Seldin, M. F. and Taketo, M. M. (1996). MesP1: a novel basic helix-loop-helix protein expressed in the nascent mesodermal cells during mouse gastrulation. *Development* **122**, 2769-78.

Saga, Y., Hata, N., Koseki, H. and Taketo, M. M. (1997). Mesp2: a novel mouse gene expressed in the presegmented mesoderm and essential for segmentation initiation. *Genes & Development* **11**, 1827-39.

Saga, Y. and Takeda, H. (2001). The making of the somite: molecular events in vertebrate segmentation. *Nature Reviews: Genetics* **2**, 835-45.

Sakai, T., Larsen, M. and Yamada, K. M. (2003). Fibronectin requirement in branching morphogenesis. *Nature* **423**, 876-81.

Sakai, Y., Meno, C., Fujii, H., Nishino, J., Shiratori, H., Saijoh, Y., Rossant, J. and Hamada, H. (2001). The retinoic acid-inactivating enzyme CYP26 is essential for establishing an uneven distribution of retinoic acid along the anterio-posterior axis within the mouse embryo. *Genes & Development* **15**, 213-25.

Sanders, E. J. (1982). Ultrastructural immunocytochemical localization of fibronectin in the early chick embryo. *Journal of Embryology and Experimental Morphology* **71**, 155-70.

Sanders, E. J. (1984). Labelling of basement membrane constituents in the living chick embryo during gastrulation. *Journal of Embryology and Experimental Morphology* **79**, 113-23.

Sanders, E. J., Khare, M. K., Ooi, V. C. and Bellairs, R. (1986). An experimental and morphological analysis of the tail bud mesenchyme of the chick embryo. *Anatomy and Embryology (Berl)* **174**, 179-85.

Sanders, E. J. and Prasad, S. (1986). Epithelial and basement membrane responses to chick embryo primitive streak grafts. *Cell Differentiation* **18**, 233-42.

Sasaki, T., Fassler, R. and Hohenester, E. (2004). Laminin: the crux of basement membrane assembly. *Journal of Cell Biology* **164**, 959-63.

Sato, Y., Yasuda, K. and Takahashi, Y. (2002). Morphological boundary forms by a novel inductive event mediated by Lunatic fringe and Notch during somitic segmentation. *Development* **129**, 3633-44.

Sawada, A., Fritz, A., Jiang, Y. J., Yamamoto, A., Yamasu, K., Kuroiwa, A., Saga, Y. and Takeda, H. (2000). Zebrafish Mesp family genes, mesp-a and mesp-b are segmentally expressed in the presomitic mesoderm, and Mesp-b confers the anterior identity to the developing somites. *Development* **127**, 1691-702.

Sawada, A., Shinya, M., Jiang, Y. J., Kawakami, A., Kuroiwa, A. and Takeda, H. (2001). Fgf/MAPK signalling is a crucial positional cue in somite boundary formation. *Development* **128**, 4873-80.

Sawada, K. and Aoyama, H. (1999). Fate maps of the primitive streak in chick and quail embryo: ingression timing of progenitor cells of each rostro-caudal axial level of somites. *International Journal of Developmental Biology* **43**, 809-15.

Scaal, M. and Christ, B. (2004). Formation and differentiation of the avian dermomyotome. *Anatomy and Embryology (Berl)* **208**, 411-24.

Schaefer, L. and Schaefer, R. M. (2010). Proteoglycans: from structural compounds to signaling molecules. *Cell and Tissue Research* **339**, 237-46.

Schaller, M. D. (2010). Cellular functions of FAK kinases: insight into molecular mechanisms and novel functions. *Journal of Cell Science* **123**, 1007-13.

Schnell, S. and Maini, P. K. (2000). Clock and induction model for somitogenesis. *Developmental Dynamics* **217**, 415-20.

Schoenwolf, G. C., Garcia-Martinez, V. and Dias, M. S. (1992). Mesoderm movement and fate during avian gastrulation and neurulation. *Developmental Dynamics* **193**, 235-48.

Schragle, J., Huang, R., Christ, B. and Prols, F. (2004). Control of the temporal and spatial Uncx4.1 expression in the paraxial mesoderm of avian embryos. *Anatomy and Embryology (Berl)* **208**, 323-32.

Schubert, F. R., Tremblay, P., Mansouri, A., Faisst, A. M., Kammandel, B., Lumsden, A., Gruss, P. and Dietrich, S. (2001). Early mesodermal phenotypes in splotch suggest a role for Pax3 in the formation of epithelial somites. *Developmental Dynamics* **222**, 506-21.

Schwarzbauer, J. E. (1991). Identification of the fibronectin sequences required for assembly of a fibrillar matrix. *Journal of Cell Biology* **113**, 1463-73.

Schwarzbauer, J. E. and DeSimone, D. W. (2011). Fibronectins, their fibrillogenesis, and in vivo functions. *Cold Spring Harbor Perspectives in Biology* **3**.

Sechler, J. L., Corbett, S. A. and Schwarzbauer, J. E. (1997). Modulatory roles for integrin activation and the synergy site of fibronectin during matrix assembly. *Molecular Biology of the Cell* **8**, 2563-73.

Sechler, J. L., Cumiskey, A. M., Gazzola, D. M. and Schwarzbauer, J. E. (2000). A novel RGD-independent fibronectin assembly pathway initiated by alpha4beta1 integrin binding to the alternatively spliced V region. *Journal of Cell Science* **113 (Pt 8)**, 1491-8.

Sechler, J. L., Takada, Y. and Schwarzbauer, J. E. (1996). Altered rate of fibronectin matrix assembly by deletion of the first type III repeats. *Journal of Cell Biology* **134**, 573-83.

Selleck, M. A. and Stern, C. D. (1991). Fate mapping and cell lineage analysis of Hensen's node in the chick embryo. *Development* **112**, 615-26.

Selleck, M. A. J. and Stern, C. D. (1992). Commitment of mesoderm cells in Hensen's node of the chick embryo to notochord and somite. *Development* **114**, 403-415.

Shanmugalingam, S. and Wilson, S. W. (1998). Isolation, expression and regulation of a zebrafish paraxis homologue. *Mechanisms of Development* **78**, 85-9.

Shen, M. M. (2007). Nodal signaling: developmental roles and regulation. *Development* **134**, 1023-34.

Sheng, G., dos Reis, M. and Stern, C. D. (2003). Churchill, a zinc finger transcriptional activator, regulates the transition between gastrulation and neurulation. *Cell* **115**, 603-13.

Showell, C., Binder, O. and Conlon, F. L. (2004). T-box genes in early embryogenesis. *Developmental Dynamics* **229**, 201-18.

Singh, P., Carraher, C. and Schwarzbauer, J. E. (2010). Assembly of fibronectin extracellular matrix. *Annual Review of Cell and Developmental Biology* **26**, 397-419.

Smyth, N., Vatansever, H. S., Murray, P., Meyer, M., Frie, C., Paulsson, M. and Edgar, D. (1999). Absence of basement membranes after targeting the LAMC1 gene results in embryonic lethality due to failure of endoderm differentiation. *Journal of Cell Biology* **144**, 151-60.

Solnica-Krezel, L. and Eaton, S. (2003). Embryo morphogenesis: getting down to cells and molecules. *Development* **130**, 4229-33.

Solursh, M., Fisher, M., Meier, S. and Singley, C. T. (1979). The role of extracellular matrix in the formation of the sclerotome. *Journal of Embryology and Experimental Morphology* **54**, 75-98.

Soshnikova, N. and Duboule, D. (2009). Epigenetic regulation of vertebrate Hox genes: a dynamic equilibrium. *Epigenetics* **4**, 537-40.

Sosic, D., Brand-Saberi, B., Schmidt, C., Christ, B. and Olson, E. N. (1997). Regulation of paraxis expression and somite formation by ectoderm- and neural tube-derived signals. *Developmental Biology* **185**, 229-43.

Sottile, J. and Hocking, D. C. (2002). Fibronectin polymerization regulates the composition and stability of extracellular matrix fibrils and cell-matrix adhesions. *Molecular Biology of the Cell* **13**, 3546-59.

Sparrow, D. B., Jen, W. C., Kotecha, S., Towers, N., Kintner, C. and Mohun, T. J. (1998). Thylacine 1 is expressed segmentally within the paraxial mesoderm of the Xenopus embryo and interacts with the Notch pathway. *Development* **125**, 2041-51.

Stern, C. D. (2004). Gastrulation in the Chick. In *Gastrulation: From Cells to Embryo*. New York: Cold Spring Harbor Laboratory Press.

Stern, C. D. (2005). Neural induction: old problem, new findings, yet more questions. *Development* **132**, 2007-21.

Stern, C. D. (2006). Evolution of the mechanisms that establish the embryonic axes. *Current Opinion in Genetics and Development* **16**, 413-8.

Stern, C. D. and Bellairs, R. (1984). Mitotic activity during somite segmentation in the early chick embryo. *Anatomy and Embryology (Berl)* **169**, 97-102.

Stern, C. D., Fraser, S. E., Keynes, R. J. and Primmett, D. R. (1988). A cell lineage analysis of segmentation in the chick embryo. *Development* **104 Suppl**, 231-44.

Stockdale, F. E., Nikovits, W., Jr. and Christ, B. (2000). Molecular and cellular biology of avian somite development. *Developmental Dynamics* **219**, 304-21.

Sun, L., Zou, Z., Collodi, P., Xu, F., Xu, X. and Zhao, Q. (2005). Identification and characterization of a second fibronectin gene in zebrafish. *Matrix Biology* **24**, 69-77.

Sun, X., Meyers, E. N., Lewandoski, M. and Martin, G. R. (1999). Targeted disruption of Fgf8 causes failure of cell migration in the gastrulating mouse embryo. *Genes & Development* **13**, 1834-46.

Swindell, E. C., Thaller, C., Sockanathan, S., Petkovich, M., Jessell, T. M. and Eichele, G. (1999). Complementary domains of retinoic acid production and degradation in the early chick embryo. *Developmental Biology* **216**, 282-96.

Tadokoro, S., Shattil, S. J., Eto, K., Tai, V., Liddington, R. C., de Pereda, J. M., Ginsberg, M. H. and Calderwood, D. A. (2003). Talin binding to integrin beta tails: a final common step in integrin activation. *Science* **302**, 103-6.

Tajbakhsh, S. and Sporle, R. (1998). Somite development: constructing the vertebrate body. *Cell* **92**, 9-16.

Takada, S., Stark, K. L., Shea, M. J., Vassileva, G., McMahon, J. A. and McMahon, A. P. (1994). Wnt-3a regulates somite and tailbud formation in the mouse embryo. *Genes & Development* **8**, 174-89.

Takahashi, S., Leiss, M., Moser, M., Ohashi, T., Kitao, T., Heckmann, D., Pfeifer, A., Kessler, H., Takagi, J., Erickson, H. P. et al. (2007a). The RGD motif in fibronectin is essential for development but dispensable for fibril assembly. *Journal of Cell Biology* **178**, 167-78.

Takahashi, Y., Inoue, T., Gossler, A. and Saga, Y. (2003). Feedback loops comprising Dll1, Dll3 and Mesp2, and differential involvement of Psen1 are essential for rostrocaudal patterning of somites. *Development* **130**, 4259-68.

Takahashi, Y., Koizumi, K., Takagi, A., Kitajima, S., Inoue, T., Koseki, H. and Saga, Y. (2000). Mesp2 initiates somite segmentation through the Notch signalling pathway. *Nature Genetics* **25**, 390-6.

Takahashi, Y., Yasuhiko, Y., Kitajima, S., Kanno, J. and Saga, Y. (2007b). Appropriate suppression of Notch signaling by Mesp factors is essential for stripe pattern formation leading to segment boundary formation. *Developmental Biology* **304**, 593-603.

Takemoto, T., Uchikawa, M., Kamachi, Y. and Kondoh, H. (2006). Convergence of Wnt and FGF signals in the genesis of posterior neural plate through activation of the Sox2 enhancer N-1. *Development* **133**, 297-306.

Takemoto, T., Uchikawa, M., Yoshida, M., Bell, D. M., Lovell-Badge, R., Papaioannou, V. E. and Kondoh, H. (2011). Tbx6-dependent Sox2 regulation determines neural or mesodermal fate in axial stem cells. *Nature* **470**, 394-8.

Tam, P. P. (1988). The allocation of cells in the presomitic mesoderm during somite segmentation in the mouse embryo. *Development* **103**, 379-90.

Tam, P. P. and Trainor, P. A. (1994). Specification and segmentation of the paraxial mesoderm. *Anatomy and Embryology (Berl)* **189**, 275-305.

Tanaka, M. and Tickle, C. (2004). Tbx18 and boundary formation in chick somite and wing development. *Developmental Biology* **268**, 470-80.

Tenin, G., Wright, D., Ferjentsik, Z., Bone, R., McGrew, M. J. and Maroto, M. (2010). The chick somitogenesis oscillator is arrested before all paraxial mesoderm is segmented into somites. *BMC Developmental Biology* **10**, 24.

Thiery, J. P., Acloque, H., Huang, R. Y. and Nieto, M. A. (2009). Epithelial-mesenchymal transitions in development and disease. *Cell* **139**, 871-90.

Thiery, J. P., Duband, J. L., Rutishauser, U. and Edelman, G. M. (1982). Cell adhesion molecules in early chicken embryogenesis. *Proceedings of the National Academy of Sciences of the United States of America* **79**, 6737-41.

Thiery, J. P. and Sleeman, J. P. (2006). Complex networks orchestrate epithelial-mesenchymal transitions. *Nature Reviews: Molecular Cell Biology* **7**, 131-42.

Thorsteinsdóttir, S., Deries, M., Cachaço, A. S. and Bajanca, F. (2011). The extracellular matrix dimension of skeletal muscle development. *Developmental Biology* **354**, 191-207.

Timpl, R. and Brown, J. C. (1996). Supramolecular assembly of basement membranes. *Bioessays* **18**, 123-32.

Tonegawa, A., Funayama, N., Ueno, N. and Takahashi, Y. (1997). Mesodermal subdivision along the mediolateral axis in chicken controlled by different concentrations of BMP-4. *Development* **124**, 1975-84.

Tonegawa, A. and Takahashi, Y. (1998). Somitogenesis controlled by Noggin. *Developmental Biology* **202**, 172-82.

Trinh, L. A. and Stainier, D. Y. (2004). Fibronectin regulates epithelial organization during myocardial migration in zebrafish. *Developmental Cell* **6**, 371-82.

Tseng, H. T. and Jamrich, M. (2004). Identification and developmental expression of Xenopus paraxis. *International Journal of Developmental Biology* **48**, 1155-8.

Turner, C. E. (2000). Paxillin interactions. *Journal of Cell Science* **113 Pt 23**, 4139-40.

Tzouanacou, E., Wegener, A., Wymeersch, F. J., Wilson, V. and Nicolas, J. F. (2009). Redefining the progression of lineage segregations during mammalian embryogenesis by clonal analysis. *Developmental Cell* **17**, 365-76.

van Eeden, F. J., Granato, M., Schach, U., Brand, M., Furutani-Seiki, M., Haffter, P., Hammerschmidt, M., Heisenberg, C. P., Jiang, Y. J., Kane, D. A. et al. (1996). Mutations affecting somite formation and patterning in the zebrafish, Danio rerio. *Development* **123**, 153-64.

Veini, M. and Bellairs, R. (1991). Early mesoderm differentiation in the chick embryo. *Anatomy and Embryology (Berl)* **183**, 143-9.

Vermot, J., Gallego Llamas, J., Fraulob, V., Niederreither, K., Chambon, P. and Dolle, P. (2005). Retinoic acid controls the bilateral symmetry of somite formation in the mouse embryo. *Science* **308**, 563-6.

Vermot, J. and Pourquié, O. (2005). Retinoic acid coordinates somitogenesis and left-right patterning in vertebrate embryos. *Nature* **435**, 215-20.

Voiculescu, O., Bertocchini, F., Wolpert, L., Keller, R. E. and Stern, C. D. (2007). The amniote primitive streak is defined by epithelial cell intercalation before gastrulation. *Nature* **449**, 1049-52.

Wahl, M. B., Deng, C., Lewandoski, M. and Pourquié, O. (2007). FGF signaling acts upstream of the NOTCH and WNT signaling pathways to control segmentation clock oscillations in mouse somitogenesis. *Development* **134**, 4033-41.

Wakely, J. and Badley, R. A. (1982). Organization of actin filaments in early chick embryo ectoderm: an ultrastructural and immunocytochemical study. *Journal of Embryology and Experimental Morphology* **69**, 169-82.

Wallin, J., Wilting, J., Koseki, H., Fritsch, R., Christ, B. and Balling, R. (1994). The role of Pax-1 in axial skeleton development. *Development* **120**, 1109-21.

Wang, H. U., Chen, Z. F. and Anderson, D. J. (1998). Molecular distinction and angiogenic interaction between embryonic arteries and veins revealed by ephrin-B2 and its receptor Eph-B4. *Cell* **93**, 741-53.

Wardle, F. C. and Papaioannou, V. E. (2008). Teasing out T-box targets in early mesoderm. *Current Opinion in Genetics and Development* **18**, 418-25.

Wedlich, D., Hacke, H. and Klein, G. (1989). The distribution of fibronectin and laminin in the somitogenesis of Xenopus laevis. *Differentiation* **40**, 77-83.

Wellik, D. M. (2009). Hox genes and vertebrate axial pattern. *Current Topics in Developmental Biology* **88**, 257-78.

Wennerberg, K., Lohikangas, L., Gullberg, D., Pfaff, M., Johansson, S. and Fassler, R. (1996). Beta 1 integrin-dependent and -independent polymerization of fibronectin. *Journal of Cell Biology* **132**, 227-38.

White, D. P., Caswell, P. T. and Norman, J. C. (2007). alpha v beta3 and alpha5beta1 integrin recycling pathways dictate downstream Rho kinase signaling to regulate persistent cell migration. *Journal of Cell Biology* **177**, 515-25.

White, P. H. and Chapman, D. L. (2005). Dll1 is a downstream target of Tbx6 in the paraxial mesoderm. *Genesis* **42**, 193-202.

Wickstrom, S. A., Lange, A., Montanez, E. and Fassler, R. (2010). The ILK/PINCH/parvin complex: the kinase is dead, long live the pseudokinase! *EMBO Journal* **29**, 281-91.

Wierzbicka-Patynowski, I. and Schwarzbauer, J. E. (2003). The ins and outs of fibronectin matrix assembly. *Journal of Cell Science* **116**, 3269-76.

Wiesner, S., Legate, K. R. and Fassler, R. (2005). Integrin-actin interactions. *Cellular and Molecular Life Sciences* **62**, 1081-99.

Wilkinson, D. G., Bhatt, S. and Herrmann, B. G. (1990). Expression pattern of the mouse T gene and its role in mesoderm formation. *Nature* **343**, 657-9.

Williams, L. W. (1910). The Somites of the Chick. *The American Journal of Anatomy* **2**, 55-100.

Wilson, V., Manson, L., Skarnes, W. C. and Beddington, R. S. (1995). The T gene is necessary for normal mesodermal morphogenetic cell movements during gastrulation. *Development* **121**, 877-86.

Winklbauer, R., Nagel, M., Selchow, A. and Wacker, S. (1996). Mesoderm migration in the Xenopus gastrula. *International Journal of Developmental Biology* **40**, 305-11.

Wittler, L., Shin, E. H., Grote, P., Kispert, A., Beckers, A., Gossler, A., Werber, M. and Herrmann, B. G. (2007). Expression of Msgn1 in the presomitic mesoderm is controlled by synergism of WNT signalling and Tbx6. *EMBO Reports* **8**, 784-9.

Wolpert, L. (2004). Much more from the chicken's egg than breakfast--a wonderful model system. *Mechanisms of Development* **121**, 1015-7.

Wong, P. C., Zheng, H., Chen, H., Becher, M. W., Sirinathsinghji, D. J., Trumbauer, M. E., Chen, H. Y., Price, D. L., Van der Ploeg, L. H. and Sisodia, S. S. (1997). Presenilin 1 is required for Notch1 and DII1 expression in the paraxial mesoderm. *Nature* **387**, 288-92.

Wood, A. and Thorogood, P. (1994). Patterns of cell behaviour underlying somitogenesis and notochord formation in intact vertebrate embryos. *Developmental Dynamics* **201**, 151-67.

Wu, C. (2001). ILK interactions. *Journal of Cell Science* **114**, 2549-50.

Xu, Q., Mellitzer, G., Robinson, V. and Wilkinson, D. G. (1999). In vivo cell sorting in complementary segmental domains mediated by Eph receptors and ephrins. *Nature* **399**, 267-71.

Yamada, K. M. and Cukierman, E. (2007). Modeling tissue morphogenesis and cancer in 3D. *Cell* **130**, 601-10.

Yamada, K. M. and Olden, K. (1978). Fibronectins--adhesive glycoproteins of cell surface and blood. *Nature* **275**, 179-84.

Yamada, K. M. and Weston, J. A. (1974). Isolation of a major cell surface glycoprotein from fibroblasts. *Proceedings of the National Academy of Sciences of the United States of America* **71**, 3492-6.

Yamada, S., Pokutta, S., Drees, F., Weis, W. I. and Nelson, W. J. (2005). Deconstructing the cadherin-catenin-actin complex. *Cell* **123**, 889-901.

Yamaguchi, T. P. (2001). Heads or tails: Wnts and anterior-posterior patterning. *Current Biology* **11**, R713-24.

Yamaguchi, T. P., Conlon, R. A. and Rossant, J. (1992). Expression of the fibroblast growth factor receptor FGFR-1/flg during gastrulation and segmentation in the mouse embryo. *Developmental Biology* **152**, 75-88.

Yamaguchi, T. P., Harpal, K., Henkemeyer, M. and Rossant, J. (1994). fgfr-1 is required for embryonic growth and mesodermal patterning during mouse gastrulation. *Genes & Development* **8**, 3032-44.

Yamaguchi, T. P., Takada, S., Yoshikawa, Y., Wu, N. and McMahon, A. P. (1999). T (Brachyury) is a direct target of Wnt3a during paraxial mesoderm specification. *Genes & Development* **13**, 3185-90.

Yang, J. T., Bader, B. L., Kreidberg, J. A., Ullman-Cullere, M., Trevithick, J. E. and Hynes, R. O. (1999). Overlapping and independent functions of fibronectin receptor integrins in early mesodermal development. *Developmental Biology* **215**, 264-77.

Yang, J. T. and Hynes, R. O. (1996). Fibronectin receptor functions in embryonic cells deficient in alpha 5 beta 1 integrin can be replaced by alpha V integrins. *Molecular Biology of the Cell* **7**, 1737-48.

Yang, J. T., Rayburn, H. and Hynes, R. O. (1993). Embryonic mesodermal defects in alpha 5 integrin-deficient mice. *Development* **119**, 1093-105.

Yasuhiko, Y., Haraguchi, S., Kitajima, S., Takahashi, Y., Kanno, J. and Saga, Y. (2006). Tbx6-mediated Notch signaling controls somite-specific Mesp2 expression. *Proceedings of the National Academy of Sciences of the United States of America* **103**, 3651-6.

Yasuhiko, Y., Kitajima, S., Takahashi, Y., Oginuma, M., Kagiwada, H., Kanno, J. and Saga, Y. (2008). Functional importance of evolutionally conserved Tbx6 binding sites in the presomitic mesoderm-specific enhancer of Mesp2. *Development* **135**, 3511-9.

Yonemura, S. (2011). Cadherin-actin interactions at adherens junctions. *Current Opinion in Cell Biology* **23**, 515-22.

Yoon, J. K., Moon, R. T. and Wold, B. (2000). The bHLH class protein pMesogenin1 can specify paraxial mesoderm phenotypes. *Developmental Biology* **222**, 376-91.

Yoon, J. K. and Wold, B. (2000). The bHLH regulator pMesogenin1 is required for maturation and segmentation of paraxial mesoderm. *Genes & Development* **14**, 3204-14.

Yoshikawa, Y., Fujimori, T., McMahon, A. P. and Takada, S. (1997). Evidence that absence of Wnt-3a signaling promotes neuralization instead of paraxial mesoderm development in the mouse. *Developmental Biology* **183**, 234-42.

Yurchenco, P. D., Amenta, P. S. and Patton, B. L. (2004). Basement membrane assembly, stability and activities observed through a developmental lens. *Matrix Biology* **22**, 521-38.

Yurchenco, P. D., Cheng, Y. S. and Colognato, H. (1992). Laminin forms an independent network in basement membranes. *Journal of Cell Biology* **117**, 1119-33.

Yurchenco, P. D. and Patton, B. L. (2009). Developmental and pathogenic mechanisms of basement membrane assembly. *Current Pharmaceutical Design* **15**, 1277-94.

Yurchenco, P. D. and Wadsworth, W. G. (2004). Assembly and tissue functions of early embryonic laminins and netrins. *Current Opinion in Cell Biology* **16**, 572-9.

Yusuf, F. and Brand-Saberi, B. (2006). The eventful somite: patterning, fate determination and cell division in the somite. *Anatomy and Embryology (Berl)* **211 Suppl 1**, 21-30.

Zaidel-Bar, R. and Geiger, B. (2010). The switchable integrin adhesome. *Journal of Cell Science* **123**, 1385-8.

Zaidel-Bar, R., Itzkovitz, S., Ma'ayan, A., Iyengar, R. and Geiger, B. (2007). Functional atlas of the integrin adhesome. *Nature Cell Biology* **9**, 858-67.

Zakany, J., Kmita, M., Alarcon, P., de la Pompa, J. L. and Duboule, D. (2001). Localized and transient transcription of Hox genes suggests a link between patterning and the segmentation clock. *Cell* **106**, 207-17.

Zamir, E. and Geiger, B. (2001a). Components of cell-matrix adhesions. *Journal of Cell Science* **114**, 3577-9.

Zamir, E. and Geiger, B. (2001b). Molecular complexity and dynamics of cell-matrix adhesions. *Journal of Cell Science* **114**, 3583-90.

Zhang, N. and Gridley, T. (1998). Defects in somite formation in lunatic fringe-deficient mice. *Nature* **394**, 374-7.

Zhang, Z., Morla, A. O., Vuori, K., Bauer, J. S., Juliano, R. L. and Ruoslahti, E. (1993). The alpha v beta 1 integrin functions as a fibronectin receptor but does not support fibronectin matrix assembly and cell migration on fibronectin. *Journal of Cell Biology* **122**, 235-42.

Zhou, X., Sasaki, H., Lowe, L., Hogan, B. L. and Kuehn, M. R. (1993). Nodal is a novel TGF-beta-like gene expressed in the mouse node during gastrulation. *Nature* **361**, 543-7.

Ziegler, W. H., Liddington, R. C. and Critchley, D. R. (2006). The structure and regulation of vinculin. *Trends in Cell Biology* **16**, 453-60.

Chapter 2

Redefining the role of ectoderm in somitogenesis: a player in the formation of the fibronectin matrix of presomitic mesoderm

Redefining the role of ectoderm in somitogenesis: a player in the formation of the fibronectin matrix of presomitic mesoderm

Pedro Rifes [1,2,*], Lara Carvalho [1,*,†], Catarina Lopes [1], Raquel P. Andrade [3], Gabriela Rodrigues [1,2], Isabel Palmeirm [3] and Sólveig Thorsteinsdóttir [1,2]

Development, 134, 3155-65, 2007

[1] Departamento de Biologia Animal e Centro de Biologia Ambiental, Faculdade de Ciências, Universidade de Lisboa, 1749-016 Lisboa, Portugal.
[2] Instituto Gulbenkian de Ciência, 2781-901 Oeiras, Portugal.
[3] Life and Health Sciences Research Institute (ICVS), School of Health Sciences, University of Minho, 4710-057 Braga, Portugal.
[*] These authors contributed equally to this work
[†] Present address: Max Planck Institute of Molecular Cell Biology and Genetics, Dresden, Germany

Contribution to the publication:

	Experimental work depicted in:									manuscript writing
	Fig. 1	Fig. 2	Fig. 3	Fig. 4	Fig. 5	Fig. 6	Fig. 7	Fig. 8	Fig. 9	
Design and concept	III	I	II	O	II	II	II	III	II	III
Execution	III	II	II	O	II	III	II	III	n.a.	
Analysis and interpretation	II	I	II	I	II	II	II	II	n.a.	

Legend:
n.a……. non applicable
O ……. no intervention
I……. minor contribution
II……. moderate contribution
III…….major contribution/full execution
Note: this contribution does not exclude other contributions, similar or not, from the remaining authors

Development 134, 3155-3165 (2007) doi:10.1242/dev.003665

Redefining the role of ectoderm in somitogenesis: a player in the formation of the fibronectin matrix of presomitic mesoderm

Pedro Rifes[1,2,*], Lara Carvalho[1,*,†], Catarina Lopes[1], Raquel P. Andrade[3], Gabriela Rodrigues[1,2], Isabel Palmeirim[3] and Sólveig Thorsteinsdóttir[1,2,‡]

The absence of ectoderm impairs somite formation in cultured presomitic mesoderm (PSM) explants, suggesting that an ectoderm-derived signal is essential for somitogenesis. Here we show in chick that the standard enzymatic treatments used for explant isolation destroy the fibronectin matrix surrounding the anterior PSM, which fails to form somites when cultured for 6 hours. By contrast, explants isolated with collagenase retain their fibronectin matrix and form somites under identical culture conditions. The additional presence of ectoderm enhances somite formation, whereas endoderm has no effect. Furthermore, we show that pancreatin-isolated PSM explants cultured in fibronectin-supplemented medium, form significantly more somites than control explants. Interestingly, ectoderm is the major producer of fibronectin (*Fn1*) transcripts, whereas all but the anterior-most region of the PSM expresses the fibronectin assembly receptor, integrin α5 (*Itga5*). We thus propose that the ectoderm-derived fibronectin is assembled by mesodermal α5β1 integrin on the surface of the PSM. Finally, we demonstrate that inhibition of fibronectin fibrillogenesis in explants with ectoderm abrogates somitogenesis. We conclude that a fibronectin matrix is essential for morphological somite formation and that a major, previously unrecognised role of ectoderm in somitogenesis is the synthesis of fibronectin.

KEY WORDS: Somitogenesis, Fibronectin, Ectoderm, Presomitic mesoderm, Integrins, Extracellular matrix, Chick

INTRODUCTION

Somites are transient segments of the paraxial mesoderm that are formed in a rostral-to-caudal progression during vertebrate embryogenesis. Each pair of somites, epithelial structures located symmetrically on either side of the neural tube, periodically detaches from the rostral end of the presomitic mesoderm (PSM), while new immature PSM tissue is added in the posterior part of the embryo. The strict temporal and spatial regulation of somitogenesis is of crucial developmental importance because segmental structures, such as the vertebrae, trunk skeletal muscles, peripheral spinal nerves and early blood vessels, develop according to the somite segmental pattern (Christ and Ordahl, 1995; Gossler and Hrabě de Angelis, 1998).

The PSM can be divided in two regions that differ not only in terms of gene expression patterns, but also in the morphology of the PSM cells. In the caudal two-thirds of the PSM, high Fgf8 activity is believed to keep cells in a mesenchymal, undifferentiated state and oscillatory expression of segmentation clock genes occurs (Dubrulle et al., 2001; Freitas et al., 2005; Palmeirim et al., 1997). As PSM cells leave this caudal immature region, crossing what has been termed the determination front and enter the anterior third of the PSM, several changes take place. The cyclic expression of clock genes comes to a halt, retinoic acid signalling progressively replaces Fgf signalling (Diez del Corral et al., 2003) and somite anterior-posterior polarity is established (Saga and Takeda, 2001). Furthermore, the first signs of morphological somite formation occur as peripheral PSM cells undergo a mesenchymal-to-epithelial transition (Duband et al., 1987; Kulesa and Fraser, 2002). Finally, in the anterior-most region of the PSM, somite boundaries are specified and formed through the activation of transcription factors of the Mesp family (Sawada et al., 2000), most likely also involving Eph-ephrin (Barrios et al., 2003; Durbin et al., 2000) and Notch signalling (Sato et al., 2002).

It has been clearly demonstrated that the molecular segmentation of the anterior PSM is an intrinsic property of the PSM and does not require signalling from neighbouring tissues (Palmeirim et al., 1997). However, morphological somite formation does not occur in isolated cultured PSMs. For somites to form, ectoderm must be in contact with the PSM (Borycki et al., 2000; Borycki et al., 1998; Correia and Conlon, 2000; Palmeirim et al., 1998), suggesting that ectodermal signals, most likely Wnts (Borycki et al., 2000; Schmidt et al., 2004), are essential for morphological somite formation.

Interactions between PSM cells and the extracellular matrix molecule fibronectin have been implicated in somitogenesis (Duband et al., 1987; George et al., 1993; Lash et al., 1984; Lash and Ostrovsky, 1986; Ostrovsky et al., 1983). Fibronectin exists in plasma and cellular forms which, when assembled into a matrix, mediate a wide variety of cellular processes such as cell spreading, migration, proliferation, survival and differentiation (Pankov and Yamada, 2002). Fibronectin matrix assembly is a complex cell-dependent process that requires the engagement of fibronectin by cell surface integrins, usually the α5β1 integrin, and fibrillogenesis involving fibronectin-fibronectin binding (Mao and Schwarzbauer, 2005; Wierzbicka-Patynowski and Schwarzbauer, 2003). Fibronectin 1 (*Fn1*)-null mouse embryos

[1]Departamento de Biologia Animal e Centro de Biologia Ambiental, Faculdade de Ciências, Universidade de Lisboa, 1749-016 Lisboa, Portugal. [2]Instituto Gulbenkian de Ciência, 2781-901 Oeiras, Portugal. [3]Life and Health Sciences Research Institute (ICVS), School of Health Sciences, University of Minho, 4710-057 Braga, Portugal.

*These authors contributed equally to this work
†Present address: Max Planck Institute of Molecular Cell Biology and Genetics, Dresden, Germany
‡Author for correspondence (e-mail: solveig@fc.ul.pt)

Accepted 2 July 2007

initiate gastrulation normally, but, although they have paraxial mesoderm, no morphologically distinguishable somites form (George et al., 1993; Georges-Labouesse et al., 1996). Furthermore, embryos null for both α5 and αV integrin subunits (*Itga5* and *Itgav*) do not assemble a fibronectin matrix and fail to form somites (Yang et al., 1999). Together, these studies suggest that interactions between the fibronectin matrix and the PSM cells are crucial for normal somitogenesis.

The main objective of the present work was to address the contribution of the ectoderm and the fibronectin matrix in somitogenesis. We show that enzymatic treatments generally used to isolate PSM explants from the surrounding tissues destroy the fibronectin matrix surrounding the PSM. When these explants are cultured for 6 hours, no somites form. By contrast, we show for the first time that when collagenase is used, the endogenous fibronectin matrix remains intact and somites form even in the absence of all surrounding tissues. Moreover, addition of exogenous fibronectin to cultured pancreatin-isolated PSMs significantly improves their ability to form somites. Interestingly, *Fn1* is primarily expressed in the ectoderm, whereas the PSM strongly expresses the fibronectin receptor *Itga5*, suggesting that ectoderm and PSM collaborate in constructing the fibronectin matrix present around the PSM. Finally, we demonstrate that inhibition of fibronectin matrix assembly in the presence of ectoderm abrogates somitogenesis. Based on these findings, we conclude that a fibronectin matrix is essential for somitogenesis and that a major role of ectoderm in this process is to provide the fibronectin protein for this matrix.

MATERIALS AND METHODS

Eggs and embryos

Fertilised chicken (*Gallus gallus*) eggs were incubated in a humidified atmosphere at 37.5°C until stage HH12-14 (Hamburger and Hamilton, 1992). Somite nomenclature follows Christ and Ordahl (Christ and Ordahl, 1995).

Cryosectioning

Embryos were fixed in 4% paraformaldehyde in phosphate buffer (77 mM Na_2HPO_4, 23 mM NaH_2PO_4, 0.12 mM $CaCl_2$) with 4% sucrose overnight at 4°C and processed for cryoembedding (Bajanca et al., 2004). Cryostat (Bright Clinicut 3020) sections (12 μm) were processed for immunohistochemistry or, if embryos had already been subjected to whole-mount in situ hybridisation, mounted in 80% glycerol in PBS and photographed.

Embryo manipulation

Embryos were pinned down on resin-coated Petri dishes with PBS containing calcium and magnesium (PBS w/$Ca^{2+}Mg^{2+}$). PSM isolation, including removal of ectoderm and/or endoderm was achieved using tungsten needles, with or without the application of enzymes: pancreatin (4×, Gibco), an enzyme extract containing trypsin; dispase (2.4 U/ml, Roche), which cleaves fibronectin and collagen type IV (Stenn et al., 1989); and collagenase type II (125 U/ml, Sigma), which digests various collagens. None of these enzymes degraded laminin (data not shown). PSM isolation with pancreatin and dispase took 3-4 minutes, whereas collagenase isolation took about 8 minutes. Pancreatin was inactivated with fetal bovine serum (FBS, Gibco), whereas dispase and collagenase were washed away with PBS w/$Ca^{2+}Mg^{2+}$.

Explant culture experiments

Embryo explants were positioned on 0.8 μm polycarbonate filters (Millipore) floating on M199 medium with 5% FBS and 10% chick serum (Palmeirim et al., 1997). In one set of experiments, the culture medium of one PSM was supplemented with 50-100 μg/ml of rat (Calbiochem) or bovine (Sigma) plasma fibronectin, whereas the contralateral PSM was incubated in control medium (medium only, or with BSA). Both plasma fibronectins produced the same results. In another set of experiments, posterior embryo explants were cultured with 50 or 100 μg/ml of a 70 kDa fibronectin fragment (Sigma). Control embryos were incubated in medium with BSA.

Statistical analysis

A factorial analysis of variance (ANOVA) was used to test for the effect of the isolation method (pancreatin versus collagenase) and the culture method (PSM with or without endoderm or ectoderm) on the capacity of PSMs to form somites. The statistical significance of predicted specific differences was then analysed using contrast analysis. A paired Student's *t*-test was used to test for differences between explants grown with or without the fibronectin supplement. Differences between control embryo explants and explants cultured with the 70 kDa fibronectin fragment were tested with *t*-tests following a square-root transformation of the data. Statistical tests were computed with the STATISTICA 6 (StatSoft) programme.

Antibodies and immunohistochemistry

Fibronectin immunohistochemistry was performed using a polyclonal antibody (Sigma, 1:400), or a monoclonal anti-cellular fibronectin antibody (clone FN-3e2; Sigma, 1:400) that recognises the EIIIA domain unique to cellular fibronectin (Barnes et al., 1995). Monoclonal anti-N-cadherin (cadherin 2) antibody (clone32; BD Transduction Laboratories, 1:100) was also used. Secondary antibodies were Alexa Fluor 488-, 546- or 568-conjugated anti-rabbit and anti-mouse IgG $F(ab')_2$ fragments (Molecular Probes, 1:1000). For F-actin staining, Alexa Fluor 568-conjugated phalloidin was used (Molecular Probes, 1:40) and TO-PRO3 (Molecular Probes, 1:500) incubated with secondary antibody and ribonuclease A (Calbiochem, 10 μg/ml) was used for nuclear staining.

Explants were fixed overnight at 4°C in 4% paraformaldehyde in PBS and washed in PBS. Both primary and secondary antibodies were incubated overnight in PBS containing 1% BSA and 0.1% Triton X-100 at room temperature, and explants were mounted in Vectashield (Vector Laboratories).

Cryosections were treated with 0.2% Triton X-100 in PBS for 20 minutes, washed in PBS and blocked for 30 minutes in 5% BSA in PBS. Incubation in primary antibody was overnight at 4°C, and incubation in secondary antibody was for 1 hour at room temperature. Sections were counterstained with 4′,6-diamidine-2-phenylidole-dihydrochloride (DAPI, 5 μg/ml in PBS, 0.1% Triton X-100).

Image acquisition and analysis

Images were acquired with an Olympus DP50 digital camera attached to an Olympus BX60 microscope equipped with epifluorescence and Nomarski optics, or with a Zeiss LSM 510 Meta confocal microscope. During confocal image acquisition, the detection parameters were adjusted to avoid under- or overexposed pixels. For fibronectin quantification, the average fluorescence intensity of six non-overlapping 75 μm-diameter regions of interest along each PSM was taken from the maximum *z*-projection of the seven most-superficial slices. The average fluorescence intensity of each PSM was normalised against its background fluorescence. ImageJ and Adobe Photoshop were used for image analysis and processing.

In situ hybridisation probes

In situ hybridisation probes for *Fn1*, *Itga5* and *Itgav* were generated. The *Fn1* probe was designed against a region present in all splice variants of the chick *Fn1* mRNA (ffrench-Constant and Hynes, 1988; Norton and Hynes, 1987). Reverse transcription (RT) PCRs were used to isolate portions of chick *Fn1*, *Itga5* and *Itgav* using the sense oligos 5′-CGTTCGTCT-CACTGGCTACA-3′, 5′-AGGTGCTGAGGGGGCAA-3′, 5′-TTCTCCA-CAGCAAACAGCC-3′ and the antisense oligos 5′-GGTCCTCTGG-ATGGGATTCT-3′, 5′-CACGACGGTGAGCGAAG-3′, 5′-ATCCTCA-CCACAATCCAGCA-3′, respectively. The DNA fragments generated were cloned into the pCRII-TOPO vector (Invitrogen) and plasmid DNA was isolated. The constructs were confirmed by sequencing.

A plasmid carrying an insert of *Paraxis* (*Tcf15*) was kindly provided by C. Jouve (Developmental Biology Institute of Marseille, Marseille, France). The digoxigenin-labelled RNA probes were obtained from linearised plasmids, according to standard procedures adapted from Sambrook et al. (Sambrook et al., 1989).

Whole-mount in situ hybridisation

Embryos and explants were fixed overnight at 4°C in 4% formaldehyde with 2 mM ethylene glycol-bis (β-amino-ethyl ether) tetra acetic acid (EGTA) in PBS, rinsed in PBT (PBS, 0.1% Tween 20), dehydrated in methanol and stored at –20°C. Whole-mount in situ hybridisation was performed according to Henrique et al. (Henrique et al., 1995), but BM Purple Substrate (Roche) was used as staining solution. Some embryos were cryosectioned as described above.

RT-PCR

PSM and epithelial somites were isolated using pancreatin. Twenty samples of each of the following were collected for RT-PCR: (1) the four posterior-most somites; (2) the anterior third of the PSM; and (3) the posterior two-thirds of the PSM. Whole embryos were collected as positive control. Samples were processed for RNA extraction using the RNeasy Mini Kit with column DNA digestion (Qiagen). Total RNA was reverse-transcribed using the RevertAid First Strand cDNA Synthesis Kit (Fermentas). PCR was performed using the primers described above. Amplification using β-actin primers was used as positive control. Reactions from which reverse transcription (RNA control) or cDNA (water control) were omitted were used as negative controls.

RESULTS

Enzymatic PSM isolation using pancreatin or dispase destroys the surrounding fibronectin matrix

Immunoreactivity for fibronectin was observed in embryo sections around the PSM and epithelial somites, as previously reported (Duband et al., 1987; Ostrovsky et al., 1983), and short strands of fibronectin immunoreactivity were distinguishable among PSM cells (Fig. 1A,B). Non-enzymatic removal of ectoderm from the anterior PSM in whole embryos revealed a network of fibrillar fibronectin-positive matrix surrounding the PSM (Fig. 1C). However, when PSMs were isolated with pancreatin or dispase, which are commonly used for this purpose, no immunoreactivity for fibronectin was detected (Fig. 1D,E). These data show that both pancreatin and dispase destroy the PSM fibronectin matrix within the time period necessary for PSM isolation. By contrast, we found that PSM isolation using collagenase preserved a fibrillar fibronectin matrix (Fig. 1F), suggesting that this is a better method for PSM isolation than pancreatin and dispase.

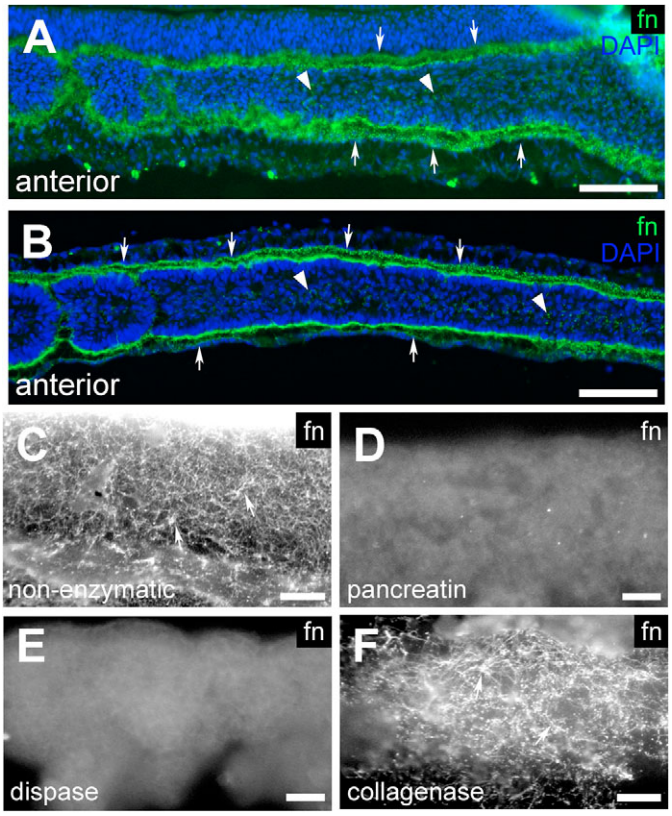

Fig. 1. Distribution of fibronectin in the chick PSM and surrounding tissues. (**A**,**B**) Longitudinal (A) and sagittal (B) sections reveal short strands of fibronectin immunoreactivity within the PSM (arrowheads in A,B), and an extensive fibronectin immunoreactivity surrounding the anterior PSM. This immunoreactivity is distinguishable from that of the neural tube, ectoderm and endoderm (arrows in A,B). (**C**) Non-enzymatic removal of ectoderm exposes fibrillar fibronectin immunoreactivity on the PSM. (**D**,**E**) By contrast, PSMs isolated with pancreatin (D) or dispase (E) are completely negative. (**F**) When collagenase is used an intact fibronectin matrix is maintained. Polyclonal anti-fibronectin (A,B) and monoclonal anti-cellular fibronectin (C-F) antibodies were used. fn, fibronectin. Scale bars: 100 μm in A,B; 25 μm in C-F.

Collagenase-isolated PSMs retain their fibronectin matrix and are able to form somites even in the absence of ectoderm

If fibronectin is important for somitogenesis, it is not surprising that PSMs isolated with pancreatin or dispase fail to form somites. However, ectoderm is able to support morphological somitogenesis even when explants are treated with these enzymes (Borycki et al., 1998; Correia and Conlon, 2000; Palmeirim et al., 1998), whereas endoderm does not (Palmeirim et al., 1998). To evaluate the role of ectoderm, endoderm and fibronectin matrix in somite formation, pancreatin or collagenase were used to isolate three types of PSM explants: PSM without any adjacent tissues (PSM), PSM with the underlying endoderm (PSM+endoderm), or PSM with the overlying ectoderm (PSM+ectoderm). Two identical explants were isolated from each embryo. One was immediately fixed and immunolabelled for fibronectin, whereas the other was cultured for 6 hours (time to form 4 somites) and processed for fibronectin immunohistochemistry and F-actin staining (Fig. 2). The number of somites formed in each case was recorded (Fig. 3).

PSMs isolated from all surrounding tissues using pancreatin were negative for fibronectin immunolabelling (Fig. 2A) and generally did not present fully formed somites after 6 hours of culture (*n*=206; Fig. 2C, Fig. 3). Curiously, in pancreatin-treated PSM+ectoderm explants, fibronectin was observed between the PSM and the ectoderm (Fig. 2G) and these formed somites after 6 hours of culture (*n*=46; Fig. 2I, Fig. 3). By contrast, although some fibronectin is preserved between the PSM and the underlying endoderm (Fig. 2D), pancreatin-treated PSM+endoderm explants rarely formed somites (*n*=19; Fig. 2F, Fig. 3).

All PSM explants treated with collagenase (*n*=157) retained a fibrillar fibronectin matrix on their surface (Fig. 2J,M,P), and exhibited fully formed somites (Fig. 2L,O,R, Fig. 3). This was true even for the PSMs cultured in complete isolation from surrounding tissues (*n*=66).

We conclude that PSMs isolated with an enzymatic treatment that retains the fibronectin matrix are able to form somites in the absence of neighbouring tissues. Pancreatin-treated PSM+ectoderm explants retain fibronectin matrix between the two tissues, which may facilitate the formation of somites. Curiously, somites rarely form in pancreatin-treated PSM+endoderm explants even though some fibronectin is retained between the two apposed tissues.

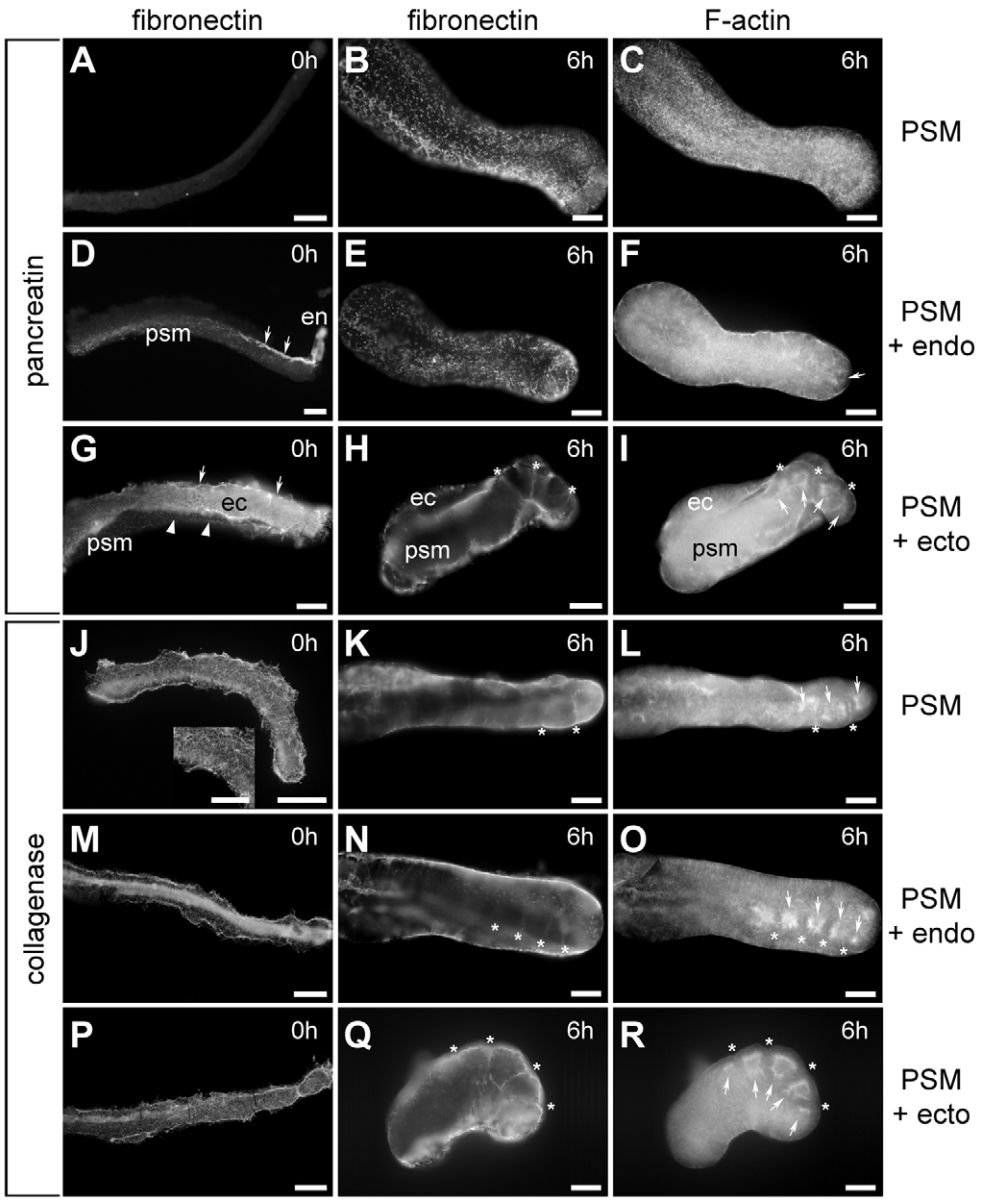

Fig. 2. Collagenase-isolated chick PSMs form somites in the absence of both ectoderm and endoderm. All explant types were either fixed immediately (0 hours, 0h) and labelled for fibronectin or cultured for 6 hours (6h) and processed for fibronectin and F-actin staining. (**A-I**) Pancreatin-isolated explants. Isolated PSMs are fibronectin-negative at 0 hours (A). At 6 hours, fibronectin staining is visible (B) but somites have not formed (C). In PSM+endoderm explants, some fibronectin immunoreactivity is present between endoderm and PSM at 0 hours (arrows in D). These explants show fibronectin immunoreactivity at 6 hours (E), but no somites have formed (arrow in F). PSM+ectoderm have fibronectin immunoreactivity between ectoderm and PSM (arrows in G), whereas the remaining PSM is negative (arrowheads in G). At 6 hours, clefts (asterisks in H,I) containing fibronectin immuoreactivity (H) and rings of F-actin staining (arrows in I) are observed. (**J-R**) Collagenase-isolated explants. All explants isolated with collagenase retain their endogenous, fibrillar (see insert in J) fibronectin matrix (J,M,P). At 6 hours, all explant types have clefts (asterisks in K,L,N,O,Q,R) containing fibronectin (K,N,Q) and several epithelialised somites (arrows in L,O,R). Anterior, right. psm, presomitic mesoderm; endo and en, endoderm; ecto and ec, ectoderm. Scale bars: 100 μm.

Ectoderm, but not endoderm, enhances the capacity of collagenase-isolated PSMs to form somites

In order to uncover the relative contribution of ectoderm, endoderm and the fibronectin matrix in morphological somite formation, we analysed our quantitative data in more detail (Fig. 3). A comparison of PSM and PSM+endoderm explants isolated with pancreatin versus collagenase, indicates that the difference in the capacity to form somites is dependent both on the enzyme (P<0.0001) and the presence of endoderm (P=0.03). To determine whether this effect is mediated by endoderm itself, or by the fibronectin retained between the two apposed tissues, we compared the somite-forming capacity of collagenase-isolated PSM and PSM+endoderm explants. No significant difference (P=0.71) in the capacity to form somites was found between these two explant types. We conclude that endoderm does not by itself enhance somite formation in cultured PSMs and that the slight increase in somite-forming capacity of pancreatin-isolated PSM+endoderm explants must be due to the fibronectin matrix that is retained between the two tissues.

We then compared PSM and PSM+ectoderm explants isolated with pancreatin versus collagenase. We found that the difference in the capacity to form somites is both dependent on the enzyme (P<0.0001) and on the presence of ectoderm (P<0.0001). Unlike in the case of endoderm, a significant interaction between these two variables was detected (P<0.0001), indicating that they mutually enhance each other's effect. To determine whether ectoderm enhances somite formation by itself, we compared collagenase-isolated PSM and PSM+ectoderm explants and found that these differ significantly in their somite-forming capacity (P<0.0001). We conclude that, although isolation with collagenase enables PSMs to form somites, the additional presence of ectoderm enhances this capacity.

Pancreatin-treated PSM+ectoderm explants retain fibronectin matrix only between ectoderm and PSM, whereas collagenase-treated PSM+ectoderm explants retain an extensive fibronectin matrix all around. A comparison between these two situations did not reveal a significant difference between the number of somites formed (P=0.075), indicating that somite formation in PSMs in

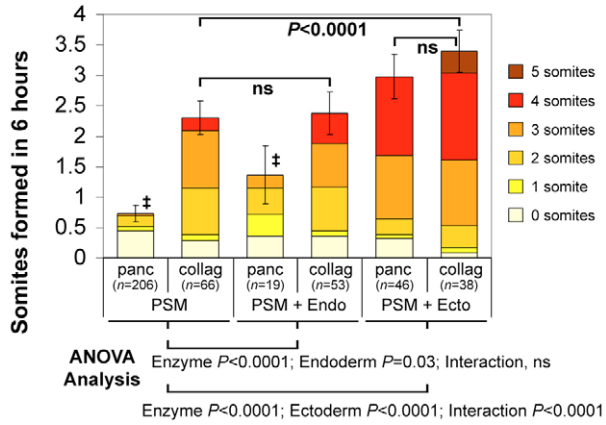

Fig. 3. Quantitative representation of the capacity of all PSM explant types treated with pancreatin or collagenase to form somites. The average number of somites formed for each explant type and enzyme treatment is depicted, and the proportion of explants forming 0, 1, 2, 3, 4 and 5 somites during the 6-hour culture period is indicated with a colour code. Note that the somites formed in PSM and PSM+endoderm explants isolated with pancreatin (marked with ‡) were frequently less compacted and had incomplete clefts as compared with all other experimental situations. A factorial ANOVA (results depicted at the bottom of the figure) followed by a contrast analysis of predicted differences (results shown in graph) were performed to test for differences among treatments. ns, not significant. Error bars represent 95% confidence limits.

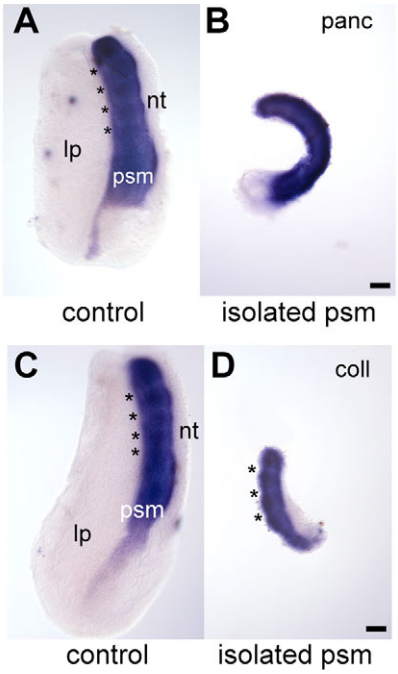

Fig. 4. *Paraxis* expression is maintained in both pancreatin- and collagenase-isolated chick PSMs cultured for 6 hours. After 6 hours of culture, control sides (intact halves, **A**,**C**) strongly express *Paraxis* in the anterior PSM in a pattern identical to that of the contralateral isolated PSMs, regardless of whether these were isolated with pancreatin (**B**) or collagenase (**D**). Only the collagenase-isolated explants formed somites (asterisks in D). Anterior, top. nt, neural tube; lp, lateral plate; psm, presomitic mesoderm; panc, pancreatin-isolated PSM; coll, collagenase-isolated PSM. Scale bars: 100 μm.

contact with ectoderm is not improved by the presence of a fibronectin matrix all around the PSM at the beginning of the culture period.

Altogether, these results demonstrate that whereas collagenase-isolated PSMs are clearly capable of forming morphological somites, the additional presence of ectoderm enhances this capacity further, whereas endoderm has no effect.

Paraxis expression is independent of ectoderm and fibronectin matrix

Paraxis expression in the anterior PSM is necessary for epithelial somite formation (Burgess et al., 1996) and it has been suggested that ectoderm is essential to induce its expression (Correia and Conlon, 2000; Sosić et al., 1997). To determine if fibronectin and/or ectoderm influence *Paraxis* expression, pancreatin- or collagenase-isolated PSMs (Fig. 4B,D) and their contralateral control halves (Fig. 4A,C) were cultured for 6 hours and assayed for *Paraxis* expression. Both pancreatin-isolated (n=11) and collagenase-isolated (n=11) PSMs showed *Paraxis* expression (Fig. 4B,D), identical to the contralateral control halves (Fig. 4A,C), although only collagenase-isolated PSMs formed somites (Fig. 4D). We conclude that *Paraxis* expression in the anterior PSM and newly formed somites is independent of all surrounding tissues and of an intact fibronectin matrix. Furthermore, *Paraxis* expression in pancreatin-isolated PSMs cultured for 6 hours is not sufficient to drive somite formation.

Exogenous fibronectin increases the ability of pancreatin-isolated PSMs to form somites

Pancreatin-isolated PSMs show a clear fibronectin-immunoreactivity after 6 hours of culture. This fibronectin matrix was recognised by a cellular fibronectin-specific antibody (Fig. 5A), indicating that it is at least partially PSM-derived and not only from the serum supplement (McKeown-Longo and Mosher, 1983). However, practically no somites were formed in these PSM explants. Thus, the possibility arises that the amount of fibronectin (PSM- plus serum-derived) available to the fibronectin-stripped PSMs is insufficient to support somite formation. PSM isolation using pancreatin or dispase removes all the endogenous fibronectin (Fig. 1D,E, Fig. 2A) and after 2 hours of culture these PSMs showed only a faint immunoreactivity for fibronectin (Fig. 5B,E). Only after 4 hours of culture had a fibronectin matrix formed, which was similar in labelling intensity to the one observed after 6 hours (Fig. 5C-E).

To determine whether the amount of fibronectin available to the PSMs could be the limiting factor for their capacity to form somites, pancreatin-isolated PSM pairs (n=20) were cultured in fibronectin-supplemented medium versus control medium. The average number of somites formed by PSMs cultured with fibronectin for 6 hours was significantly higher (P=0.002) than that formed by the contralateral PSMs grown in control medium (Fig. 5F-J). Cells of PSMs cultured with fibronectin had aligned, elongated nuclei and apical enrichment of F-actin and N-cadherin, which was not observed in PSMs cultured in control medium (Fig. 6, compare B,E with A,D). In fact, cell morphology in PSMs cultured with fibronectin was very similar to that of collagenase-isolated PSMs (Fig. 6, compare B,E with C,F). We conclude that the culture of fibronectin-stripped PSMs in fibronectin-supplemented medium significantly improves their capacity to form somites and that their cells exhibit a morphology typical of somitic cells.

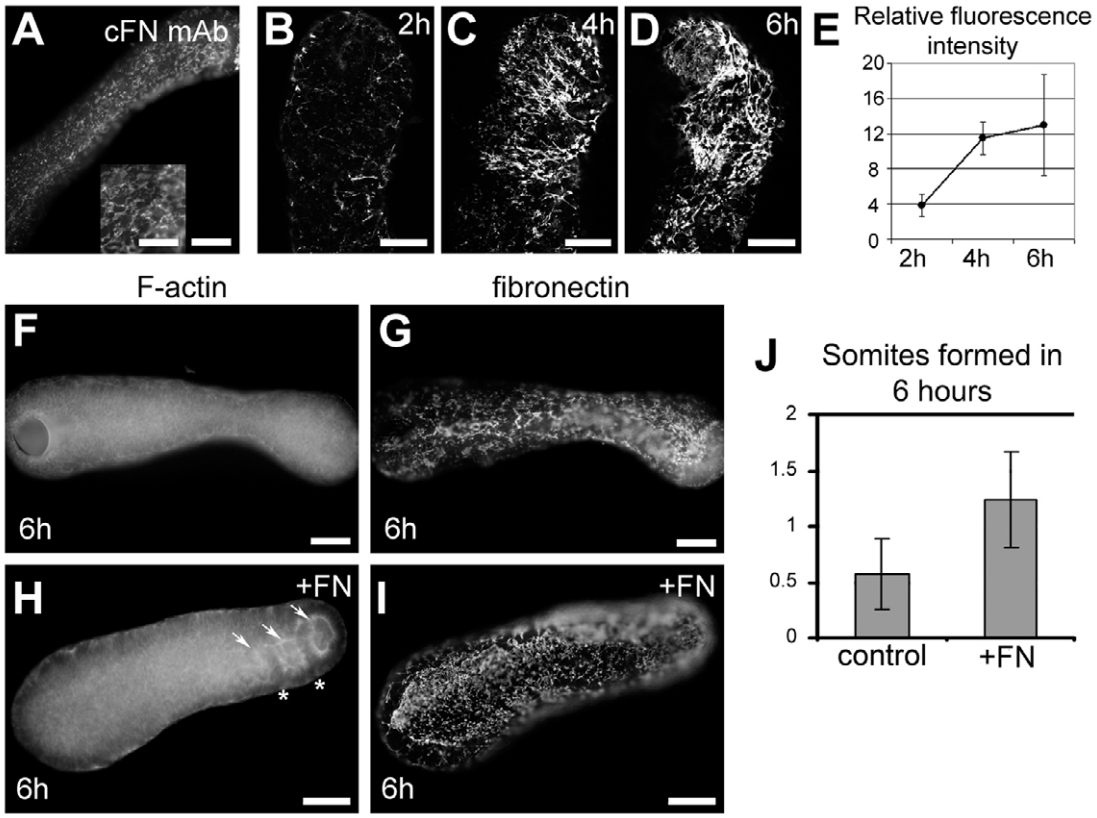

Fig. 5. Partial rescue of somite formation in pancreatin-isolated PSMs cultured with exogenous fibronectin. (**A**) Pancreatin-isolated chick PSMs present immunoreactivity for cellular fibronectin after 6 hours in culture. (**B-D**) *z*-projection of confocal images of dispase-isolated PSMs cultured for 2 hours (B) show faint fibronectin immunoreactivity, whereas after 4 (C) and 6 (D) hours it is more extensive. (**E**) Average fluorescence labelling intensity relative to background in dispase-isolated PSMs cultured for 2 (*n*=7), 4 (*n*=4) and 6 hours (*n*=6). (**F-I**) Contralateral pancreatin-isolated PSMs, cultured in control (F,G) or fibronectin-supplemented (H,I) medium and stained for F-actin (F,H) and fibronectin (G,I). (**J**) Bar chart of the average number of somites formed (*n*=20 pairs) showing that PSMs cultured with fibronectin form significantly more somites (*P*=0.002). Error bars represent 95% confidence limits. cFN, cellular fibronectin; +FN, PSM cultured in fibronectin-supplemented medium. Scale bars: 100 μm in A,F-I; 50 μm in A insert, B-D.

PSM and ectoderm collaborate in the assembly of the PSM fibronectin matrix

Our previous observations indicate that although isolated PSMs are able to produce and assemble a fibronectin matrix in culture, the amount of fibronectin available to them is insufficient to support somitogenesis. This led us to investigate where fibronectin is normally produced.

In situ hybridisation for chick *Fn1* transcripts revealed strong expression in the ectoderm and in the posterior part of epithelial somites (Fig. 7A-D). Furthermore, *Fn1* was expressed in the endoderm underlying anterior PSM and somites (Fig. 7B-D). Unexpectedly, *Fn1* mRNA was not detected in the rostral PSM and only a faint signal was present in the caudal PSM (Fig. 7B,C). This was confirmed by removal of the ectoderm prior to fixation (Fig. 7E-I). Interestingly, RT-PCR analysis showed that both anterior and posterior PSM express *Fn1* mRNA (Fig. 7J), which is in accordance with the cellular fibronectin immunoreactivity present on pancreatin-isolated PSMs after 6 hours of culture (Fig. 5A). Together, these data demonstrate that the major site of *Fn1* transcription is the ectoderm overlying the PSM, whereas the PSM expresses only low levels of *Fn1* mRNA.

Our next step was to identify where the integrins known to mediate fibronectin fibrillogenesis (Yang et al., 1999) are expressed. The main integrin responsible for fibronectin fibrillogenesis, *Itga5*, was strongly expressed in the posterior two-thirds of the PSM (Fig. 7L,N), whereas *Itgav* transcripts were not detected in the PSM by in situ hybridisation (data not shown). Little or no *Itga5* mRNA expression was detected in the anterior-most PSM (Fig. 7L,M), but was again detected in epithelial somites (Fig. 7L). These data demonstrate that ectoderm is the major source of fibronectin, whereas the PSM expresses *Itga5*, the receptor necessary for its assembly into a fibrillar matrix.

Inhibition of fibronectin matrix assembly in the presence of ectoderm inhibits somite formation

We have shown that somite formation occurs in collagenase-isolated PSMs and in pancreatin-isolated PSMs cultured with fibronectin. Our results also demonstrated that although collagenase-isolated PSMs were able to form somites, the presence of ectoderm improved this capacity further. We now show that ectoderm is the major producer of fibronectin protein in the region of the PSM. The question arises, is the beneficial effect of ectoderm due to its production of fibronectin or does it provide some other essential signal to the PSM that contributes to somitogenesis?

To test this hypothesis, we cultured posterior embryo explants for 12 hours in medium containing a 70 kDa fragment of fibronectin known to block fibronectin fibrillogenesis (McKeown-Longo and Mosher, 1985). Thus, fibronectin matrix assembly is blocked in the

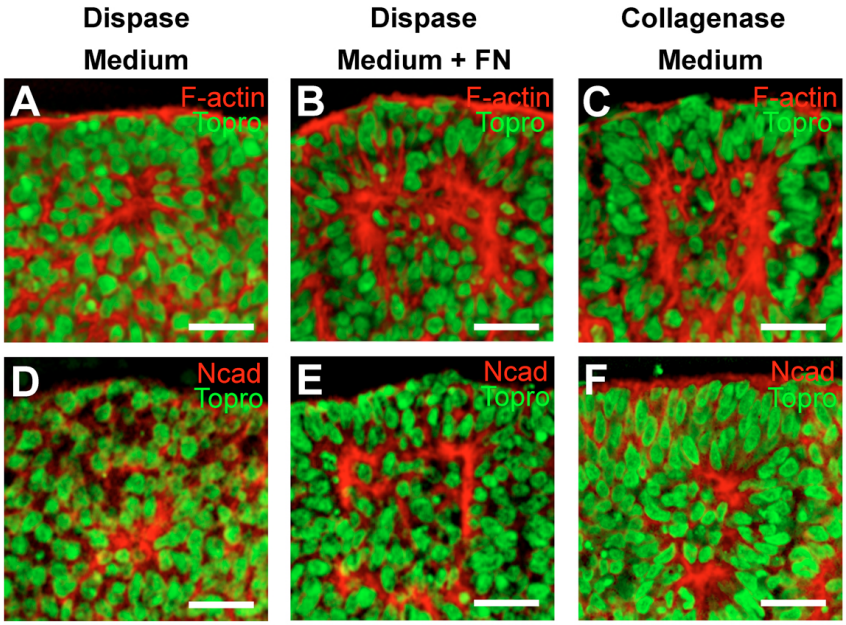

Fig. 6. F-actin and N-cadherin distribution in dispase-isolated PSMs cultured with and without fibronectin. Somite III regions (i.e. somite –II at 0 hours) of dispase-isolated chick PSMs after 6 hours of culture in control medium show only small foci of F-actin (**A**) and N-cadherin (**D**) clustering. By contrast, the same region of dispase-isolated PSMs cultured with fibronectin shows a prominent apical enrichment of F-actin (**B**) and N-cadherin (**E**) and a nuclear alignment and elongation typical in epithelial somites (B,E). Interestingly, this cellular arrangement is very similar to that observed in collagenase-treated PSMs (**C**,**F**). Anterior, left. Scale bars: 25 μm.

presence of ectoderm. Endoderm was removed from one side of the embryo to improve the accessibility of the peptide, while the other side was kept intact. Control embryos formed the expected 7-8 somites (Fig. 8A,C,E). However, when explants were cultured in the presence of 50 μg/ml of the fibronectin peptide (Fig. 8B,E), somitogenesis was less efficient (this was only significant in the absence of endoderm; P=0.005). Strikingly, when embryos were cultured in the presence of 100 μg/ml of the peptide, somitogenesis was practically abolished, both in the presence (P=0.002) and absence (P=0.001) of endoderm (Fig. 8D,E). We conclude that fibronectin matrix assembly is absolutely necessary for morphological somite formation, even when ectoderm is left intact over the PSM.

DISCUSSION

PSMs isolated from all surrounding tissues form somites if their fibronectin matrix is left intact

The notion that fibronectin might be an important player in somitogenesis is not new. A fibronectin matrix outlines epithelial somites in both chick and mouse and its distribution pattern in the PSM shows a more complex matrix anteriorly than posteriorly, such that it has been suggested that this matrix is progressively laid down as the PSM matures (Lash et al., 1984; Lash and Ostrovsky, 1986; Ostrovsky et al., 1983; Ostrovsky et al., 1988). Experiments involving the addition of fibronectin to dissociated chick PSM cells caused their aggregation, suggesting that fibronectin might normally play a role in compacting and/or increasing the cell-cell adhesiveness of anterior PSM cells (Lash et al., 1984; Lash et al., 1987). In agreement with this, we show that adding exogenous fibronectin to pancreatin-isolated PSMs significantly improved their capacity to form somites.

In *Fn1*-null mouse embryos, paraxial mesoderm initially forms normally but does not generate any morphologically distinguishable somites (Georges-Labouesse et al., 1996). The *Fn1*-null phenotype thus represents one of the most severe somitogenesis phenotypes in a single mouse gene (reviewed by Pourquié, 2001). Moreover, a fibronectin matrix is required for normal somitogenesis and axial extension in *Xenopus* (Marsden and DeSimone, 2003) and both *fn1* and *itga5* knock-down interfere with somite epithelialisation and boundary maintenance in zebrafish (Julich et al., 2005; Koshida et al., 2005).

Many authors have reported that PSMs cultured in the absence of all surrounding tissues do not form somites (Borycki et al., 1998; Borycki et al., 2000; Correia and Conlon, 2000; Lash et al., 1984; Lash and Ostrovsky, 1986; Lash and Yamada, 1986; Linker et al., 2003; Packard, 1976; Packard, 1980; Palmeirim et al., 1998). In all these studies, PSMs were isolated with pancreatin (which contains trypsin), trypsin or dispase. Here we demonstrate that 3-4 minutes of exposure to pancreatin or dispase is sufficient to remove all fibronectin immunoreactivity from isolated PSM, whereas collagenase-isolated PSMs retain their fibronectin matrix and form somites. We thus show for the first time that isolated PSMs can form somites in the absence of all surrounding tissues as long as the fibronectin matrix is preserved. We propose that the major cause for the reported failure in morphological somite formation in isolated PSMs is that the enzymes commonly used for their isolation degrade the fibronectin matrix.

Ectoderm and PSM collaborate to produce PSM fibronectin matrix

Our results demonstrate that ectoderm strongly expresses *Fn1*, whereas the PSM expresses very little (see proposed model in Fig. 9). Cultured ectoderm assembles an extensive, basally located fibronectin matrix (Newgreen and Thiery, 1980), showing that ectodermal *Fn1* expression results in the production of fibronectin, which is predominantly secreted basally towards the PSM. Furthermore, fibronectin-positive ‘dense bodies’ appear to come off the basal surface of the ectoderm as fibronectin-positive extracellular material accumulates on the mesoderm (Sanders, 1986). In fact, extracellular matrix material has been described as travelling freely between germ layers in the early chick embryo (Harrisson et al., 1985). Thus, we suggest that the bulk of the PSM fibronectin matrix originates from fibronectin protein produced and secreted by the ectoderm (Fig. 9).

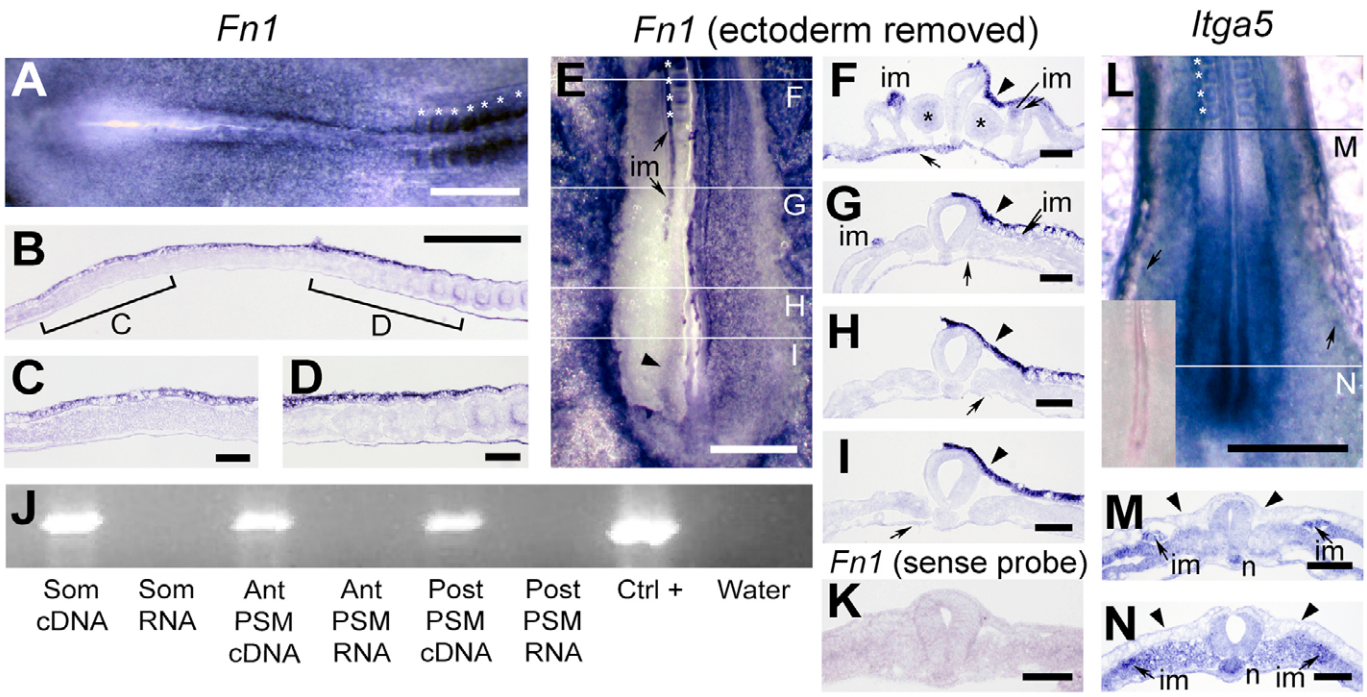

Fig. 7. mRNA expression pattern of fibronectin (*Fn1*) and its integrin receptor (*Itga5*) in the PSM and surrounding tissues. (**A-D**) In situ hybridisation for *Fn1* on HH12-14 stage chick embryos shows that *Fn1* mRNA is strongly expressed in the ectoderm overlying the PSM (A-D) and in the posterior part of epithelial somites (A,B,D). Endoderm is negative posteriorly but expression is detected at the level of anterior PSM and epithelial somites (B-D). PSM appears negative for *Fn1* mRNA except for a faint staining posteriorly (B,C). (**E-I**) Removal of ectoderm before fixation confirms this pattern and shows that *Fn1* expression is very strong in the intermediate mesoderm (E,F,G). (**J**) However, *Fn1* expression is detectable in both the anterior third and posterior two-thirds of the PSM by RT-PCR. (**K**) Negative hybridisation control with *Fn1* sense probe. (**L-N**) In situ hybridisation for *Itga5* shows that it is strongly expressed in the posterior two-thirds of the PSM and in epithelial somites. Insert (L) shows sense probe control. Sections of *Itga5*-hybridised embryos show that the signal in PSM is faint anteriorly (M), but strong posteriorly (N). *Itga5* is also expressed in notochord, intermediate (arrows) and lateral mesoderm (M,N), and extraembryonic blood vessels (arrows in L). Faint staining is detectable in neural tube and ectoderm (arrowheads, M,N). Anterior, up. *, Epithelial somite; im, intermediate mesoderm; n, notochord; som, somites; ant PSM, anterior PSM; post PSM, posterior PSM; Ctrl+, positive control (whole embryo cDNA); RNA, reverse-transcription omitted; water, cDNA omitted. Scale bars: 500 μm in A,B,E,L; 100 μm in C,D,F-K,M,N.

The posterior two-thirds of the PSM strongly express *Itga5*. Immunoreactivity for the β1 integrin subunit has been shown to be enriched on the surface of the PSM and is much lower within the PSM (Duband et al., 1986; Krotoski et al., 1986). Given that fibronectin matrix accumulates almost exclusively on the surface of the PSM, we suggest that α5β1 protein is enriched on the outer surface of the PSM where it regulates fibronectin assembly (Fig. 9).

Our results also show that the amount of fibronectin available to the PSM is crucial for the formation of a fibronectin matrix that can support somitogenesis. As the PSM-derived fibronectin is not sufficient to support somitogenesis, the PSM appears to depend on an external source of fibronectin to construct its matrix. Our observations strongly suggest that this external source is ectoderm.

A new role for ectoderm in morphological somite formation

It is clear that *Paraxis* is necessary for somitogenesis (Burgess et al., 1996), and its long-term expression depends on the overlying ectoderm (Correia and Conlon, 2000; Schmidt et al., 2004; Sosić et al., 1997). However, *Paraxis* expression is maintained in the paraxial mesoderm for up to 10 hours without any interaction with ectoderm (Linker et al., 2005), which agrees with our observation of strong *Paraxis* expression in isolated PSMs cultured for 6 hours (Palmeirim et al., 1998) (this study). Thus, although ectoderm is essential to maintain *Paraxis* in the dermomyotome (Linker et al., 2005), it is dispensable for initial *Paraxis* expression in PSM and early somites.

Our results instead provide evidence of a previously unrecognised role of ectoderm in somitogenesis, which is the production of the bulk of fibronectin necessary for morphological somite formation. However, we also show that if enough fibronectin has assembled into a matrix in the anterior PSM, the ectoderm is no longer required for somite formation. How can these results be reconciled with the existing literature that advocates an essential signalling role of ectoderm in morphological somite formation? We suggest that when ectoderm is removed from the full extension of the chick PSM in ovo (Sosić et al., 1997), or from the caudal PSM (Schmidt et al., 2004), somites do not form because the PSM is deprived of the major source of fibronectin necessary to construct its matrix (Fig. 9). In fact, if ectoderm is replaced over the PSM after its manipulation, there is little effect on somitogenesis (Packard et al., 1993). Conversely, we propose that when ectoderm is physically separated from the anterior PSM, epithelial somites form (Linker et al., 2005) because the fibronectin matrix in the anterior PSM remains undamaged. Furthermore, when dispase-treated PSMs are cultured within a bag of tail ectoderm, somite formation is

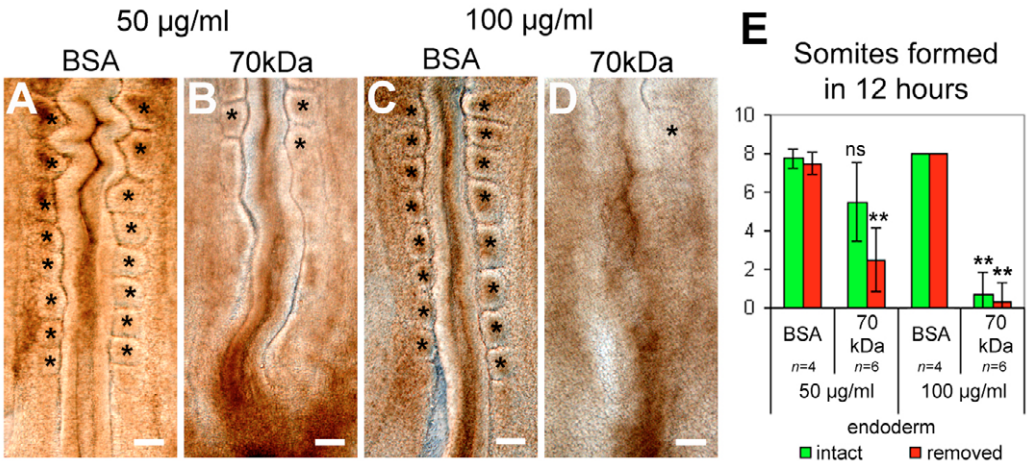

Fig. 8. A 70 kDa peptide containing the fibronectin assembly domain inhibits somitogenesis in embryo explants cultured for 12 hours. (**A-D**) Ventral view of chick embryo explants cultured with BSA (control) or the 70 kDa fibronectin fragment. Endoderm was removed on the left while the other side was kept intact. Embryos incubated with BSA form the expected number of somites in 12 hours (A,C), whereas embryos cultured with the 70 kDa fibronectin fragment form fewer somites (B,D). When embryos are cultured with 100 µg/ml of the peptide, somitogenesis is practically abolished (D). (**E**) Bar chart of the results obtained in A-D. Error bars represent 95% confidence limits. *, Somites formed in culture; BSA, bovine serum albumin; 70 kDa, 70 kDa fibronectin fragment; ns, not significant; **, $P \leqslant 0.005$. Scale bars: 100 µm.

partially restored (Correia and Conlon, 2000). We show that pancreatin-treated PSMs significantly increased their ability to form somites when cultured in fibronectin-enriched medium. It is thus tempting to suggest that the ectoderm bags used by Correia and Conlon (Correia and Conlon, 2000) provided a rich source of fibronectin protein to the dispase-isolated PSMs, allowing them to assemble a fibronectin matrix and partially restore somitogenesis. We propose that for morphological somites to form, PSMs need a major external source of fibronectin – the overlying ectoderm – in order to build a fibronectin matrix able to support somite formation.

Does ectoderm play additional roles in morphological somite formation?

Although the role of Wnts in the segmentation clock and in the differentiation of epithelial somites is well documented (reviewed by Auhehla and Pourquié, 2006; Rida et al., 2004; Yusuf and Brand-Saberi, 2006), their role in the epithelialisation of somites is much less clear. Wnt6, the only Wnt expressed in the ectoderm overlying the anterior PSM (Cauthen et al., 2001; Rodriguez-Niedenfuhr et al., 2003; Schubert et al., 2002), is the most likely candidate to play a role in somite formation. Wnt6-expressing cells placed in the caudal PSM after ectoderm removal rescue *Paraxis*, *Pax3* and *MyoD* expression after 18 hours of culture (Schmidt et al., 2004). However, expression of these genes is independent of somite epithelialisation (Linker et al., 2005; Palmeirim et al., 1998; Burgess et al., 1996; Wilson-Rawls et al., 1999) (this study). Furthermore, our results show that somites form in collagenase-isolated PSMs in the absence of ectoderm and that somitogenesis is severely affected when fibronectin matrix assembly is inhibited in its presence. These data therefore strongly argue against a direct role of ectodermal Wnts on the epithelialisation of the anterior PSM. Although ectodermal canonical Wnt signalling cannot be ruled out as a player in morphological somite formation [some somite-like condensations form in dispase-isolated quail PSM explants cultured with LiCl (Borycki et al., 2000)], our experiments show that its role in somite epithelialisation can only be minor in comparison with that of the fibronectin matrix.

Fibronectin matrix assembly as a part of the somitogenesis machinery

We have demonstrated that the PSM fibronectin matrix is essential for morphological somite formation. Fibronectin matrix assembly is a complex process (reviewed by Wierzbicka-Patynowski and Schwarzbauer, 2003; Mao and Schwarzbauer, 2005) and its strengthening and maintenance is dependent on the amount of free fibronectin available for continuous incorporation, even after an initial fibrillar matrix has formed. This might explain why collagenase-isolated PSM+ectoderm explants form significantly more somites than collagenase-isolated PSMs. Since ectoderm produces fibronectin during the 6-hour culture period, the matrix of PSMs cultured with ectoderm increases in strength, whereas PSMs isolated without ectoderm rely on the matrix they have at the time of isolation. The 70 kDa fibronectin fragment used in our experiments prevents the fibronectin-fibronectin binding essential for the formation of new fibrils and it also binds to and displaces fibronectin within young fibrils (McKeown-Longo and Mosher, 1985), explaining its dramatic effect on somite formation. We propose that the presence of ectoderm promotes a continuous fibronectin fibrillogenesis that maintains and increases the strength of the PSM fibronectin matrix, essential to support somitogenesis.

Is the PSM fibronectin matrix solely providing a structural framework or could fibronectin also be playing an instructive role? Studies of *Xenopus* convergent extension have demonstrated that fibronectin affects cadherin-mediated cell-cell adhesion, which is important for morphogenetic movements (Marsden and DeSimone, 2003). Fibronectin signalling through α5β1 integrin upregulates N-cadherin expression in cultured myoblasts (Huttenlocher et al., 1998). Since N-cadherin has been implicated in somitogenesis (Horikawa et al., 1999; Linask et al., 1998; Radice et al., 1997) and the presence of fibronectin correlates with the cellular redistribution

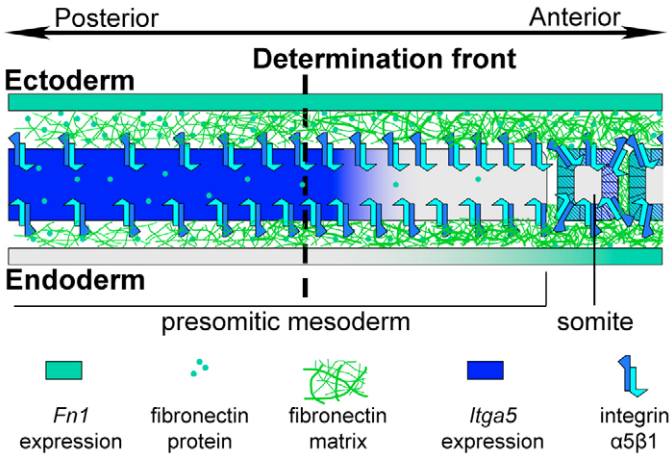

Fig. 9. Model of fibronectin assembly in the chick PSM. Sagittal view of PSM and first epithelial somite, showing ectoderm dorsally and endoderm ventrally. Based on our data, we suggest that PSM fibronectin matrix assembly occurs primarily in the posterior two-thirds of the PSM and that the fibronectin matrix in the anterior-most PSM is (if left unperturbed) sufficiently extensive to support somite formation. We propose that ectoderm is the major source of fibronectin protein for this matrix, and that only a minor contribution comes from the PSM itself. The PSM does however express α5β1 integrin, which is essential for the assembly process. Although *Itga5* mRNA is not detected in the anterior PSM, we hypothesise that the α5β1 protein remains on its surface. *Itga5* mRNA is again detected in epithelial somites, whereas *Fn1* is expressed in their posterior half, suggesting a potential role in the stabilisation of somite clefts (Koshida et al., 2005). According to our model, ectoderm ablation over the posterior two-thirds of the PSM compromises fibronectin matrix assembly and the formation of somites by the underlying PSM. By contrast, ectoderm ablation over the anterior-most PSM, if performed without destroying the endogenous fibronectin matrix, does not affect somite formation.

of N-cadherin and F-actin (this study), α5β1-mediated signalling might affect N-cadherin during somitogenesis. Integrin α5β1 and fibronectin have also been shown to regulate cell behaviour during convergent extension in *Xenopus* (Davidson et al., 2006). This is controlled by small GTPases of the Rho family (Fukata et al., 2003), which have been implicated in the regulation of the mesenchymal-to-epithelial transition of the anterior PSM (Nakaya et al., 2004).

In summary, we conclude that fibronectin is an essential player in somitogenesis and that the PSM fibronectin matrix is the product of a collaboration between the PSM and the overlying ectoderm. We propose that the continuous build-up of the fibronectin matrix is essential for somitogenesis and that the removal of this matrix or the inhibition of its assembly compromises morphological somite formation. It is also tempting to suggest that the increasing complexity of the fibronectin matrix might transmit specific signals, so that cell behaviour in the anterior PSM changes, promoting epithelialisation. Whether and how fibronectin collaborates with other factors to achieve this morphological transition into somites will be interesting issues to explore.

We thank Gabriel G. Martins and Fernanda Bajanca for helpful suggestions during the course of this work and for reading the manuscript; Jorge Palmeirim for statistical advice; Luís Marques for valuable help; and C. Jouve for cDNA. Financial support was from Fundação para a Ciência e a Tecnologia (FCT)/FEDER projects POCTI/BCI/40754/2001 and POCI/BIA-BCM/59201/2004 and the FP6/EU Network of Excellence 'Cells into Organs' of which P.R., C.L., R.P.A., G.R., I.P. and S.T. are members. L.C. was supported by the European Social Fund contract 1/3.2/PRODEP/2001. R.P.A. was supported by FCT (SFRH/BPD/9432/2002).

References

Aulehla, A. and Pourquié, O. (2006). On periodicity and directionality of somitogenesis. *Anat. Embryol.* **211**, Suppl. 1, 3-8.
Bajanca, F., Luz, M., Duxson, M. J. and Thorsteinsdóttir, S. (2004). Integrins in the mouse myotome: Developmental changes and differences between the epaxial and hypaxial lineage. *Dev. Dyn.* **231**, 402-415.
Barnes, J. L., Torres, E. S., Mitchell, R. J. and Peters, J. H. (1995). Expression of alternatively spliced fibronectin variants during remodeling in proliferative glomerulonephritis. *Am. J. Pathol.* **147**, 1361-1371.
Barrios, A., Poole, R. J., Durbin, L., Brennan, C., Holder, N. and Wilson, S. W. (2003). Eph/Ephrin signaling regulates the mesenchymal-to-epithelial transition of the paraxial mesoderm during somite morphogenesis. *Curr. Biol.* **13**, 1571-1582.
Borycki, A. G., Mendham, L. and Emerson, C. P., Jr (1998). Control of somite patterning by Sonic hedgehog and its downstream signal response genes. *Development* **125**, 777-790.
Borycki, A., Brown, A. M. and Emerson, C. P., Jr (2000). Shh and Wnt signaling pathways converge to control Gli gene activation in avian somites. *Development* **127**, 2075-2087.
Burgess, R., Rawls, A., Brown, D., Bradley, A. and Olson, E. N. (1996). Requirement of the *paraxis* gene for somite formation and musculoskeletal patterning. *Nature* **384**, 570-573.
Cauthen, C. A., Berdougo, E., Sandler, J. and Burrus, L. W. (2001). Comparative analysis of the expression patterns of *Wnts* and *Frizzleds* during early myogenesis in chick embryos. *Mech. Dev.* **104**, 133-138.
Christ, B. and Ordahl, C. P. (1995). Early stages of chick somite development. *Anat. Embryol.* **191**, 381-396.
Correia, K. M. and Conlon, R. A. (2000). Surface ectoderm is necessary for the morphogenesis of somites. *Mech. Dev.* **91**, 19-30.
Davidson, L. A., Marsden, M., Keller, R. and DeSimone, D. W. (2006). Integrin α5β1 and fibronectin regulate polarized cell protrusions required for Xenopus convergence and extension. *Curr. Biol.* **16**, 833-844.
Diez del Corral, R., Olivera-Martinez, I., Goriely, A., Gale, E., Maden, M. and Storey, K. (2003). Opposing FGF and retinoid pathways control ventral neural pattern, neuronal differentiation, and segmentation during body axis extension. *Neuron* **40**, 65-79.
Duband, J. L., Rocher, S., Chen, W. T., Yamada, K. M. and Thiery, J. P. (1986). Cell adhesion and migration in the early vertebrate embryo: location and possible role of the putative fibronectin receptor complex. *J. Cell Biol.* **102**, 160-178.
Duband, J. L., Dufour, S., Hatta, K., Takeichi, M., Edelman, G. M. and Thiery, J. P. (1987). Adhesion molecules during somitogenesis in the avian embryo. *J. Cell Biol.* **104**, 1361-1374.
Dubrulle, J., McGrew, M. J. and Pourquié, O. (2001). FGF signaling controls somite boundary position and regulates segmentation clock control of spatiotemporal Hox gene activation. *Cell* **106**, 219-232.
Durbin, L., Sordino, P., Barrios, A., Gering, M., Thisse, C., Thisse, B., Brennan, C., Green, A., Wilson, S. and Holder, N. (2000). Anteroposterior patterning is required within segments for somite boundary formation in developing zebrafish. *Development* **127**, 1703-1713.
ffrench-Constant, C. and Hynes, R. O. (1988). Patterns of fibronectin gene expression and splicing during cell migration in chicken embryos. *Development* **104**, 369-382.
Freitas, C., Rodrigues, S., Saúde, L. and Palmeirim, I. (2005). Running after the clock. *Int. J. Dev. Biol.* **49**, 317-324.
Fukata, M., Nakagawa, M. and Kaibuchi, K. (2003). Roles of Rho-family GTPases in cell polarisation and directional migration. *Curr. Opin. Cell Biol.* **15**, 590-597.
George, E. L., Georges-Labouesse, E. N., Patel-King, R. S., Rayburn, H. and Hynes, R. O. (1993). Defects in mesoderm, neural tube and vascular development in mouse embryos lacking fibronectin. *Development* **119**, 1079-1091.
Georges-Labouesse, E. N., George, E. L., Rayburn, H. and Hynes, R. O. (1996). Mesodermal development in mouse embryos mutant for fibronectin. *Dev. Dyn.* **207**, 145-156.
Gossler, A. and Hrabě de Angelis, M. (1998). Somitogenesis. *Curr. Top. Dev. Biol.* **38**, 225-287.
Hamburger, V. and Hamilton, H. L. (1992). A series of normal stages in the development of the chick embryo. 1951. *Dev. Dyn.* **195**, 231-272.
Harrisson, F., Van Hoof, J., Vanroelen, C. and Vakaet, L. (1985). Transfer of extracellular matrix components between germ layers in chimaeric chicken-quail blastoderms. *Cell Tissue Res.* **239**, 643-649.
Henrique, D., Adam, J., Myat, A., Chitnis, A., Lewis, J. and Ish-Horowicz, D. (1995). Expression of a Delta homologue in prospective neurons in the chick. *Nature* **375**, 787-790.

Horikawa, K., Radice, G., Takeichi, M. and Chisaka, O. (1999). Adhesive subdivisions intrinsic to the epithelial somites. *Dev. Biol.* **215**, 182-189.
Huttenlocher, A., Lakonishok, M., Kinder, M., Wu, S., Truong, T., Knudsen, K. A. and Horwitz, A. F. (1998). Integrin and cadherin synergy regulates contact inhibition of migration and motile activity. *J. Cell Biol.* **141**, 515-526.
Jülich, D., Geisler, R. and Holley, S. A. (2005). Integrinα5 and delta/notch signaling have complementary spatiotemporal requirements during zebrafish somitogenesis. *Dev. Cell* **8**, 575-586.
Koshida, S., Kishimoto, Y., Ustumi, H., Shimizu, T., Furutani-Seiki, M., Kondoh, H. and Takada, S. (2005). Integrinα5-dependent Fibronectin accumulation for maintenance of somite boundaries in zebrafish embryos. *Dev. Cell* **8**, 587-598.
Krotoski, D. M., Domingo, C. and Bronner-Fraser, M. (1986). Distribution of a putative cell surface receptor for fibronectin and laminin in the avian embryo. *J. Cell Biol.* **103**, 1061-1071.
Kulesa, P. M. and Fraser, S. E. (2002). Cell dynamics during somite boundary formation revealed by time-lapse analysis. *Science* **298**, 991-995.
Lash, J. W. and Ostrovsky, D. (1986). On the formation of somites. *Dev. Biol. N. Y.* **2**, 547-563.
Lash, J. W. and Yamada, K. M. (1986). The adhesion recognition signal of fibronectin: a possible trigger mechanism for compaction during somitogenesis. In *Somites in Developing Embryos* (ed. R. Bellairs, D. Ede and J. W. Lash), pp. 201-208. New York: Plenum Press.
Lash, J. W., Seitz, A. W., Cheney, C. M. and Ostrovsky, D. (1984). On the role of fibronectin during the compaction stage of somitogenesis in the chick embryo. *J. Exp. Zool.* **232**, 197-206.
Lash, J. W., Linask, K. K. and Yamada, K. M. (1987). Synthetic peptides that mimic the adhesive recognition signal of fibronectin: differential effects on cell-cell and cell-substratum adhesion in embryonic chick cells. *Dev. Biol.* **123**, 411-420.
Linask, K. K., Ludwig, C., Han, M. D., Liu, X., Radice, G. L. and Knudsen, K. A. (1998). N-cadherin/catenin-mediated morphoregulation of somite formation. *Dev. Biol.* **202**, 85-102.
Linker, C., Lesbros, C., Stark, M. R. and Marcelle, C. (2003). Intrinsic signals regulate the initial steps of myogenesis in vertebrates. *Development* **130**, 4797-4807.
Linker, C., Lesbros, C., Gros, J., Burrus, L. W., Rawls, A. and Marcelle, C. (2005). β-Catenin-dependent Wnt signalling controls the epithelial organisation of somites through the activation of *paraxis*. *Development* **132**, 3895-3905.
Mao, Y. and Schwarzbauer, J. E. (2005). Fibronectin fibrillogenesis, a cell-mediated matrix assembly process. *Matrix Biol.* **24**, 389-399.
Marsden, M. and DeSimone, D. W. (2003). Integrin-ECM interactions regulate cadherin-dependent cell adhesion and are required for convergent extension in *Xenopus*. *Curr. Biol.* **13**, 1182-1191.
McKeown-Longo, P. J. and Mosher, D. F. (1983). Binding of plasma fibronectin to cell layers of human skin fibroblasts. *J. Cell Biol.* **97**, 466-472.
McKeown-Longo, P. J. and Mosher, D. F. (1985). Interaction of the 70,000-mol-wt amino-terminal fragment of fibronectin with the matrix-assembly receptor of fibroblasts. *J. Cell Biol.* **100**, 364-374.
Nakaya, Y., Kuroda, S., Katagiri, Y. T., Kaibuchi, K. and Takahashi, Y. (2004). Mesenchymal-epithelial transition during somitic segmentation is regulated by differential roles of Cdc42 and Rac1. *Dev. Cell* **7**, 425-438.
Newgreen, D. and Thiery, J. P. (1980). Fibronectin in early avian embryos: synthesis and distribution along the migration pathways of neural crest cells. *Cell Tissue Res.* **211**, 269-291.
Norton, P. A. and Hynes, R. O. (1987). Alternative splicing of chicken fibronectin in embryos and in normal and transformed cells. *Mol. Cell. Biol.* **7**, 4297-4307.
Ostrovsky, D., Cheney, C. M., Seitz, A. W. and Lash, J. W. (1983). Fibronectin distribution during somitogenesis in the chick embryo. *Cell Differ.* **13**, 217-223.
Ostrovsky, D., Sanger, J. W. and Lash, J. W. (1988). Somitogenesis in the mouse embryo. *Cell Differ.* **23**, 17-25.
Packard, D. S., Jr (1976). The influence of axial structures on chick somite formation. *Dev. Biol.* **53**, 36-48.
Packard, D. S., Jr (1980). Somitogenesis in cultured embryos of the Japanese quail, *Coturnix coturnix japonica*. *Am. J. Anat.* **158**, 83-91.
Packard, D. S., Jr, Zheng, R. Z. and Turner, D. C. (1993). Somite pattern regulation in the avian segmental plate mesoderm. *Development* **117**, 779-791.
Palmeirim, I., Henrique, D., Ish-Horowicz, D. and Pourquié, O. (1997). Avian hairy gene expression identifies a molecular clock linked to vertebrate segmentation and somitogenesis. *Cell* **91**, 639-648.
Palmeirim, I., Dubrulle, J., Henrique, D., Ish-Horowicz, D. and Pourquié, O. (1998). Uncoupling segmentation and somitogenesis in the chick presomitic mesoderm. *Dev. Genet.* **23**, 77-85.
Pankov, R. and Yamada, K. M. (2002). Fibronectin at a glance. *J. Cell Sci.* **115**, 3861-3863.
Pourquié, O. (2001). Vertebrate somitogenesis. *Annu. Rev. Cell Dev. Biol.* **17**, 311-350.
Radice, G. L., Rayburn, H., Matsunami, H., Knudsen, K. A., Takeichi, M. and Hynes, R. O. (1997). Developmental defects in mouse embryos lacking N-cadherin. *Dev. Biol.* **181**, 64-78.
Rida, P. C., Le Minh, N. and Jiang, Y. J. (2004). A Notch feeling of somite segmentation and beyond. *Dev. Biol.* **265**, 2-22.
Rodríguez-Niedenführ, M., Dathe, V., Jacob, H. J., Pröls, F. and Christ, B. (2003). Spatial and temporal pattern of *Wnt-6* expression during chick development. *Anat. Embryol.* **206**, 447-451.
Saga, Y. and Takeda, H. (2001). The making of the somite: molecular events in vertebrate segmentation. *Nat. Rev. Genet.* **2**, 835-845.
Sambrook, S. K., Fritsch, E. F. and Maniatis, T. (1989). *Molecular Cloning: A Laboratory Manual*. Cold Spring Harbor: Cold Spring Harbor Laboratory Press.
Sanders, E. J. (1986). Mesoderm migration in the early chick embryo. In *Developmental Biology. A comprehensive Synthesis.* (ed. Browder L.W.), pp. 449-480. New York: Plenum Press.
Sato, Y., Yasuda, K. and Takahashi, Y. (2002). Morphological boundary forms by a novel inductive event mediated by Lunatic fringe and Notch during somitic segmentation. *Development* **129**, 3633-3644.
Sawada, A., Fritz, A., Jiang, Y. J., Yamamoto, A., Yamasu, K., Kuroiwa, A., Saga, Y. and Takeda, H. (2000). Zebrafish Mesp family genes, *mesp-a* and *mesp-b* are segmentally expressed in the presomitic mesoderm, and Mesp-b confers the anterior identity to the developing somites. *Development* **127**, 1691-1702.
Schmidt, C., Stoeckelhuber, M., McKinnell, I., Putz, R., Christ, B. and Patel, K. (2004). Wnt 6 regulates the epithelialisation process of the segmental plate mesoderm leading to somite formation. *Dev. Biol.* **271**, 198-209.
Schubert, F. R., Mootoosamy, R. C., Walters, E. H., Graham, A., Tumiotto, L., Munsterberg, A. E., Lumsden, A. and Dietrich, S. (2002). *Wnt6* marks sites of epithelial transformations in the chick embryo. *Mech. Dev.* **114**, 143-148.
Sosić, D., Brand-Saberi, B., Schmidt, C., Christ, B. and Olson, E. N. (1997). Regulation of *paraxis* expression and somite formation by ectoderm- and neural tube-derived signals. *Dev. Biol.* **185**, 229-243.
Stenn, K. S., Link, R., Moellmann, G., Madri, J. and Kuklinska, E. (1989). Dispase, a neutral protease from *Bacillus polymyxa*, is a powerful fibronectinase and type IV collagenase. *J. Invest. Dermatol.* **93**, 287-290.
Wierzbicka-Patynowski, I. and Schwarzbauer, J. E. (2003). The ins and outs of fibronectin matrix assembly. *J. Cell Sci.* **116**, 3269-3276.
Wilson-Rawls, J., Hurt, C. R., Parsons, S. M. and Rawls, A. (1999). Differential regulation of epaxial and hypaxial muscle development by Paraxis. *Development* **126**, 5217-5229.
Yang, J. T., Bader, B. L., Kreidberg, J. A., Ullman-Cullere, M., Trevithick, J. E. and Hynes, R. O. (1999). Overlapping and independent functions of fibronectin receptor integrins in early mesodermal development. *Dev. Biol.* **215**, 264-277.
Yusuf, F. and Brand-Saberi, B. (2006). The eventful somite: patterning, fate determination and cell division in the somite. *Anat. Embryol.* **211**, Suppl. 1, 21-30.

Chapter 3

Dynamic 3D cell rearrangements guided by a fibronectin matrix underlie somitogenesis

Dynamic 3D cell rearrangements guided by a fibronectin matrix underlie somitogenesis.

Gabriel G. Martins [1,2], Pedro Rifes [1,2], Rita Amândio [1,2], Gabriela Rodrigues [1,2] , Isabel Palmeirm [3] and Sólveig Thorsteinsdóttir [1,2]

PLoS One 4, e7429, 2009

[1] Departamento de Biologia Animal e Centro de Biologia Ambiental, Faculdade de Ciências, Universidade de Lisboa, 1749-016 Lisboa, Portugal.
[2] Instituto Gulbenkian de Ciência, 2781-901 Oeiras, Portugal.
[3] Life and Health Sciences Research Institute (ICVS), School of Health Sciences, University of Minho, 4710-057 Braga, Portugal.

Contribution to the publication:

	Experimental work depicted in:							manuscript writing
	Fig. 1	Fig. 2	Fig. 3	Fig. 4	Fig. 5	Fig. 6	Supp. Fig. 1	
Design and concept	I	I	II	III	III	I	O	II
Execution	I/II	O	II	III	III	n.a.	O	
Analysis and interpretation	I/II	I	II	III	III	n.a.	O	

Legend:
n.a……. non applicable
O …….. no intervention
I……. minor contribution
II…… moderate contribution
III……major contribution/full execution
Note: this contribution does not exclude other contributions, similar or not, from the remaining authors

OPEN ACCESS Freely available online

PLoS one

Dynamic 3D Cell Rearrangements Guided by a Fibronectin Matrix Underlie Somitogenesis

Gabriel G. Martins[1,2]*, Pedro Rifes[1,2], Rita Amândio[1,2], Gabriela Rodrigues[1,2], Isabel Palmeirim[3], Sólveig Thorsteinsdóttir[1,2]*

1 Centro de Biologia Ambiental, Departamento de Biologia Animal Faculdade de Ciências, Universidade de Lisboa, Lisboa, Portugal, **2** Instituto Gulbenkian de Ciência, Oeiras, Portugal, **3** Life and Health Sciences Research Institute (ICVS), School of Health Sciences, University of Minho, Braga, Portugal

Abstract

Somites are transient segments formed in a rostro-caudal progression during vertebrate development. In chick embryos, segmentation of a new pair of somites occurs every 90 minutes and involves a mesenchyme-to-epithelium transition of cells from the presomitic mesoderm. Little is known about the cellular rearrangements involved, and, although it is known that the fibronectin extracellular matrix is required, its actual role remains elusive. Using 3D and 4D imaging of somite formation we discovered that somitogenesis consists of a complex choreography of individual cell movements. Epithelialization starts medially with the formation of a transient epithelium of cuboidal cells, followed by cell elongation and reorganization into a pseudostratified epithelium of spindle-shaped epitheloid cells. Mesenchymal cells are then recruited to this medial epithelium through accretion, a phenomenon that spreads to all sides, except the lateral side of the forming somite, which epithelializes by cell elongation and intercalation. Surprisingly, an important contribution to the somite epithelium also comes from the continuous egression of mesenchymal cells from the core into the epithelium via its apical side. Inhibition of fibronectin matrix assembly first slows down the rate, and then halts somite formation, without affecting pseudopodial activity or cell body movements. Rather, cell elongation, centripetal alignment, N-cadherin polarization and egression are impaired, showing that the fibronectin matrix plays a role in polarizing and guiding the exploratory behavior of somitic cells. To our knowledge, this is the first 4D *in vivo* recording of a full mesenchyme-to-epithelium transition. This approach brought new insights into this event and highlighted the importance of the extracellular matrix as a guiding cue during morphogenesis.

Citation: Martins GG, Rifes P, Amândio R, Rodrigues G, Palmeirim I, et al. (2009) Dynamic 3D Cell Rearrangements Guided by a Fibronectin Matrix Underlie Somitogenesis. PLoS ONE 4(10): e7429. doi:10.1371/journal.pone.0007429

Editor: Patrick Callaerts, Katholieke Universiteit Leuven, Belgium

Received May 10, 2009; **Accepted** September 16, 2009; **Published** October 15, 2009

Funding: This work was supported by the Portuguese Fundação para a Ciência e a Tecnologia (FCT) and the POCI 2010 program (III Community Support Framework)/FEDER through project POCI/BIA-BCM/59201/2004 as well as by the Network of Excellence "Cells into Organs"(EU/FP6). GGM was supported through a fellowship from FCT (SFRH/BPD/18907/2004), PR was supported by a PhD grant from FCT (SFRH/BD/37423/2007) and RA was supported with IEFP and FCT grants. The funders had no role in the study design, data collection and analysis, decision to publish, or preparation of the manuscript.

Competing Interests: The authors have declared that no competing interests exist.

* E-mail: gaby@fc.ul.pt (GGM); solveig@fc.ul.pt (ST)

Introduction

Imaging morphogenesis in live embryos and tissues has revealed that cells are much more dynamic than previously thought, changing their shape and behavior in ways that our interpretation of successive static images of developmental stages could not have predicted [1–5]. Analysis of cell behavior *in vivo* has caused a revival of the concept that morphogenesis is generated through the modulation of mechanical properties of cells, affecting their shape and relationship with the surroundings [6–9]. The extracellular matrix (ECM) surrounding cells *in vivo* is a key regulator of their shape, differentiation state and motile behavior [10–12]. Cell engagement of the ECM through integrins (or other receptors), in turn affects the mechanical state of the cytoskeleton and often also translates the mechanical forces of the ECM into chemical signals intracellularly [7,13–15]. Furthermore, cell-ECM engagement is known to modulate cell-cell adhesion, another important player in the regulation of morphogenesis [16]. Thus, to fully understand morphogenesis *in vivo* we must know how cells behave during morphogenetic events and how they interact with, and are influenced by the surrounding ECM.

Metamerization of the vertebrate axial musculoskeletal, nervous and circulatory systems is established during development as a result of the transformation of a mass of mesenchymal cells, which make up the presomitic mesoderm (PSM), into a series of epithelial somites located on both sides of the neural tube [17,18]. Somites are formed in a periodic fashion (every 90 minutes in the chick) emerging from the rostral end of the PSM as spheres of epithelial cells organized centripetally around a mesenchymal somitocoel [19–21]. Much is known about the molecular mechanisms which define the periodic positioning of somitic boundaries as well as the rostro-caudal polarity of somites [22–24]. However, almost nothing is known about how cell shape and behavior are altered as the mesenchymal PSM transforms into epithelial somites.

A fibronectin (FN) matrix surrounds the PSM and recently formed somites [25,26] and inactivation of the FN gene (*Fn1*) in the mouse prevents somitogenesis [27,28]. More recently, the importance of FN in somitogenesis has also been established in zebrafish [29,30], *Xenopus laevis* [31,32] and chick [33]. We have demonstrated that in chick, the FN matrix surrounding the PSM is generated through collaboration between ectoderm and PSM: the ectoderm produces FN which is then assembled by integrin $\alpha5\beta1$

expressed by PSM cells. Furthermore, when FN matrix assembly is blocked, somitogenesis fails [33]. These results explain the requirement of ectoderm for morphological somite formation [34,35] and demonstrate that FN needs to be assembled into a matrix in order to support somitogenesis. However, in spite of these recent advances, we still do not know how the FN matrix affects the transformation of mesenchymal PSM cells into epithelial somitic cells.

To better understand somite morphogenesis *in vivo*, and how a mesenchyme-to-epithelium transition occurs in the embryo, we have improved procedures for 3D imaging both live and fixed chick embryos. We first obtained detailed images of fixed embryos revealing the cellular organization of the PSM and early somites as well as the 3D organization of the surrounding ECM. We then used two-photon live imaging to obtain 3D videos (4D images) of cell dynamics during somite formation. Our results show that PSM cells are highly dynamic, exhibiting constant protrusive activity and cell body movements, and that somite epithelialization involves the progressive organization of these dynamic cells into an aster-like arrangement, a process that takes much longer than the 90 minute interval of each new boundary formation. This reveals and also clarifies the nature and sequence of events in a surprisingly complex morphogenetic process, involving two distinct stages of epithelialization and multiple concurrent cell movements, some of which had not been previously described as contributing to somitogenesis. Perturbation of *de novo* FN matrix assembly does not inhibit the dynamic behavior of PSM cells but impairs cell elongation and alignment, N-cadherin polarization and egression of cells from the somitocoel into the epithelium. These results provide new insights into the complexity of the mesenchyme-to-epithelium transition underlying somitogenesis and demonstrate how a FN matrix is essential to guide dynamic cells into an epithelial structure.

Materials and Methods

Embryos and immunohistochemistry

Fertilized chicken eggs were incubated at 38°C until the stages of interest. Embryos and explants were fixed overnight in 4% paraformaldehyde in phosphate buffered saline (PBS) at 4°C, permeabilized with 1% Triton-X100, and incubated overnight with antibodies and dyes diluted in 1% bovine serum albumin (BSA) in PBS. The following antibodies were used: anti-FN (1:400; Sigma), anti-laminin (1:100, Sigma), anti N-cadherin (clone 32, 1:100, BD Biosciences), and the appropriate Alexa Fluor-conjugated secondary antibodies (Molecular Probes). Embryos and explants were treated with ribonuclease A (10 μg/ml, Sigma) and counterstained using ToPro3 (1:500, Molecular Probes), slowly dehydrated in methanol and cleared with methylsalicylate (Sigma). Somite nomenclature follows that of Pourquié and Tam [36] where the forming somite is defined as somite 0 (s0), formed somites rostral to it are sI, sII and so forth, and prospective somites (PSM caudal to s0) are defined as s-I, s-II and so on.

Embryo preparation and culture for live-imaging

Stage HH4-5 [37] embryos were microinjected *in ovo* over the anterior primitive streak, with the PCAAGS-GFP vector [38] at a low concentration (0.8–1.4 μg/ml) which, after electroporation, resulted in a mosaic of GFP-positive and GFP-negative cells which facilitated the identification of individual cells within the tissues of interest. An Electro Square Porator ECM830 (BTX Genomics Inc) was used to deliver three to five 25–50 ms 9V pulses, spaced 350 μsec, applying a sharpened tungsten anode under the embryo and a platinum wire cathode above the PSM-prospective territory [39]. After re-incubating overnight, normally developing GFP-expressing embryos were collected with vitelline membranes using a paper ring (Whatman #1) and cleaned in warmed Hanks Balanced Salt Solution (Sigma). Embryos were then mounted ventral-side down over a 0.4 μm pore size Transwell-collagen-coated membrane (Costar, Life Sciences) which was placed on 35 mm diameter #1.5 glass-bottom Petri dishes (World Precision Instruments). The mounted embryo was bathed with Medium 199 (Sigma) with 5% fetal bovine serum and 10% chick serum (culture medium M199) as previously described [40] and the Petri dish placed on a heated stage insert (PECON Tempcontrol 37) inside a custom built microscope incubator box assuring that the embryo, objective and stage were kept at 37–38°C during time-lapse image recording.

Confocal and two-photon image acquisition

Images of fixed and immunostained embryos and explants were acquired on either a Leica SPE or a Zeiss LSM 510 confocal system. Stacks of optical sections spanning the thickness of the rostral-most PSM and recently formed somites were acquired using a 20x/0.7NA dry or a 40x/1.4NA oil-immersion objectives. 3D images of live embryos were acquired using a Zeiss LSM 510 NLO system coupled to a Ti:Sa IR pulsed laser, pumped by a 5W Verdi laser, and tuned for 880 nm. PSMs of live embryos were scanned dorso-ventrally (approximately 120 μm) using a 20x 0.7NA objective, repeated every 10 minutes for a period of 6–8 hours; bright-field images were acquired simultaneously.

Inhibition of FN fibrillogenesis

A 70 kDa amino-terminal FN fragment (100 μg/ml; Sigma) was used to inhibit FN matrix assembly [41] as in [33]. For live imaging, embryos were first cultured under the microscope in M199 medium until they formed one somite pair (to ensure normal development) after which the medium was replaced with new warmed M199 containing either the 70 kDa fragment, or BSA (100 μg/ml; Sigma) as a control. In another set of experiments, embryo explants were cultured for 6 hours over a Millipore filter floating on M199 medium [40], containing the 70 kDa fragment (or BSA in controls), after which they were labeled and processed for confocal microscopy as already described.

Image analysis and quantifications

Z-stacks of confocal and two-photon images were processed and converted using ImageJ (http://rsb.info.nih.gov/ij) and the LOCI's Bio-Formats plugin (http://www.loci.wisc.edu/ome/formats.html), before 3D reconstructions and analysis using Amira v4.1.2 (Visage Imaging, Inc.) and Imaris v5.7.2 (Bitplane, Inc) softwares. The z-depth was rescaled to compensate for refractive index mismatch (by 1.33x in the case of live embryos or by 1.52x in fixed embryos when imaged with dry lenses) and embryo drift was corrected in Amira by 3D reconstructing each time-point 3D stack and repositioning it so that the center of the first formed somite remained stationary.

The Amira software was used to obtain 3D surface reconstructions of PSMs, somites and their somitocoels (by manual segmentation and iso-surfacing of volumes), as well as volume renderings of the 3D distribution of FN, laminin and N-cadherin. 3D coordinates of the somitocoel centroid, basal and apical ends of rostral and caudal somite cells were used to calculate the cell length (= Euclidean distance between the cell's apical and basal ends), and centripetal alignment of fusiform epitheloid cells (= angle formed between the somitocoel's centroid, and the cell's basal [vertex] and apical ends; Figure S1A). These measurements were done at two time points in each embryo (n = 3; n = 20 cells/

embryo [10 rostral and 10 caudal]) and differences between s0 and sII stages as well as between rostral and caudal cells were evaluated using a repeated measures ANOVA. Differences between treatments (*i.e.* control *versus* 70 kDa fragment-treated (n = 3 embryos; n = 20 cells/embryo [10 rostral and 10 caudal])) were evaluated using a nested ANOVA, where the effects on rostral and caudal cells were evaluated separately.

Cell densities in somitocoel and somite epithelium were estimated from the nuclear labeling within the manually segmented volumes (see above) by calculating the average grey intensity *per* μm^3 and further normalizing to the average intensity of the neural tube at the same axial level. Only somites fully separated from the PSM (≥ sI) were measured and because an ANOVA revealed no significant differences between somites within each treatment, we pooled the different somites to an average *per* explant for each parameter measured, and evaluated differences between treatments (*i.e.* control *versus* 70 kDa fragment-treated) using a *t*-test.

Timing of somite formation and staging were determined by analyzing bright-field image sequences in ImageJ and scoring the appearance of new clefts. Using the 4D images in the Amira software we scored the number of pseudopodia formed by cells of control and 70 kDa fragment-treated embryos and using the Imaris software we manually tracked cell-body movements in 3D, and calculated track lengths and net displacement (distance between initial and final position; Figure S1B) of caudal *versus* rostral cells of control and 70 kDa fragment-treated embryos (n = 3 per treatment; 20 cells per embryo); measurements per treatment were pooled and differences evaluated using a *t*-test. We also determined the fate of PSM cells that were initially either peripheral or in the core and calculated the percentage that became elongated and centripetally aligned (*i.e.* epitheloid) at the end of the video, in control *versus* 70 kDa fragment-treated embryos.

All quantifications are summarized in Table S1. Statistical analysis was performed using JMP!In V4.0 (SAS institute) or Statistica 8.0 (StatSoft).

Results

Somite formation involves two stages of epithelialization and contact with a FN matrix

To better understand how cells are organized as somites form, we used N-cadherin immunolabeling and ToPro3 nuclear staining to study cell morphology and polarization in the rostral PSM and newly formed somites. At the level of s-II and s-I, medial peripheral PSM cells are cuboidal (Figure 1A), with round basal nuclei (Figure 1B) and apically polarized N-cadherin (Figure 1A). We define this layer of medial cuboidal cells with the basal side facing outwards as the first stage of somite epithelialization. At the s0 level and further rostrally, medial cells are spindle-shaped (Figure 1A), their nuclei are oval and not aligned basally (Figure 1C), N-cadherin is restricted apically (Figure 1A), and thick basal tapering extensions connect these cells to surrounding tissues (Figure 1D). We define this pseudostratified layer of polarized epithelial cells with basal protrusive activity as the second stage of epithelialization. Other cells in the rostral PSM are polygonal, widely spaced, do not present a noticeable orientation or epithelial organization, and N-cadherin is homogeneously distributed on their surface (Figure 1A).

Eventually, all peripheral cells in a mature somite reach the second stage of epithelialization, but not simultaneously on all sides. In s0, cells in rostral and lateral sides are still non-polarized, unaligned and polygonal, while on all other sides, the peripheral cells have polarized N-cadherin, are spindle-shaped and aligned centripetally (Figure 1A, 1E, 1E′, 1G and 1G′; Video S1). Consequently, a 3D reconstruction of the apical N-cadherin staining reveals a "3D adhesion basket" opened rostrally and laterally (Figure 1F, 1F′ and 1F″).

The PSM is surrounded by an extracellular matrix containing FN [26,33] and laminin [26]. Laminin immunoreactivity appears as discrete spots distributed homogeneously over the rostral-most PSM and newly formed somite (Figure 1H). This indicates that the laminin matrix is still in early stages of assembly [42–44] and only forms a continuous basement membrane later. In contrast, a dense fibrillar FN matrix surrounds the rostral PSM (Figure 1H and 1I; Video S2), and numerous FN fibrils penetrate the tissue (Figure 1J and 1J′). Cables of FN fibrils often align along pseudopodia (data not shown) and are especially frequent at the forming inter-somitic cleft (Figure 1J and 1J′; Video S2), suggesting that cells exert traction forces or use the FN matrix for structural support. We conclude that FN is the likely ECM ligand for the basal protrusions of PSM cells during somite formation.

The pseudostratified somite epithelium arises through a dynamic process initiated medially

The data from fixed embryos showed that the mesenchyme-to-epithelium transition underlying somite formation appears to occur progressively around the somite. To analyze this phenomenon *in vivo*, we obtained 4D images centered on PSM level s-II over time, until this area assembled as a new somite and reached sII (Figure 2; Video S3). Interestingly, during the whole period, cells displayed highly dynamic protrusive and motile activities (Figure 2B and 2B′), even after becoming incorporated into the epithelium (Video S3 and Table S1). Close analysis of the videos allowed us to discriminate a number of different morphogenetic movements underlying somite epithelialization: *i*) Medial cuboidal cells elongate and become spindle-shaped (Figure 2A and Video S3, blue cell). *ii*) Mesenchymal cells adjacent to these medial spindle-shaped cells attach "one-by-one" to their basal ends and "zip" along their surface, becoming elongated and centripetally aligned (Figure 2A and Video S3, red cells), a process best described as cell accretion. Accretion first spreads to the ventral and dorsal PSM side, then to the caudal side of s0 (compare Figure 2A+3h with 2A+4h), only reaching the rostral side in late s0/sI (compare Figure 2A+4h with 2A+5h). *iii*) Epithelialization of the lateral side occurs last (≥sI; compare Figure 2A+5h with 2A+6h) and involves yet another mechanism: cells from the lateral-most PSM and the core elongate, intercalate and condense into an epithelium (Figure 2A and Video S3, yellow cells). This movement seems to be responsible for the medio-lateral narrowing and dorso-ventral thickening of the prospective somite and its detachment from the intermediate mesoderm (Figure 1E and E′). Throughout the image recording period we also observed a fourth type of morphogenetic movement: *iv*) Egression of cells from the center of the PSM/somites (Figure 2A and Video S3, green cell) outwards into the forming epithelium. Ingression from the epithelium to the core also occurred, but was less frequent, hence the somitocoel became progressively smaller (Figure 2, black dotted contours). Core cells egress by extending protrusions which penetrate the apical cell-cell adhesions, and then undergoing amoeboid movements that translocate the cell body into the epithelium where cells become spindle-shaped and centripetally aligned (Figure 2A and Video S3 green cell). Furthermore, *v*) we recorded cells "jumping" from one prospective somite to another as previously described by [1]. The fact that cells freely switch between periphery and core, and between adjacent somite

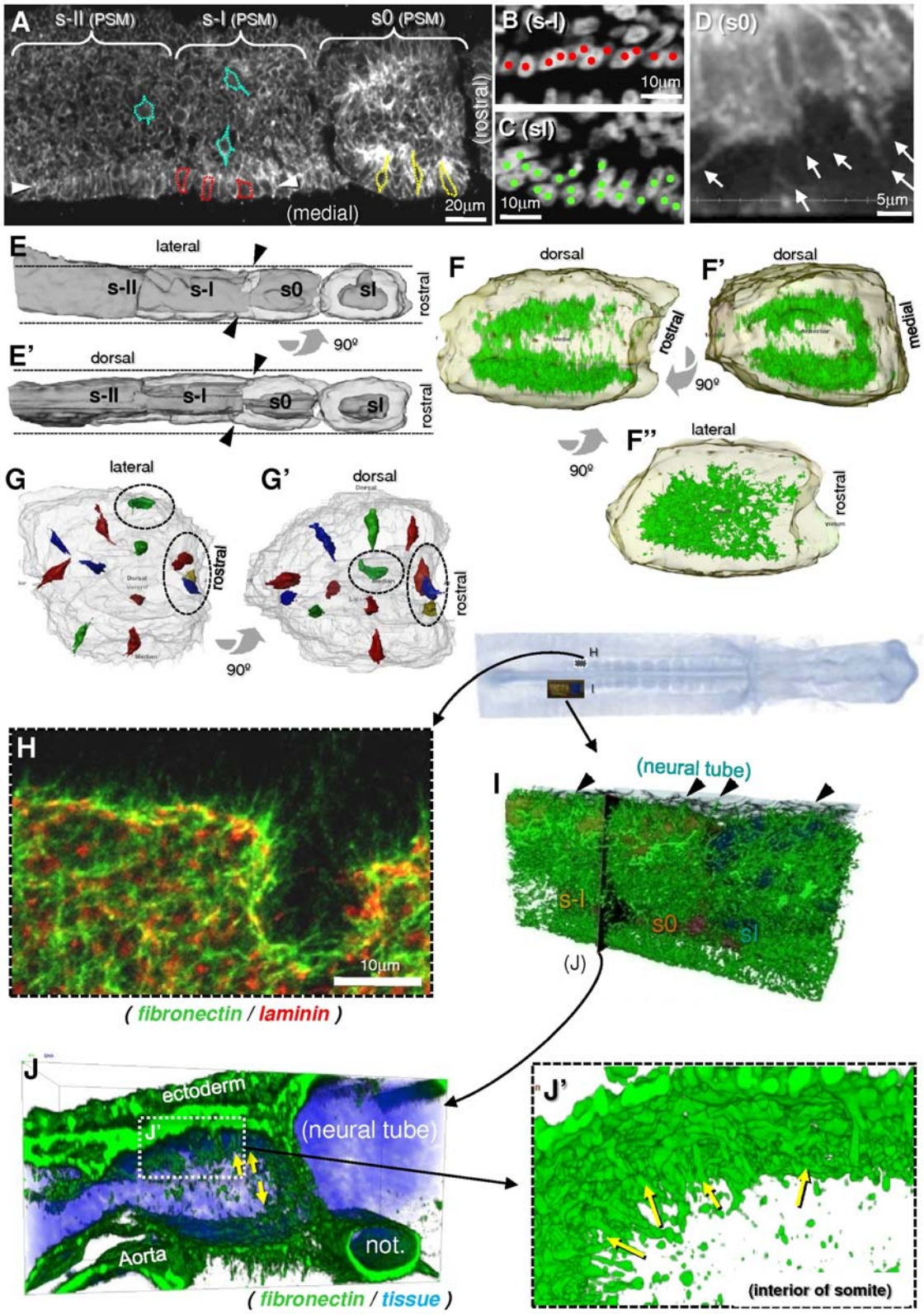

Figure 1. Cell organization, polarization and matrix organization in rostral PSM and epithelial somites (see also Videos S1 and S2). **A**) Coronal confocal section of chick embryo PSM immunostained for N-cadherin showing s-II, s-I and s0. Different cell shapes can be recognized: mesenchymal polygonal cells (blue), medial cuboidal cells (red) which are aligned forming a cuboidal epitheloid layer (between arrowheads) and elongated spindle-shaped cells (yellow). Red cells in s-I have started elongating and yellow cells in s0 are spindle-shaped. **B** and **C**) Coronal confocal sections of a chick embryo PSM stained for DNA showing a detail of the medial epithelium at the level of s-I (B) where cell nuclei are round and basally aligned (red dots), and at level sI (C), where they are oval-shaped and non-aligned basally as in a pseudostratified epithelium (green dots). **D**) Coronal confocal section of a chick embryo PSM stained for N-cadherin, showing in detail the extension of pseudopodia that connect the PSM cells to

their surroundings. **E**) 3D surface reconstruction of the rostral PSM and sI showing a dorsal (E) and medial view (E′). Transparent surface represents the epithelium and in dark gray the mesenchymal core. The s0 somite is still inserted in the "socket-like" PSM [1], but indentations (arrowheads) reveal where the inter-somitic cleft will soon appear. The rostral and lateral sides of s0 are still mesenchymal. As a result of cell rearrangements between s-II and sI, the PSM narrows medio-laterally and thickens dorso-ventrally (dotted lines in E and E′). **F**) 3D surface reconstruction (white transparent surface) of s0 somite viewed medially (F), rostrally (F′) and dorsally (F″), showing a volume reconstruction of N-cadherin immunostaining (green) inside. N-cadherin is enriched in the medial, dorsal, ventral and caudal sides, and less so in rostral and lateral sides. Thus the N-cadherin-staining forms a 3D "adhesion basket" in s0. **G**) 3D surface reconstruction (white transparent surface) of s0 somite viewed dorsally (G) and medially (G′) showing representative cells in the epithelial layer inside, also surface reconstructed (multiple colors). Rostral and lateral cells are elongated but not yet oriented centripetally (dotted circles), while cells in other sides are already aligned. See also Video S1. **H**) Projection of tangential confocal coronal sections FN-positive fibrils (green) extending away from somite surface, and demonstrating a patchy pattern of laminin immunoreactivity (red). **I**) 3D volume reconstruction of FN matrix organization (green) surrounding the rostral PSM including s-I and s0 (brown surface) and sI (blue surface). Rostral is to the right and medial to the top. Cables of FN connect the PSM and sI to surrounding tissues (arrowheads). **J**) Rostral view of FN matrix in a 3D volume reconstructed transversal slab of PSM as shown in I (black plane) at the level of the forming cleft between s-I and s0. Dorsal is upwards, medial is to the right. Cables of FN penetrate inwards into the interior of the somite (yellow arrows), along the lateral surface of epitheloid cells, and between somites, into the nascent cleft. Tissues are represented in light blue. J′ is a detail of panel J, showing the cables of FN penetrating the intersomitic cleft. The tissues have been digitally removed to show only the FN matrix (green).
doi:10.1371/journal.pone.0007429.g001

territories suggests that either cell fate choices are flexible, or that differently committed cells sort according to their fate.

We conclude that somite formation is a complex process involving a combination of multiple morphogenetic movements that occur continuously over a period of at least 6 hours, without noticeable periodic changes of cell behavior every 90 minutes. Furthermore, the somitic epithelium is clearly not a "conventional" epithelium, as its cells retain many characteristics of mesenchymal cells. Hence, we will refer to these cells as epitheloid rather than epithelial cells.

Inhibition of FN matrix assembly impairs PSM cell elongation and alignment without affecting cell dynamics

We have previously shown that somitogenesis is impaired when embryo explants are cultured with the 70 kDa N-terminal FN fragment [33], known to inhibit the incorporation and assembly of endogenous FN molecules into fibrils [41]. As our live imaging data demonstrates that somitogenesis involves extensive cell movements and basal protrusive activity towards the surrounding FN matrix, we analyzed the effect of perturbing FN matrix assembly on PSM cell behavior.

Embryos cultured in medium with BSA (control, Figure 3A) form three or four somites in 6 hours, and an even fibrillar network of FN matrix can be observed (Figure 3C). In contrast, embryos cultured with the 70 kDa FN fragment (Figure 3B) form only one or two somites and the FN matrix has numerous large holes interspersed with dense agglomerates of FN (Figure 3D). Analysis of bright-field image sequences of live-imaged control embryos (n = 3) showed that new somitic clefts form every 80–87 minutes (Figure 3A and 3E), as expected. In contrast, fragment-treated embryos (n = 4) took 145 minutes to form the first somite pair and only two out of four embryos gave rise to a second somite pair, which formed in 150 minutes (Figure 3B and 3E). Thus the disruption of the FN matrix first delays and then effectively halts the formation of new somites.

Analysis of cell movements in 4D images of treated embryos showed that, despite the perturbation of the FN matrix, the medial wall of cuboidal epitheloid cells forms and the movements of accretion, egression and condensation still occur (Video S4). In control and fragment-treated embryos (n = 3; 20 cells/embryo each) cell bodies moved an average distance of 39.6 μm/37.6 μm every 90 minutes, for a net displacement of only 4.8 μm/5.5 μm, respectively (Table S1). This demonstrates the dynamic nature of cells within the rostral PSM and shows that this dynamic behavior is not affected when FN matrix assembly is perturbed ($P = 0.1468$ and $P = 0.1582$, respectively). Although the 4D images do not permit resolution of fine filopodial protrusions, we scored the formation of pseudopodia and found that embryos treated with the 70 kDa fragment formed the same number of pseudopodia as control embryos (Table S1) showing that the dynamic behavior is preserved. Despite this, the PSM cells of the fragment-treated embryos never formed the expected aster-like arrangement of control somites (compare Figure 2A+6h with Figure 3B′), most likely due to a defect in cell organization (Figure 3B″).

To test this, we measured the alignment and lengths of PSM/somitic cells. In control embryos, cells that were at s-II level at time 0 h had been incorporated in sII after 6 hours of culture (Figure 3A), while in fragment-treated embryos (n = 3) these cells only reached a s0-like organization which we designate "s0" (Figure 3B and 3F). Notably, both rostral and caudal cells from control sII are significantly more elongated and aligned than the equivalent cells from the "s0" (Figure 3F). Thus the FN matrix plays a crucial role in cell elongation and alignment during somitogenesis.

We next assessed whether the elongation and alignment of cells in "s0" is equivalent to an s0. Normally, in a forming somite, the caudal side epithelializes before the rostral one (Figure 1; [45]. Comparing cell elongation and alignment in s0 *versus* "s0" reveals no differences rostrally, but caudal "s0" cells are significantly less elongated and less aligned than in s0 (Figure 3F). This demonstrates that "s0" somites are not just delayed, but that the epithelialization of their caudal walls also is greatly impaired.

We conclude that an intact FN matrix is not essential for the pseudopodial or motile behavior of PSM cells, but is required to orient their dynamic behavior and guide them into an aster-like arrangement.

FN matrix plays a crucial role in N-cadherin polarization during somitogenesis

In order to assess whether perturbing the FN matrix also affects the apical polarization of N-cadherin, embryo explants were cultured for 6 hours with BSA (n = 4; Figure 4A) or the 70 kDa FN fragment (n = 6; Figure 4D) and immunostained for N-cadherin. Analysis of our results showed that in control explants, s0 cells have started to polarize their N-cadherin apically (Figure 4A′) and sIII cells are elongated, aligned and have apically polarized N-cadherin (Figure 4A′). In contrast, in fragment-treated explants (n = 6; Figure 4D), the axial equivalent to s0 of controls have an "s-III" morphology and do not show any sign of epithelialization (Figure 4D′). The axial equivalent to control sIII cells have only reached an "s0" morphology with cuboidal medial cells and present only a slight apical enrichment of N-cadherin (Figure 4D″). 3D reconstruction of the N-cadherin labeling further confirms the differences between control and 70 kDa fragment-treated explants. The s0 in control embryos has a "3D adhesion basket" opened

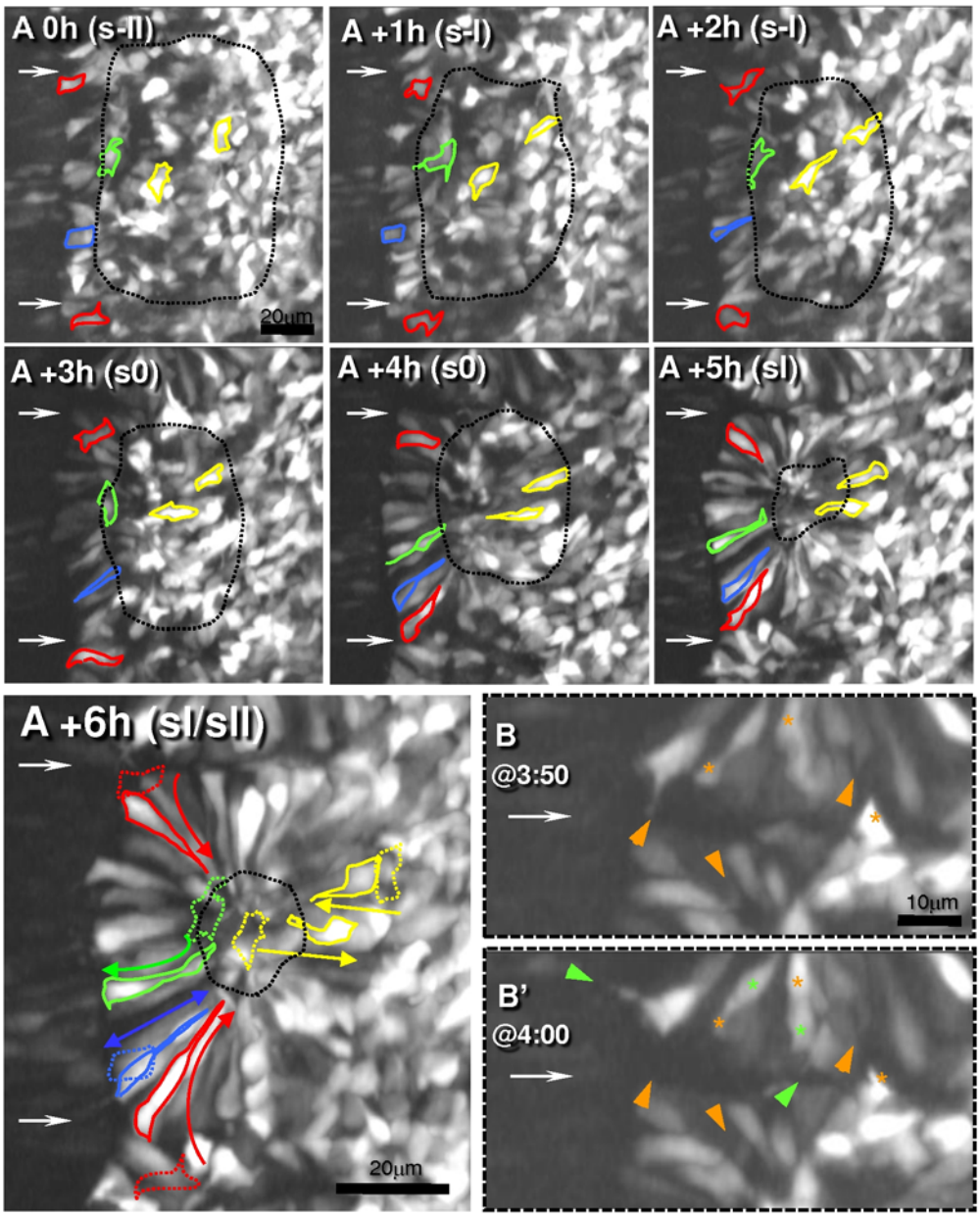

Figure 2. Morphogenetic movements during somite formation in chick embryos (see also Video S3). A) Panels represent seven time-points (spaced 1 hour) of a 4D two-photon imaging sequence (each is a 3D reconstructed 30 μm coronal ''slab'' through the somite's equator (rostral is to the top, medial to the left) of embryos expressing a mosaic of GFP-positive and negative cells. Thin horizontal arrows point to areas where intersomitic boundaries form. Five cells were traced (outlined in color) to depict different morphogenetic movements: *i*) Cuboidal medial cells elongate and become spindle-shaped (blue). *ii*) Some cells are recruited to the medial epithelium via accretion (red) and undergo a change in shape and orientation to conform to the orientation of medial elongated cells. *iii*) Lateral PSM cells and core mesenchymal cells (both yellow) converge and elongate. *iv*) Core cells egress (green) into the epithelium, becoming spindle-shaped and centripetally aligned. In the last panel (A+6h) the initial positions of the cells (A+0h) are drawn with dotted lines, and colored arrows represent the overall morphogenetic movements. The size of the mesenchymal region, *i.e.* the somitocoel (black dotted lines) becomes progressively smaller during these 6 hours. **B**) Detailed view of time-points 3:50 (B) and 4:00 (B′) showing pseudopodia retracting (orange arrowheads) and new ones forming (green arrowheads), similar to the tapering extension observed in fixed embryos (see Figure 1D and last segment of Video S3). Furthermore, massive cytoplasm movements inside cells are also visible (asterisks; where green marks cytoplasm translocations; see also Video S3). These movements occurred throughout the image recording period indicating that the dynamic behavior was retained even after cells became epitheloid.
doi:10.1371/journal.pone.0007429.g002

rostrally and laterally (Figure 4B) and in sII it has formed a ball (Figure 4C). In contrast, the two equivalent tissues in fragment-treated explants have no obvious apical polarization of N-cadherin (''s-II''; Figure 4E) or have a defective ''3D adhesion'' basket with the caudal side opened (''s0''; Figure 4F). Thus in addition to cell elongation and alignment abnormalities (Figure 3F), the cells of fragment-treated explants also show impaired N-cadherin polarization which in ''s0'' is most severe caudally.

We further noticed that perturbing the FN matrix also affects somites that were already formed before culture. In control

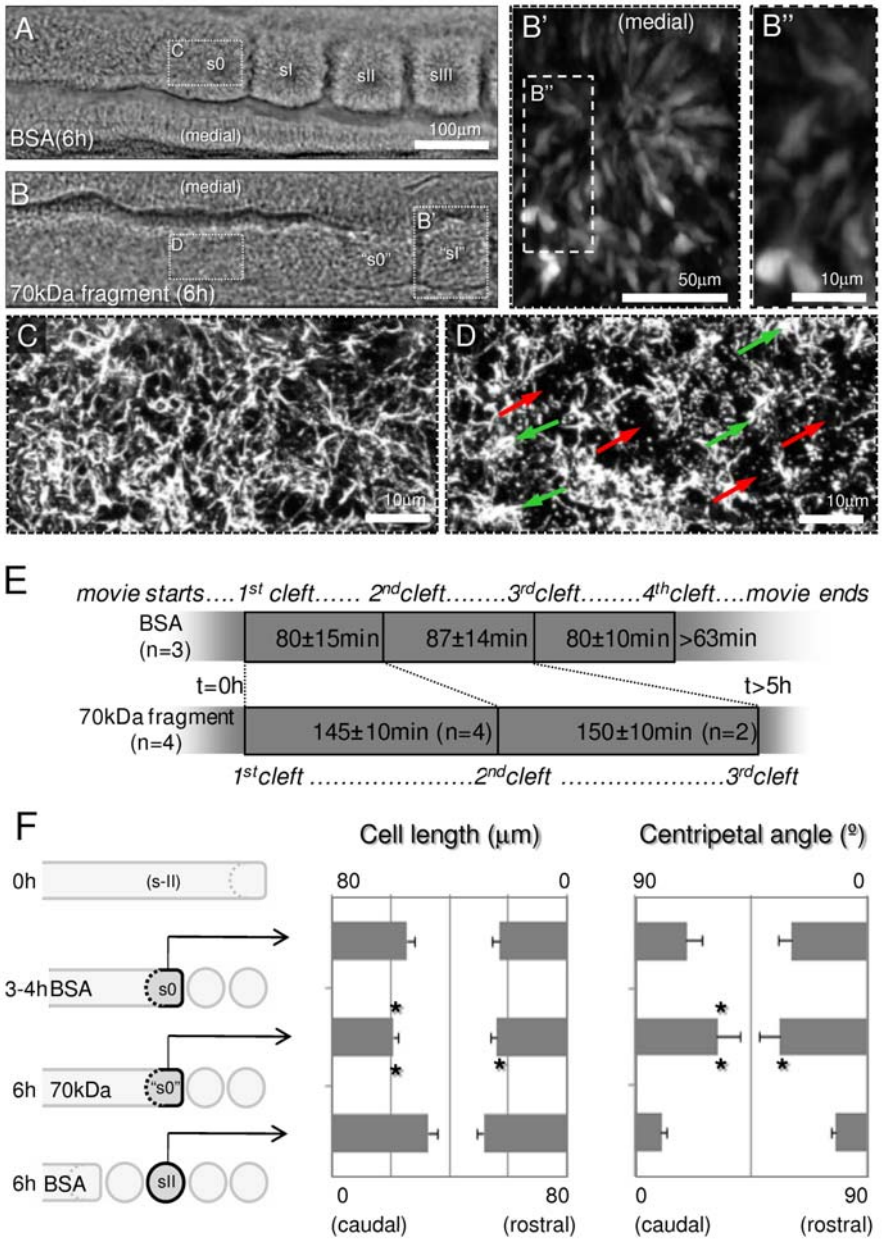

Figure 3. Inhibiting FN matrix assembly impairs somite formation by affecting cell elongation and alignment. A and **B**) Bright-field images showing equivalent halves of embryos cultured for 6 hours either under control (BSA) conditions (A) or with the 70 kDa FN fragment (B). The control embryo formed three complete somites (sI-sIII) and an advanced s0 (A), while the 70 kDa fragment-treated embryo formed only one somite (marked "sI") and an incipient "s0" (B). B' is a two-photon section showing an "sI" of a GFP-electroporated and 70 kDa fragment-treated embryo showing impaired cell elongation and alignment (see also Video S4), particularly in the caudal side (B"; compare with Figure 2A+6h). **C** and **D**) FN matrix covering the dorsal surface of the PSM at equivalent axial positions of control explants (s0, C) and explants treated with the 70kDa fragment ("s-II", D). Ectoderm-associated FN was digitally removed to show only the PSM FN matrix. Explants treated with the 70 kDa fragment (D) show numerous large holes in the FN matrix (red arrows) interspersed with dense agglomerates of FN (green arrows), contrasting with the more uniform fibrillar matrix of control explants (C). **E**) Timing of intersomitic cleft formation as determined from analysis of bright-field time-lapse image sequences. Control embryos (n = 3) formed three new somites in approximately 4 hours, while experimental embryos (n = 4) took almost 5 hours to form either one (n = 2) or two (n = 2) new somites. **F**) Graphical representation of cell lengths and centripetal angles of rostral (n = 10 cells/embryo) *versus* caudal (n = 10 cells/embryo) somitic cells in control embryos at mid-culture (s0, n = 3), experimental embryos at 6 hours ("s0", n = 3) and control embryos at 6 hours (sII, n = 3). Comparing cells in "s0" with the equivalent cells of control embryos, which had matured to sII stage, showed that caudal cells were significantly less elongated and aligned ($P<0.001$) in the "s0", and so were rostral cells ($P = 0.004$ and $P<0.001$, respectively). Comparing cells in "s0" to cells of control s0 revealed significant differences in caudal cell elongation ($P<0.001$) and alignment ($P = 0.007$) whereas no differences in those parameters were detected rostrally ($P = 0.643$ and $P = 0.368$, respectively). Error bars represent 95% confidence intervals. Asterisks represent significant differences of "s0" when compared to sII (bottom asterisk) or s0 (upper asterisk).
doi:10.1371/journal.pone.0007429.g003

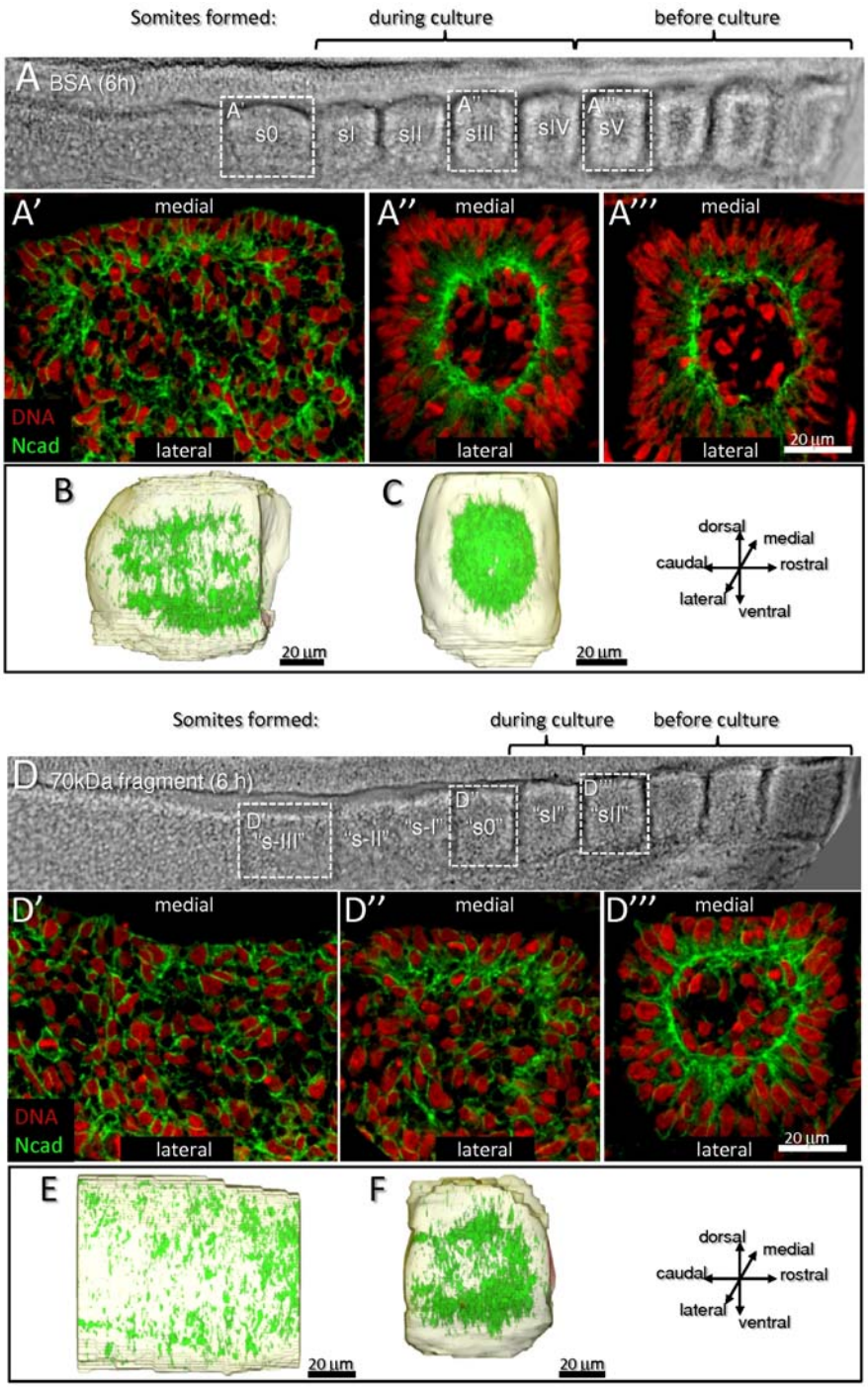

Figure 4. N-cadherin fails to polarize apically when FN fibrillogenesis is inhibited. Bright field (A, D), coronal confocal sections (A′, A″, A‴, D′, D″, D′‴) of control (A) and 70 kDa FN fragment-treated (D) explants cultured for 6 hours, immunostained for N-cadherin (green) and labeled for DNA (red) and 3D surface reconstruction with N-cadherin labeling (green in B,C,E,F) of selected volumes. **A**) Control explants form four new somites. In s0 (A′), medial cells are starting to elongate and to polarize their N-cadherin apically. In sIII (A″) and sV (A‴), cells have become centripetally aligned, with oval-shaped nuclei and apically restricted N-cadherin immunoreactivity. **B–C**) Lateral view of N-cadherin labeling shows a ''3D adhesion basket'' in s0 (B). By sIII (C) the N-cadherin labeling has become more apically restricted and has closed rostrally and laterally thus forming a ball. **D**) 70 kDa fragment-treated explants form one or two somites; the depicted embryo formed one (''sI'') and has an advanced ''s0''. The tissue at the same axial level as A′ (''s-III'', D′) shows no sign of epithelialization or cell elongation. Medial cells in the forming somites of 70kDa fragment-treated explants (''s0'', D″; axially equivalent to A″) show incipient elongation and N-cadherin polarization. Cells of somites that had formed before culture (''sII'', D‴) are less polarized and less elongated than cells at the equivalent axial level in control explants (sV). **E–F**) Lateral view of N-cadherin labeling in 70kDa fragment-treated explants show dispersed N-cadherin localization in the ''s-III'' (axial equivalent to B). The ''s0'' (axial equivalent to C) depicts a more intense labeling in the rostral portion, resulting in an ''adhesion basket'' that is opened caudally.
doi:10.1371/journal.pone.0007429.g004

explants, sI cells progressed to sV during the 6 hour culture and were elongated, centripetally aligned with apically restricted N-cadherin (Figure 4A″). Cells at sI level in 70 kDa fragment-treated explants, did not develop into a typical sV (Figure 4A″), but remain less elongated and display less polarized N-cadherin immunoreactivity (Figure 4D″). In fact, these cells were even less elongated and less polarized than cells in a control sIII (Figure 4A″). This shows that the FN matrix not only promotes cell elongation and polarization during the formation of new somites, but is also crucial to maintain the epithelial state of already formed somites.

Egression of core cells into the somite epithelium requires an intact FN matrix

We noticed that in embryos cultured with the 70 kDa fragment, somites have unusually large somitocoels, suggesting a possible defect in the recruitment of core cells into the epithelium. To address this, we started by tracking individual cells in the 4D images. In control embryos (n = 3), 95% of tracked core cells (n = 35/37 cells) from s-II became epitheloid after 6–8 hours, while in experimental embryos (n = 3) only 29% of tracked core cells (n = 10/35 cells) became part of the epithelium (Table S1), suggesting a defect in the egression of cells from the core to the periphery. To further quantify this phenomenon, we measured the volumes of somites formed and their somitocoels during a 6 hour culture period in control (n = 4) and 70 kDa fragment-treated (n = 6) explants (Figure 5A and 5B). Total volume of somites does not differ significantly, but in 70 kDa fragment-treated explants the somitocoels are significantly larger, representing 13.2% of the total volume of the somite, in contrast to only 6.5% in control explants (Figure 5C; Table S1). Furthermore, in control embryos, somitocoel cell density is lower than that of the surrounding epithelium while in fragment-treated embryos it is as high as in the epithelium (Figure 5D). This strongly suggests that the ability of core cells to egress into, and become part of the somitic epithelium is seriously hampered when FN fibrillogenesis is inhibited.

Discussion

Somite epithelialization is a complex and continuous event

The chick PSM segments every 90 minutes, giving rise to a new somite. This periodicity is achieved through a molecular segmentation clock, evidenced by oscillations of gene expression in the PSM, which is the hallmark of somitogenesis [23,24]. Here we used 3D live imaging of the full chick PSM in a mosaic of GFP-labeled and non-labeled cells to study the cellular transformations involved in somite formation. Surprisingly, our time-lapse images revealed that the epithelialization of the forming somite does not occur in a periodic fashion every 90 minutes. Rather, a continuous series of events, spanning a period of at least 6 hours, bring about the assembly of cells into the epithelial somite, which only becomes complete as it reaches stage sII.

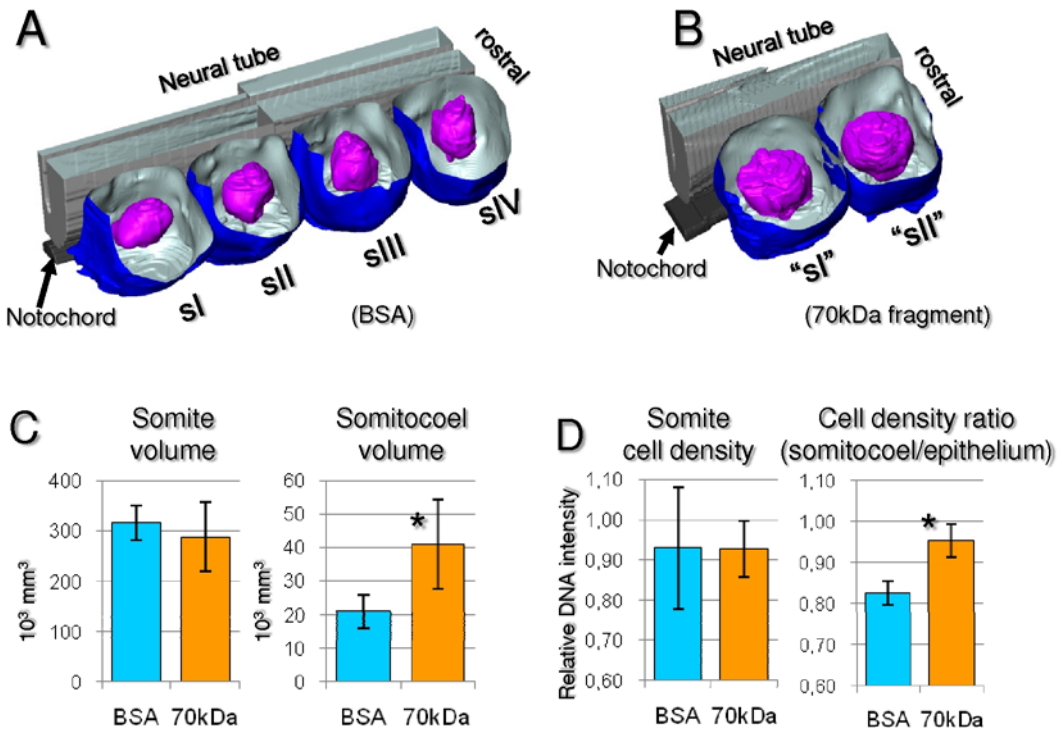

Figure 5. Inhibition of FN fibrillogenesis impairs egression of cells from the somitocoel to the somite epithelium. A–B) Representative examples of 3D surface reconstructions of somites (blue; dorsal cap digitally removed) and their somitocoels (purple) formed in embryo explants at the end of 6 hours of culture with BSA (n = 4; A) or with 70 kDa fragment (n = 6; B). Three of the six explants treated with the fragment formed two somites as depicted in B; the remaining ones formed only one somite. **C**) Quantification of somite and somitocoel volumes and cell densities (fluorescence intensity of DNA labeling). Only somites fully separated from the PSM (≥ sI) were measured. Since an ANOVA revealed no significant differences between somites formed during the 6 hour culture period within each treatment, we pooled the measurements of the different somites to an average *per* explant (C). There is no significant difference ($P = 0.129$) in somite volume between control and fragment-treated explants, but somitocoels of fragment-treated explants are significantly larger ($P < 0.0001$). **D**) Quantification of cell density in the whole somites shows no difference ($P = 0.990$) between control and 70 kDa fragment-treated explants. However, the cell density ratio (somitocoel/epithelial portion) is significantly higher ($P = 0.043$) in somites of 70 kDa fragment-treated explants. Bars represent 95% confidence intervals.
doi:10.1371/journal.pone.0007429.g005

Our data show that somitogenesis involves two distinct epithelialization events. Although it has previously been reported that the chick PSM shows signs of precocious epithelialization [18,46,47] and that the somitic epithelium is pseudostratified [19,21], it has gone largely unnoticed that these two epithelia are morphologically distinct and that the cuboidal epithelium of the rostral PSM is characteristic of its medial cells.

The transformation of the mesenchymal chick PSM into epitheloid cells starts medially with the formation of the cuboidal epithelium. These cells later elongate into a pseudostratified arrangement and while doing so, they recruit adjacent cells by accretion (Figure 6A). It has been shown that medial PSM cells form somites autonomously, whereas lateral PSM cells require the presence of medial ones [48]. By showing that both steps of epithelialization start medially and that these medial cells recruit adjacent cells into the forming epithelium, our images provide evidence that reinforces the idea that medial cells have an organizing function during somitogenesis. Although accretion has not previously been identified for somitogenesis, it is known to occur, for example during notochord development [49,50] and primordial germ cell cluster formation [51].

The lateral side of the chick somite epithelializes last when lateral mesenchymal cells rearrange by intercalating and elongating into a centripetal arrangement (Figure 6A), reminiscent of the convergence and extension movements of dorsal mesoderm cells in amphibian embryos [52].

Finally, egression of cells from the forming somitocoel is an unexpectedly large contributor to the somitic epithelium (Figure 6A). In fact, core cells are as likely to end up in the peripheral epitheloid layer as peripheral cells. The observation that an epithelium can assemble from mesenchymal cells egressing into it from the apical side and aligning along the existing epitheloid cells is unexpected and few other examples exist [53]. High-resolution time-lapse imaging of situations where an epithelium assembles from a group of mesenchymal cells (e.g. vasculogenesis; condensation of the metanephric mesenchyme during kidney development) should clarify whether this mechanism is a general feature of mesenchyme-to-epithelium transitions.

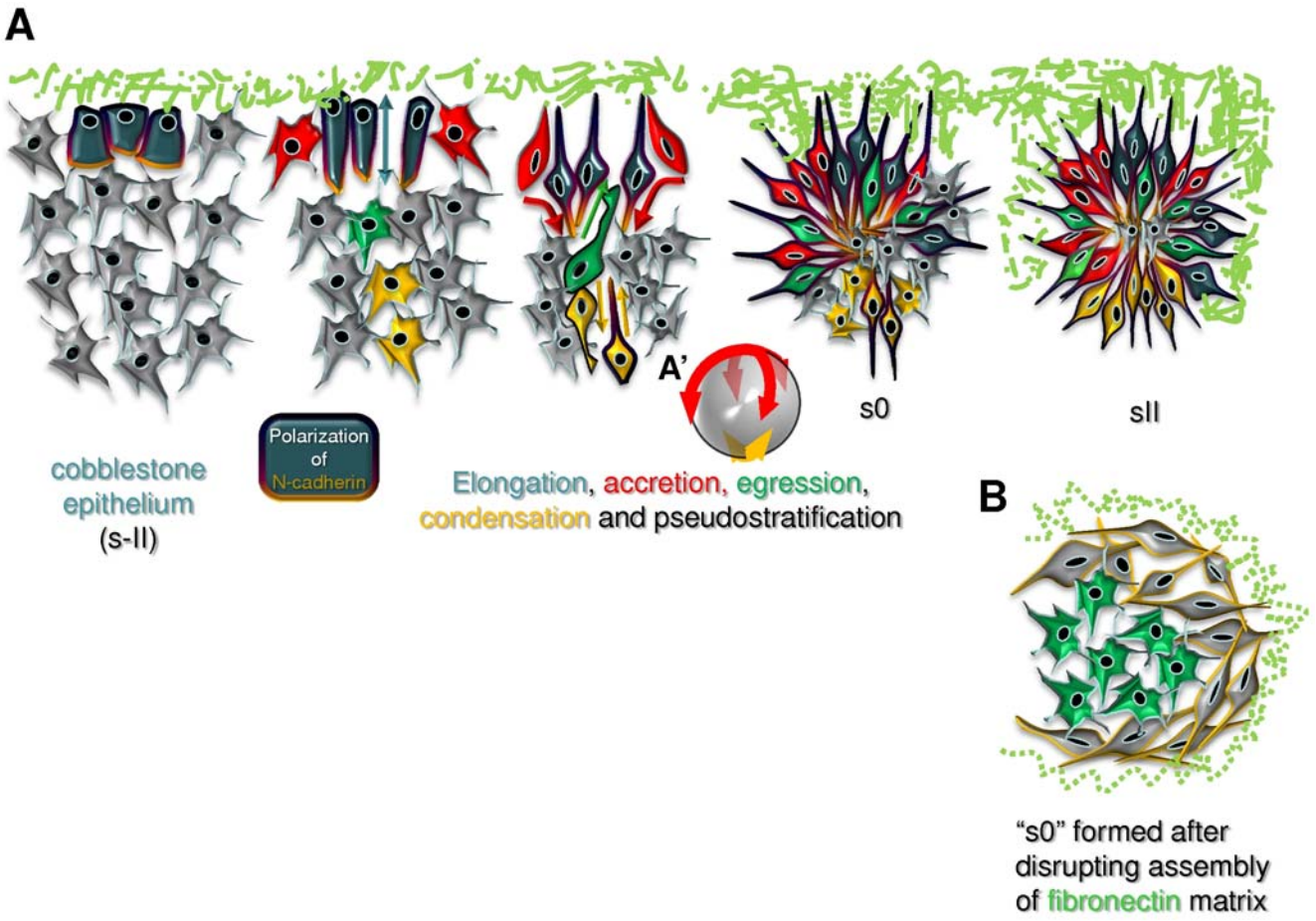

Figure 6. Model of morphological somite formation and morphogenetic movements. A) Schematic representation of a "hypothetical" coronal slice representing stages of somite formation. Medial is up and rostral to the right. The different morphogenetic movements that contribute to the assembly of the somite epithelium are represented: Medial cells first become cuboidal with basal nuclei (dark green cells), then these cells elongate and recruit other cells to the epitheloid layer via accretion (red cells); accretion spreads ventrally and dorsally (not shown), and eventually to the caudal and rostral side. Simultaneously, cells egress from the core into the epitheloid layer (green cells), and, finally, at the lateral side of the somite, cells elongate, intercalate and condense (yellow cells). In s0, the rostral and lateral sides epithelialization is only completed after the somite separates from the PSM. The FN matrix is depicted in green. **A**' depicts how the accretion and condensation "spread" through the whole somite to complete the "spherical" ball of epitheloid cells. **B**) When the assembly of the FN matrix is disrupted, PSM cells (especially caudal cells) do not polarize or orient centripetally and core cells fail to egress into the epithelium.
doi:10.1371/journal.pone.0007429.g006

The assembly of the somitic epithelium is a dynamic process and the dynamic behavior of its cells continues after the somite forms. The constant translocations of cell bodies within the epitheloid layer may be a response to continuous cell recruitment into this epithelium through egression, which gives it the pseudostratified appearance. Pseudostratification seems to be typical of embryonic epithelia which rest on FN-rich and laminin-sparse matrices [8] as is the case of rostral PSM and early somites. We conclude that the somitic epithelium is clearly not a conventional epithelium, neither morphologically nor behaviorally, as its cells retain several mesenchymal characteristics. Future live imaging studies should address whether pseudostratification in embryonic epithelia represents a structural organization *per se* or whether it simply reflects that these embryonic epitheloid tissues are formed by cells which are highly dynamic and in transit (as is the case of somite cells which later disperse and move on to give rise to different tissues of the adult organism).

The FN matrix orients PSM cells into an aster-like somite conformation

Our previous studies revealed that the FN matrix of the PSM is the product of a collaboration between ectoderm and PSM, where ectoderm provides the bulk of the FN protein, and the PSM cells assemble this FN into a fibrillar matrix [33]. Furthermore, the 70 kDa FN fragment inhibits somitogenesis [33] by halting *de novo* FN fibrillogenesis [41,54,55]. Here we show that culture of embryo explants in the presence of the 70 kDa FN fragment for 6 hours causes a disruption in the FN matrix, as evidenced by large holes and areas with apparently collapsed fibrils. A similar effect is seen in cultured cells where an already assembled matrix is progressively lost if FN molecules are not continuously added to it [56]. Thus, young FN matrices are in a constant turnover and inhibiting FN matrix assembly gradually leads to a net loss of matrix [56]. Observing cell behavior in 3D time-lapse images of live embryos cultured in the presence of the 70 kDa FN fragment gave us the unique opportunity to determine what aspects of somitogenesis fail as the surrounding FN matrix weakens over time.

The dynamic behavior of PSM cells suggests that they are continuously sensing and adjusting to the surroundings (other tissues and the ECM). Our results show that the inhibition of FN matrix assembly does not affect PSM cell movements and pseudopodial activity, but perturbs N-cadherin polarization, cell elongation, centripetal alignment and egression (Figure 6B). This suggests that the FN matrix normally serves as a cue that orients the dynamic behavior of PSM cells, polarizes the cell-cell adhesions to the apical side and serves as a basal anchoring point essential for cell elongation and alignment. FN matrices are crucial in inducing cell elongation and polarization in young embryonic epithelia before they mature and assemble their laminin-containing basement membranes [57–59]. Furthermore, FN matrices also induce cell elongation and orient protrusive activity during dorsal mesoderm development in *Xenopus* [60]. Many studies have also provided evidence of cross-talk between FN signaling and cadherins [16]. For example, a basal FN matrix polarizes N-cadherin to the apical domain of zebrafish myocardial cells [58] and downregulates E-cadherin basally in cleft cells of branching epithelia [57]. Furthermore, in *Xenopus* mesoderm, β1 integrin signaling modulates C-cadherin adhesiveness to the "correct" level to permit tissue rearrangements [61]. In fact, the presence of FN around the rostral PSM correlates with an increase in cell-cell adhesion between PSM cells [62–64]. Thus a FN matrix is important both as a basal orienting cue and in polarizing cell-cell adhesion to the apical side in several developing systems. These basal and apical attachments are essential for creating and maintaining the tensile strength that supports cell elongation and cell body movements, and in turn may also modulate the cytoskeleton and intracellular signaling pathways thereby controlling cell shape and differentiation [7]. Moreover, we also saw a loss of N-cadherin polarization and cell elongation in somites that were already formed before the addition of the 70 kDa FN fragment. Therefore, cues from a basal FN matrix seem to be crucial, not only to induce, but also to maintain somite cell polarization and elongation.

Egression is significantly impaired when FN matrix assembly is perturbed, demonstrating that an intact FN matrix is required to support and direct cell egression. FN matrices are flexible and elastic and are extensively modifiable by cell traction forces [65–67]. The presence of cables of FN penetrating the somite epithelium indicates that somitocoel cells may pull on the matrix to bring themselves into their final position. We propose that without the presence of a strong and continuous matrix, many cells fail to egress and remain in the somitocoel, resulting in fewer cells in the epithelium.

The FN matrix aids somitic cleft formation

It has previously been hypothesized that somite epithelialization starts at the rostral border of s0 continuing in the caudal direction and finishing at the caudal border as it separates from the PSM [1]. However, more recent observations suggested that, in the chick embryo, the caudal part of s0 epithelializes first [45,68]. Our analysis of cell shape and orientation, cell movements and the organization of the N-cadherin "3D adhesion basket" in s0 provide a formal demonstration that the caudal wall indeed epithelializes well before the rostral one (Figure 6A).

Work in recent years has established that cleft formation involves a cross-talk between cells caudal and rostral to the forming cleft, whereby cells caudal to the prospective boundary (rostral side of s-I) instruct cells rostral to the boundary (caudal side of s0) to epithelialize [68]. The transcription factor *Mesp2/Meso-1* expressed in the cells caudal to the prospective boundary upregulates *EphA4* expression in these cells [46,69]. Subsequent binding between EphA4 and EphrinB2 present on the cells rostral to the boundary, induces a signaling event that downregulates the activity of the GTPase Cdc42, leading to cell epithelialization [69]. Interestingly, these authors demonstrate that EphrinB2 signaling not only downregulates Cdc42 activity, but also acts through yet another unknown mechanism to promote cleft formation. Here we show that the inhibition of FN fibrillogenesis dramatically affects the caudal side of the somite, indicating that FN plays a crucial role in its epithelialization. EphrinB1 and EphrinB2 reverse signaling have been shown to increase the affinity of β1 integrins for FN, stimulating cell attachment and motility on a FN matrix [70,71]. Thus, during somite boundary formation, EphrinB2 signaling may increase integrin engagement to the FN matrix in a cell autonomous manner. Consequently, accreting caudal s0 cells would bring the external FN matrix into the forming cleft with them, a process also seen during cleft formation in salivary gland branching morphogenesis [4]. Newly synthesized FN is then assembled to fill in the space between the gland bud surface and the cells at the leading edge of the cleft, thus stabilizing the cleft further [4]. *Itga5* mRNA is expressed in newly formed somites and *Fn1* mRNA is expressed in their caudal half [33], indicating that newly assembled FN may play the same role in the somitic clefts. Therefore we propose that EphrinB2 signaling would promote epithelialization in two complementary ways: (1) by lowering the activity of Cdc42 promoting epithelialization [69] and (2) by stimulating the binding of caudal s0 cells to the FN matrix which, in turn, induces N-cadherin polarization, cell elongation and centripetal alignment. In agreement with this, *Ephrin-B2a* and *Fn1*

have been shown to collaborate in somite cleft formation and maintenance in zebrafish [29].

Conclusion

Here we present data indicating that during chick somite formation the FN matrix acts as a fibrillar network that spatially orients the highly dynamic mesenchymal PSM cells, bringing them into the aster-like arrangement of spindle-shaped cells characteristic of the epithelial somite. We propose that it does so by inducing the polarization of N-cadherin to the apical domain of PSM cells, thus reinforcing cell-cell adhesions, and by serving as a basal anchoring scaffold, giving PSM cells a second point of attachment essential for acquiring the tensile strength necessary for elongation and orientation in 3D. We further propose that when EphrinB2 reverse signaling induces the somitic cleft, caudal s0 cells adhere strongly to the FN matrix, accreting cells pull the superficial FN matrix into the cleft and then new somite-derived FN is assembled to fill in the cleft, stabilizing it. Finally, it is tempting to speculate that the progressive accumulation of FN in the cleft promotes the alignment and polarization of the cells in the rostral side of the following somite. In this scenario, a fibrillar FN network is absolutely crucial to package cells into a somite.

Supporting Information

Figure S1 Cell shape and movement measurements. A) Diagram representing the cell's length (distance a-b) and centripetal alignment angle (α; note that the smaller the angle, the better aligned a cell is). "a" represents cell's apical end, "b" the cell's basal end, and "c" is the somitocoel's centroid. See materials and methods for more details. B) 3D reconstruction of tracks of cells whose cell body movement was used to the calculate full track length (magenta line) and net cell body displacement (white vector). Rostral is to the right and lateral to the top. Bright-yellow spheres represent the position of the cell bodies of tracked cells in the last time-point. GFP-expressing cells are 3D reconstructed in transparent light green.
Found at: doi:10.1371/journal.pone.0007429.s001 (1.35 MB TIF)

Table S1 Effect of inhibiting FN matrix assembly on PSM cell protrusive and motile activity, elongation and alignment, and probability of egressing. Values presented are averages ±95% confidence intervals.
Found at: doi:10.1371/journal.pone.0007429.s002 (0.07 MB DOC)

Video S1 3D surface reconstruction of an s0 stage somite and of cells in the epithelial layer showing their typical shape and orientation. The somite is oriented rostral towards the right, dorsal upwards. Cells in rostral wall are not centripetally oriented. During the second 3D rotation, the surface of reconstructed cells changes color to show apical accumulation of N-cadherin (green). Cells that are well oriented have most N-cadherin accumulated on the apical end, i.e. towards the interior of the somite. For more details refer to Figure 1 of the manuscript.
Found at: doi:10.1371/journal.pone.0007429.s003 (5.50 MB MOV)

Video S2 Organization of the FN matrix in the nascent somite. The video is an animation showing all sides of the 3D reconstruction of fibronectin (green) matrix organized around somite sI (blue), s0 (dark brown) and s-I (light brown). Rostral is to the right. The "outward cables" of FN are clearly seen radiating from the surface of the somites in formation. In the middle of the Video only s0 is depicted, to show how the fibronectin matrix is organized on all sides; the medial wall is less well covered with fibronectin than the dorsal and ventral walls. The caudal and cranial walls of s0 are not yet covered with FN. In the last segment of the video, the surface of the PSM and sI somite are removed to show only the FN, and the "inward cables" penetrating the PSM, especially in the prospective cleft. For more details refer to Figure 1.
Found at: doi:10.1371/journal.pone.0007429.s004 (10.22 MB MOV)

Video S3 Multiphoton 4D image sequence of GFP expressing-cells in chick embryo PSM showing cell movements during somite formation. First segment of the video shows a portion of the PSM of a chick embryo (rostral is upwards, medial is to the left). In the beginning only one somite is formed, but at the end of 6 hours four new somites have formed. After zooming into a single somite the details of individual cell movements are shown. Several different morphogenetic stereotypical movements are identified in cells with different colors. Blue represents elongation of a medial cell, red cell accretion in the rostral and caudal walls, green egression, and yellow mesenchymal elongation and intercalation in the lateral wall. In the end, a zoom of a forming intersomitic cleft shows the continuous extension and retraction of pseudopodia. For more details refer to Figure 2 of the manuscript.
Found at: doi:10.1371/journal.pone.0007429.s005 (8.03 MB MOV)

Video S4 Effect of treatment with 70kDa FN fragment on rate of somite formation and cell movements The video starts by showing two side-by-side bright-field image sequences of a control (BSA; upper panel) and 70kDa treated embryo (bottom panel), to compare rates of somite formation. FN matrix assembly disruption slows down and eventually halts somite formation and prevents cells from organizing into an aster of spindle-shaped centripetally aligned cells. In the last segment of the Video formation of pseudopodia is shown in "freezed-frames", demonstrating that pseudopodial activity is not affected by the inhibition of FN fibrillogenesis. For more details refer to Figure 3 of the manuscript.
Found at: doi:10.1371/journal.pone.0007429.s006 (9.37 MB MOV)

Acknowledgments

The authors are grateful to Tsuyoshi Momose for providing PCAAGS-GFP vector, Pedro Almeida for helping with formulas to calculate 3D distances and angles, Nuno Moreno and Ricardo Henriques for support with the two-photon system and ImageJ macros, Ana Tavares for help with embryo culture and Ana Rainho and Jorge Palmeirim for precious statistical advice. We also thank Rui Martinho, Élio Sucena, Leonor Saúde and all members of our laboratory for helpful discussions.

Author Contributions

Conceived and designed the experiments: GGM PR GR IP ST. Performed the experiments: GGM PR RA. Analyzed the data: GGM PR RA ST. Contributed reagents/materials/analysis tools: GGM IP ST. Wrote the paper: GGM PR RA GR IP ST.

References

1. Kulesa PM, Fraser SE (2002) Cell dynamics during somite boundary formation revealed by time-lapse analysis. Science 298: 991–995.
2. Ribeiro C, Neumann M, Affolter M (2004) Genetic control of cell intercalation during tracheal morphogenesis in Drosophila. Curr Biol 14: 2197–2207.
3. Haas P, Gilmour D (2006) Chemokine signaling mediates self-organizing tissue migration in the zebrafish lateral line. Dev Cell 10: 673–680.
4. Larsen M, Wei C, Yamada KM (2006) Cell and fibronectin dynamics during branching morphogenesis. J Cell Sci 119: 3376–3384.

5. Voiculescu O, Bertocchini F, Wolpert L, Keller RE, Stern CD (2007) The amniote primitive streak is defined by epithelial cell intercalation before gastrulation. Nature 449: 1049–1052.
6. Hay ED (2005) The mesenchymal cell, its role in the embryo, and the remarkable signaling mechanisms that create it. Dev Dyn 233: 706–720.
7. Ingber DE (2006) Mechanical control of tissue morphogenesis during embryological development. Int J Dev Biol 50: 255–266.
8. Shook DR, Keller R (2008) Epithelial type, ingression, blastopore architecture and the evolution of chordate mesoderm morphogenesis. J Exp Zoolog B Mol Dev Evol 310: 85–110.
9. Montell DJ (2008) Morphogenetic cell movements: diversity from modular mechanical properties. Science 322: 1502–1505.
10. Danen EH, Sonnenberg A (2003) Integrins in regulation of tissue development and function. J Pathol 201: 632–641.
11. Daley WP, Peters SB, Larsen M (2008) Extracellular matrix dynamics in development and regenerative medicine. J Cell Sci 121: 255–264.
12. Ghajar CM, Bissell MJ (2008) Extracellular matrix control of mammary gland morphogenesis and tumorigenesis: insights from imaging. Histochem Cell Biol 130: 1105–1118.
13. Larsen M, Artym VV, Green JA, Yamada KM (2006) The matrix reorganized: extracellular matrix remodeling and integrin signaling. Curr Opin Cell Biol 18: 463–471.
14. Harburger DS, Calderwood DA (2009) Integrin signalling at a glance. J Cell Sci 122: 159–163.
15. Vicente-Manzanares M, Choi CK, Horwitz AR (2009) Integrins in cell migration–the actin connection. J Cell Sci 122: 199–206.
16. Chen X, Gumbiner BM (2006) Crosstalk between different adhesion molecules. Curr Opin Cell Biol 18: 572–578.
17. Gossler A, Hrabe de Angelis M (1998) Somitogenesis. Curr Top Dev Biol 38: 225–287.
18. Stockdale FE, Nikovits W Jr, Christ B (2000) Molecular and cellular biology of avian somite development. Dev Dyn 219: 304–321.
19. Williams LW (1910) The Somites of the chick. The American Journal of Anatomy 2: 55–100.
20. Lipton BH, Jacobson AG (1974) Analysis of Normal Somite Development. Developmental Biology 38: 73–90.
21. Bellairs R (1979) The mechanism of somite segmentation in the chick embryo. J Embryol Exp Morphol 51: 227–243.
22. Saga Y (2007) Segmental border is defined by the key transcription factor Mesp2, by means of the suppression of Notch activity. Dev Dyn 236: 1450–1455.
23. Andrade RP, Palmeirim I, Bajanca F (2007) Molecular clocks underlying vertebrate embryo segmentation: A 10-year-old hairy-go-round. Birth Defects Res C Embryo Today 81: 65–83.
24. Dequeant ML, Pourquie O (2008) Segmental patterning of the vertebrate embryonic axis. Nat Rev Genet 9: 370–382.
25. Ostrovsky D, Cheney CM, Seitz AW, Lash JW (1983) Fibronectin distribution during somitogenesis in the chick embryo. Cell Differ 13: 217–223.
26. Duband JL, Dufour S, Hatta K, Takeichi M, Edelman GM, et al. (1987) Adhesion molecules during somitogenesis in the avian embryo. J Cell Biol 104: 1361–1374.
27. George EL, Georges-Labouesse EN, Patel-King RS, Rayburn H, Hynes RO (1993) Defects in mesoderm, neural tube and vascular development in mouse embryos lacking fibronectin. Development 119: 1079–1091.
28. Georges-Labouesse EN, George EL, Rayburn H, Hynes RO (1996) Mesodermal development in mouse embryos mutant for fibronectin. Dev Dyn 207: 145–156.
29. Koshida S, Kishimoto Y, Ustumi H, Shimizu T, Furutani-Seiki M, et al. (2005) Integrinalpha5-dependent Fibronectin accumulation for maintenance of somite boundaries in zebrafish embryos. Dev Cell 8: 587–598.
30. Julich D, Geisler R, Holley SA (2005) Integrinalpha5 and delta/notch signaling have complementary spatiotemporal requirements during zebrafish somitogenesis. Dev Cell 8: 575–586.
31. Kragtorp KA, Miller JR (2006) Regulation of somitogenesis by Ena/VASP proteins and FAK during Xenopus development. Development 133: 685–695.
32. Kragtorp KA, Miller JR (2007) Integrin alpha5 is required for somite rotation and boundary formation in Xenopus. Dev Dyn 236: 2713–2720.
33. Rifes P, Carvalho L, Lopes C, Andrade RP, Rodrigues G, et al. (2007) Redefining the role of ectoderm in somitogenesis: a player in the formation of the fibronectin matrix of presomitic mesoderm. Development 134: 3155–3165.
34. Packard DS, Jacobson AG (1976) Influence of Axial Structures on Chick Somite Formation. Developmental Biology 53: 36–48.
35. Palmeirim I, Dubrulle J, Henrique D, Ish-Horowicz D, Pourquie O (1998) Uncoupling segmentation and somitogenesis in the chick presomitic mesoderm. Dev Genet 23: 77–85.
36. Pourquie O, Tam PP (2001) A nomenclature for prospective somites and phases of cyclic gene expression in the presomitic mesoderm. Dev Cell 1: 619–620.
37. Hamburger V, Hamilton HL (1951) A Series of Normal Stages in the Development of the Chick Embryo. Journal of Morphology 88: 49–&.
38. Momose T, Tonegawa A, Takeuchi J, Ogawa H, Umesono K, et al. (1999) Efficient targeting of gene expression in chick embryos by microelectroporation. Dev Growth Differ 41: 335–344.
39. Psychoyos D, Stern CD (1996) Fates and migratory routes of primitive streak cells in the chick embryo. Development 122: 1523–1534.
40. Palmeirim I, Henrique D, Ish-Horowicz D, Pourquie O (1997) Avian hairy gene expression identifies a molecular clock linked to vertebrate segmentation and somitogenesis. Cell 91: 639–648.
41. McKeown-Longo PJ, Mosher DF (1985) Interaction of the 70,000-mol-wt amino-terminal fragment of fibronectin with the matrix-assembly receptor of fibroblasts. J Cell Biol 100: 364–374.
42. Kuhl U, Timpl R, von der MK (1982) Synthesis of type IV collagen and laminin in cultures of skeletal muscle cells and their assembly on the surface of myotubes. Dev Biol 93: 344–354.
43. Thorsteinsdottir S (1992) Basement membrane and fibronectin matrix are distinct entities in the developing mouse blastocyst. Anat Rec 232: 141–149.
44. Yurchenco PD, Amenta PS, Patton BL (2004) Basement membrane assembly, stability and activities observed through a developmental lens. Matrix Biol 22: 521–538.
45. Nakaya Y, Kuroda S, Katagiri YT, Kaibuchi K, Takahashi Y (2004) Mesenchymal-Epithelial Transition during Somitic Segmentation Is Regulated by Differential Roles of Cdc42 and Rac1. Dev Cell 7: 425–438.
46. Saga Y, Takeda H (2001) The making of the somite: molecular events in vertebrate segmentation. Nat Rev Genet 2: 835–845.
47. Dubrulle J, Pourquie O (2004) Coupling segmentation to axis formation. Development 131: 5783–5793.
48. Freitas C, Rodrigues S, Charrier JB, Teillet MA, Palmeirim I (2001) Evidence for medial/lateral specification and positional information within the presomitic mesoderm. Development 128: 5139–5147.
49. Sausedo RA, Schoenwolf GC (1993) Cell Behaviors Underlying Notochord Formation and Extension in Avian Embryos - Quantitative and Immunocytochemical Studies. Anatomical Record 237: 58–70.
50. Sausedo RA, Schoenwolf GC (1994) Quantitative-Analyses of Cell Behaviors Underlying Notochord Formation and Extension in Mouse Embryos. Anatomical Record 239: 103–112.
51. McLaren A, Lawson KA (2005) How is the mouse germ-cell lineage established? Differentiation 73: 435–437.
52. Keller R, Davidson L, Edlund A, Elul T, Ezin M, et al. (2000) Mechanisms of convergence and extension by cell intercalation. Philosophical Transactions of the Royal Society B-Biological Sciences 355: 897–922.
53. Schock F, Perrimon N (2002) Molecular mechanisms of epithelial morphogenesis. Annu Rev Cell Dev Biol 18: 463–493.
54. Wierzbicka-Patynowski I, Schwarzbauer JE (2003) The ins and outs of fibronectin matrix assembly. J Cell Sci 116: 3269–3276.
55. Mao Y, Schwarzbauer JE (2005) Fibronectin fibrillogenesis, a cell-mediated matrix assembly process. Matrix Biol 24: 389–399.
56. Sottile J, Hocking DC (2002) Fibronectin polymerization regulates the composition and stability of extracellular matrix fibrils and cell-matrix adhesions. Mol Biol Cell 13: 3546–3559.
57. Sakai T, Larsen M, Yamada KM (2003) Fibronectin requirement in branching morphogenesis. Nature 423: 876–881.
58. Trinh LA, Stainier DY (2004) Fibronectin regulates epithelial organization during myocardial migration in zebrafish. Dev Cell 6: 371–382.
59. Zhou X, Rowe RG, Hiraoka N, George JP, Wirtz D, et al. (2008) Fibronectin fibrillogenesis regulates three-dimensional neovessel formation. Genes Dev 22: 1231–1243.
60. Davidson LA, Marsden M, Keller R, DeSimone DW (2006) Integrin alpha5beta1 and fibronectin regulate polarized cell protrusions required for Xenopus convergence and extension. Curr Biol 16: 833–844.
61. Marsden M, DeSimone DW (2003) Integrin-ECM interactions regulate cadherin-dependent cell adhesion and are required for convergent extension in Xenopus. Curr Biol 13: 1182–1191.
62. Bellairs R, Curtis ASG, Sanders EJ (1978) Cell Adhesiveness and Embryonic Differentiation. Journal of Embryology and Experimental Morphology 46: 207–213.
63. Lash JW, Seitz AW, Cheney CM, Ostrovsky D (1984) On the role of fibronectin during the compaction stage of somitogenesis in the chick embryo. J Exp Zool 232: 197–206.
64. Lash JW, Yamada KM (1986) The adhesion recognition signal of fibronectin: a possible trigger mechanism for compaction during somitogenesis. In: Bellairs R, Ede D, Lash JW, eds (1986) Somites in Developing Embryo. New York, . pp 201–208.
65. Ohashi T, Kiehart DP, Erickson HP (2002) Dual labeling of the fibronectin matrix and actin cytoskeleton with green fluorescent protein variants. J Cell Sci 115: 1221–1229.
66. Davidson LA, Dzamba BD, Keller R, DeSimone DW (2008) Live imaging of cell protrusive activity, and extracellular matrix assembly and remodeling during morphogenesis in the frog, Xenopus laevis. Dev Dyn 237: 2684–2692.
67. Zamir EA, Rongish BJ, Little CD (2008) The ECM moves during primitive streak formation–computation of ECM versus cellular motion. PLoS Biol 6: e247.
68. Sato Y, Yasuda K, Takahashi Y (2002) Morphological boundary forms by a novel inductive event mediated by Lunatic fringe and Notch during somitic segmentation. Development 129: 3633–3644.
69. Watanabe T, Sato Y, Saito D, Tadokoro R, Takahashi Y (2009) EphrinB2 coordinates the formation of a morphological boundary and cell epithelialization during somite segmentation. Proc Natl Acad Sci U S A 106: 7467–7472.

70. Huynh-Do U, Vindis C, Liu H, Cerretti DP, McGrew JT, et al. (2002) Ephrin-B1 transduces signals to activate integrin-mediated migration, attachment and angiogenesis. J Cell Sci 115: 3073–3081.

71. Meyer S, Hafner C, Guba M, Flegel S, Geissler EK, et al. (2005) Ephrin-B2 overexpression enhances integrin-mediated ECM-attachment and migration of B16 melanoma cells. Int J Oncol 27: 1197–1206.

Supporting information for:

Martins, G. G., Rifes, P., Amândio, R., Rodrigues, G., Palmeirim, I. and Thorsteinsdóttir, S. (2009). Dynamic 3D cell rearrangements guided by a fibronectin matrix underlie somitogenesis. *PLoS One* **4**, e7429.

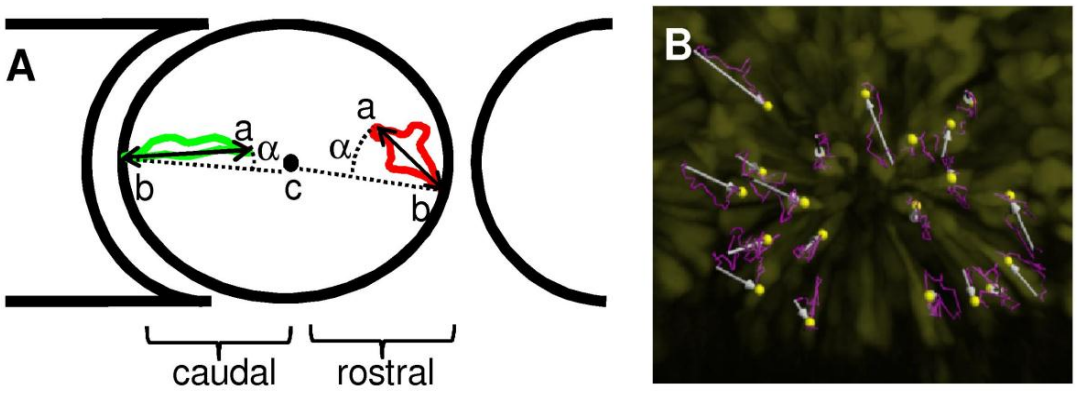

Figure S1. Cell shape and movement measurements. A) Diagram representing the cell's length (distance a-b) and centripetal alignment angle (a; note that the smaller the angle, the better aligned a cell is). ''a'' represents cell's apical end, ''b'' the cell's basal end, and ''c'' is the somitocoel's centroid. See materials and methods for more details. B) 3D reconstruction of tracks of cells whose cell body movement was used to calculate full track length (magenta line) and net cell body displacement (white vector). Rostral is to the right and lateral to the top. Bright-yellow spheres represent the position of the cell bodies of tracked cells in the last time-point. GFP-expressing cells are 3D reconstructed in transparent light green.

Chapter 4

Extracellular matrix assembly and 3D organization during paraxial mesoderm development in the chick embryo

Extracellular matrix assembly and 3D organization during paraxial mesoderm development in the chick embryo

Pedro Rifes [1,2] and Sólveig Thorsteinsdóttir [1,2]

Developmental Biology **368**, 370-81, 2012

[1] Departamento de Biologia Animal e Centro de Biologia Ambiental, Faculdade de Ciências, Universidade de Lisboa, 1749-016 Lisboa, Portugal.
[2] Instituto Gulbenkian de Ciência, 2781-901 Oeiras, Portugal.

Contribution to the publication:

	Experimental work depicted in:							manuscript writing
	Fig. 1	Fig. 2	Fig. 3	Fig. 4	Fig. 5	Supp. Movies	Supp. Figures	
Design and concept	III	III	III	III	III	III	III	III
Execution	III	III	III	III	III	III	III	
Analysis and interpretation	III	III	III	III	III	III	III	

Legend:
n.a……. non applicable
O ……. no intervention
I……. minor contribution
II……. moderate contribution
III…….major contribution/full execution
Note: this contribution does not exclude other contributions, similar or not, from the remaining authors

Developmental Biology 368 (2012) 370–381

Contents lists available at SciVerse ScienceDirect

Developmental Biology

journal homepage: www.elsevier.com/locate/developmentalbiology

Extracellular matrix assembly and 3D organization during paraxial mesoderm development in the chick embryo

Pedro Rifes [a,b,*], Sólveig Thorsteinsdóttir [a,b,*]

[a] Centro de Biologia Ambiental/Departamento de Biologia Animal, Faculdade de Ciências, Universidade de Lisboa, Lisbon, Portugal
[b] Instituto Gulbenkian de Ciência, Oeiras, Portugal

ARTICLE INFO

Article history:
Received 30 January 2012
Received in revised form
1 June 2012
Accepted 2 June 2012
Available online 13 June 2012

Keywords:
Paraxial mesoderm
Somite development
3D reconstruction
Fibronectin
Laminin
Extracellular matrix
Morphogenesis
Chick embryo

ABSTRACT

The extracellular matrix (ECM) is a major player in the microenvironment governing morphogenesis. However, much is yet to be known about how matrix composition and architecture changes as it influences major morphogenetic events. Here we performed a detailed, 3D analysis of the distribution of two ECM components, fibronectin and laminin, during the development of the chick paraxial mesoderm. By resorting to whole mount double immunofluorescence and confocal microscopy, we generated a detailed 3D map of the two ECM components, revealing their supra-cellular architecture *in vivo*, while simultaneously retaining high resolution cellular detail.

We show that fibronectin assembly occurs at the surface of the presomitic mesoderm (PSM), where a gradual increase in the complexity of the fibronectin matrix accompanies PSM maturation. In the rostral PSM, where somites form, fibronectin fibrils are thick and densely packed and some occupy the cleft which comes to separate the newly formed somite from the PSM. Our 3D approach revealed that laminin matrix assembly starts at the PSM surface as small dispersed patches, which are always localized closer to cells than the fibronectin matrix. These patches gradually grow and coalesce with neighboring patches, but do not generate a continuous laminin sheet, not even on epithelial somites and dermomyotome, suggesting that these epithelia develop in contact with a fenestrated laminin matrix. Unexpectedly, as the somite differentiates, its fibronectin and laminin matrices are maintained, thus initially containing both the epithelial dermomyotome and the mesenchymal sclerotome within the somite segment.

Our analysis provides unprecedented details of the progressive *in vivo* assembly and 3D architecture of fibronectin and laminin matrices during paraxial mesoderm development. These data are consistent with the hypothesis that progressive ECM assembly and subsequent 3D organization are active driving and containing forces during tissue development.

Introduction

Early embryos are characterized by massive cell and tissue remodeling, which result in the formation of the basic units of the body plan. The dynamic reciprocity between the genetic program of development and the surrounding microenvironment ensures the adequate coordination of embryonic cells during morphogenesis (Nelson and Bissell, 2006). However, how cells perceive the extracellular morphogenetic signals and change shape or position in response to those signals has been mostly provided by two-dimensional *in vitro* studies, and the adequate translation of such knowledge into the physiological third dimension of developing tissues *in vivo* has proven challenging. The extracellular matrix (ECM), the main component of the extracellular microenvironment, is assembled into a complex three dimensional network that serves as a supportive scaffold for cells and tissues (Frantz et al., 2010). ECM components undergo assembly and turnover, and provide attachment sites for the dynamic cell-ECM interactions involved in guiding cells and shaping embryonic tissues (Goody and Henry, 2010; Ingber, 2006; Larsen et al., 2006a; Rozario and DeSimone, 2010). However, despite the recent advances in setting up 3D systems *in vitro* (Frantz et al., 2010), we still know very little about the 3D microenvironment surrounding cells during embryonic tissue formation and morphogenesis.

In this study we focus on the chick paraxial mesoderm, a unique embryonic tissue with regard to cell and tissue remodeling, and the alterations in two ECM components, fibronectin and laminin, during its development. Paraxial mesoderm development starts when, as a consequence of gastrulation, the mesenchymal presomitic

* Corresponding authors at: Departamento de Biologia Animal, Faculdade de Ciências, Universidade de Lisboa 1749-016, Lisboa, Portugal. Fax: +351 217500028.
E-mail addresses: pgrifes@fc.ul.pt (P. Rifes), solveig@fc.ul.pt (S. Thorsteinsdóttir).

0012-1606/$ - see front matter © 2012 Elsevier Inc. All rights reserved.
http://dx.doi.org/10.1016/j.ydbio.2012.06.003

mesoderm (PSM) comes to lie on both sides of the forming neural tube. Following several hours of maturation, a cleft is created in the rostral PSM and cells rostral to the cleft undergo a mesenchyme to epithelium transition, pinching off as an epithelial somite. A few hours later, the ventral portion of the somite undergoes an epithelium to mesenchyme transition and gives rise to the sclerotome, precursor of the axial skeleton, while the dorsal part retains the epithelial configuration, becoming the dermomyotome, from which the trunk and limb muscles and dorsal dermis derive (Gossler and Hrabě de Angelis, 1998; Kalcheim and Ben-Yair, 2005; Pourquié, 2001). Since somites are formed sequentially in a rostral to caudal fashion, at a given developmental stage, each segment represents a different stage of the developmental program of the paraxial mesoderm, and thus, the rostro-caudal axis reflects a developmental continuum of the undergoing cell rearrangements, such as the transitions between mesenchymal and epithelial states.

Fibronectin is an extracellular glycoprotein essential for somitogenesis in all vertebrate embryo models (George et al., 1993; Jülich et al., 2005; Koshida et al., 2005; Kragtorp and Miller, 2007; Rifes et al., 2007). Fibronectin assembly into a fibrillar matrix starts with the binding of the secreted, compact form of the fibronectin molecule to integrin receptors on the cell surface. Fibronectin is subsequently unfolded and assembled into fibrils which grow in size through the progressive addition of more and more fibronectin molecules (Mao and Schwarzbauer, 2005; Singh et al., 2010; Wierzbicka-Patynowski and Schwarzbauer, 2003). In spite of its clear implication in numerous morphogenesis models (Larsen et al., 2006a; Pankov and Yamada, 2002; Rozario and DeSimone, 2010), our understanding on how this ECM molecule regulates somitogenesis is still incomplete. We know that in the chick embryo, both the fibronectin matrix surrounding the PSM (Duband et al., 1987; Ostrovsky et al., 1983; Rifes et al., 2007) and the continuous supply of new fibronectin protein from the overlying ectoderm are essential for the correct orchestration of PSM cells into an epithelial somite (Rifes et al., 2007). However, a thorough analysis of how this matrix is organized during the morphogenesis of the paraxial mesoderm is still lacking.

Laminins are a major component of basement membranes, and their assembly is a prerequisite for the incorporation and organization of other basement membrane constituents (Yurchenco and Patton, 2009; Yurchenco and Wadsworth, 2004). Laminins are heterotrimeric molecules composed of α,β, and γ chains (Durbeej, 2010; Thorsteinsdóttir et al., 2011). Laminins 111 and 511 are thought to be the first laminins to be synthesized in the embryo, at least during mouse development (Miner and Yurchenco, 2004; Thorsteinsdóttir et al., 2011; Yurchenco and Patton, 2009) and are essential for mouse development beyond E5.5 (Smyth et al., 1999). A laminin-containing basement membrane lines all epithelia and is believed to be required for the acquisition of epithelial polarity (Bryant and Mostov, 2008; Nelson, 2009). However, little is known about its role during the formation of the epithelial somite and during the transformation of the somite into dermomyotome and sclerotome. Analysis of sectioned chick and mouse embryos indicates that a laminin matrix surrounds epithelial somites and remains on the dermomyotome after sclerotome dispersal (Bajanca et al., 2004; Duband et al., 1987). However it is difficult to evaluate its organization as sectioning provides a transverse view of the tissue surfaces. Thus, a detailed analysis of whole mount embryos remains to be done.

In this study we use whole mount double immunofluorescence, high resolution confocal imaging and 3D reconstruction techniques to analyze the 3D pattern of the ECM components fibronectin and laminin during paraxial mesoderm development in chick embryos. The 3D reconstruction of the whole stack of confocal images allowed us to digitally dissect the different tissues and analyze them individually without compromising their morphology. We first analyzed the pattern of fibronectin and laminin associated with the ectoderm and endoderm, which are permanent epithelia, therefore serving as a reference when evaluating the ECM patterns in the paraxial mesoderm. We then focused on the organization of the fibronectin and laminin matrices during three key events in the paraxial mesoderm: PSM maturation, the formation and maturation of the epithelial somite, and somite differentiation into dermomyotome and sclerotome. Our results reveal a progressive assembly of both ECM molecules over time. They show that a fibronectin-rich microenvironment is in a position to support PSM maturation and somite formation, whereas both matrices may play complementary roles in somite maturation and the containment of somite derivatives within the segment.

Material and methods

Eggs and embryos

Fertile eggs were obtained from commercial sources (Sociedade Agrícola Quinta da Freiria, Portugal) and incubated for 48 h at 38 °C. Stage 12 embryos (Hamburger and Hamilton, 1992) were collected, the head and heart were dissected away to reduce embryo thickness, and embryos were fixed overnight in 4% paraformaldehyde in phosphate buffered saline (PBS), at 4 °C.

Somite staging was according to Pourquié and Tam (2001), were the forming somite (rostral end of the PSM) is termed somite 0, or s0. Roman numerals (negative for PSM) are used to refer the position of paraxial tissue relative to somite 0; e.g. sI, sII, sIII etc, for formed somites and s-I ("s minus 1"), s-II, s-III, etc, for progressively more caudal somite-length portions of the PSM (Pourquié and Tam, 2001).

Immunofluorescence and confocal imaging

After fixation embryos were extensively washed in PBS, permeabilized in 1% Triton X-100 in PBS for 30 min and incubated in 5% bovine serum albumin (BSA) in PBS for 3 h at room temperature. Primary antibodies were rabbit polyclonal anti-laminin 111 (Sigma-Aldrich L9393, 1:100), which recognizes all laminins containing an α1, β1 or γ1 chain, mouse monoclonal anti-chick fibronectin (DSHB, clone B3/D6, 1:100), and rabbit polyclonal anti-ZO-1 (Zymed 40–2200, 1:100), a component of tight junctions. Secondary antibodies were Alexa Fluor® 488- and 568-conjugated anti-rabbit and anti-mouse IgG F(ab')$_2$ fragments, (Invitrogen, 1:1000). All antibodies were diluted in PBS with 1% BSA and 0.1% Triton X-100. Embryos were incubated in primary antibodies for 48 h at 4 °C, followed by extensive washing in PBS before being incubated with the secondary antibodies for 24 h together with To-Pro 3 (Invitrogen, 1:500) and ribonuclease A (Sigma, 10 μg/ml) to counterstain nuclei. After a final wash in PBS, embryos were slowly dehydrated in a graded series of methanol in PBS (increasing the methanol concentration by 5–10% per step) and stored in 100% methanol at −20 °C until needed. Selected embryos were slowly brought to room temperature, cleared in graded methyl salicylate in methanol (25%, 50%, and 75%) and mounted in 100% methyl salicylate beneath an n0 coverslip (Martins et al., 2009). Confocal images were acquired on a Leica SPE with an APO 40 × 1.15 N.A. oil immersion lens. The different channels were acquired sequentially, generating stacks of images with a 0.5 μm *z*-step. Double labeling with the two ECM antibodies was performed in all the experiments shown. This approach allowed us to visualize the relative distribution of the fibronectin and laminin ECMs in the same embryo. Single labeling experiments gave the same results (data not shown).

Image analysis

The confocal stacks were imported and analyzed with Amira V.5.3.3 (Visage Imaging Inc.) software. The original stacks of raw images were used to perform the rendering of the immunolabeling into the 3D volumes used for all subsequent analyses and for digital segmentation (Supplementary Movie 1). Image analysis was performed using simple box-shaped regions of interest, volume editing of regions of interest and precise manual segmentation of selected tissues, or a combination of these (see Fig. 1B and Supplementary Movie 2). To analyze the matrix associated with ectoderm and endoderm, these tissues were selected during the segmentation. For the analysis of the matrix of PSM and somites, a 10 to 15 μm thick layer of either the dorsal or ventral surface was selected. No image optimization was performed on the laminin or fibronectin labeling except for histogram corrections to reduce background (less than 10% of the gray levels). The To-Pro 3 (DNA) labeling was further subjected to a 3D Gaussian filter to improve nuclear shape. Localization details on rendered volumes were solved by resorting to the original confocal image sequences, which are simultaneously managed by the Amira software. This software feature allowed for simultaneous analysis of optical planes from the whole stack of images, in either the original *xy* acquisition plane, or any other orientation necessary.

To assess laminin coverage, selected areas (with negligible curvature) of each tissue surface (average 1800 μm^2/area) were thresholded to select the laminin labeling, and the percentage of selected pixels was scored. A total of 51 areas from 4 embryos (3–5 areas per location, 10 locations) were scored.

Images of volumes were exported from Amira, and *z*-views of confocal stacks were collected with ImageJ, and exported as tiff files in both cases. Adobe Illustrator and Photoshop were used to edit and assemble plates.

Movies were created using the Amira DemoMaker module to manage and direct CameraPath and CameraRotate modules, generating through the MovieMaker module a sequence of tiff images. ImageJ Fiji software was used for further editing, such as adding text, pausing, combining and concatenating image sequences, and to transform the image sequence into a movie file.

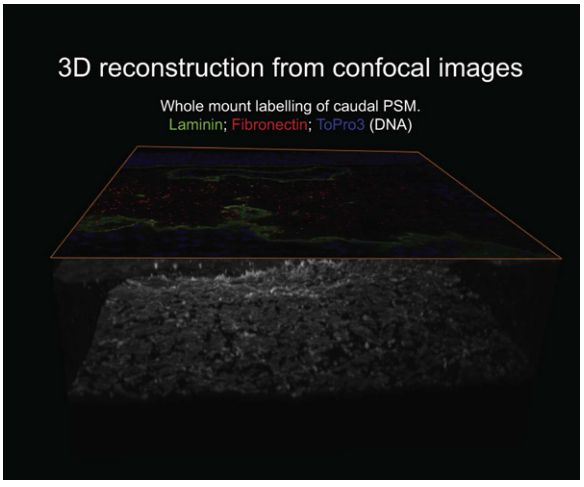

Movie 1. 3D reconstruction from confocal images: Whole mount confocal imaging of the chick embryo at the level of the caudal PSM (one side), and the subsequent 3D reconstruction of the fibronectin, laminin, and To-Pro 3 (DNA) labeling. Note the thick ectoderm covering the paraxial and lateral mesoderm, the thin endoderm lining the ventral side, and the neural tube on the right with the notochord underneath it. http://dx.doi.org/10.1016/j.ydbio.2012.06.003.

Results and discussion

Laminin is the predominant extracellular matrix component lining the ectoderm and endoderm

In order to characterize the ECM organization of the epithelial phenotype in the embryo, we first analyzed the pattern of the laminin and fibronectin immunoreactivity associated with the ectoderm, an example of a mature embryonic epithelium, and the endoderm, a recently formed embryonic epithelium. Using the complete stack of confocal images, we reconstructed in 3D the double immunolabeling of the whole tissue (pictured in Fig. 1A; Supplementary Movie 1), and through digital segmentation of the 3D reconstruction, individualized the immunoreactivity of both ECMs (pictured in Fig. 1B; Supplementary Movie 2, see Materials and Methods).

The digital individualization of the ectoderm epithelium (dark blue in Fig. 1A, B) allowed us to discriminate the fibronectin labeling of the ectoderm (Fig. 1C, E), from the interstitial fibronectin matrix filling the space between the tissues in the chick embryo (Duband et al., 1987; Rifes et al., 2007). At all axial levels studied, numerous fibronectin-stained globules, but not fibrils, are found immediately ventral to the ectoderm (Fig. 1C, F), while a continuous sheet of laminin labeling lines its basal side (Fig. 1D, G, Supplementary Movie 3). Interestingly, the fibronectin-positive globules are found within this continuous laminin-positive basement membrane (Fig. 1F–J, arrows in 1H, J) as well as between the ectodermal basement membrane and the mesoderm (arrowheads in Fig. 1H). Unlike the ectoderm, the endoderm, a thin and elastic epithelium that lies on the ventral side of the embryo (yellow in Fig. 1A, B), displays, clear differences in ECM organization between different axial levels (Supplementary Movie 3). Caudally, near Hensen's node, the laminin matrix has numerous holes (Fig. 1O), which gradually disappear as development proceeds (compare Fig. 1O with L, R). Fibronectin is visible as numerous short fibrils, in the vicinity of the laminin holes, although not filling them (Fig. 1N, P). Where the laminin labeling is continuous, no fibronectin matrix is detected (asterisks in Fig. 1N, O). Beneath the rostral two thirds of the PSM and further rostrally, the endoderm is lined with a continuous laminin sheet (Fig. 1L, R), and fibronectin immunoreactivity is restricted to a few short fibrils (Fig. 1K, M). Notably, beneath the formed somites, small fibronectin-rich globular shapes are observed on the basal side of the endoderm (Fig. 1Q). As observed for ectoderm, this globular fibronectin labeling did not co-localize with the laminin staining (Fig. 1S), which was always located closer to the basal side of the epithelium (Fig. 1T).

We conclude that these embryonic epithelia are lined with a continuous laminin sheet, characteristic of a mature basement membrane (LeBleu et al., 2007). Only the caudal endoderm displays a discontinuous laminin matrix, with holes decreasing in size and frequency as it matures indicating a progressive assembly of its basement membrane. On the other hand, a fibronectin matrix is practically absent from these two epithelia whereas a strong globular fibronectin staining is associated with them. This globular fibronectin staining is spatially coincident with the expression of *Fn1* by ectoderm and rostral endoderm (Rifes et al., 2007), suggesting that the globules represent the compact form of secreted fibronectin (Singh et al., 2010; Wierzbicka-Patynowski and Schwarzbauer, 2003).

A progressive increase in fibronectin matrix complexity accompanies the maturation of the presomitic mesoderm

To evaluate the distribution pattern of fibronectin and laminin in association with the paraxial mesoderm (PSM and somites), we

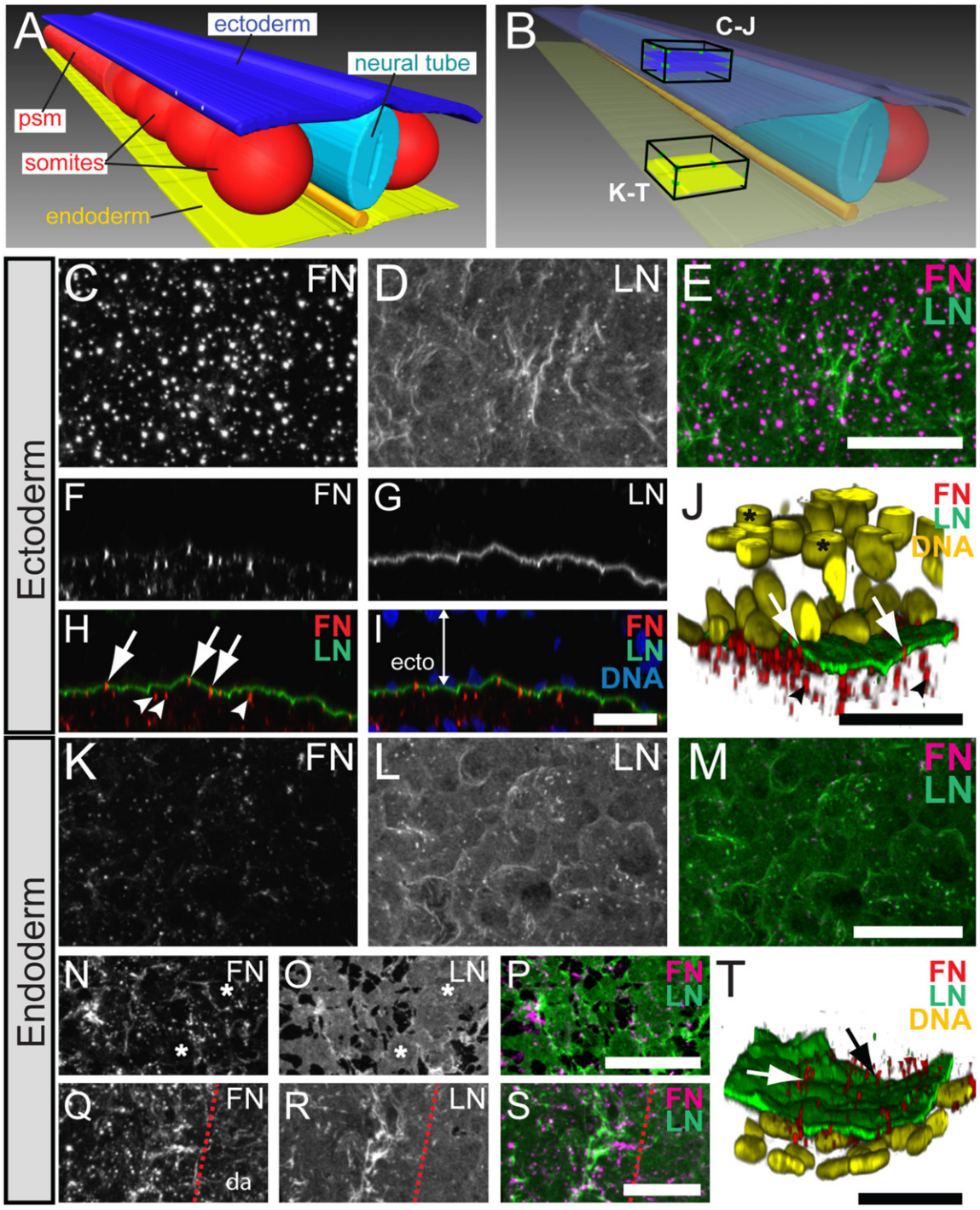

Fig. 1. Fibronectin and laminin organization of ectoderm and endoderm. (A) 3D representation of the paraxial mesoderm (red) and its surrounding tissues, ectoderm (dark blue), neural tube (light blue), notochord (orange), and endoderm (yellow). (B) The technique of digital segmentation of the 3D reconstructed tissues (in transparent colors) allowed the individualization of a portion of each tissue, such as representative regions of the ectoderm (opaque blue within box) and endoderm (opaque yellow within box). See Supplementary Movies 1 and 2. (C–E) Digitally segmented portion of the 3D reconstruction of fibronectin (C) and laminin (D) immunoreactivity (merged in E) of ectoderm (equivalent to boxed blue region in B) viewed from the paraxial mesoderm. The basal side of ectoderm is covered by a globular fibronectin immunoreactivity (C, E) and a continuous laminin-positive sheet (D, E). (F–I) Transverse slice (*z*-axis) through the stack of confocal images displayed in C–E (dorsal on top), showing that the fibronectin-positive globules (F, H, I) are localized extracellularly, below the ectoderm, either embedded within (arrows in H) or ventral to (arrowheads in H) the laminin-positive basement membrane (G, H, I). (J) Perspective view of a portion of the 3D reconstruction of nuclear staining (yellow) in the ectoderm with its associated fibronectin (red) and laminin (green) immunoreactivity. The nuclei are present at different levels, showing the stratified nature of the ectoderm (note the flattened nuclei on top, asterisk). Laminin is localized on the basal side of the ectoderm, whereas fibronectin-positive globules are either within the basement membrane (arrows) or ventral to it (arrowheads). (K–T) Digitally segmented portion of the 3D reconstructed fibronectin (K, N, Q) and laminin (L, O, R) immunoreactivity of endoderm (as in boxed yellow region in B; merged images in M, P, S) viewed from the paraxial mesoderm at three different axial levels: rostral PSM (K–M), caudal PSM (N–P) and somite X (Q–S). At the level of the rostral PSM, endoderm has a few specks of fibronectin immunoreactivity (K, M) and a continuous laminin-positive basement membrane (L, M). Endoderm at the level of the caudal PSM is characterized by a fibronectin-positive matrix of short fibrils (N) and a discontinuous sheet of laminin immunoreactivity (O). Note that where the laminin staining forms a continuous sheet (asterisks), the fibronectin staining is decreased or absent (N–P). Underneath somite X, globular fibronectin-positive bodies are visible covering the endoderm directly facing the sclerotome (Q). Interestingly, these globular bodies are not observed at the endoderm–dorsal aorta interface (right of dashed line), where a faint fibrillar matrix is visible, even though the laminin staining is similar in both locations (R). (T) Perspective view of a 3D reconstruction of the endoderm epithelium underneath the rostral PSM, with its nuclei (yellow), fibronectin (red) and laminin (green) immunostaining. Note that nuclei are flatter than in the ectoderm and all in one plane. A laminin-positive basement membrane covers the endoderm on its basal side, while fibronectin-positive fibrils take a perpendicular orientation, reaching the paraxial mesoderm (arrows). See Supplementary Movie 3 for a comparison of all three locations. FN: fibronectin; LN: laminin, DNA: To-Pro 3 staining; psm: presomitic mesoderm; ecto: ectoderm; da: dorsal aorta-endoderm interface area. Scale bars=20 μm.

analyzed 3D reconstructions of these two ECMs through transverse views of slabs of tissue (Fig. 2A, white arrow) and surface segmentations (Fig. 2A, orange arrow). Comparative analysis of the fibronectin and laminin matrix along the axis from caudal to rostral provides a temporal scale of *in vivo* matrix assembly. The cells that ingress during gastrulation at the caudal end of the embryo, have degraded their previous fibronectin and laminin matrices (Nakaya et al., 2008; Sanders and Prasad, 1986), and, as they populate the caudal PSM, start the assembly of new ECMs.

Fibronectin labeling in the caudal PSM is in the form of globules and short thin fibrils (arrows in Fig. 2B) which we believe corresponds to the punctate pattern of fibronectin observed in avian embryo sections (Duband et al., 1987; Krotoski et al., 1986; Ostrovsky et al., 1983; Rifes et al., 2007). A fibronectin matrix, composed of well-spaced thin fibrils, intermingled with a globular-shaped immunoreactivity (Fig. 2D, F), fills the space between the PSM and the neighboring tissues (arrowheads in Fig. 2B). The globular fibronectin staining is particularly abundant on the dorsal PSM surface (Fig. 2D; Supplementary Movie 4), reflecting the proximity to the *Fn1*-expressing ectoderm (Rifes et al., 2007). Laminin staining is faint throughout the caudal PSM (Fig. 2C; Supplementary Movie 4), and only a few speckles are located on the PSM surface (Fig. 2E, G).

The rostral PSM shows a clear change in the organization of both fibronectin and laminin compared to the caudal PSM. Fibronectin is now organized into an extensive fibrillar matrix which surrounds the PSM and extends towards the neighboring tissues (compare Fig. 2B and H), and long fibrils penetrate into the PSM in a radial fashion (arrowheads in Fig. 2H, Supplementary Movie 5). The digitally individualized PSM surfaces display a dense meshwork of compact and thick fibrils (Fig. 2L, N), with numerous fibronectin-rich globules on the dorsal surface of the PSM (Fig. 2L, L'), but not on the ventral side (Fig. 2N) where the endoderm is negative for *Fn1* transcripts (Rifes et al., 2007). Disperse patches of laminin matrix delineate the rostral PSM surface (Fig. 2I, J, M, O; Supplementary Movie 5). This pattern coincides with the presence of aligned nuclei in the peripheral PSM (Fig. 2K; Supplementary Figure S1), representing the early signs of epithelialization (Dubrulle and Pourquié, 2004; Martins et al., 2009). The laminin patches are always located closer to the PSM surface than the fibrillar fibronectin matrix (Fig. 2K, K′). Within the PSM, dispersed laminin patches are, like fibronectin, enriched in the center of the PSM (Fig. 2H, I), and are often located adjacent to non-fibrillar fibronectin staining (Fig. 2K″).

We conclude that fibronectin fibrillogenesis occurs rapidly at the PSM surface, and it continues throughout PSM maturation, thickening the fibrillar matrix surrounding the paraxial tissue. Our observations give a 3D morphological view which supports the proposal that a gradient of fibronectin immunoreactivity exists in the PSM (Ostrovsky et al., 1988). Fibronectin fibrillogenesis in cultured cells follows a pattern where fibronectin molecules attach to the cell surface (Peters and Mosher, 1987), then short fibrils form and extend between adjacent cells or connect

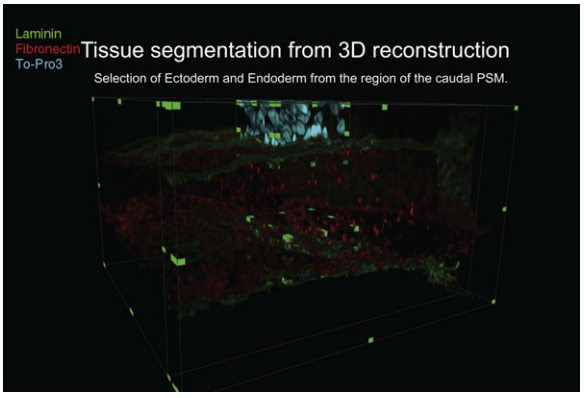

Movie 2. Tissue segmentation from 3D reconstruction: 3D reconstruction of fibronectin, laminin, and To-Pro 3 (DNA) labeling at the level of the caudal PSM, as in Movie 1. First: digital selection of a 20 μm thick slab along the rostro-caudal axis. Second: manual segmentation of an area of the labeling associated with ectoderm and endoderm, followed by a close-up of the ectoderm. Note the globular fibronectin labeling embedded within the laminin staining on the basal side of the ectoderm, compared to the fenestrated laminin matrix and dispersed fibronectin fibrils on the endoderm. http://dx.doi.org/10.1016/j.ydbio.2012.06.003.

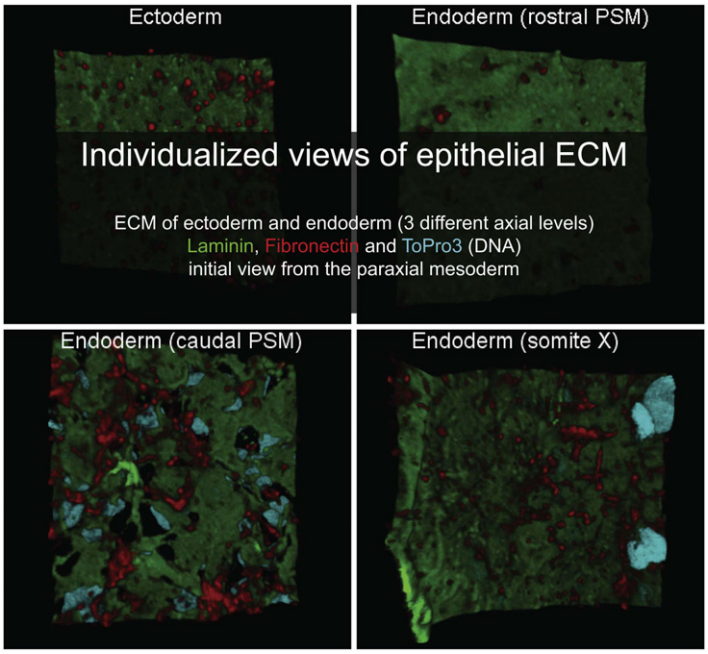

Movie 3. Individualized views of ECM of ectoderm and endoderm: Comparative perspective views of selected portions (35 μm wide) obtained though digital segmentation of fibronectin, laminin, and To-Pro 3 (DNA) labeling of the ectoderm and endoderm. Four different locations are displayed; ectoderm and endoderm underneath the rostral PSM, endoderm underneath the caudal PSM and endoderm under somite X. Note that in the last image, the nuclei of the dorsal aorta are visible on the right side of the dorsal view. http://dx.doi.org/10.1016/j.ydbio.2012.06.003.

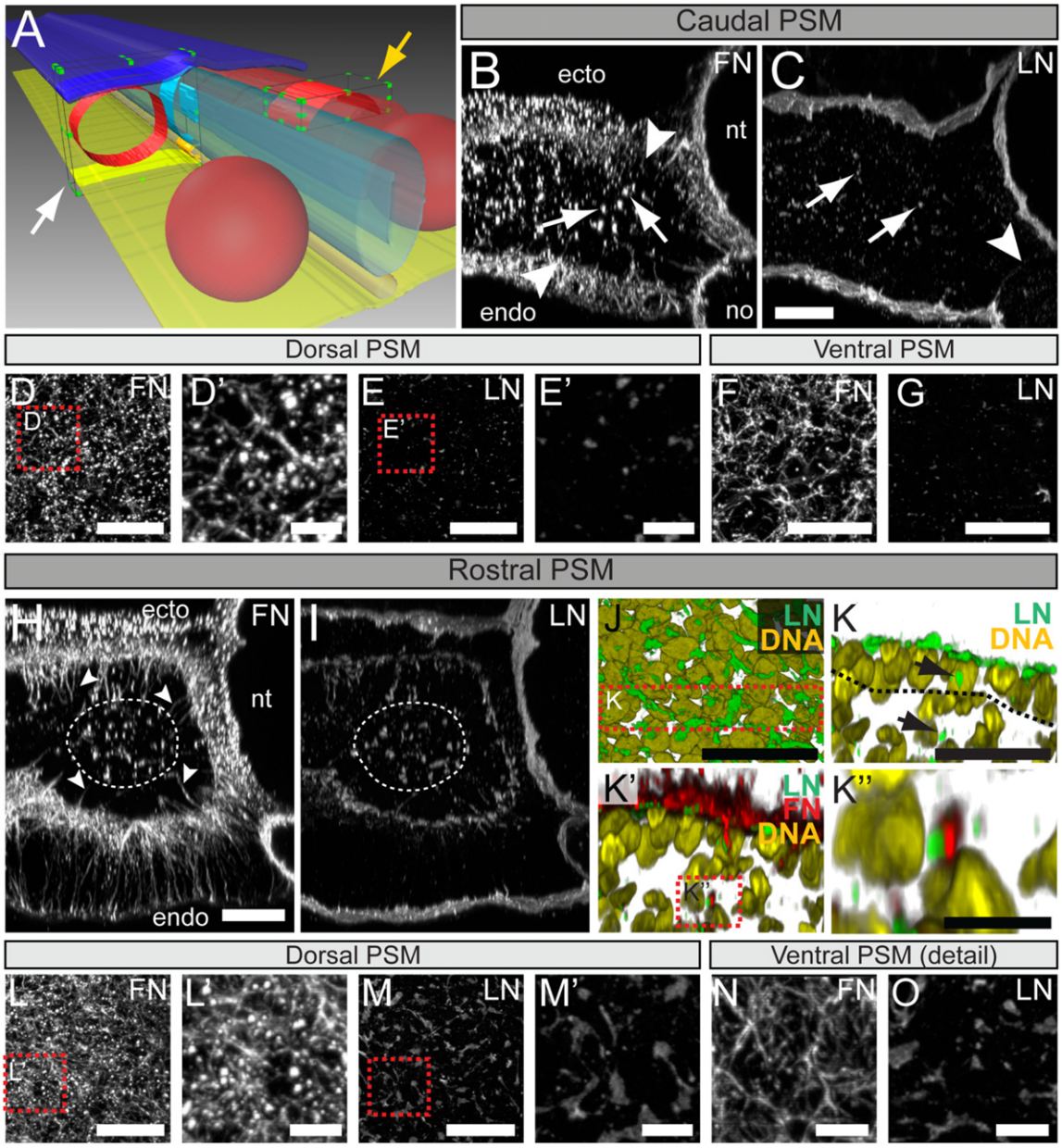

Fig. 2. Fibronectin forms an increasingly complex matrix along the caudo-rostral axis of the PSM while laminin is organized in sparse patches. (A) 3D representation of the paraxial mesoderm (red) and surrounding tissues, with examples of the digital segmentation performed (see Supplementary Movie 2). White arrow: selection of a 20 μm thick transverse slab of a 3D reconstruction of immunolabeling of the paraxial mesoderm (as in B, C, H, I). Yellow arrow: segmentation of the surface immunoreactivity (10–15 μm) from the whole 3D reconstruction of a tissue, here exemplified with the dorsal facet of the paraxial mesoderm (yellow arrow; as in D, E, J, L, M). (B–C) Transverse slab from the 3D reconstruction of fibronectin (B) and laminin (C) immunoreactivity of the caudal PSM shows a globular fibronectin staining within the PSM (arrows in B) and fibrillar fibronectin staining surrounding this tissue (arrowheads in B). Faint laminin immunoreactivity is detectable within the PSM (arrows in C), which contrasts with the strong basement membrane staining of the ectoderm, endoderm and neural tube (C). A thick fibronectin-positive matrix surrounds the notochord (no in B), but, in contrast, laminin staining around the notochord is faint (arrowhead in C). Note the strong globular staining associated with the fibrillar fibronectin matrix between the PSM and ectoderm but not between the PSM and endoderm (B). (D–E) Dorsal view of a 3D reconstruction of the fibronectin (D,D′) and laminin (E,E′) immunoreactivity on the dorsal facet of the caudal PSM shows a fibrillar fibronectin-positive matrix with numerous globular forms (D,D′) but only a few specs of laminin (E,E′). (F–G) Ventral view of 3D reconstruction of fibronectin (F) and laminin (G) immunoreactivity of the ventral facet displays a similar fibrillar fibronectin staining but little globular staining (F). Like on the dorsal side, the laminin staining is limited to a few dispersed specs (G). (H–I) Transverse slab from the 3D reconstruction of fibronectin (H) and laminin (I) labeling in the rostral PSM shows a globular fibronectin staining within the PSM (dashed circle in H) and between mesoderm and ectoderm and mesoderm and neural tube. An extensive fibrillar fibronectin-positive matrix surrounds the rostral PSM (H). Numerous fibronectin fibrils penetrate the PSM radially (arrowheads in H) and others link the PSM to neighboring tissues. Laminin immunoreactivity is detected within the PSM (dashed circle in I) in a similar pattern to that observed for fibronectin and a discontinuous laminin matrix surrounds the rostral PSM. (J) Dorsal view of the peripheral PSM layer (20 μm) showing the dispersed patches of laminin staining and the nuclei located underneath. (K) Transverse view of a portion of J, showing the peripheral layer of aligned nuclei (dashed line), a sign of the initiation of epithelialization. Laminin immunoreactivity is primarily organized in patches on the outer (basal) side of peripheral PSM cells. A few laminin-positive specs are also seen within the PSM (arrows). The basal laminin matrix of peripheral PSM cells is always positioned closer to the cells than the fibronectin matrix surrounding the PSM (K′). It is of interest to note that specs of laminin staining within the PSM are associated with fibronectin-positive material; although generally adjacent to each other; fibronectin and laminin never co-localized in the same structure (K″). (L–M) In the rostral PSM, the dorsal fibronectin-positive matrix (L) is much denser when compared to the one of caudal PSM (D) and more fibrils can be observed (L′) than caudally (D′). Laminin immunoreactivity on the dorsal PSM surface is organized in dispersed patches (M), larger than the patches observed further caudally (E). (N–O) An extensive fibronectin-positive fibrillar matrix is also observed on the ventral side of the PSM (N) but unlike the situation dorsally (L′), no globular fibronectin staining is detectable. Laminin immunoreactivity on the ventral side of the PSM is organized in dispersed patches (O), analogous to the pattern observed on the dorsal side (M′). Scale bars = 5 μm (D′, E′, K″, L′, M′, N, O) and 20 μm (all other images). FN: fibronectin; LN: laminin, DNA: To-Pro 3 staining; ecto: ectoderm; endo: endoderm; nt: neural tube; no: notochord.

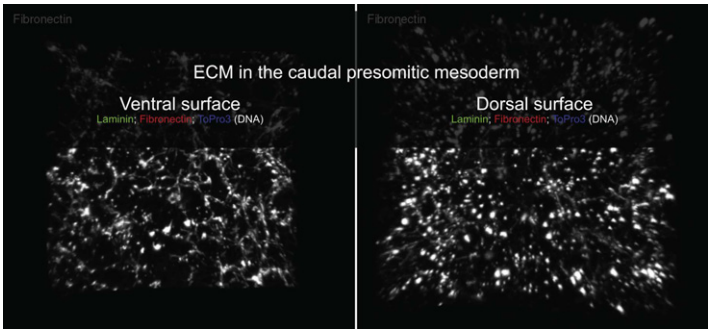

Movie 4. ECM in the caudal presomitic mesoderm: Segmented portion (50 μm wide) of fibronectin, laminin, and To-Pro 3 (DNA) labeling on the ventral (on the left) and dorsal (on the right) surface of the caudal PSM (starts with view from outside the PSM). http://dx.doi.org/10.1016/j.ydbio.2012.06.003.

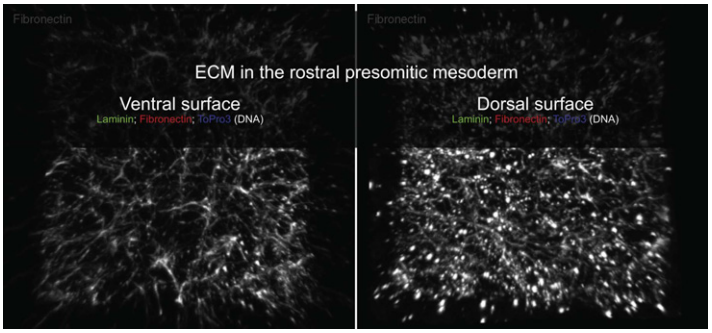

Movie 5. ECM in the rostral presomitic mesoderm: Segmented portion (50 μm wide) of fibronectin, laminin, and To-Pro 3 (DNA) labeling on the ventral (on the left) and dorsal (on the right) surface of the caudal PSM (starts with view from outside the PSM). http://dx.doi.org/10.1016/j.ydbio.2012.06.003.

them to their substrate (McDonald et al., 1987). Fibronectin matrix assembly in the PSM, however, appears to occur quickly, and does not pass through the stage of short fibrils at cell–cell boundaries. We propose that the PSM, being a 3D tissue composed of small, highly motile mesenchymal cells (Bénazéraf et al., 2010; Delfini et al., 2005; Martins et al., 2009), assembles its peripheral fibronectin matrix from globules to fibrils. The continuous supply and incorporation of new fibronectin molecules then progressively stabilizes and strengthens the matrix, as has been observed in cultured cells (Sottile and Hocking, 2002), thickening and elongating the existing network into a complex fibrillar matrix (Mao and Schwarzbauer, 2005; Singh et al., 2010; Wierzbicka-Patynowski and Schwarzbauer, 2003).

In summary, the laminin matrix in the rostral PSM is sparse and in the form of patches adjacent to the peripheral epithelializing PSM cells, indicating that the epithelialization process does not rely on a basement membrane. In contrast, the fibronectin matrix becomes progressively more complex from the caudal to the rostral PSM, culminating in a dense matrix which is essential for somite formation (Rifes et al., 2007). Our data are consistent with an hypothesis where a build-up of a fibronectin matrix may be viewed as part of the PSM maturation program. In this scenario, a fibronectin matrix of adequate complexity would, together with lowered fibroblast growth factor levels and increased retinoic acid and sonic hedgehog levels (Aulehla and Pourquié, 2010; Resende et al., 2010), be an essential condition of the rostral PSM microenvironment for somite formation to occur successfully.

Somite clefts are rapidly filled with a fibrillar fibronectin matrix and lined with laminin patches

A new somite (somite I) separates from the rostral PSM when a gap within the tissue is created (Fig. 3A), establishing the earliest somitic boundary. The somitic boundary comprises not only the space created between cells, the somitic cleft, but also the two opposing epithelializing somitic borders (Supplementary Figure S2). The somitic clefts are filled with a rich fibronectin matrix, while each of the opposing borders is lined with a patchy laminin matrix (Fig. 3B). The newly formed cleft revealed numerous fibronectin fibrils organized in a centripetal fashion (Fig. 3C), suggesting that fibrils are rapidly dragged from the PSM surface into the cleft, aiding tissue separation. The boundary between somite I and II (see Fig. 3A), older by one round of somite formation and thus slightly more mature, is almost fully filled with a dense fibrillar fibronectin matrix (Fig. 3D). These results show that fibronectin rapidly fills the somitic cleft and suggests that *de novo* production by somites (Rifes et al., 2007) may promote a burst in matrix assembly thus stabilizing the somitic boundary, as occurs during zebrafish somitogenesis (Koshida et al., 2005). Interestingly, fibronectin remodeling during cleft formation of the salivary gland follows similar dynamics. Localized fibronectin assembly at the gland surface promotes cleft formation (Onodera et al., 2010; Sakai et al., 2003), but cleft growth requires the continuous wedging in of the initial fibronectin matrix concomitantly with the assembly of a new matrix (Larsen et al., 2006b). As somite I forms, the cells which border the newly formed cleft epithelialize. However, they do so at different times; the caudal border of somite I epithelializes before the rostral border of the PSM (see Fig. 3A; Supplementary Fig S2) (Martins et al., 2009; Sato et al., 2002; Watanabe et al., 2009). Laminin staining of the rostral border of the PSM (Fig. 3E) showed some patches of laminin, most concentrated towards the center of the tissue but also large laminin-negative areas (asterisks in Fig. 3E). At the caudal border of somite I, the laminin patches were slightly denser albeit still enriched in the center of the tissue (Fig. 3F). The borders on both sides of the second cleft were more evenly covered with patches of laminin (Figs. 3G and H) than the

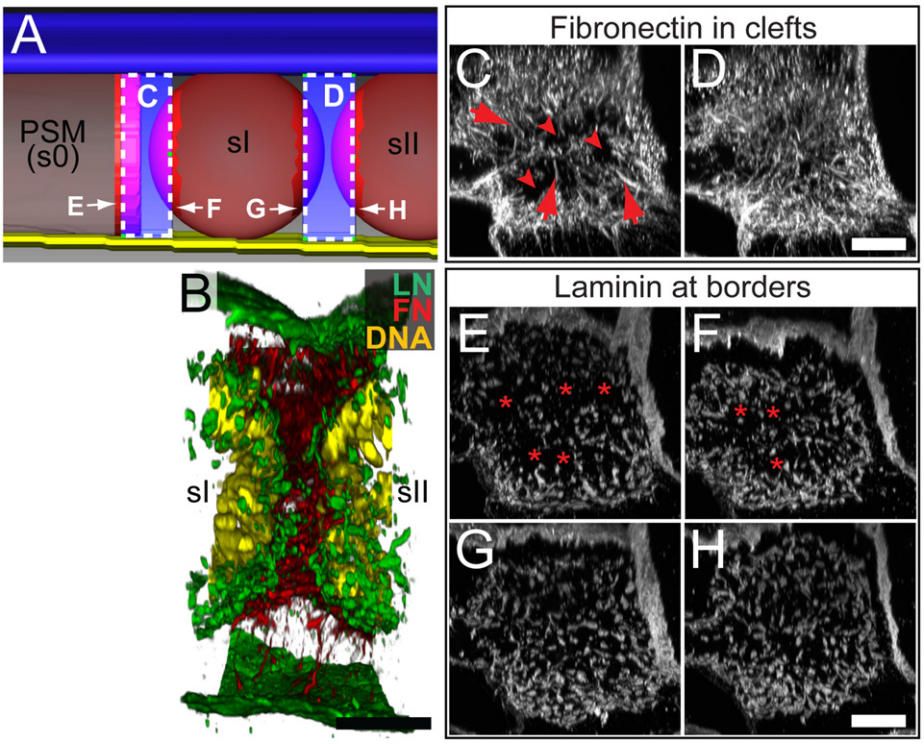

Fig. 3. Newly formed somite clefts are rapidly filled with a fibronectin matrix and lined with patches of laminin. (A) Lateral view of a 3D representation of the rostral PSM and most recent somites (I and II) and respective boundaries. The clefts are filled with fibronectin (volumes C and D, transparent blue) while the borders are lined with laminin (surfaces E, F and G, H, in red) The most recent somitic boundary separates the rostral-most part of the PSM (somite 0) from somite I (see Materials and Methods for nomenclature). Dorsal to the top, paraxial mesoderm in transparent red, ectoderm in opaque blue, and endoderm in yellow. (B) Lateral view of the 3D reconstruction of fibronectin (red), laminin (green) and nuclei (yellow) labeling of a representative boundary between somite I and somite II (cleft D with borders G and H). While a complex fibronectin matrix fills the cleft, both borders are lined with a patchy laminin matrix. Note that to aid visualization, only the medial half of the fibronectin labeling is displayed here, and a 10 μm wide slab of the DNA labeling, through the middle of the somite is shown. (C,D) 3D reconstruction (rostral view of a 20 μm thick slab) of the fibronectin staining in somite clefts. The first cleft (C) displays centripetally arranged fibronectin-positive fibrils (arrows) with fibronectin-negative areas in between (arrowheads). The second cleft (D) retains the pattern of centripetally arranged fibrils, but the spaces in between are now filled with a dense fibronectin matrix. (E–H) Segmentation of the 3D reconstruction of the laminin staining in the somite cleft borders (viewed from the cleft). The laminin immunoreactivity is organized in dispersed patches amidst large laminin-negative areas (asterisks) on the borders of the first cleft (E and F), while the borders of the second cleft (G and H) show a homogeneous distribution of the laminin patches. FN: fibronectin; LN: laminin, DNA: To-Pro 3 staining; PSM: presomitic mesoderm; s0: somite 0; sI: somite I; sII: somite II. Scale bars = 20 μm.

first cleft. Therefore, as observed for the rostral PSM, epithelializing surfaces are lined with dispersed patches of laminin, showing that the epithelialization process in the paraxial mesoderm is not dependent on a continuous basement membrane.

Epithelial somites are surrounded by a thick fibronectin matrix and a discontinuous pericellular laminin matrix

The most recently formed somite, somite I, is covered by a dense fibrillar fibronectin matrix which spreads over the somite surface and connects to the surrounding tissues (Fig. 4A–C). Fibronectin fibrils are thicker than observed around the PSM (compare Fig. 4B, C with Fig. 2H, L, N) indicating that fibronectin fibrillogenesis still continues. Also, the fibronectin fibrils covering the epithelial somite I (Supplementary Figure S3) are less parallel to the tissue surface than on the rostral PSM (compare Supplementary Movies 5 and 6), probably as the result of the cell rearrangements occuring during the compaction of the epithelial somite (Martins et al., 2009). Numerous fibronectin fibrils penetrate the somitic epithelium towards the somitocoel, albeit less abundantly than in the rostral PSM (compare Fig. 4A with Fig. 2H). Cells are known to deform the matrix as they engage and pull it (Ohashi et al., 1999). We therefore suggest that these radial fibronectin fibrils reflect the movement of cells between the paraxial mesoderm core and its surface (Martins et al. 2009). As the epithelial somite is formed and the peripheral epitheliod layer is established, PSM cells become less motile (Delfini et al. 2005) and the egression movements diminish (Martins et al. 2009). In accordance with this, somite V, which has reached full maturity as a sphere of epitheloid cells (Supplementary Figure S4), only displays a few radial fibronectin fibrils (Fig. 4D). Furthermore, the fibronectin matrix surrounding somite V has developed into a complex mat of shorter, thicker and more closely packed fibrils than observed earlier (compare Fig. 4E′ with Figs. 2L′ and 4B′).

A patchy laminin labeling fully surrounds somite I (Fig. 4F; Supplementary Figure S5; Supplementary Movie 6). However, the individual patches of laminin matrix now cover a bigger area than observed in the rostral PSM, and some neighboring patches have coalesced (compare Fig. 2M, O with Fig. 4G, H). This trend continues in somite V where the area covered by laminin-positive patches has become even larger (compare Fig. 4G, H with 4J, K). Nevertheless, the laminin matrix is far from forming a basement membrane sheet such as those lining the ectoderm and endoderm, indicating that epithelial somites do not require a continuous basement membrane for their development. Unexpectedly, in both somite I and V, the ventral surface of the somite appears to have a larger area occupied by laminin than the dorsal surface (Fig. 4G, H and J, K; Fig. 5L; Supplementary Movies 6 and 7; also see next section).

Fibronectin and laminin matrices contain cells within the somite after its subdivision into dermomyotome and sclerotome

In somite X, the separation of the dorsal and ventral halves of the somite into dermomyotome and sclerotome is well underway

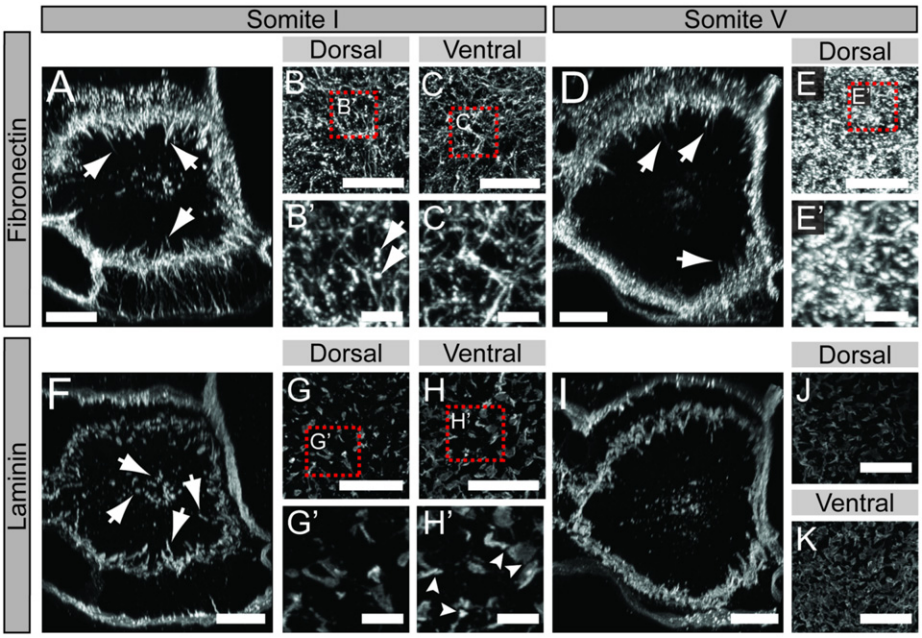

Fig. 4. The epithelial somite is surrounded by an extensive network of fibronectin fibrils and a growing laminin-positive basement membrane. 3D reconstructions of the fibronectin and laminin immunolabeling in somite I (A, F) and somite V (D, I), selected as 20 μm transverse slabs through the middle of the reconstructed somites (dorsal to the top), and segmented portions (10–15 μm thick) of the dorsal (B, E, G, J) and ventral (C, H, K) somite surfaces, viewed from outside the somite. See representation in Fig. 2A and Supplementary Movies 6 and 7 for somite I and somite V, respectively. (A) A thick fibrillar fibronectin matrix surrounds somite I, with several long fibrils penetrating the somite epithelium (arrows). A globular staining is also visible in the somitocoel. (B, C) The fibronectin-stained fibrils on the dorsal (B) and ventral (C) surface of somite I are densely interweaved. Fibronectin-positive globules are visible in the dorsal matrix (arrows in B′) but are uncommon in the ventral one (C′). (D) The surface of somite V is covered with a strong fibronectin labeling, but at this stage, only a few fibrils penetrate the somite epithelium (arrows). A globular staining remains in the somitocoel. (E) The fibronectin-positive matrix covering somite V consists of a compact mat of short fibrils (E, E′). (F): A transverse view of the laminin staining shows the continuous laminin-positive matrix lining epithelia, such as ectoderm, endoderm, neural tube and notochord. In contrast, a discontinuous, patchy matrix surrounds somite I. Specks of laminin are also observed in the somitocoel and within the somite epithelium (arrows). (G, H): The laminin staining on the surface of somite I is organized into separate patches (G, H). These patches are generally separated on the dorsal surface (G′) but ventrally, many patches connect with each other (H′, arrowheads), thus showing a larger laminin coverage than dorsally. (I) Transverse view of the 3D reconstruction of laminin labeling shows a denser but still discontinuous laminin matrix surrounding somite V. (J, K) Detailed views of the dorsal and ventral surface of somite V revealed that the number of interconnected patches is overall much larger than at the previous stage. Interestingly, the laminin network is considerably denser on the ventral side (K) compared to the dorsal side (J). FN: fibronectin; LN: laminin, DNA: To-Pro 3 staining. Scale bars=20 μm (A–K) or 5 μm (B′, C′, E′, G′, H′).

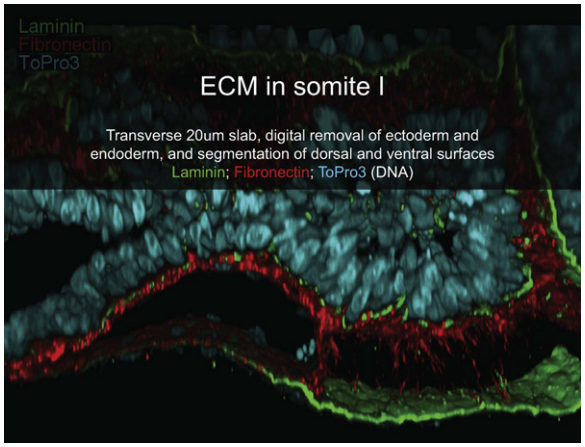

Movie 6. ECM in somite I: Selection of a 20 μm thick transverse slab of the 3D reconstruction of fibronectin, laminin, and To-Pro 3 (DNA) labeling in the middle of somite I. First: ectoderm and endoderm digitally removed. Second: digital selection of the dorsal and then ventral surface of the somite (plus adjacent intermediate mesoderm and neural tube). http://dx.doi.org/10.1016/j.ydbio.2012.06.003.

(Fig. 5A, D; Supplementary Figure S6). A dense mat of fibronectin matrix covers the dorsal side of the dermomyotome (Fig. 5B, B′). Laminin immunoreactivity is also seen lining the basal (dorsal) side (Fig. 5D), but it is still far from continuous (Fig. 5E, E′; Supplementary Movie 8). Rather, the dermomyotomal laminin matrix remains organized in patches, reminiscent of the laminin matrix of somite V (compare Figs. 4J and 5E). Thus, as in the case of the epithelial somite, the dermomyotome develops in the presence of a fenestrated laminin matrix.

Sclerotome formation is considered to involve an epithelium to mesenchyme transition of the ventral somite but, surprisingly, although the ventral part of the somite clearly downregulates the epithelial tight junction marker ZO-1 (Supplementary Figure S6), we did not observe a degradation of the ECM surrounding the segment (Fig. 5A, D, G, H; Supplementary Figure S7) and perhipheral nuclei remain aligned (Fig. 5G–J; Supplementary Figures S6 and S7; Solursh et al., 1979). Altogether these observations suggest that, despite the ventral loss of epithelial markers, the ECM inherited from the epithelial somite aids in the maintenance of the segment compartment, at least in these early stages of differentiation. Sclerotome formation is known to involve the synthesis and secretion of hyaluronic acid and chondroitin sulphate proteoglycans, leading to the expansion of the extracellular space and dispersal of the sclerotomal cells (Solursh et al., 1979). Thus it is tempting to suggest that the increase in laminin coverage on the ventral somite (Fig. 4G, H, J, K; Fig. 5L) may provide enough matrix to counterbalance this sclerotomal expansion. Our data are thus consistent with the notion that sclerotome formation is a particular form of EMT, where despite the loss of cell–cell adhesion/epithelial markers (Duband et al. 1987), cell–matrix interactions are initially kept, containing the somitic cells within the segment.

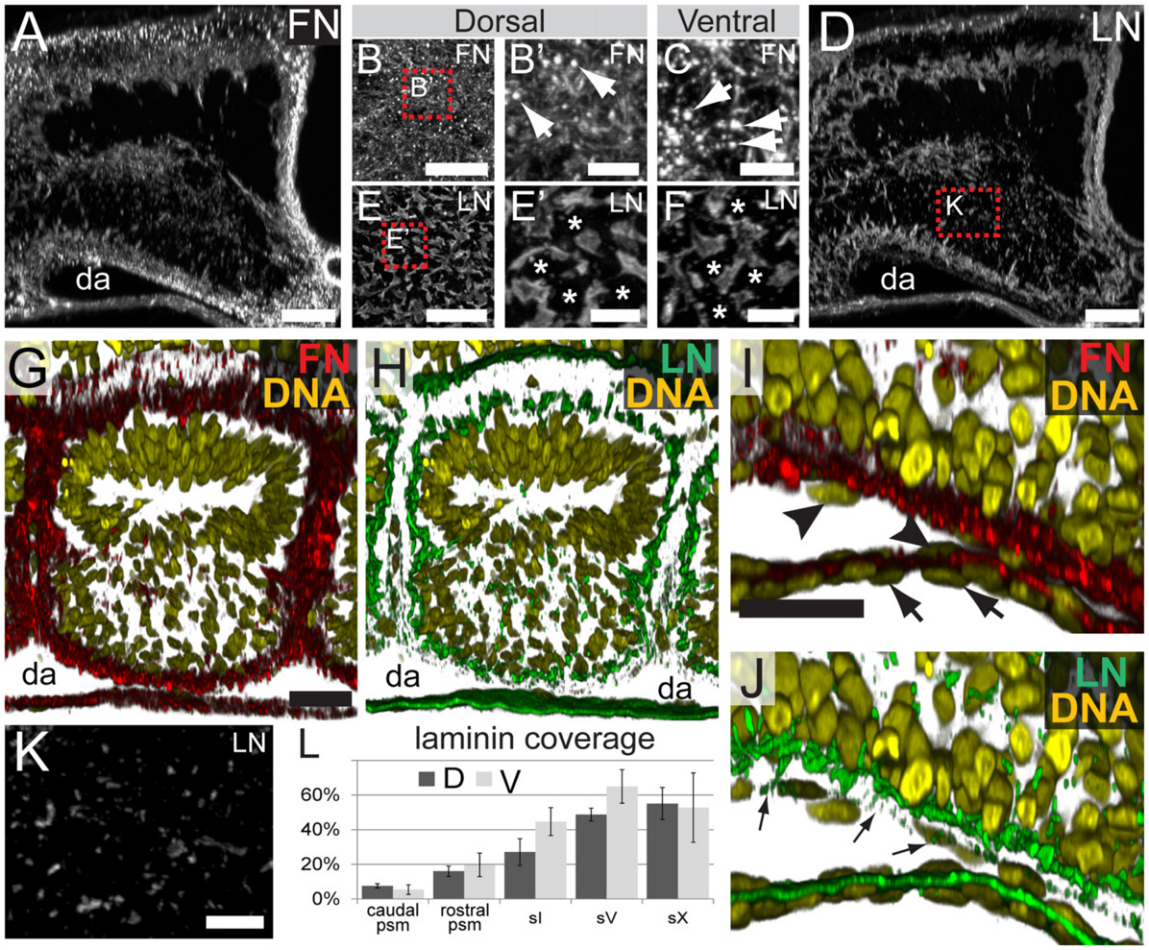

Fig. 5. Fibronectin and laminin matrices during dermomyotome and sclerotome formation. (A) Transverse view of a 20 μm slab through a 3D reconstruction of fibronectin labeling of somite X which has differentiated into dermomyotome and sclerotome. A fibronectin-positive matrix fills the space between the ectoderm and the dermomyotome and a dispersed fibronectin immunolabeling is present within the sclerotome. See Supplementary Movie 8. (B, C) Segmented portions of the 3D fibronectin labeling on the dorsal (B) and ventral (C) surface of somite X, viewed from outside the somite. The dorsal fibronectin matrix is composed of compact short fibrils (B) and fibronectin-positive globules (arrows in B′). The fibronectin matrix covering the ventral surface of the sclerotome has more space between the fibrils and numerous fibronectin rich globules (arrows) are concentrated at the sclerotome–endoderm interface (C). (D) Transverse view of the same slab as in A, but showing the 3D reconstruction of the laminin immunolabeling. Both the dorsal surface of somite X (basal surface of the dermomyotome) and the ventral surface of the sclerotome are covered with a strong laminin labeling. Specks of laminin are visible throughout the sclerotome (box). (E, F) Segmented portions of the 3D laminin labeling of the dorsal (E) and ventral (F) surfaces of somite X, viewed from outside the somite. Numerous interconnected patches of laminin are observed both dorsally and ventrally, but they are separated by laminin-negative areas (asterisks in E′ and F). (G, H) Lateral view of a 10 μm sagittal slab trough the 3D reconstruction of fibronectin (G) and laminin (H) labeling (and nuclear staining) of somite X. The dermomyotomal nuclei are elongated and arranged in an inverted U shape. Note that nuclei at the periphery of the sclerotome are rounder but aligned. The fibronectin labeling (G) fills in the spaces between the somites and the surrounding tissues, while a patchy laminin matrix lines, not only the dermomyotome, but also the sclerotome (H). (I, J) Detail of transverse view of a 10 μm slab through the 3D reconstruction of the fibronectin (I) and laminin (J) labeling (and nuclear staining) of somite X, centered at the sclerotome–endoderm–dorsal aorta interface. Note the laminin-positive matrix (J) delineating the peripheral nuclei of the sclerotome which are aligned compared to the other sclerotomal nuclei located towards the central sclerotome. The flat nuclei of the dorsal aorta (arrowheads in I) can be distinguished from the endodermal nuclei (arrows in I) and a fibronectin matrix is located between these two tissues and between the dorsal aorta and the sclerotome. Note the different laminin matrices (J); the continuous lining of the endoderm, the patchy coverage of the sclerotome and the faint laminin immunoreactivity lining the dorsal aorta dorsally (arrows in J). (K) Detailed dorsal view of the box in D, showing the laminin labeling within the sclerotome. Several patches and specks are dispersed within the sclerotome. (L) Quantification of the area covered by laminin on the dorsal versus ventral surface of the paraxial mesoderm throughout the caudal–rostral axis. Laminin coverage increases in a caudal to rostral fashion both dorsally and ventrally. However, at somite stages I and V, laminin coverage is greater ventrally than dorsally, but after sclerotome formation (somite X) the coverage again becomes equivalent dorsally and ventrally. FN: fibronectin; LN: laminin, DNA: To-Pro 3 staining; da: dorsal aorta; psm: presomitic mesoderm. Scale bars=20 μm (A, B, C, D, E, G, H, I, J) or 5 μm (B′, C′, E′, F, K).

Conclusions

We applied a 3D approach to studying ECM organization during paraxial mesoderm development and provided unprecedented resolution of the matrix and its relationship with cells during the various maturation steps of this tissue. We show that, immediately following gastrulation, globular fibronectin is assembled into a fibrillar matrix at the PSM surface and its complexity progressively increases as the PSM matures (Supplementary Table 1), culminating in a matrix which has been shown to support somite formation (Rifes et al., 2007). A fibronectin matrix may also be necessary to maintain the architecture of the segment after somites have formed, as has been shown for zebrafish (Snow et al., 2008). In fact, we found that both a fibronectin and a laminin matrix remain around the segment even after sclerotome dispersal. An interesting issue to address in the future is whether this containment represents a developmental step in sclerotome morphogenesis and/or whether it plays a role in the adequate spatial organization of other

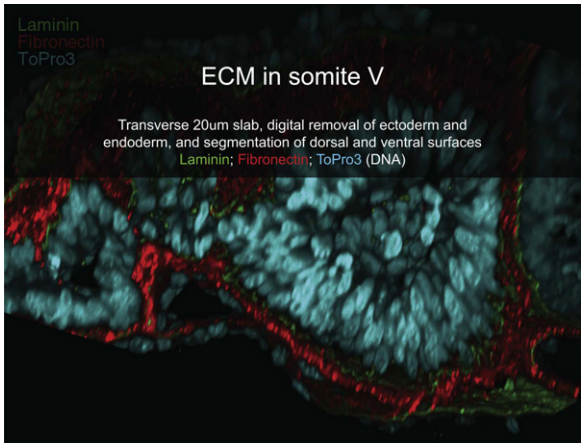

Movie 7. ECM in somite V: Selection of a 20 μm thick transverse slab of the 3D reconstruction of fibronectin, laminin, and To-Pro 3 (DNA) labeling in the middle of somite V. First: ectoderm and endoderm digitally removed. Second: digital selection of the dorsal and then ventral surface of the somite (plus adjacent intermediate mesoderm, dorsal aorta and neural tube). http://dx.doi.org/10.1016/j.ydbio.2012.06.003.

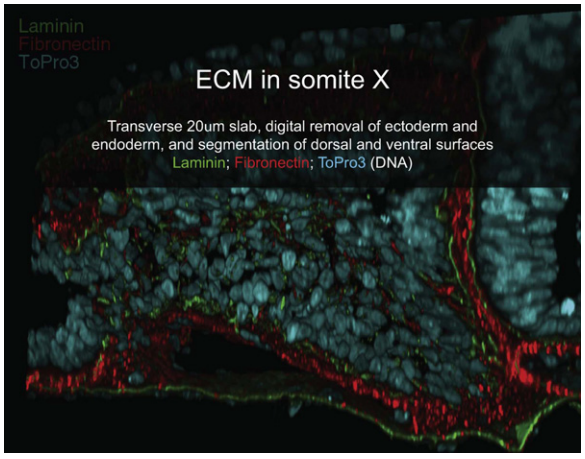

Movie 8. ECM in somite X: Selection of a 20 μm thick transverse slab of the 3D reconstruction of fibronectin, laminin, and To-Pro 3 (DNA) labeling in the middle of somite X. First: ectoderm and endoderm digitally removed. Second: digital selection of the dorsal and then ventral surface of the somite (plus adjacent intermediate mesoderm, dorsal aorta and neural tube). http://dx.doi.org/10.1016/j.ydbio.2012.06.003.

cell types, such as endothelial or neural crest cells, which use the somite segment as a guide for their migration (Jones and Li, 2007; Loring and Erickson, 1987; Tosney et al., 1994).

Our 3D approach also revealed that laminin is assembled into small and dispersed matrix patches on the PSM surface, which are not easily appreciated in sections. Most likely for that reason, previous studies using sectioned material reported an absence of laminin around the chick PSM (Duband et al., 1987; Krotoski et al., 1986). Our data further revealed that these laminin patches grow and coalesce in a progressive fashion as the paraxial mesoderm matures (Supplementary Table 1). However, a continuous basement membrane sheet does not form. Even in somite X the laminin labeling on the basal dermomyotome surface was fenestrated, suggesting that a continuous lining is not necessary for the normal development of this epithelium. In the mouse embryo, a study of the organization of the laminin matrix throughout all stages of dermomyotome development showed that it never becomes continuous (Deries et al., 2012). We thus propose that laminin matrices exist in two forms: a continuous form, resulting from coalesced patches, essential for the development and maintenance of certain tissues, such as permanent epithelia; and a fenestrated patchwork form, sufficient to guide the development of transient cell types, such as epithelial somites and dermomyotome, without ever fully isolating them from surrounding cells and their signals.

This study highlights the importance of visualizing the organizational status of ECMs, rather than just their presence/absence, during tissue morphogenesis. It further shows that the investment in high quality whole mount preparations for confocal imaging, and the processing of stacks of confocal images with one of the many available 3D rendering softwares, leads to a fuller, more accurate 3D understanding of ECM organization. We believe that this study illustrates the great advantage of a 3D perspective when observing and analyzing complex biological events.

Acknowledgments

We thank Gabriel G. Martins for his help with the 3D reconstruction software and initial analysis, Marianne Deries for her critical reading of the manuscript, and all members of our group for helpful discussions. The B3/D6 antibody was developed by D.M. Fambrough and was obtained from the Developmental Studies Hybridoma Bank, developed under the auspices of the NICHD and maintained by The University of Iowa, Department of Biology, Iowa City, IA52242, USA.

This work was financed by Fundação para a Ciência e a Tecnologia (Portugal) project PTDC/SAU-OBD/103771/2008 and PR was supported by Fundação para a Ciência e a Tecnologia, grant number SFRH/BD/37423/2007.

Appendix A. Supporting information

Supplementary data associated with this article can be found in the online version at http://dx.doi.org/10.1016/j.ydbio.2012.06.003.

References

Aulehla, A., Pourquié, O., 2010. Signaling gradients during paraxial mesoderm development. Cold Spring Harb. Perspect. Biol. 2, a000869.
Bajanca, F., Luz, M., Duxson, M.J., Thorsteinsdóttir, S., 2004. Integrins in the mouse myotome: developmental changes and differences between the epaxial and hypaxial lineage. Dev. Dyn. 231, 402–415.
Bénazéraf, B., Francois, P., Baker, R.E., Denans, N., Little, C.D., Pourquié, O., 2010. A random cell motility gradient downstream of FGF controls elongation of an amniote embryo. Nature 466, 248–252.
Bryant, D.M., Mostov, K.E., 2008. From cells to organs: building polarized tissue. Nat. Rev. Mol. Cell Biol. 9, 887–901.
Delfini, M.C., Dubrulle, J., Malapert, P., Chal, J., Pourquié, O., 2005. Control of the segmentation process by graded MAPK/ERK activation in the chick embryo. Proc. Natl. Acad. Sci., USA 102, 11343–11348.
Deries, M., Gonçalves, A.B., Vaz, R., Martins, G.G., Rodrigues, G., Thorsteinsdóttir, S., 2012. Extracellular matrix remodeling accompanies axial muscle development and morphogenesis in the mouse. Dev. Dyn. 241, 350–364.
Duband, J.L., Dufour, S., Hatta, K., Takeichi, M., Edelman, G.M., Thiery, J.P., 1987. Adhesion molecules during somitogenesis in the avian embryo. J. Cell Biol. 104, 1361–1374.
Dubrulle, J., Pourquié, O., 2004. Coupling segmentation to axis formation. Development 131, 5783–5793.
Durbeej, M., 2010. Laminins. Cell Tissue Res. 339, 259–268.
Frantz, C., Stewart, K.M., Weaver, V.M., 2010. The extracellular matrix at a glance. J. Cell Sci. 123, 4195–4200.
George, E.L., Georges-Labouesse, E.N., Patel-King, R.S., Rayburn, H., Hynes, R.O., 1993. Defects in mesoderm, neural tube and vascular development in mouse embryos lacking fibronectin. Development 119, 1079–1091.
Goody, M.F., Henry, C.A., 2010. Dynamic interactions between cells and their extracellular matrix mediate embryonic development. Mol. Reprod. Dev. 77, 475–488.
Gossler, A., Hrabě de Angelis, M., 1998. Somitogenesis. Curr. Top. Dev. Biol. 38, 225–287.

Hamburger, V., Hamilton, H.L., 1992. A series of normal stages in the development of the chick embryo. 1951. Dev. Dyn. 195, 231–272.
Ingber, D.E., 2006. Mechanical control of tissue morphogenesis during embryological development. Int. J. Dev. Biol. 50, 255–266.
Jones, C.A., Li, D.Y., 2007. Common cues regulate neural and vascular patterning. Curr. Opin. Genet. Dev. 17, 332–336.
Jülich, D., Geisler, R., The Tübingen 2000 Screen Consortium, Holley, S.A., 2005. Integrinα5 and delta/notch signaling have complementary spatiotemporal requirements during zebrafish somitogenesis. Dev. Cell 8, 575–586.
Kalcheim, C., Ben-Yair, R., 2005. Cell rearrangements during development of the somite and its derivatives. Curr. Opin. Genet. Dev. 15, 371–380.
Koshida, S., Kishimoto, Y., Ustumi, H., Shimizu, T., Furutani-Seiki, M., Kondoh, H., Takada, S., 2005. Integrinα5-dependent fibronectin accumulation for maintenance of somite boundaries in zebrafish embryos. Dev. Cell 8, 587–598.
Kragtorp, K.A., Miller, J.R., 2007. Integrin α5 is required for somite rotation and boundary formation in *Xenopus*. Dev. Dyn. 236, 2713–2720.
Krotoski, D.M., Domingo, C., Bronner-Fraser, M., 1986. Distribution of a putative cell surface receptor for fibronectin and laminin in the avian embryo. J. Cell Biol. 103, 1061–1071.
Larsen, M., Artym, V.V., Green, J.A., Yamada, K.M., 2006a. The matrix reorganized: extracellular matrix remodeling and integrin signaling. Curr. Opin. Cell Biol. 18, 463–471.
Larsen, M., Wei, C., Yamada, K.M., 2006b. Cell and fibronectin dynamics during branching morphogenesis. J. Cell Sci. 119, 3376–3384.
LeBleu, V.S., MacDonald, B., Kalluri, R., 2007. Structure and function of basement membranes. Exp. Biol. Med. 232, 1121–1129.
Loring, J.F., Erickson, C.A., 1987. Neural crest cell migratory pathways in the trunk of the chick embryo. Dev. Biol. 121, 220–236.
Mao, Y., Schwarzbauer, J.E., 2005. Fibronectin fibrillogenesis, a cell-mediated matrix assembly process. Matrix Biol. 24, 389–399.
Martins, G.G., Rifes, P., Amândio, R., Rodrigues, G., Palmeirim, I., Thorsteinsdóttir, S., 2009. Dynamic 3D cell rearrangements guided by a fibronectin matrix underlie somitogenesis. PLoS One 4, e7429.
McDonald, J.A., Quade, B.J., Broekelmann, T.J., LaChance, R., Forsman, K., Hasegawa, E., Akiyama, S., 1987. Fibronectin's cell-adhesive domain and an amino-terminal matrix assembly domain participate in its assembly into fibroblast pericellular matrix. J. Biol. Chem. 262, 2957–2967.
Miner, J.H., Yurchenco, P.D., 2004. Laminin functions in tissue morphogenesis. Annu. Rev. Cell. Dev. Biol. 20, 255–284.
Nakaya, Y., Sukowati, E.W., Wu, Y., Sheng, G., 2008. RhoA and microtubule dynamics control cell-basement membrane interaction in EMT during gastrulation. Nat. Cell Biol. 10, 765–775.
Nelson, C.M., Bissell, M.J., 2006. Of extracellular matrix, scaffolds, and signaling: tissue architecture regulates development, homeostasis, and cancer. Annu. Rev. Cell. Dev. Biol. 22, 287–309.
Nelson, W.J., 2009. Remodeling epithelial cell organization: transitions between front–rear and apical–basal polarity. Cold Spring Harb. Perspect. Biol 1, a000513.
Ohashi, T., Kiehart, D.P., Erickson, H.P., 1999. Dynamics and elasticity of the fibronectin matrix in living cell culture visualized by fibronectin-green fluorescent protein. Proc. Natl. Acad. Sci., USA 96, 2153–2158.
Onodera, T., Sakai, T., Hsu, J.C., Matsumoto, K., Chiorini, J.A., Yamada, K.M., 2010. Btbd7 regulates epithelial cell dynamics and branching morphogenesis. Science 329, 562–565.
Ostrovsky, D., Cheney, C.M., Seitz, A.W., Lash, J.W., 1983. Fibronectin distribution during somitogenesis in the chick embryo. Cell Differ 13, 217–223.
Pankov, R., Yamada, K.M., 2002. Fibronectin at a glance. J. Cell Sci. 115, 3861–3863.
Peters, D.M., Mosher, D.F., 1987. Localization of cell surface sites involved in fibronectin fibrillogenesis. J. Cell Biol. 104, 121–130.
Pourquié, O., 2001. Vertebrate somitogenesis. Annu. Rev. Cell. Dev. Biol. 17, 311–350.
Pourquié, O., Tam, P.P., 2001. A nomenclature for prospective somites and phases of cyclic gene expression in the presomitic mesoderm. Dev. Cell 1, 619–620.
Resende, T.P., Ferreira, M., Teillet, M.A., Tavares, A.T., Andrade, R.P., Palmeirim, I., 2010. Sonic hedgehog in temporal control of somite formation. Proc. Natl. Acad. Sci., USA 107, 12907–12912.
Rifes, P., Carvalho, L., Lopes, C., Andrade, R.P., Rodrigues, G., Palmeirim, I., Thorsteinsdóttir, S., 2007. Redefining the role of ectoderm in somitogenesis: a player in the formation of the fibronectin matrix of presomitic mesoderm. Development 134, 3155–3165.
Rozario, T., DeSimone, D.W., 2010. The extracellular matrix in development and morphogenesis: a dynamic view. Dev. Biol. 341, 126–140.
Sakai, T., Larsen, M., Yamada, K.M., 2003. Fibronectin requirement in branching morphogenesis. Nature 423, 876–881.
Sanders, E.J., Prasad, S., 1986. Epithelial and basement membrane responses to chick embryo primitive streak grafts. Cell Differ. 18, 233–242.
Sato, Y., Yasuda, K., Takahashi, Y., 2002. Morphological boundary forms by a novel inductive event mediated by Lunatic fringe and Notch during somitic segmentation. Development 129, 3633–3644.
Singh, P., Carraher, C., Schwarzbauer, J.E., 2010. Assembly of fibronectin extracellular matrix. Annu. Rev. Cell. Dev. Biol. 26, 397–419.
Smyth, N., Vatansever, H.S., Murray, P., Meyer, M., Frie, C., Paulsson, M., Edgar, D., 1999. Absence of basement membranes after targeting the *LAMC1* gene results in embryonic lethality due to failure of endoderm differentiation. J. Cell Biol. 144, 151–160.
Snow, C.J., Peterson, M.T., Khalil, A., Henry, C.A., 2008. Muscle development is disrupted in zebrafish embryos deficient for fibronectin. Dev. Dyn. 237, 2542–2553.
Solursh, M., Fisher, M., Meier, S., Singley, C.T., 1979. The role of extracellular matrix in the formation of the sclerotome. J. Embryol. Exp. Morphol. 54, 75–98.
Sottile, J., Hocking, D.C., 2002. Fibronectin polymerization regulates the composition and stability of extracellular matrix fibrils and cell–matrix adhesions. Mol. Biol. Cell 13, 3546–3559.
Thorsteinsdóttir, S., Deries, M., Cachaço, A.S., Bajanca, F., 2011. The extracellular matrix dimension of skeletal muscle development. Dev. Biol. 354, 191–207.
Tosney, K.W., Dehnbostel, D.B., Erickson, C.A., 1994. Neural crest cells prefer the myotome's basal lamina over the sclerotome as a substratum. Dev. Biol. 163, 389–406.
Watanabe, T., Sato, Y., Saito, D., Tadokoro, R., Takahashi, Y., 2009. EphrinB2 coordinates the formation of a morphological boundary and cell epithelialization during somite segmentation. Proc. Natl. Acad. Sci., USA 106, 7467–7472.
Wierzbicka-Patynowski, I., Schwarzbauer, J.E., 2003. The ins and outs of fibronectin matrix assembly. J. Cell Sci. 116, 3269–3276.
Yurchenco, P.D., Patton, B.L., 2009. Developmental and pathogenic mechanisms of basement membrane assembly. Curr. Pharm. Des. 15, 1277–1294.
Yurchenco, P.D., Wadsworth, W.G., 2004. Assembly and tissue functions of early embryonic laminins and netrins. Curr. Opin. Cell Biol. 16, 572–579.

Supplementary information for:

Rifes, P. and Thorsteinsdóttir, S. (2012). Extracellular matrix assembly and 3D organization during paraxial mesoderm development in the chick embryo. *Developmental Biology* **368**, 370-81.

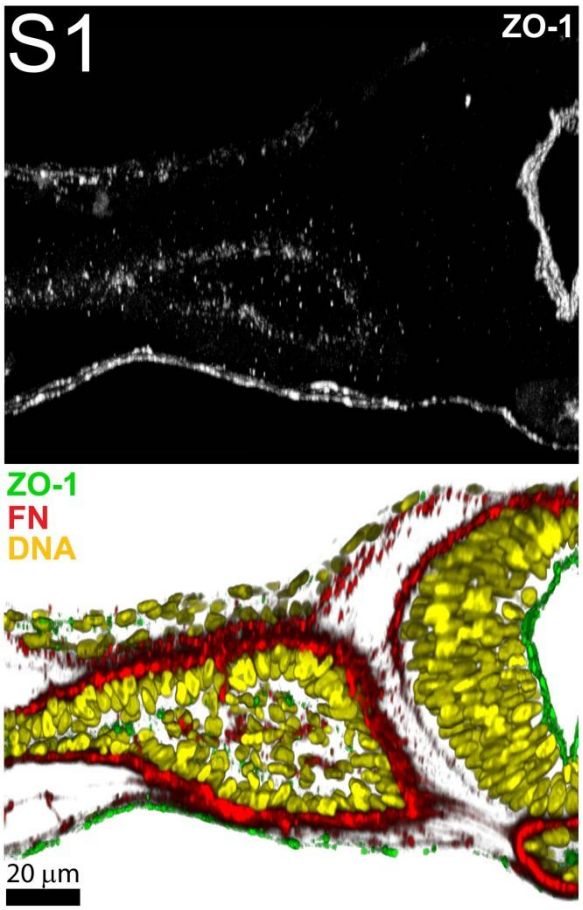

Supplementary Figure S1: Upper panel: Rostral view of a 20 µm thick transverse slab through the 3D reconstruction of epithelial apical marker ZO-1 labelling in the rostral PSM. Note the insipient ZO-1 labelling on the apical side of the epithelializing cells (aligned nuclei) in the periphery of the PSM. Compare with the strong ZO-1 labelling visible apically on neural tube cells (on the right). Lower panel: View of the ZO-1 immunostaining (green) combined with fibronectin (red) and nuclear (yellow) labelling (thickness of transverse slab was reduced to 10 µm to allow better visualization).

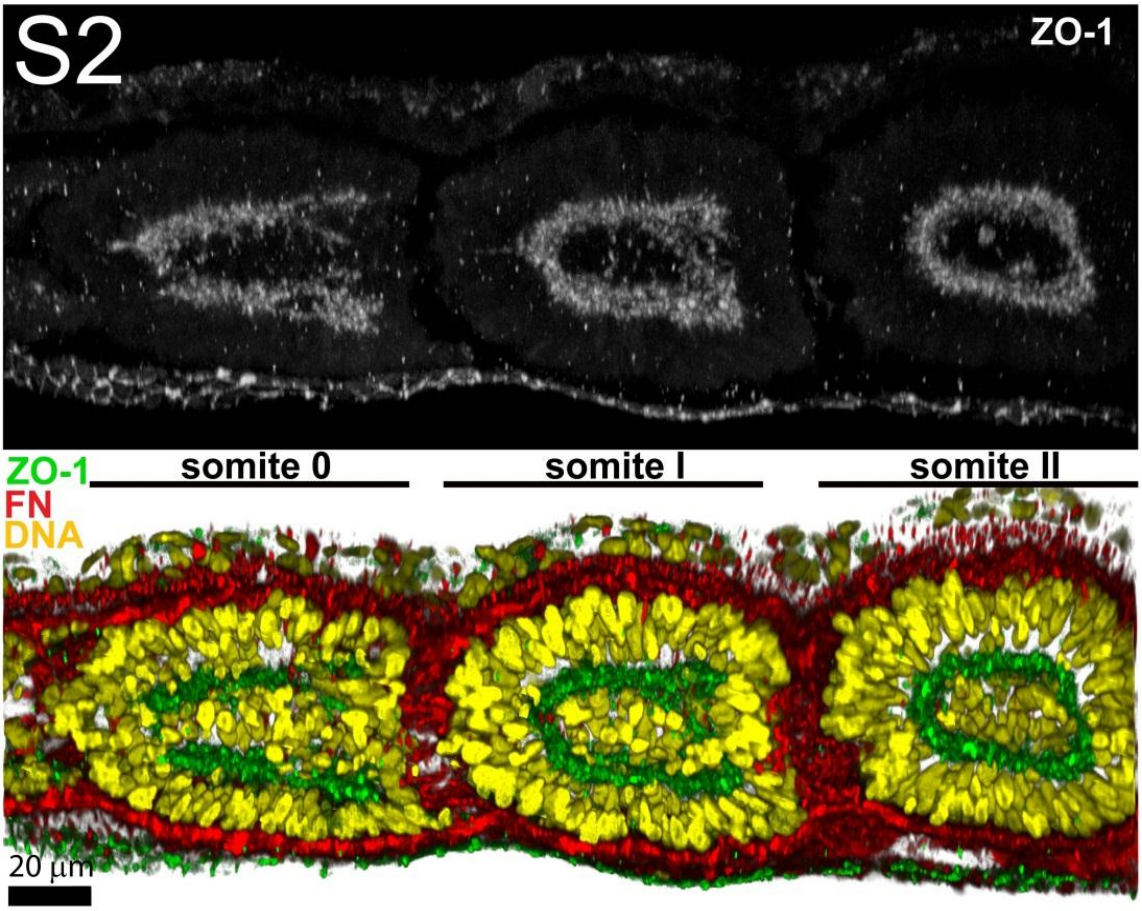

Supplementary Figure S2: Upper panel: Side view of a 20 µm thick sagittal slab through the 3D reconstruction of ZO-1 labelling comprising the rostral end of the PSM (s0) and the first somites (sI and sII). Note that somite 0 displays a “c”-shape labelling for ZO-1, a pattern which is also still visible in somite I of this embryo, demonstrating the later epithelialization of the rostral facet compared to the caudal one. Lower panel: View of the ZO-1 immunostaining (green) combined with fibronectin (red) and nuclear (yellow) labelling (thickness of transverse slab: 10 µm).

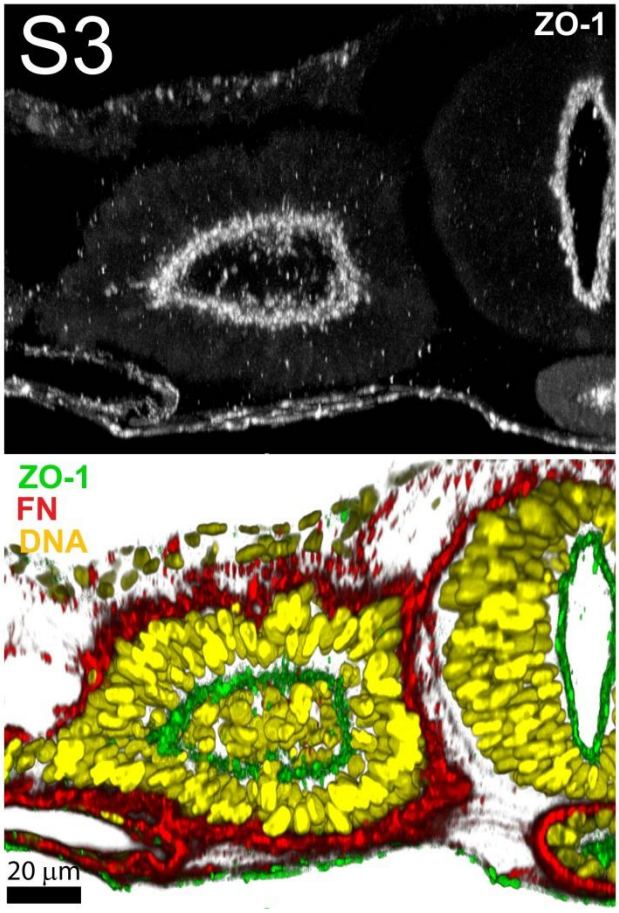

Supplementary Figure S3: Upper panel: Rostral view of a 20 µm thick transverse slab through the 3D reconstruction of ZO-1 labelling in the most recently formed somite (sI). Note the clear ring (a ball in 3D) of ZO-1, marking the apical side of the epithelioid outer portion of the somite. Lower panel: View of the ZO-1 immunostaining (green) combined with fibronectin (red) and nuclear (yellow) labelling (thickness of transverse slab: 10 µm).

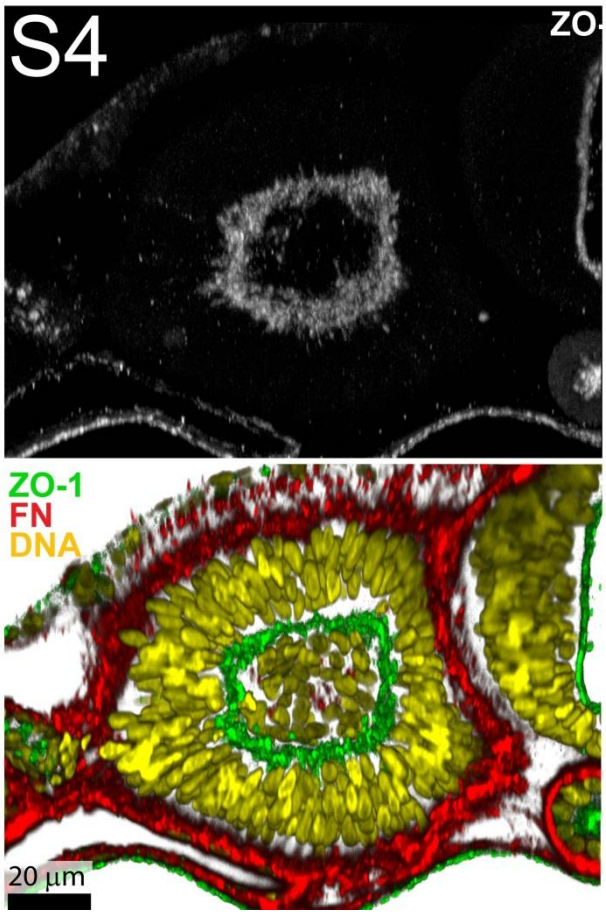

Supplementary Figure S4: Upper panel: Rostral view of a 20 µm thick transverse slab through the 3D reconstruction of ZO-1 labelling in mature epithelial somite (sV). Note the clear separation of the mesenchymal somitocoel from the remaining epithelial array of somitic cells strongly labelled with apical ZO-1. Lower panel: View of the ZO-1 immunostaining (green) with fibronectin (red) and nuclear (yellow) labelling (thickness of transverse slab: 10 µm).

Supplementary Figure S5: Rostral view of a transverse slab through the 3D reconstruction of the combined fibronectin (red), laminin (green), and nuclear (yellow) labeling in somite I (see Figures 4A and 4F), with a slab thickness of 10 µm to allow better tissue visualization. Arrowheads point to the laminin matrix of somite I, which is located closer to somitic cells than the fibronectin matrix.

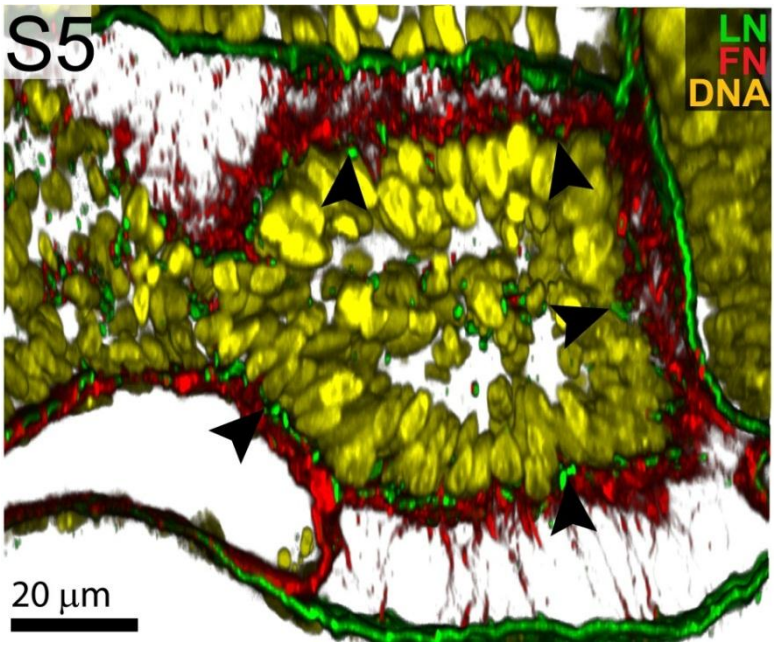

Supplementary Figure S6: Upper panel: Rostral view of a 20 µm thick transverse slab through the 3D reconstruction of ZO-1 labelling in the differentiating somite X. Note that the strong apical ZO-1 labelling is restricted to the dermomyotomal epithelia, and absent from the sclerotome, composed of dispersed cells with an outer layer of aligned cells. Lower panel: View of the ZO-1 immunostaining (green) combined with fibronectin (red) and nuclear (yellow) labelling (thickness of transverse slab: 10 µm).

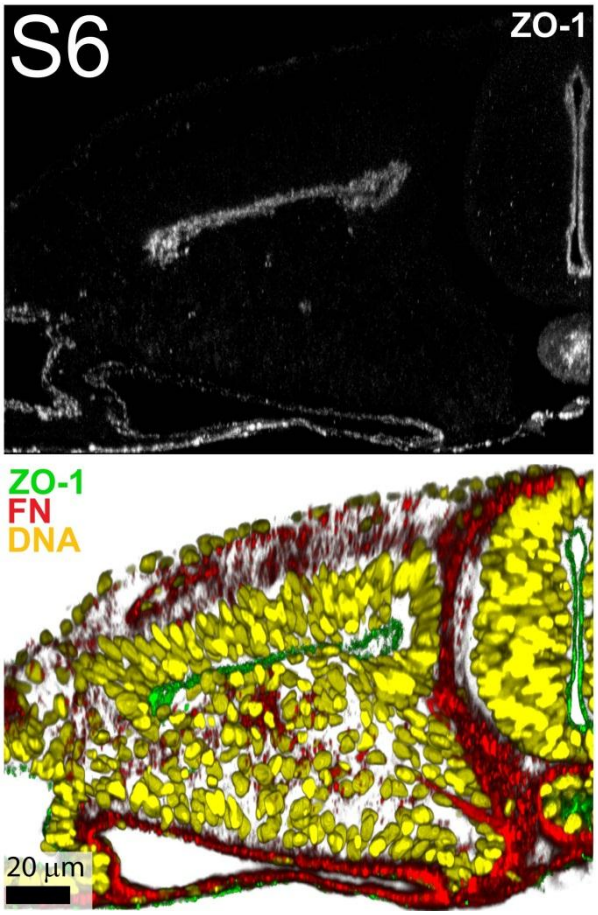

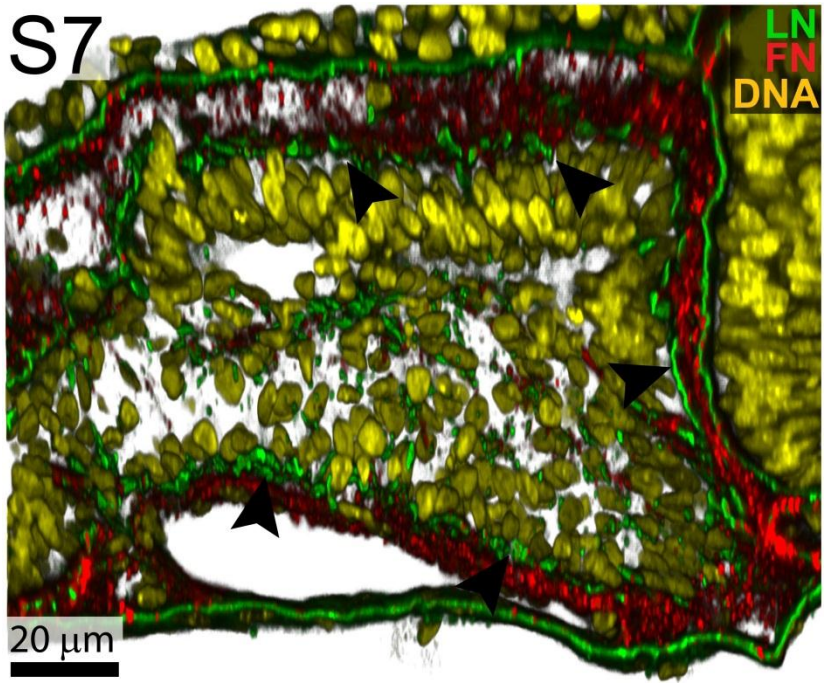

Supplementary Figure S7: Rostral view of a transverse slab through the 3D reconstruction of the combined fibronectin (red), laminin (green), and nuclear (yellow) labeling in somite X (see Figures 5A and 5D), with a slab thickness of 10 µm to allow better tissue visualization. Note that both the epithelial dermomyotome and the dispersed sclerotome are delimited by fibronectin and laminin matrices. Arrowheads point to the laminin matrix of somite X, which is located closer to somitic cells than the fibronectin matrix.

Supplementary Table 1: ECM organization at tissue surfaces

		Embryonic Epithelia		Paraxial Mesoderm				
				Caudal				**Rostral**
		Ectoderm	Endoderm	Caudal PSM	Rostral PSM	Somite I	Somite V	Somite X
Fibronectin	fibrils	-	- -/+ (caudal)	+ ; long, thin	++ ; long, thick	+++ ; long, thick	+++ ; short, thick	DM: ++ ; short, thick Sc: + ; short, thick
	globules	+++	- + (rostral)	++ (dorsal) + (ventral)	++ (dorsal) - (ventral)	++ (dorsal) -/+ (ventral)	++ (dorsal) + (ventral)	DM: ++ Sc: ++
Laminin	patches	-	-	-	-/+	+	++	++
	sheet	+++	+++ (except caudal holes)	-	-	-	-	-

Legend: - absent; -/+ few; + to +++, present with increasing abundance;
DM, Dermomyotome; Sc, Sclerotome

Chapter 5

Effect of cell tension inhibitors on somitogenesis in chicken (*Gallus gallus*) embryos

Effect of cell tension inhibitors on somitogenesis in chicken (*Gallus gallus*) embryos

Pedro Rifes [1,2] and Sólveig Thorsteinsdóttir [1,2]

Manuscript in preparation

[1] Departamento de Biologia Animal e Centro de Biologia Ambiental, Faculdade de Ciências, Universidade de Lisboa, 1749-016 Lisboa, Portugal.
[2] Instituto Gulbenkian de Ciência, 2781-901 Oeiras, Portugal.

Contribution to the publication:

	Experimental work depicted in:										manuscript writing
	Fig. 1	Fig. 2	Fig. 3	Fig. 4	Fig. 5	Fig. 6	Fig. 7	Fig. 8	Fig. 9	Supp. Fig. 1	
Design and concept	III	III	III	III	III	III	III	III	III	III	III
Execution	III	III	III	III	III	III	III	III	III	III	
Analysis and interpretation	III	III	III	III	III	III	III	III	III	III	

Legend:
n.a……. non applicable
O ……. no intervention
I……. minor contribution
II……. moderate contribution
III…….major contribution/full execution
Note: this contribution does not exclude other contributions, similar or not, from the remaining authors

Effect of cell tension inhibitors on somitogenesis in chicken (*Gallus gallus*) embryos

Pedro Rifes [1,2] and Sólveig Thorsteinsdóttir [1,2]

[1] Departamento de Biologia Animal e Centro de Biologia Ambiental, Faculdade de Ciências, Universidade de Lisboa, 1749-016 Lisboa, Portugal.

[2] Instituto Gulbenkian de Ciência, 2781-901 Oeiras, Portugal.

Abstract

Cells exert force on their surroundings and neighboring cells, allowing for cell displacements or shape changes, essential for sculpting tissues and creating new forms. Cells generate their internal tension using the actomyosin contractile system, in which the non-muscle myosin II (NMMII) is the main player. Recent years provided numerous examples of the involvement of cell tension in almost all aspects of cell behavior, although we still know very little regarding the role of cell tension in complex systems, such as embryo morphogenesis.

Here we investigate the role of cell-derived tension during a conspicuous, morphogenetic event, characteristic of vertebrate embryogenesis: somite formation. The presomitic mesoderm (PSM) is a continuous mesenchymal tissue which gives rise to separate blocks of cells, the somites. The PSM is sleeved with a rich extracellular matrix (ECM) and somite formation is dependent on the ECM component fibronectin, apparently used as an attachment site necessary for the coordinated rearrangement of the mesenchymal PSM into an epithelial somite.

In this report, we first analyzed the acquisition of epithelial traits that distinguish the formed epithelial somite sphere, from the non-segmented PSM. We then

investigated the effect of cell tension inhibitors on the formation of the epithelial somite. While the epithelialization of the PSM is abrogated in the presence of blebbistatin, an inhibitor of NMMII activity, the epithelium-specific characteristics of mature somites appear to partially hold the somitic segment.

Interestingly, we found that blebbistatin also interferes with the somitic rostro-caudal (RC) genetic program, which takes place concomitantly with somitogenesis. The blebbistatin treatment altered the expression of *Meso1*, the key initiator of the RC program and exerted its effect in the caudal, non-determined PSM, influencing the positioning *Meso1* striped expression. The effect on *Meso1* expression is reproduced, with increased penetrance, using an inhibitor against the NMMII activator Rock, which is known to act downstream of cell-ECM adhesions.

Our results show that the morphogenetic epithelialization process is a tension dependent process. Quite surprisingly, they also indicate that the positional regulation of the RC genetic program may be fine-tuned by a tension dependent mechanism.

Keywords: cell tension, non-muscle myosin II, blebbistatin, somite, somitogenesis, mesenchyme, epithelia, ZO-1, rostro-caudal polarity.

Abbreviations and acronyms: non-muscle myosin II, NMMII; extracellular matrix, ECM; rostro-caudal, RC; *zonula occludens* protein 1, ZO-1; atypical protein kinase C, aPKC.

Introduction

The importance of mechanical forces in the regulation of biological events was perceived over a century ago. However, only in the last few years, research in mechanobiology has benefitted from the advent of new tools that enable the measurement and manipulation of mechanical forces (see Eyckmans et al., 2011). Various types of externally applied forces, such as traction, physical strain or fluid flow, can influence cell behavior and fate in an outside-in fashion, but all cells, even non-muscle cells, can generate force (Eyckmans et al., 2011; Ingber, 2006; Schwartz and DeSimone, 2008). Cells exert force on the surrounding environment, on neighboring cells, and even generate and modulate their internal cell tension, essential for probing the mechanical properties of their milieu (Chen, 2008; Eyckmans et al., 2011; Geiger et al., 2009; Lopez et al., 2008; Parsons et al., 2010; Schwartz and DeSimone, 2008).

Cells generate force mainly through the actin-myosin contractile system, where myosins are the active sliding cross bridges between the actin filaments. Of the large myosin family, non-muscle myosin II (NMMII) is the ubiquitous force generator in non-contractile cells (Clark et al., 2007; Vicente-Manzanares et al., 2009). Several kinase pathways can induce the formation of the active, phosphorylated form of NMMII, therefore regulating the ATP-dependent activity of NMMII, and consequently, cell tension (Vicente-Manzanares et al., 2009). NMMII can be activated internally, but external cues such as an extracellular attachment point to exert force are major force regulators, allowing for the adequate cellular response, such as cell adhesion or migration (Vicente-Manzanares et al., 2009). For example, cells in suspension decrease their internal tension upon the initial attachment to an extracellular matrix (ECM)-coated substrate, allowing for cell spreading, but rapidly increase it, resulting in the formation of firm cell-ECM adhesion structures (Danen et al., 2002, see Huveneers and Danen, 2009). These cell-ECM contacts, mediated by integrin receptors (Barczyk et al., 2010), serve not only as mechanotransduction centers for cells to perceive their environment but also elicit the cells' response, by tethering it to its milieu (Geiger et al., 2009; Parsons et al., 2010; Schwartz and DeSimone, 2008).

In *in vitro* culture conditions, the regulation of cell tension is also essential to expand the initial cell-cell contacts resulting from exploratory actin-based membrane extensions (Cavey and Lecuit, 2009). Moreover, maturation of intercellular adhesions between epithelial cells provides strong cohesiveness to epithelial tissues, which act as fundamental shaping entities during embryonic morphogenesis (Quintin et al., 2008). Embryonic morphogenetic events are excellent examples where the coordination of forces within cells, between cells and with their surroundings is essential to generate a supracellular architecture (Lecuit and Lenne, 2007; Quintin et al., 2008). Although research on invertebrate embryos (mainly *D. melanogaster* and *C. elegans*) has provided some important insight into this field, there is little light on the mechanical biology of vertebrate embryogenesis (Eyckmans et al., 2011).

Somitogenesis is a fundamental morphogenic event in vertebrate embryogenesis, involving the periodic detachment of individual epithelial blocks of cells from an original continuum of mesenchymal cells. These blocks, or spheres of cells, called somites, are originated from the mesenchymal presomitic mesoderm (PSM), and together they compose the paraxial mesoderm, which flanks both sides of the axially located neural tube (Gossler and Hrabě de Angelis, 1998). Somites are transient structures that give rise to the metamerized axial skeleton and to the skeletal musculature in the body. Somitogenesis takes place at the rostral end of the PSM in a reiterated fashion with a species-specific periodicity, while at the same time the embryo elongates caudally and generates new PSM (Gossler and Hrabě de Angelis, 1998; Maroto et al., 2005; Pourquié, 2011).

In the chick embryo, massive cell rearrangements occur during somite formation, choreographing paraxial mesoderm cells into an epithelial sphere, containing a mesenchymal core, the somitocoel (Kulesa and Fraser, 2002; Martins et al., 2009). Little is known about how paraxial cells perform such a morphogenic event, although the ECM component fibronectin surrounding the chicken PSM (Duband et al., 1987; Ostrovsky et al., 1983; Rifes et al., 2007; Rifes and Thorsteinsdóttir, 2012) has been shown to be essential for somite formation (Rifes et al., 2007). Furthermore, fibronectin and its specific cell receptors appear to be a common requirement for somite formation in all vertebrate embryogenesis models studied (George et al., 1993; Georges-Labouesse et al.,

1996; Goh et al., 1997; Jülich et al., 2005; Koshida et al., 2005; Kragtorp and Miller, 2007; Yang et al., 1993).

As somites form, they already portray a rostro-caudal (RC) polarity which is fundamental to impose the subsequent metameric organization onto neural tube and neural crest derivatives (Gossler and Hrabě de Angelis, 1998; Keynes and Stern, 1988). Although somites are formed as a single unit, differential gene expression patterns clearly depict the two distinct, rostral and caudal moieties (Dequeant and Pourquié, 2008; Kuan et al., 2004; Saga and Takeda, 2001). The foundations for this RC polarity are established before there is any sign of overt segmentation in the rostral PSM, and are visible through the striped expression of the *Meso1* gene (Buchberger et al., 1998). Localized upregulation of *Mesp2* (mouse homolog of *Meso1*) in the rostral PSM (Saga et al., 1996; Saga et al., 1997) results from a still unclear mechanism, but which involves the Tbx6 transcription factor and the active Notch intra-cellular domain (NICD; (Yasuhiko et al., 2006). *Mesp2/Meso1* expression eventually becomes restricted to the rostral moiety of the prospective somite, leading to a local downregulation Notch signaling (Sasaki et al., 2011), discriminating it from the remaining Notch-active, *Dll1*-expressing caudal portion (reviewed in (Saga, 2007; Saga, 2012).

In this study we investigate the behavior of the actin cytoskeleton, cell junction and polarity markers in the acquisition of the epithelial phenotype during somite formation and then specifically address the involvement of cell tension in this process. We observe the rapid formation of polarized and mature cell-cell adhesions concomitantly with somite detachment, which last throughout somite development. The presence of cell-tension inhibitory drugs strongly impairs the formation of new somites, and affects, although much less strongly, the morphology of already formed epithelial spheres. Moreover, our results also show that NMMII inhibition perturbs the initiation of the RC specification program of the PSM. Thus the tension-generating pathway downstream of integrin-ECM interactions may be a major pathway regulating the upregulation of the RC program. Our study provides the first evidence implicating intra- and intercellular forces in the PSM differentiation program as well as in somite epithelialization.

Materials and Methods

Eggs and embryos

Fertile eggs were obtained from commercial sources (Sociedade Agrícola Quinta da Freiria, Portugal) and incubated for 48 hours at 38ºC, until the desired stage (11-13, (Hamburger and Hamilton, 1992). Somite staging was according to (Pourquié and Tam, 2001), were the forming somite (rostral end of the PSM) is termed somite 0, or S0, for short. Roman numerals (negative for PSM) are used to refer the position of paraxial tissue relative to somite 0; e.g. SI, SII, SIII etc, for formed somites and S-I ("S minus 1"), S-II, S-III, etc, for progressively more caudal somite-length portions of the PSM (Pourquié and Tam, 2001).

Antibodies, inhibitory drugs and other reagents

For primary immunodetection we used the following antibodies: ZO-1 (Zymed ref. 40-2200, 1:100); N-cadherin (BD Biosciences ref. C-70320, 1:100); aPKC (Santa Cruz Biotechnology ref. sc-216, 1:100). For counterstaining we used Alexa 488-conjugated phalloidin (Invitrogen, ref. A12379, 1:40), ToPro3 (Invitrogen, ref. T3605, 1:500), the latter in conjunction with ribonuclease A (Sigma, 10 µg/ml) to improve nuclear signal. For detection of the primary antibodies we used the adequate secondary goat anti-mouse and anti-rabbit Alexa 488, Alexa 568 or Alexa 546-conjugated F'ab fragments from Invitrogen. All antibody dillutions were made in phosphate buffered saline (PBS) with 1% bovine serum albumin.

Blebbistatin in DMSO solution from Calbiochem (ref. 203389) was used at a 20 µM or 50 µM in culture medium (see below), both concentrations yielding the same results. RockOut from Calbiochem (ref. 555553) was used at 50 µM. Equal volumes of DMSO (Sigma-Aldrich) were used as controls for both drugs. The RGD and RGE peptides were synthetized at the Netherlands Cancer Institute (Huveneers 2008). A cell adhesion assay to fibronectin confirmed the inhibitory effect of the RGD peptide (data not shown), in agreement with the extensive literature on this effect (Danen et al., 2002; Pierschbacher and Ruoslahti, 1984; Takahashi et al., 2007, see Ruoslahti, 1996; Singh et al., 2010).

Embryo explants and culture

Embryos were collected and cultured as explants as previously described (Palmeirim et al., 1997; Rifes et al., 2007). In short, pinned down embryos were bisected along the midline, cut transversally rostral to the fourth somite and excluding the Hensen's node, thus producing an explant consisting of all the PSM and the first four somites, with all neighboring tissues intact. Explants were placed on top of a polycarbonate filter floating on M199 culture medium with 5% fetal bovine serum and 10% chick serum (Palmeirim et al., 1997), and also containing the indicated drug or the adequate volume of the control vehicle. Isolated PSMs were prepared as previously reported (Rifes et al., 2007); after the collection of the intact control side, the contralateral side was treated with pure dispase (2,4 U/ml, Roche), locally pipetted (less than 100µl) onto the pinned down, PBS immersed embryo, to release the PSM, and both sides were incubated in parallel for 6 hours.

Immunofluorescence and *in situ* hybridization

Cryosectioning was performed on whole embryos fixed with 4% paraformaldehyde in 0.12 M phosphate buffer containing 4% sucrose, subsequently embedded in 7.5% gelatin in 0.12 M phosphate buffer containing 15% sucrose and frozen as described previously (Bajanca et al., 2004). Cryostat sections (20-30 µm thick) were processed for immunofluorescence as previously described (Rifes et al., 2007), or if embryos had already been subjected to *in situ* hybridization, sections (10-15 µm thick) were counterstained with 5 µg/ml 4',6-diamidine-2-phenylidole-dihydrochloride (DAPI) in 0.1% Triton X-100 in PBS.

Explants were fixed with 4% paraformaldehyde and processed for whole-mount immunodetection as previously described (Martins et al., 2009; Rifes and Thorsteinsdóttir, 2012). *In situ* hybridization using DIG-labeled RNA probes was performed as described previously (Henrique et al., 1995) with minor alterations (Rifes et al., 2007). RNA probes were synthetized from linearized plasmids, which have been previously described: Dll1 (Henrique et al., 1995; Palmeirim et al., 1997), Meso1 (Buchberger et al., 1998), Tbx18 (Tanaka and Tickle, 2004), using standard techniques.

Sample preparation and imaging

Whole mount explants were gradually dehydrated and embedded in methylsalicylate (Sigma-Aldrich) as described previously (Martins et al., 2009; Rifes and Thorsteinsdóttir, 2012), except for phalloidin-labelled embryos and explants, were a shorter series of ethanol dehydration was used. Both ethanol and methanol rapidly disrupt the quality of the phalloidin staining, but the faster ethanol dehydration followed by immediate image acquisition reduces the effect to a negligible measure (data not shown). Cryostat sections were mounted in Vectashield (Vector Laboratories).

Immunofluorescence images of whole mounts and cryostat sections were taken on a confocal Leica SPE microscope with an APO 40x 1.15 N.A. oil immersion lens, following imaging acquisition steps described previously (Rifes and Thorsteinsdóttir, 2012). Imaging of explants processed for *in situ* hybridization was performed using a Zeiss LUMAR Stereoscope with oblique illumination, coupled to an Axiocam-cooled charge-coupled device. Cryosections of embryos processed for *in situ* hybridization were imaged with an Olympus DP50 digital camera mounted on an Olympus BX60 microscope equipped with epifluorescence and Nomarski optics.

Image analysis was performed using ImageJ (http://rsb.info.nih.gov/ij/) and when a fuller 3D view of stacks of confocal images was necessary we resorted to the Amira V.5.3.3 (Visage Imaging Inc.) software. Image histogram corrections were performed on ImageJ and exported as TIFF files. For the analysis of *in situ* hybridization patterns along the PSM we used the ImageJ plugin “Straighten” (Kocsis et al., 1991). Alignment of straightened paraxial mesoderm images, the remaining image editing and composition of plates was performed using Adobe Illustrator CS4 and Adobe Photoshop CS4.

Results and Discussion

Formation of the somitic sphere involves a rapid upregulation and apical localization of the tight junction protein ZO-1

N-cadherin is the main cell-cell adhesion molecule present in the PSM of chicken embryos (Duband et al., 1987; Hatta et al., 1987). It is responsible for the integrity of the PSM mesenchyme and is also involved in the formation of the epithelial somite (Duband et al., 1987; Linask et al., 1998). Although not essential for the formation of somites (Linask et al., 1998; Radice et al., 1997), this *adherens* junction protein is present on the surface of all PSM cells and its apical enrichment accompanies the epithelialization process (Duband et al., 1987; Martins et al., 2009; Rifes et al., 2007) and data not shown). Therefore, in order to discriminate the establishment of the somitic epithelium, we attempted to identify a component of matured cell-cell adhesions characterizing epithelial somites, but not present in the mesenchymal PSM.

To this end we analyzed the immunoreactivity for the *zonula occludens* protein 1 (ZO-1), a pivotal cytoplasmic protein constituent of the tight junction-associated protein complex, characteristic of epithelia (Hartsock and Nelson, 2008). The analysis using sagittal sections allowed the simultaneous comparison of the ZO-1 labeling in the paraxial mesoderm with that of neighboring epithelial tissues, such as the over- and underlying ectoderm and endoderm, respectively. As previously described for epithelia, ectoderm and endoderm cells show strong, dot-like ZO-1 labeling on their apical side (arrowheads in Fig. 1B,F,J), which represents the visible confocal sagittal depiction of the apical adhesion belt, characteristic of epithelial cells (see Eckert and Fleming, 2008). In contrast, we could not observe any ZO-1 labeling on cells throughout the PSM, neither in the caudal mesenchymal PSM (data not shown), nor in the rostral PSM (Fig. 1A-H), where an epithelioid arrangement in the peripheral cell layer has been reported (Duband et al., 1987; Dubrulle and Pourquié, 2004; Martins et al., 2009; Rifes and Thorsteinsdóttir, 2012). Despite the cell alignment, evidenced by aligned nuclei (Fig. 1C and G), visible in the rostral PSM (including somite 0) and the elongated format of the cytoskeleton of the peripheral cells (Fig. 1A and E), no mature, ZO-1-rich cell-cell adhesions were visible (Fig. 1B and F). However, the first formed somite, somite I, which

has recently detached from the rostral PSM , depicted a clear ZO-1 labeling, encompassing the apical extremity of the peripheral epitheloid cells (Fig. 1J).Thus, together with the strong apical F-actin enrichment (Fig. 1I), this ZO-1 rich apical adhesion ring (in fact, a ball in the spherical 3D somite), clearly sets the separation between the mesenchymal somitocoel and the epithelial cell periphery (Fig. 1K, L).The strong apical F-actin enrichment and ZO-1 localization was retained in the more rostral mature epithelial somites (Fig, 2A-D). In accordance to our previous observations (Rifes and Thorsteinsdóttir, 2012), but contrary to others, (Duband et al., 1987, see Christ et al., 2007), at the somite VII level, the apical adhesion "ring" was still visible, complete both dorsally and ventrally, with no obvious signs of de-epithelialization (Fig. 2E-H). By somite X, a ventral downregulation of ZO-1 is visible (Fig. 2J) demarcating the sclerotomal compartment, clearly distinguishable from the epithelial, dorsally located dermomyotome (Fig. 2I-L). Our results thus show that in HH 11-12 embryos, sclerotome formation starts after the SVII stage is reached and is clearly ongoing in SX. This is considerably later than described by other authors, which report sclerotome dispersal occurring in SIV-SV (see Christ et al., 2007; Christ et al., 2000; Monsoro-Burq, 2005). We believe that the somite level at which sclerotomal de-epithelialization is visible varies between embryos of different stages. This hypothesis could explain, at least partially, the difference between our results obtained with stage HH 11-12 embryos (two days of incubation) and these previous reports on sclerotomal formation (see Christ et al., 2004; Christ et al., 2007; Monsoro-Burq, 2005),which focus on later stages, i.e. three days of incubation.

We also analyzed the location of the atypical protein kinase C (aPKC), an ubiquitous protein involved in cell polarization processes, whose apical location is essential for the establishment of apico-basal polarity in epithelial cells (Bryant and Mostov, 2008; Martin-Belmonte and Perez-Moreno, 2012). Preliminary results indicate that the pattern of aPKC localization accompanies that of ZO-1, since both are absent throughout the PSM and present in an apical pattern in somites and the surrounding epithelia (data not shown). These observations are in accordance with previous results

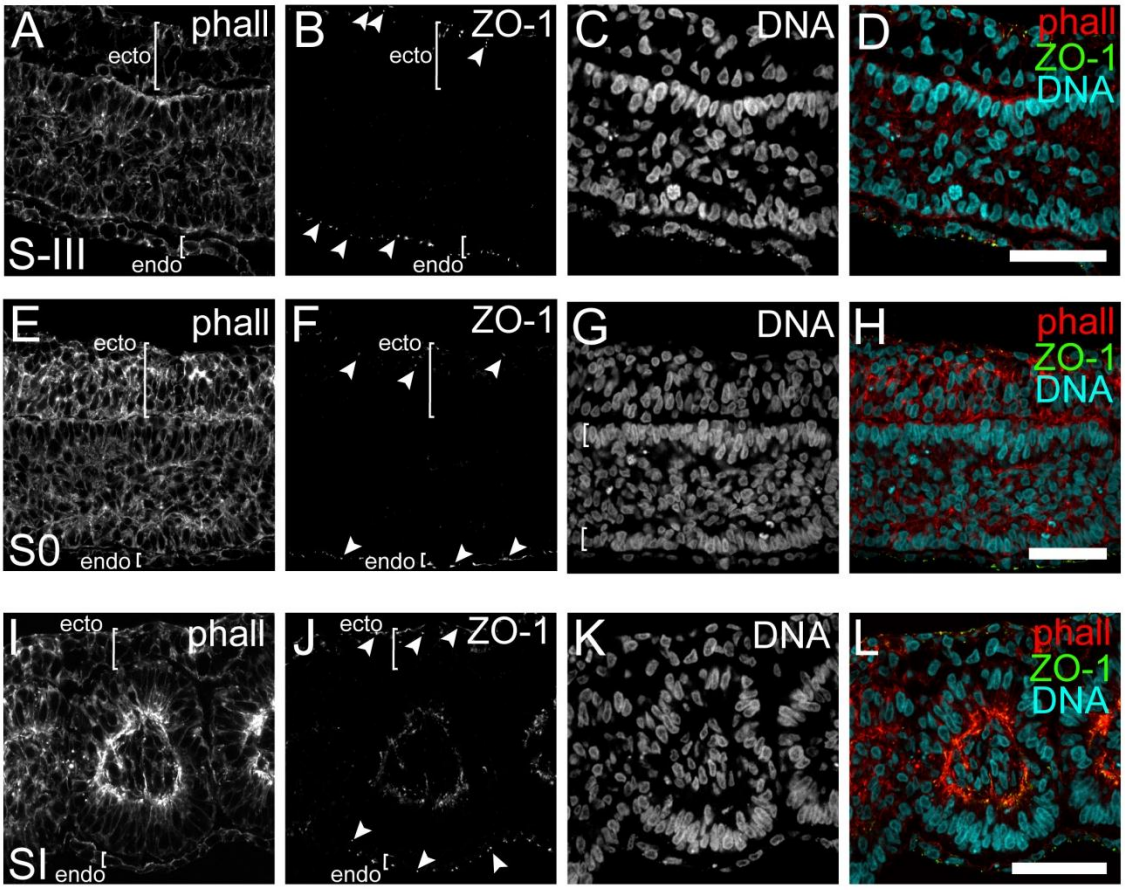

Figure 1. Sagittal views of f-actin and ZO-1 localization during PSM epithelialization and somite formation. Peripheral cells in the rostral PSM (A-D) show signs of an epithelioid organization, with elongated actin cytoskeleton (A) and aligned nuclei (C). However apically localized ZO-1 staining is not present in the PSM (B), contrasting with the clearly visible ZO-1 staining in the apposed endoderm and ectoderm (brackets in A and B), in the form of strong apical dots (arrowheads in B). Despite the eminence of somite detachment, sagittal views of S0 (E-H) showed no signs of ZO-1 apical localization (F), though nuclei (G) and f-actin (E) staining shows an aligned, epithelioid organization of the peripheral PSM, clearly distinguishable from the mesenchymal PSM core (H). The most recently formed somite, SI (I-L), reveals a clear ZO-1 labeling, restricted to the apical end of the peripheral epithelial layer (J). Concordantly, f-actin staining (I) is also strongly enriched apically, and the peripheral nuclei are aligned and distinct from the ones in the somitocoel (K, L). Dorsal is on top and rostral to the right. Phall: phalloidin f-actin staining; DNA: ToPro-3 nuclear staining; endo: endoderm; ecto: ectoderm. Scale bars represent 50 µm.

on the activity of Cdc42 during somitogenesis (Nakaya et al., 2004), a crucial cytoplasmic protein involved in the establishment of the apical identity during baso-apical polarization of epithelial cells (Bryant and Mostov, 2008; Iden and Collard, 2008).

Furthermore, we conclude that the rapid appearance of apical ZO-1 characterizes the transformation of the rostral PSM (S0) into somite I. Thus, our results show that although a pre-epithelialization process occurs in the PSM, the formation of the epithelial somite involves the rapid acquisition of particular epithelial characteristics. Our observations indicate that on top of the cadherin-mediated cell-cell adhesion present in the PSM, somite formation involves the activation of the apical polarity machinery and consequent formation of tight junctions.

NMMII activity is essential for PSM cell alignment and rearrangement into a somite

In order to investigate the role of cell tension in somitogenesis, we cultured chick embryo-half explants in the presence of the non-muscle myosin II (NMMII) inhibitor blebbistatin (Straight et al., 2003), while the contra-lateral embryo half-explants were cultured in the presence of DMSO for the same amount of time. Blebbistatin does not interfere with the actin binding properties of NMMII, but rather blocks it in an actin-detached state (Kovacs et al., 2004). Given the sequential feature of somitogenesis, within a single explant, containing the whole PSM and the first four somites, we can observe the effect of the inhibitory drug on several paraxial mesoderm events: (1) the maturation of the rostral PSM, (2) the pinching off of the somitic segment and (3) maturation of the epithelial somite. Macroscopic observation of explants cultured in the presence of blebbistatin *versus* vehicle revealed severe inhibition of somite formation in the blebbistatin-exposed sides with these explants forming on average 2.1 fewer somites than the control side (n=24), which is consistent with previous studies (Chuai et al., 2006; Wei et al., 2001). To gain clues about how this inhibition in somite formation occurs at the cellular level, we performed a detailed analysis of the PSM morphology of these two types of explants using confocal microscopy imaging.

The control DMSO-treated embryo-half explants underwent somite formation normally, showing both the peripheral cell alignment in the rostral PSM and the rapid apical enrichment of F-actin as somite I forms (Fig. 3A-C). In the presence of 50 µM of blebbistatin, the contralateral PSMs showed no signs of peripheral cell alignment. Rather, F-actin labeling appeared dispersed, with no signs of any particular cell-cell interactions (Fig. 3D), similar to the caudal, mesenchymal PSM (data not shown, (Rifes et

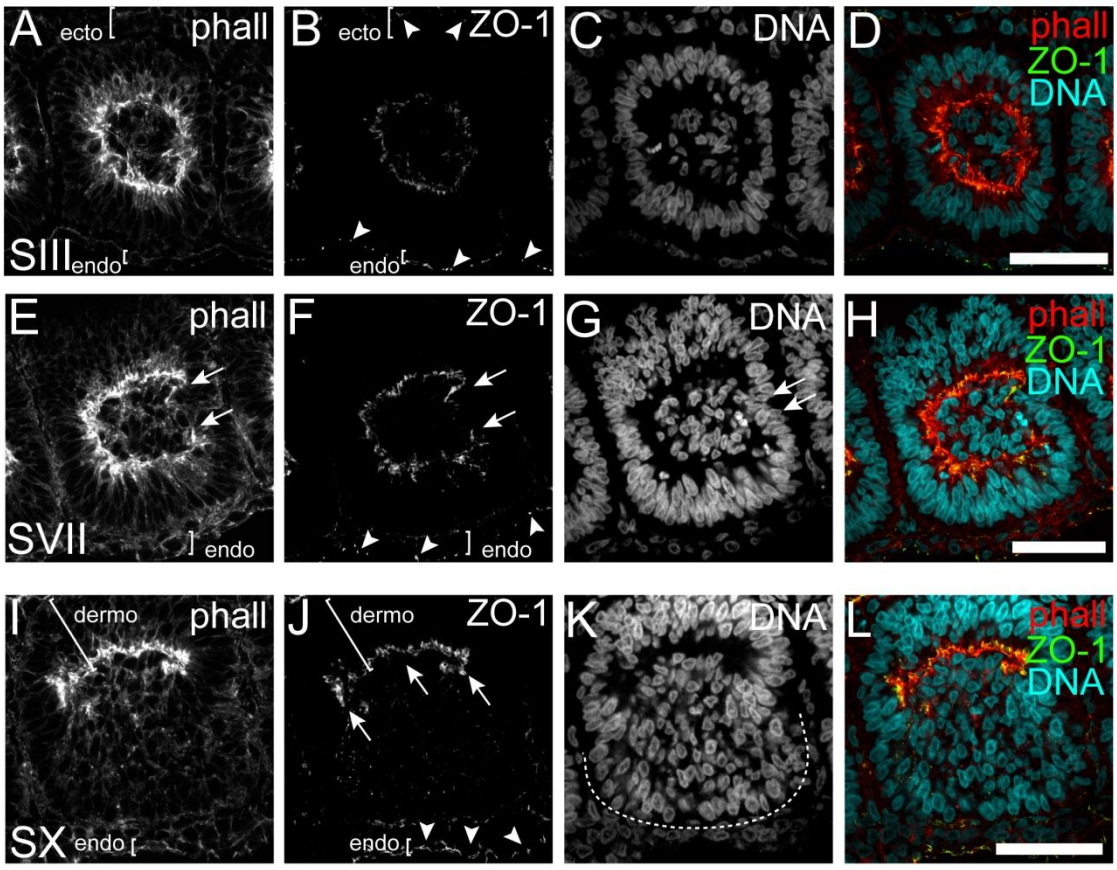

Figure 2. Sagittal views of f-actin and ZO-1 localization during somite maturation and initial compartmentalization. In the mature epithelial somite, SIII (A-D), the outer epithelial layer remains evident, with f-actin localization enriched at the apical end of cells (A) and peripheral nuclei are clearly aligned (C). ZO-1 labeling remains clearly visible apically (B), and the intensity of the labeling remains similar compared to SI (see Fig. 1J) and to the labeling in the ectoderm and endoderm (arrowheads). By SVII (E-H), the epithelialization of the outer cell layer is visible around the whole somitic segment, when taking into account the three criteria used: the apically enriched f-actin (E), aligned nuclei (G) and ZO-1 labeling (F). No obvious signs of de-epithelialization are visible in the ventral portion of the somite, though a kink in the aligned nuclei and interruption in the apical labeling is visible in the rostral region (between arrows in E, F and G). In somite X (I-L), the formation of the first somitic compartments is evident: the dorsally located dermomyotome (brackets in I, J) retains the apically enriched actin cytoskeleton (I), ZO-1 staining (J, arrows) and aligned nuclei (K, L). In contrast, in the ventral side, the de-epithelialized sclerotome shows no signs of an epitheliod organization, though the outer cells remain aligned and restricted to the somitic segment (dotted line in K, Rifes et al., 2012). Dorsal is on top and rostral to the right. Phall: phalloidin f-actin staining; DNA: ToPro-3 nuclei staining; endo: endoderm; Dermo: dermomyotome. Scale bars represent 50 µm.

al., 2007). In the area where SI should have formed, no sign of somitic boundaries was detectable, neither by cellular alignment, nor through apical enrichment of F-actin (Fig. 3D-F).

In a more rostral area of the explants, where somites would normally be present (compare Fig. 3G-I with J-L), the peripheral cells in the rostral PSM before culture were unable, in the presence of blebbistatin, to rearrange their aligned cytoskeleton and nuclei into the apically enriched somitic "ring" (compare Fig. 3G-I with J-L). Rather, the NMMII-inhibited explants showed numerous F-actin-enriched foci dispersed throughout the paraxial tissue (Fig. 3J), and the somitic segment was only depicted by an incipient nuclear alignment (arrowheads in Fig. 3K). The presence of these numerous foci indicates that the actin-polymerizing machinery associated with cell-cell adhesion (Harris and Tepass, 2010) is active in individual cells but does not get organized into an apical actin ring that links several cells into a continuum, as occurs in control explants.

Interestingly, somites which had formed before culture (stages SI and SII) showed more resilience to the effect of the inhibitor (compare Fig. 3M-O and P-R). Somites were clearly individualized, and the distinction between the peripheral layer and the somitocoel was still visible (Fig. 3R), although the mesenchymal portion appeared greatly expanded compared to the control side (compare Fig. 3Q and N). The apical enrichment of F-actin in the peripheral layer of the somites remains evident, but cell elongation within this layer was severely impaired (compare Fig. 3P and M).

NMMII activity is required for the establishment of mature cell-cell adhesions during somite formation

In order to further comprehend the role of NMMII-derived cell tension in somitogenesis, we analyzed the effect of blebbistatin on N-cadherin and ZO-1 localization in the paraxial tissue. We first investigated if blebbistatin treatment disrupted the epithelial characteristics of embryonic epithelia in general. Epithelial tissues other than somites (e.g. ectoderm and neural tube) did not show obvious signs of altered morphology after treatment of explants with blebbistatin (data not shown) and these epithelial cells displayed ZO-1 labeling in the form of apical adhesion belts, in a similar pattern as observed in control explants (Supplementary Fig. 1). In fact, it has

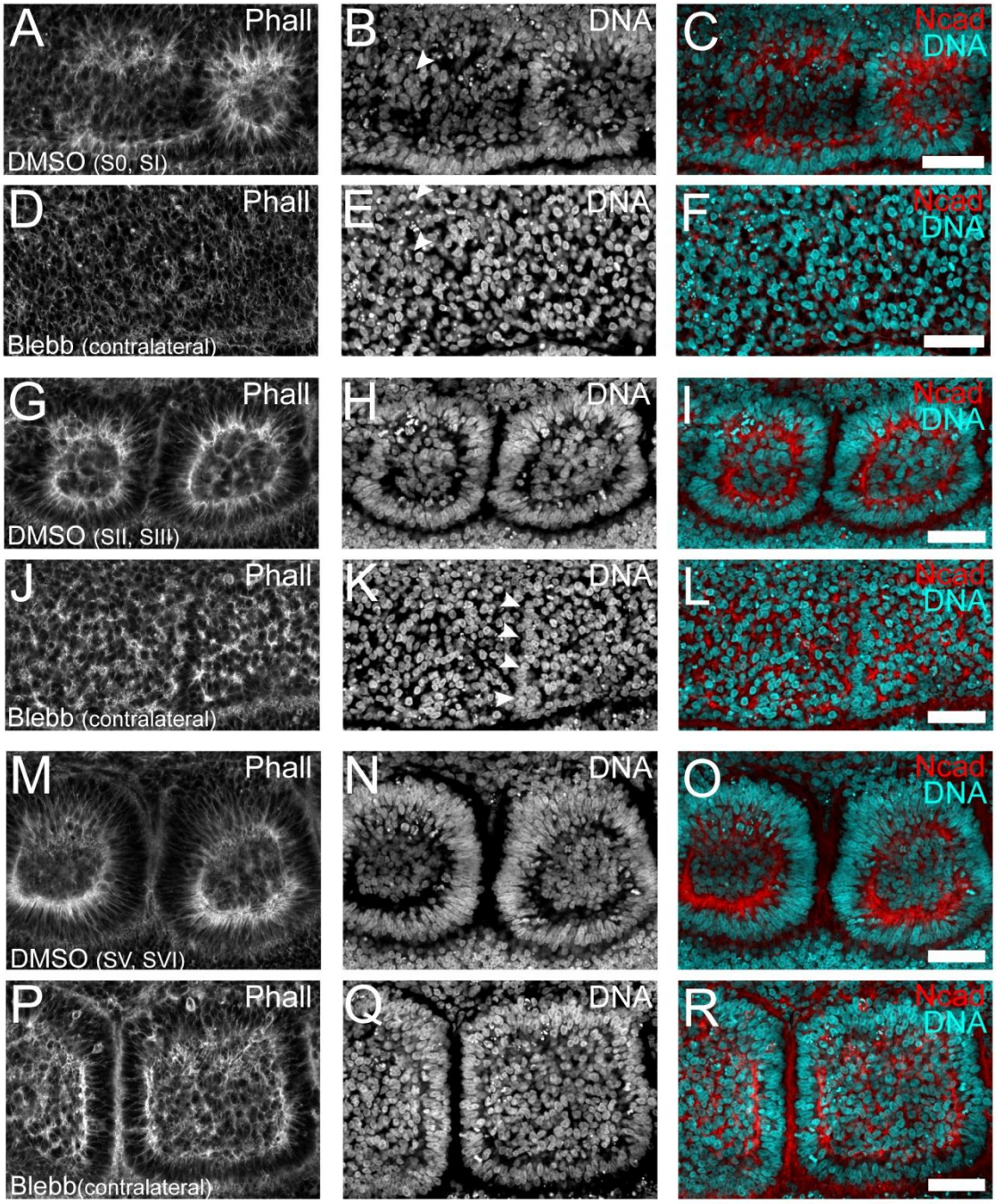

Figure 3. NMMII inhibition perturbs somite formation. In the presence of only the vehicle, DMSO (A-C), rostral PSM epithelialization occurs normally, with f-actin apical enrichment (A) and nuclear alignment (B) in S0 and SI. At the same axial level in the contralateral blebbistatin-treated explant (D-F), no signs of epithelial arrangement or of the somitic segment are present, with only dispersed f-actin staining (D) and nonaligned nuclear organization (E). Further rostrally, DMSO-treated explants depict markedly epithelial somites formed during culture (G-I), composed of the outer cell layer with aligned nuclei (H) and elongated cells with apically enriched actin (G). At the same axial level in the contralateral blebbistatin-treated explant (D-F), no signs of epithelial arrangement or of the somitic segment are present, with only dispersed f-actin staining (D) and nonaligned nuclear organization (E). (**Continues on next page →**)

previously been shown that, epithelial sheets of cultured cells retain their apical ZO-1-rich adhesion belt when blebbistatin is added (Miyake et al., 2006). Thus no significant effect is seen on ZO-1 in these epithelial tissues.

Cells that were at the rostral end of the PSM before explant culture with blebbistatin did not show any polarization or enrichment of either N-cadherin or ZO-1 (Fig. 4A and B). No signs of the somitic segment were visible, and in line with the F-actin and nuclear staining, the N-cadherin and ZO-1 staining resembled that normally found in caudal PSM (data not shown). In contrast, the contralateral DMSO-treated side clearly showed the initial ZO-1 apical accumulation and the assembly of the N- cadherin "basket" typical of a forming somite (Martins et al., 2009), Fig. 4A and B). Thus, intracellular tension is a requirement for the pre-epithelialization observable in the rostral PSM, and for establishing the cell-cell adhesions supporting somite formation.

The somite-forming epithelialization process initiated before culture (i.e. S0 before culture) was also abrogated by blebbistatin (Fig. 4M-P). The complete apical "ring" of N-cadherin enrichment and ZO-1 localization, visible at the contralateral position in the control explant (Fig. 4I-L) was completely absent on the blebbistatin-treated side. Few dispersed and local enrichments of N-cadherin and ZO-1 (Fig. 4M and N) were visible but the somitic segment was barely recognizable (Fig. 4O and P).

(**Continued from previous page**) Further rostrally, DMSO-treated explants depict markedly epithelial somites formed during culture (G-I), composed of the outer cell layer with aligned nuclei (H) and elongated cells with apically enriched actin (G). At the equivalent axial level in the treated explant (J-L), the somitic segments were severely affected, but still noticeable, with nuclei more or less lined up at the inter-somitic border (K, arrowheads). On the other hand, filamentous actin congregates into separate foci (J), with no particular arrangement (L). Somites formed before culture matured in the presence of DMSO vehicle (M-O), with an outer layer of elongated, apically polarized (M) and aligned cells (N) clearly distinguishable from the mesenchymal somitocoel. These epithelial and mesenchymal portions of the somitic segment are also visible at the equivalent axial level in the contralateral blebbistatin-treated side (P-R). Nevertheless, the somitocoel is notoriously enlarged and the outer layer narrower, the latter depicting apical f-actin enrichment (P) even though cells are shorter (compare nuclear elongation in Q with N). Somite staging refers to control DMSO-treated explants at the end of culture. Dorsal is on top and rostral to the right. Blebb: Blebbistatin; Phall: phalloidin f-actin staining; DNA: ToPro-3 nuclear staining. Scale bars represent 50 μm.

On the other hand, somites formed before the explants were exposed to blebbistatin were individualized and overall retained their epithelioid morphology (Fig. 4U-X). Nevertheless their mesenchymal somitocoel was expanded (compare Fig. 4S and W) and although the outer layer depicted a clear N-cadherin (Fig. 4U) and ZO-1 labeling (Fig. 4V), this labeling was interrupted, failing to form a continuous apical "ring" of N-cadherin and ZO-1 like observed in the control (compare Fig. 4Q-T with U-X).

We thus conclude that blebbistatin has a strong effect on the cells of the non-epithelial and recently epithelialized paraxial mesoderm, preventing them to advance normally in their morphogenesis program. In contrast, it has a milder effect on cells in the mature epithelial somites, indicating that it is the ZO-1-rich apical cell adhesions, and not the N-cadherin-rich adhesions already present on cells in the PSM that locks somite cells in the epithelial layer. This is in agreement with the blebbistatin-induced abrogation of *adherens* junction maturation and initial formation of tight junction complexes in cell culture (Miyake et al., 2006), in contrast to the failure to interfere with already formed junctions of epithelia in 3D (Yu et al., 2008). Our results show that the somitic epithelialization process has an absolute requirement for NMMII generated tension, while the perturbation of NMMII generated tension after the cohesiveness of the somitic epithelium has been established, partially protects the integrity of the segment from the effect of the inhibitory drugs.

Cell-derived tension contributes to the establishment of the R-C somite polarity

The formation of the intersomitic boundaries separating the somitic segments is concomitant with the visible display of a RC polarity within the segment. Several lines of evidence show that somitic RC polarity specification occurs before overt segmentation (Aoyama and Asamoto, 1988; Dequeant and Pourquié, 2008; Keynes and Stern, 1984). However, precise chicken embryo manipulation indicated that the final RC determination can be adjusted with the formation of an intersomitic boundary (Sato and Takahashi, 2005, see Takahashi and Sato, 2008). Therefore, we asked whether the described abrogation of intersomitic fissures by blebbistatin interfered with the determination of RC polarity in somites.

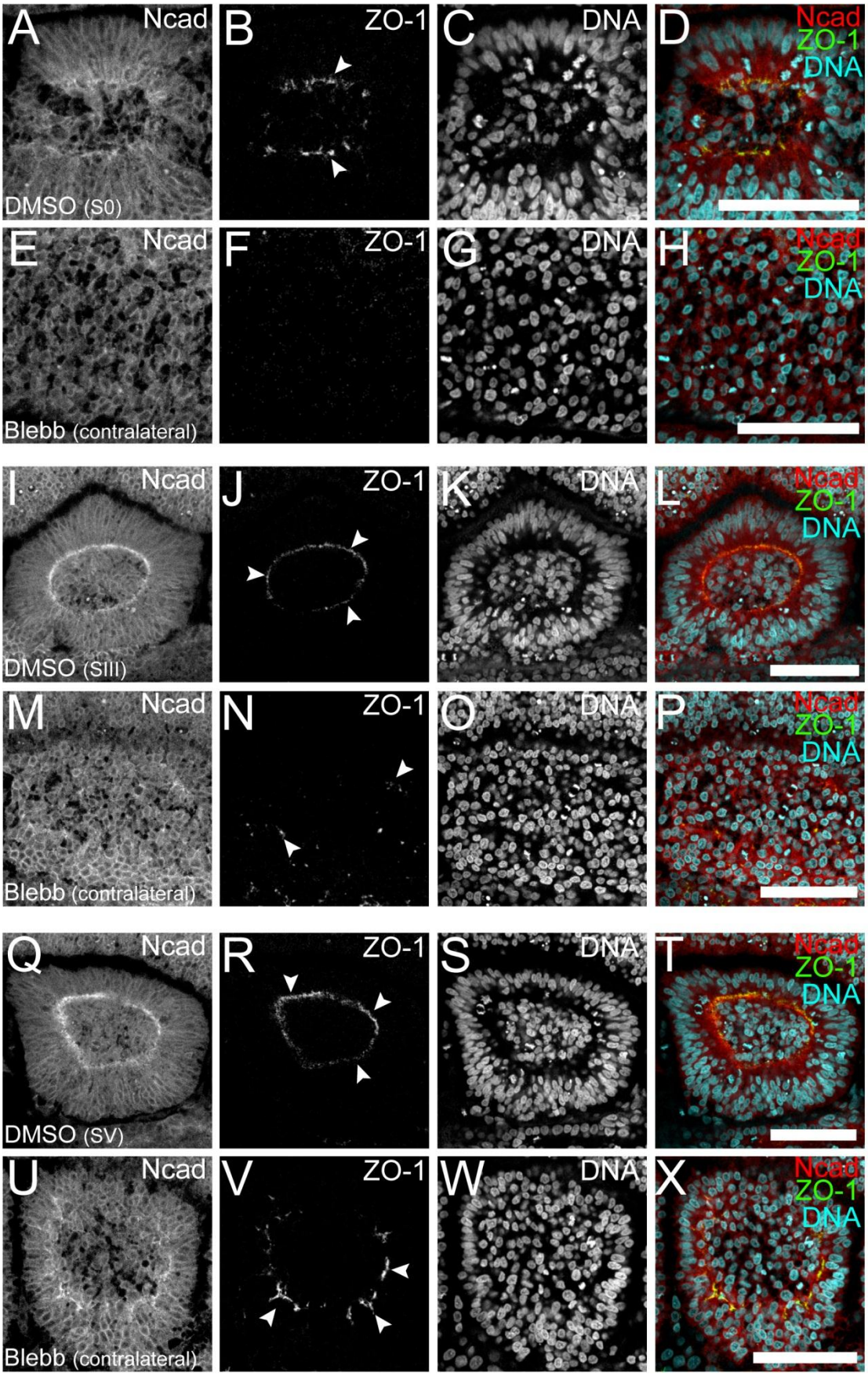

Figure 4. Blebbistatin affects the establishment of N-cadherin and ZO-1-rich cell-cell adhesions.

(Legend on the next page →)

We first investigated the expression of Delta-like 1 (*Dll1*), which conspicuously changes from a strong expression throughout the PSM to a caudal stripe in somites (Henrique et al., 1995; Palmeirim et al., 1998). We observed no alterations between the blebbistatin-treated side and DMSO treated control explant (3/3, Fig. 5A). Four new stripes of *Dll1* expression, corresponding to the 6 hour (4x90min) culture, were clearly visible, both in the control explant, with four new somites, and in the NMMII-inhibited side, with only one or two new somites. Preliminary results also indicate a normal acquisition of rostral identity, with the expression of *Tbx18* (Haenig and Kispert, 2004; Tanaka and Tickle, 2004) apparently being identical in contralateral control and experimental explants (data not shown).

We then analyzed the expression of *Meso1*, the key initiator of RC polarity in the somite, in contralateral control and experimental embryo halves. Although the majority of the pairs showed similar *Meso1* expression patterns (17/26, Fig. 5B) a significant portion depicted conspicuous differences between explants halves (9/26, Fig. 5C and D). We observed differences in the number of bands of *Meso1* expression (4/26, Fig. 5C), clearly indicating that the cycle of activation and suppression of *Meso1* in the rostral PSM was altered by the blebbistatin treatment. Moreover, we also observed

(Figure in previous page) **Figure 4. Blebbistatin affects the establishment of N-cadherin and ZO-1-rich cell-cell adhesions.** The forming somite (S0) in the control explant (A-D) clearly depicts the peripheral cell layer with apically enriched N-cadherin (A), strong but interrupted ring of apical ZO-1 (B, arrowheads) and an aster-like nuclear arrangement (C, D). At the equivalent axial level in the contralateral explant (E-H), the presence of blebbistatin abolishes all signs of polarized cell adhesions (E, F) and nuclear alignment (G). In DMSO treated explants, the forming somite (I-L) matures into a complete sphere of epithelial, apically polarized and adherent cells (I, J), surrounding the mesenchymal somitocoel (K). On the contralateral side (M-P), NMMII inhibition abolishes somite formation, inhibiting N-cadherin polarization (M) and dispersing ZO-1 adhesions (arrowheads in N) and perturbing the alignment of as visualized by the absence of aligned nuclei (O). Somites formed before culture mature in DMSO-treated explants (Q-T) and retain their outer epithelial layer (Q, R), demarcated from the somite core (S). The blebbistatin-treated side (U-X) partly retains the apical enrichment of N-cadherin (U), though the apical ZO-1 ring becomes fragmented (V, arrowheads) and the somitocoel expands (W). Somite staging refers to control DMSO-treated explants at the end of culture. Dorsal is on top and rostral to the right. Blebb: Blebbistatin; Ncad: N-cadherin; DNA: ToPro-3 nuclei staining. Arrowheads point to ZO-1 labeling. Scale bars represent 50 µm.

explants pairs were *Meso1* expression was located more rostrally in NMMI-inhibited explants than in the control side (5/26, Fig. 5D). The different effects of blebbistatin on *Dll1* and *Meso1* expression were unexpected, given that in mouse embryos, the expression of *Mesp2*, the Meso1 homolog, at the S-I position leads to the repression of Notch signaling (Sasaki et al., 2011) that underlies the caudal restriction of *Dll1* expression (see Saga, 2012).

It has been reported that in chicken embryos, the regulation of *Dll1* expression is an autonomous property of the PSM (Linker et al., 2003; Palmeirim et al., 1998), but there is no information regarding *Meso1*. We found that PSMs isolated from all surrounding tissues, depict, after 6 hours of culture, a striped *Meso1* expression pattern identical to that of the paraxial mesoderm on the intact contralateral side (6/6, Fig 6A). Thus, *Meso1* is, along with *Dll1*, *Notch1* (Linker et al., 2003; Palmeirim et al., 1998), and the cycling gene *Hairy1* (Palmeirim et al., 1997) upregulated normally in isolated PSMs in explant culture, and is thus independent of the presence of surrounding tissues, at least in the first 6 hours of culture.

In the mouse embryo, approximately one somite cycle (i.e. 120 minutes) lie between the detection of *Meso1* mRNA and protein in somite -I (Morimoto et al., 2005; Saga, 2007) and the consequent downregulation of *Dll1* in the rostral part of somite 0 (Bettenhausen et al., 1995; Takahashi et al., 2000, see Saga, 2007)). In chicken embryos, *Meso1* is expressed in S-I (Fig. 6B), or in S-II and sometimes even in the two positions (Buchberger et al., 1998). No antibody to detect the Meso1 protein is currently available. On the other hand, *Dll1* expression in chicken embryos is only caudally-restricted in the mature somite (SI; Fig. 6C and D), indicating that at least 2 somite cycles, i.e. 180 minutes, take place after *Meso1* upregulation in the PSM.

However, even if this species difference in the lag between *Meso1* expression and the caudal restriction of *Dll1* mRNA is potentially interesting, it does not explain why *Dll1* expression in unaffected while *Meso1* expression is affected after culture with blebbistatin for 6 hour. Rather, our results show that all events related to RC polarity, i.e. either rostral downregulation of *Dll1*or *Meso1* upregulation, which occurred rostral to the S-III position (before culture) were unaffected by the blebbistatin

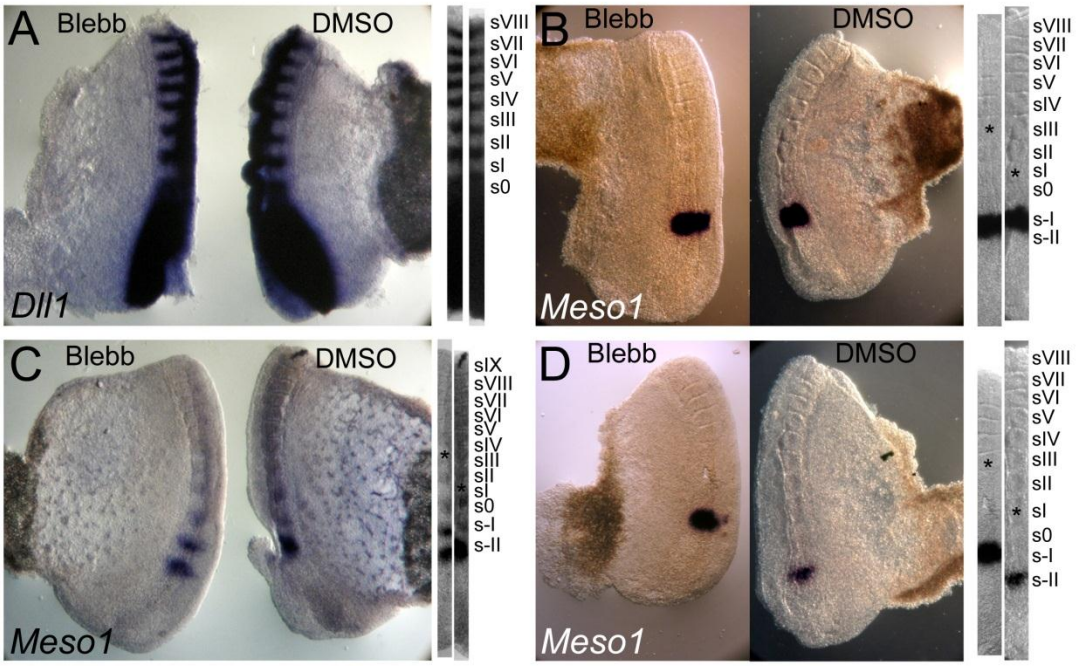

Figure 5. Inhibition of NMMII activity interferes with spatial regulation of Meso1 expression but Dll1 expression is normal. Comparison of paraxial mesoderm expression patterns in explants cultured under control conditions (DMSO; right) or in the presence of NMMII inhibitor blebbistatin (Blebb, left). Digital alignment of the two paraxial mesoderms (two bars on the right of each image), using the most caudal pair of formed somites observed on both sides as a reference. Asterisks mark S0 at the end of the culture period. The caudal-restricted expression of Dll1 (A) in somites was identical between the control side (right) and the blebbistatin treated explant (left), in somites formed both before and during culture. Though the Meso1 banded expression is similar between contralateral explants in some cases (B), we also observe explant pairs with different numbers of bands (C) or where Meso1 expression is localized more rostrally on the blebbistatin-treated side (D). Rostral is up.

treatment. This conclusion is in line with the proposed determination front being situated at the S-IV location, separating the rostral PSM from the caudal unspecified paraxial tissue (Dubrulle and Pourquié, 2002). Accordingly, when somite length portions of the PSM are RC inverted in locations rostral to front results, the original RC polarity is maintained, while more caudally located inverted portions adopt the new RC polarity (Dubrulle et al., 2001). Our results thus indicate that the upregulation of *Meso1* is unaffected by cell tension in the rostral, determined PSM, but, in contrast, cells localized in the caudal, undetermined region of the PSM are sensitive to cell tension and blocking it leads to the perturbation of a mechanism necessary for correct *Meso1* expression later on.

Opposing gradients of morphogens such as Wnts, FGFs and retinoic are involved in spatial location of the determination front (Aulehla et al., 2003; Diez del Corral et al., 2003; Dubrulle et al., 2001; Sawada et al., 2001) and *Meso1* expression (Aulehla and Pourquié, 2008; Delfini et al., 2005; Moreno and Kintner, 2004). Therefore our results point to the hypothesis that cell-derived tension can modulate these signaling gradients and the determination front, altering the spatial regulation of *Meso1* expression. Notwithstanding, alterations of *Meso1* expression in blebbistatin-treated, non-determined PSM should be investigated in further detail so that this surprising relationship between cell tension and the timely expression of *Meso1* is identified.

Inhibition of cell-fibronectin interactions by excess RGD peptide is ineffective in interfering with somitogenesis

The interaction between the $\alpha5\beta1$ integrin and the RGD site on fibronectin, has been reported to be particularly important both for regulation of cell tension and also in somite formation. Integrin $\alpha5\beta1$ interaction with the RGD sequence of fibronectin (Pierschbacher and Ruoslahti, 1984), elicits a strong $\alpha5\beta1$-fibronectin binding (Friedland et al., 2009), and modulates cell tension allowing for the initial cell spreading and the consequent strong adherence to the substrate in culture (Danen et al., 2002, see Geiger et al., 2009; Huveneers and Danen, 2009). This strong integrin $\alpha5\beta1$ fibronectin via the RGD site is essential for the assembly of a fibronectin matrix (Schwarzbauer, 1991; Yamada and Kennedy, 1984, see Singh et al., 2010) and also for mouse somitogenesis (Takahashi et al., 2007). Therefore we asked whether the RGD-integrin interaction is involved in the formation of somites in chicken embryos.

In cell culture, the presence of excess RGD peptide in the medium leads to the occupation of all the available integrin-binding pockets, inhibiting cell adhesion and integrin function (Pierschbacher and Ruoslahti, 1984; Yamada and Kennedy, 1984, see Harburger and Calderwood, 2009; Barczyk et al., 2010)). After a 6 hour culture with RGD, embryo explants showed no difference in somite formation when compared to the contralateral half cultured in the presence of the non-functional, control RGE (Fig. 7A-D). Unexpectedly, both halves formed the 4 respective somites, and with no alteration in the expression of *Meso1* (6/6, Fig. 7A and B) or *Dll1* (6/6, Fig 7C and D). However,

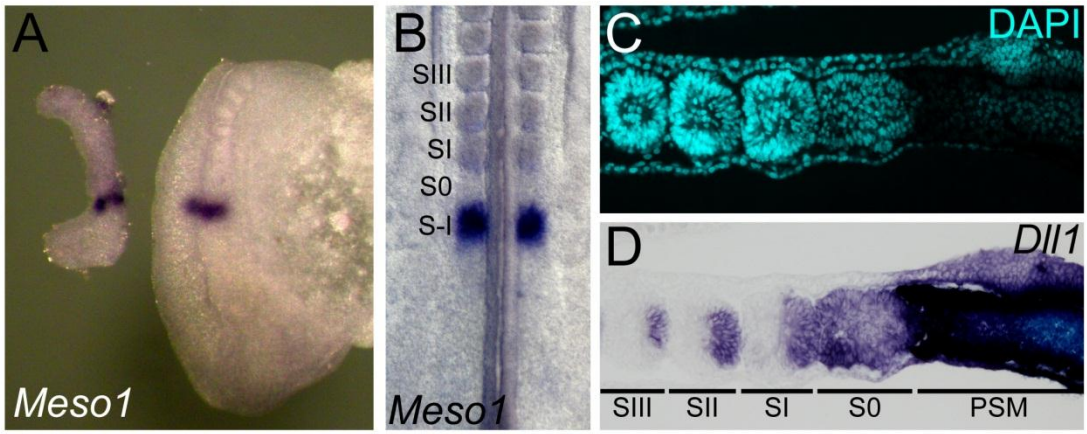

Figure 6. **Meso1 and Dll1 expression in the PSM**. The upregulation of Meso1 expression in isolated PSMs cultured for 6 hours (A, left) parallels the Meso1 expression on the contralateral intact half cultured for the same amount of time(right). Both are similar to the banded expression in non-cultured intact embryos (B). Sagittal views of nuclear staining (DAPI, C) and Dll1 expression (D) in the rostral PSM and somites. Dll1 expression is restricted to the caudal halves of formed somites (SI, SII, SIII), but in the forming somite (S0) it is expressed in the whole segment. Thus approximately 3 somite cycles (i.e. 4.5 hours) go by between the expression of Meso1 in S-I and the establishment of RC somite polarity when measured by the caudal restriction of Dll1 expression in SI (see text for details). Rostral is up in A and B; rostral is to the left and dorsal on top in C and D.

literature reporting the functional effect of excess RGD peptide in 3D embryonic systems is quite scarce (e.g. Boucaut et al., 1984; Boucaut et al., 1985, see Schwarzbauer and DeSimone, 2011). In fact, we could not find any report where the addition of the RGD peptide had an inhibitory effect on cells already adherent to a complex, mature, 3D matrix, such as that surrounding the paraxial mesoderm in chicken embryos (Rifes et al., 2007; Rifes and Thorsteinsdóttir, 2012). Actually, it has become increasingly noticeable that cell-ECM interactions *in vivo* may not completely follow the mechanisms and dynamics reported for cell culture on 2D rigid substrates, due to the complexity of a 3D matrix (Harunaga and Yamada, 2011). The availability and arrangement of adhesive domains in ECM molecules in 3D matrices is far greater that on flat substrates. Therefore, we speculate that the dramatic increase in quantity and quality of RGD sites, available in a densely 3D fibrillar fibronectin matrix (Rifes and Thorsteinsdóttir, 2012), compared to 2D matrices, renders the effect of "excess" RGD peptide on cell-fibronectin binding quite negligible. Thus, other molecular tools will have to be used to be able to investigate the role of cell binding to the RGD site of fibronectin in somite formation in the chicken embryo.

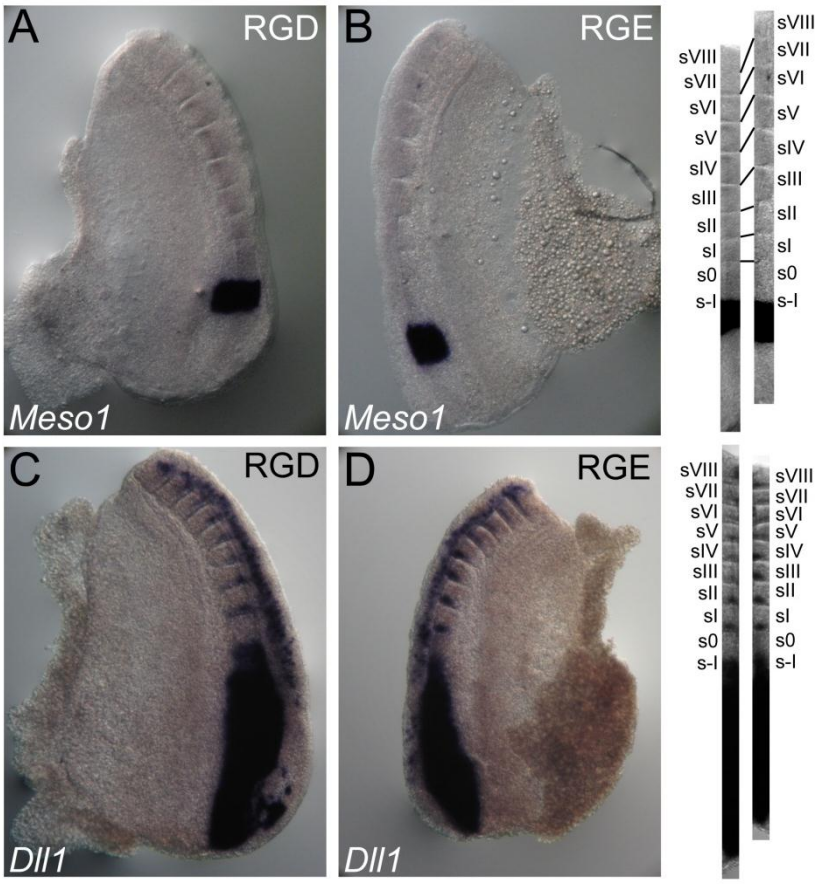

Figure 7. The presence of integrin binding pep-tide RGD does not interfere with somite formation or RC polarity. The presence of 0.9 mM RGD peptide, which inhibits integrin attachment to a fibronectin substrate in cultured cells, does not alter the expression of Meso1 (A) nor Dll1 (C), when compared contralateral embryo-halves incubated with the RGE non-functional peptide (B, D). Digital alignment of the contralateral paraxial mesoderms hybridized for Meso1 expression depicted in A and B (top row, on right) or of the contralateral paraxial mesoderms hybridized for Dll1 expression depicted in C and D (bottom row, on right) shows that there is no difference in the number of somites formed during culture nor any alterations in the expression domains of these two genes. Rostral is up.

Rho Kinase activity inhibition by RockOut strongly interferes with the positioning of Meso1 expression

In cell culture, the attachment and consequent cell spreading to a fibronectin substrate involves a $\alpha 5\beta 1$ downstream modulation of RhoA-dependent cell tension (Danen et al., 2002; Huveneers and Danen, 2009; Ren et al., 1999). Rho kinase I and II (ROCK-I, ROCK-II) are the effectors of RhoA on the cell's actomyosin contractility, acting both as direct promoters of NMMII activity and as inhibitors of the activity of myosin

phosphatase, the main NMMII inhibitor (Conti and Adelstein, 2008; Vicente-Manzanares et al., 2009). Given the importance of the fibronectin ECM in the formation of somites, we postulated that ROCK-I and –II should be downstream of the integrin ECM-receptor to elicit the adequate cell tension essential for somite formation. Therefore, using the same method described above, we cultured chicken embryo explant halves in the presence of the ROCK-I and –II inhibitor, RockOut (Yarrow et al., 2005), or DMSO as control. In the presence of RockOut somite formation is severely impaired (they form 2,15 fewer somites than the control side in 6 hours of culture, n= 8), similar to the effect of blebbistatin, though, macroscopically, the formed somites were clearer in the RockOut-treated explants (compare Fig. 4 and 8). Remarkably our *in situ* hybridization results from these explants show that RockOut disrupts the expression of *Meso1* in all cases studied (n=8/8; Fig. 8 A and B). The effect of the ROCK inhibitor on *Meso1* is thus more penetrant than the effect of blebbistatin; 8/8 explant pairs depict a clearly different expression pattern of *Meso1*, either in the number of bands (3/8) or in their position (5/8). Therefore these results clearly show that ROCK-regulated cell tension is necessary for the correct upregulation in time and space of *Meso1*. Interestingly, the knock-down of integrin 1 resulted in the abolition of *Meso1* expression (Rallis 2010), providing further evidence for a role of an integrin-ROCK relationship in the control of tension and subsequently the regulation of *Meso1*.

Given this result, future studies should first evaluate the cellular effects of RockOut during paraxial mesoderm morphogenesis, such as the effect on cell shape and organization, actin cytoskeleton and cell polarity, comparing with the effects obtained with blebbistatin. Moreover, and although the mechanism of *Meso1* upregulation is unknown in the chicken embryo, it would be interesting to verify whether the RockOut treatment also alters either the rostral domain of *Tbx6* expression and, even more interestingly, whether it impacts on the regular oscillatory pattern of any of the Notch-related cycling genes.

For now, our results demonstrate that cell tension is essential for somite formation and furthermore raise the possibility that it also controls the temporally and spatially correct upregulation of *Meso-1* in the PSM. This raises the exciting prospect

that cell tension may play a profound and previously unknown role in regulating somitogenesis.

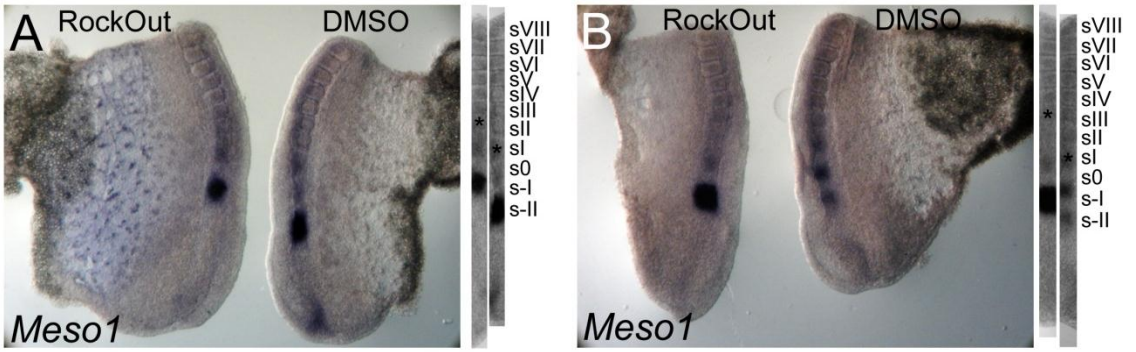

Figure 8. Inhibition of Rho Kinase (Rock) activity impairs somite formation and disturbs Meso1 expression. Comparison of Meso1 expression in contralateral embryo explant halves incubated with DMSO (DMSO, right) or with the Rock inhibitor RockOut (RockOut, left) for the same amount of time. Meso1 expression is different in control and drug treated explants, either showing Meso1 expression located more rostrally in the RockOut-treated explants compared to the contralateral control (A) or the number of Meso1 expression bands is different between experimental and control explants (B). Rostral is up.

Conclusion

Our results show that somite formation is accompanied by a rapid, cell-tension dependent reinforcement of apical cell-cell adhesions, in the form of tight junction formation. Once established, these matured adhesions lock the epithelial cell layer, separating it from the mesenchymal somitocoel. Remarkably, and contrary to previous whole embryo cultures (Bénazéraf et al., 2010), our embryo half-explants show that cell-tension also interferes with the expression of *Meso1*, and that the tension-dependent event controlling *Meso1* expression occurs caudal to the determination front. Although we were not successful in blocking cell-ECM engagement with the excess of free RGD peptide commonly used in 2D cell culture, most likely because of the overwhelming availability of this binding sequence in a mature 3D ECM environment (Rifes and Thorsteinsdóttir, 2012), other approaches indicate that an integrin downstream signal can regulate the underlying genetic somitogenesis program (Girós et al., 2011) in a Notch-independent way (Rallis et al., 2010). Future studies will address the exciting

possibility that cell-tension created through cell-ECM binding may regulate the genetic program underlying somitogenesis.

References

Aoyama, H. and Asamoto, K. (1988). Determination of somite cells: independence of cell differentiation and morphogenesis. *Development* **104**, 15-28.

Aulehla, A. and Pourquié, O. (2008). Oscillating signaling pathways during embryonic development. *Current Opinion in Cell Biology* **20**, 632-7.

Aulehla, A., Wehrle, C., Brand-Saberi, B., Kemler, R., Gossler, A., Kanzler, B. and Herrmann, B. G. (2003). Wnt3a plays a major role in the segmentation clock controlling somitogenesis. *Developmental Cell* **4**, 395-406.

Bajanca, F., Luz, M., Duxson, M. J. and Thorsteinsdóttir, S. (2004). Integrins in the mouse myotome: developmental changes and differences between the epaxial and hypaxial lineage. *Developmental Dynamics* **231**, 402-15.

Barczyk, M., Carracedo, S. and Gullberg, D. (2010). Integrins. *Cell and Tissue Research* **339**, 269-80.

Bénazéraf, B., Francois, P., Baker, R. E., Denans, N., Little, C. D. and Pourquié, O. (2010). A random cell motility gradient downstream of FGF controls elongation of an amniote embryo. *Nature* **466**, 248-52.

Bettenhausen, B., Hrabě de Angelis, M., Simon, D., Guenet, J. L. and Gossler, A. (1995). Transient and restricted expression during mouse embryogenesis of Dll1, a murine gene closely related to Drosophila Delta. *Development* **121**, 2407-18.

Boucaut, J. C., Darribère, T., Boulekbache, H. and Thiery, J. P. (1984). Prevention of gastrulation but not neurulation by antibodies to fibronectin in amphibian embryos. *Nature* **307**, 364-7.

Boucaut, J. C., Darribère, T., Li, S. D., Boulekbache, H., Yamada, K. M. and Thiery, J. P. (1985). Evidence for the role of fibronectin in amphibian gastrulation. *Journal of Embryology and Experimental Morphology* **89 Suppl**, 211-27.

Bryant, D. M. and Mostov, K. E. (2008). From cells to organs: building polarized tissue. *Nature Reviews: Molecular Cell Biology* **9**, 887-901.

Buchberger, A., Seidl, K., Klein, C., Eberhardt, H. and Arnold, H. H. (1998). cMeso-1, a novel bHLH transcription factor, is involved in somite formation in chicken embryos. *Developmental Biology* **199**, 201-15.

Cavey, M. and Lecuit, T. (2009). Molecular bases of cell-cell junctions stability and dynamics. *Cold Spring Harbor Perspectives in Biology* **1**, a002998.

Chen, C. S. (2008). Mechanotransduction - a field pulling together? *Journal of Cell Science* **121**, 3285-92.

Christ, B., Huang, R. and Scaal, M. (2004). Formation and differentiation of the avian sclerotome. *Anatomy and Embryology (Berl)* **208**, 333-50.

Christ, B., Huang, R. and Scaal, M. (2007). Amniote somite derivatives. *Developmental Dynamics* **236**, 2382-96.

Christ, B., Huang, R. and Wilting, J. (2000). The development of the avian vertebral column. *Anatomy and Embryology (Berl)* **202**, 179-94.

Chuai, M., Zeng, W., Yang, X., Boychenko, V., Glazier, J. A. and Weijer, C. J. (2006). Cell movement during chick primitive streak formation. *Developmental Biology* **296**, 137-49.

Clark, K., Langeslag, M., Figdor, C. G. and van Leeuwen, F. N. (2007). Myosin II and mechanotransduction: a balancing act. *Trends in Cell Biology* **17**, 178-86.

Conti, M. A. and Adelstein, R. S. (2008). Nonmuscle myosin II moves in new directions. *Journal of Cell Science* **121**, 11-8.

Danen, E. H., Sonneveld, P., Brakebusch, C., Fassler, R. and Sonnenberg, A. (2002). The fibronectin-binding integrins alpha5beta1 and alphavbeta3 differentially modulate RhoA-GTP loading, organization of cell matrix adhesions, and fibronectin fibrillogenesis. *Journal of Cell Biology* **159**, 1071-86.

Delfini, M. C., Dubrulle, J., Malapert, P., Chal, J. and Pourquié, O. (2005). Control of the segmentation process by graded MAPK/ERK activation in the chick embryo. *Proceedings of the National Academy of Sciences of the United States of America* **102**, 11343-8.

Dequeant, M. L. and Pourquié, O. (2008). Segmental patterning of the vertebrate embryonic axis. *Nature Reviews: Genetics* **9**, 370-82.

Diez del Corral, R., Olivera-Martinez, I., Goriely, A., Gale, E., Maden, M. and Storey, K. (2003). Opposing FGF and retinoid pathways control ventral neural pattern, neuronal differentiation, and segmentation during body axis extension. *Neuron* **40**, 65-79.

Duband, J. L., Dufour, S., Hatta, K., Takeichi, M., Edelman, G. M. and Thiery, J. P. (1987). Adhesion molecules during somitogenesis in the avian embryo. *Journal of Cell Biology* **104**, 1361-74.

Dubrulle, J., McGrew, M. J. and Pourquié, O. (2001). FGF signaling controls somite boundary position and regulates segmentation clock control of spatiotemporal Hox gene activation. *Cell* **106**, 219-32.

Dubrulle, J. and Pourquié, O. (2002). From head to tail: links between the segmentation clock and antero-posterior patterning of the embryo. *Current Opinion in Genetics and Development* **12**, 519-23.

Dubrulle, J. and Pourquié, O. (2004). Coupling segmentation to axis formation. *Development* **131**, 5783-93.

Eckert, J. J. and Fleming, T. P. (2008). Tight junction biogenesis during early development. *Biochimica et Biophysica Acta* **1778**, 717-28.

Eyckmans, J., Boudou, T., Yu, X. and Chen, C. S. (2011). A hitchhiker's guide to mechanobiology. *Developmental Cell* **21**, 35-47.

Friedland, J. C., Lee, M. H. and Boettiger, D. (2009). Mechanically activated integrin switch controls alpha5beta1 function. *Science* **323**, 642-4.

Geiger, B., Spatz, J. P. and Bershadsky, A. D. (2009). Environmental sensing through focal adhesions. *Nature Reviews: Molecular Cell Biology* **10**, 21-33.

George, E. L., Georges-Labouesse, E. N., Patel-King, R. S., Rayburn, H. and Hynes, R. O. (1993). Defects in mesoderm, neural tube and vascular development in mouse embryos lacking fibronectin. *Development* **119**, 1079-91.

Georges-Labouesse, E. N., George, E. L., Rayburn, H. and Hynes, R. O. (1996). Mesodermal development in mouse embryos mutant for fibronectin. *Developmental Dynamics* **207**, 145-56.

Girós, A., Grgur, K., Gossler, A. and Costell, M. (2011). alpha5beta1 integrin-mediated adhesion to fibronectin is required for axis elongation and somitogenesis in mice. *PLoS One* **6**, e22002.

Goh, K. L., Yang, J. T. and Hynes, R. O. (1997). Mesodermal defects and cranial neural crest apoptosis in alpha5 integrin-null embryos. *Development* **124**, 4309-19.

Gossler, A. and Hrabě de Angelis, M. (1998). Somitogenesis. *Current Topics in Developmental Biology* **38**, 225-87.

Haenig, B. and Kispert, A. (2004). Analysis of TBX18 expression in chick embryos. *Development Genes and Evolution* **214**, 407-11.

Hamburger, V. and Hamilton, H. L. (1992). A series of normal stages in the development of the chick embryo. 1951. *Developmental Dynamics* **195**, 231-72.

Harburger, D. S. and Calderwood, D. A. (2009). Integrin signalling at a glance. *Journal of Cell Science* **122**, 159-63.

Harris, T. J. and Tepass, U. (2010). Adherens junctions: from molecules to morphogenesis. *Nature Reviews: Molecular Cell Biology* **11**, 502-14.

Hartsock, A. and Nelson, W. J. (2008). Adherens and tight junctions: structure, function and connections to the actin cytoskeleton. *Biochimica et Biophysica Acta* **1778**, 660-9.

Harunaga, J. S. and Yamada, K. M. (2011). Cell-matrix adhesions in 3D. *Matrix Biology* **30**, 363-8.

Hatta, K., Takagi, S., Fujisawa, H. and Takeichi, M. (1987). Spatial and temporal expression pattern of N-cadherin cell adhesion molecules correlated with morphogenetic processes of chicken embryos. *Developmental Biology* **120**, 215-27.

Henrique, D., Adam, J., Myat, A., Chitnis, A., Lewis, J. and Ish-Horowicz, D. (1995). Expression of a Delta homologue in prospective neurons in the chick. *Nature* **375**, 787-90.

Huveneers, S. and Danen, E. H. (2009). Adhesion signaling - crosstalk between integrins, Src and Rho. *Journal of Cell Science* **122**, 1059-69.

Iden, S. and Collard, J. G. (2008). Crosstalk between small GTPases and polarity proteins in cell polarization. *Nature Reviews: Molecular Cell Biology* **9**, 846-59.

Ingber, D. E. (2006). Cellular mechanotransduction: putting all the pieces together again. *FASEB Journal* **20**, 811-27.

Jülich, D., Geisler, R., Consortium, T. S. and Holley, S. A. (2005). Integrinalpha5 and delta/notch signaling have complementary spatiotemporal requirements during zebrafish somitogenesis. *Developmental Cell* **8**, 575-86.

Keynes, R. J. and Stern, C. D. (1984). Segmentation in the vertebrate nervous system. *Nature* **310**, 786-9.

Keynes, R. J. and Stern, C. D. (1988). Mechanisms of vertebrate segmentation. *Development* **103**, 413-29.

Kocsis, E., Trus, B. L., Steer, C. J., Bisher, M. E. and Steven, A. C. (1991). Image averaging of flexible fibrous macromolecules: the clathrin triskelion has an elastic proximal segment. *Journal of Structural Biology* **107**, 6-14.

Koshida, S., Kishimoto, Y., Ustumi, H., Shimizu, T., Furutani-Seiki, M., Kondoh, H. and Takada, S. (2005). Integrinalpha5-dependent fibronectin accumulation for maintenance of somite boundaries in zebrafish embryos. *Developmental Cell* **8**, 587-98.

Kovacs, M., Toth, J., Hetenyi, C., Malnasi-Csizmadia, A. and Sellers, J. R. (2004). Mechanism of blebbistatin inhibition of myosin II. *Journal of Biological Chemistry* **279**, 35557-63.

Kragtorp, K. A. and Miller, J. R. (2007). Integrin alpha5 is required for somite rotation and boundary formation in Xenopus. *Developmental Dynamics* **236**, 2713-20.

Kuan, C. Y., Tannahill, D., Cook, G. M. and Keynes, R. J. (2004). Somite polarity and segmental patterning of the peripheral nervous system. *Mechanisms of Development* **121**, 1055-68.

Kulesa, P. M. and Fraser, S. E. (2002). Cell dynamics during somite boundary formation revealed by time-lapse analysis. *Science* **298**, 991-5.

Lecuit, T. and Lenne, P. F. (2007). Cell surface mechanics and the control of cell shape, tissue patterns and morphogenesis. *Nature Reviews: Molecular Cell Biology* **8**, 633-44.

Linask, K. K., Ludwig, C., Han, M. D., Liu, X., Radice, G. L. and Knudsen, K. A. (1998). N-cadherin/catenin-mediated morphoregulation of somite formation. *Developmental Biology* **202**, 85-102.

Linker, C., Lesbros, C., Stark, M. R. and Marcelle, C. (2003). Intrinsic signals regulate the initial steps of myogenesis in vertebrates. *Development* **130**, 4797-807.

Lopez, J. I., Mouw, J. K. and Weaver, V. M. (2008). Biomechanical regulation of cell orientation and fate. *Oncogene* **27**, 6981-93.

Maroto, M., Dale, J. K., Dequeant, M. L., Petit, A. C. and Pourquié, O. (2005). Synchronised cycling gene oscillations in presomitic mesoderm cells require cell-cell contact. *International Journal of Developmental Biology* **49**, 309-15.

Martin-Belmonte, F. and Perez-Moreno, M. (2012). Epithelial cell polarity, stem cells and cancer. *Nature Reviews: Cancer* **12**, 23-38.

Martins, G. G., Rifes, P., Amandio, R., Rodrigues, G., Palmeirim, I. and Thorsteinsdóttir, S. (2009). Dynamic 3D cell rearrangements guided by a fibronectin matrix underlie somitogenesis. *PLoS One* **4**, e7429.

Miyake, Y., Inoue, N., Nishimura, K., Kinoshita, N., Hosoya, H. and Yonemura, S. (2006). Actomyosin tension is required for correct recruitment of adherens junction components and zonula occludens formation. *Experimental Cell Research* **312**, 1637-50.

Monsoro-Burq, A. H. (2005). Sclerotome development and morphogenesis: when experimental embryology meets genetics. *International Journal of Developmental Biology* **49**, 301-8.

Moreno, T. A. and Kintner, C. (2004). Regulation of segmental patterning by retinoic acid signaling during Xenopus somitogenesis. *Developmental Cell* **6**, 205-18.

Morimoto, M., Takahashi, Y., Endo, M. and Saga, Y. (2005). The Mesp2 transcription factor establishes segmental borders by suppressing Notch activity. *Nature* **435**, 354-9.

Nakaya, Y., Kuroda, S., Katagiri, Y. T., Kaibuchi, K. and Takahashi, Y. (2004). Mesenchymal-epithelial transition during somitic segmentation is regulated by differential roles of Cdc42 and Rac1. *Developmental Cell* **7**, 425-38.

Ostrovsky, D., Cheney, C. M., Seitz, A. W. and Lash, J. W. (1983). Fibronectin distribution during somitogenesis in the chick embryo. *Cell Differentiation* **13**, 217-23.

Palmeirim, I., Dubrulle, J., Henrique, D., Ish-Horowicz, D. and Pourquié, O. (1998). Uncoupling segmentation and somitogenesis in the chick presomitic mesoderm. *Developmental Genetics* **23**, 77-85.

Palmeirim, I., Henrique, D., Ish-Horowicz, D. and Pourquié, O. (1997). Avian hairy gene expression identifies a molecular clock linked to vertebrate segmentation and somitogenesis. *Cell* **91**, 639-48.

Parsons, J. T., Horwitz, A. R. and Schwartz, M. A. (2010). Cell adhesion: integrating cytoskeletal dynamics and cellular tension. *Nature Reviews: Molecular Cell Biology* **11**, 633-43.

Pierschbacher, M. D. and Ruoslahti, E. (1984). Cell attachment activity of fibronectin can be duplicated by small synthetic fragments of the molecule. *Nature* **309**, 30-3.

Pourquié, O. (2011). Vertebrate segmentation: from cyclic gene networks to scoliosis. *Cell* **145**, 650-63.

Pourquié, O. and Tam, P. P. (2001). A nomenclature for prospective somites and phases of cyclic gene expression in the presomitic mesoderm. *Developmental Cell* **1**, 619-20.

Quintin, S., Gally, C. and Labouesse, M. (2008). Epithelial morphogenesis in embryos: asymmetries, motors and brakes. *Trends in Genetics* **24**, 221-30.

Radice, G. L., Rayburn, H., Matsunami, H., Knudsen, K. A., Takeichi, M. and Hynes, R. O. (1997). Developmental defects in mouse embryos lacking N-cadherin. *Developmental Biology* **181**, 64-78.

Rallis, C., Pinchin, S. M. and Ish-Horowicz, D. (2010). Cell-autonomous integrin control of Wnt and Notch signalling during somitogenesis. *Development* **137**, 3591-601.

Ren, X. D., Kiosses, W. B. and Schwartz, M. A. (1999). Regulation of the small GTP-binding protein Rho by cell adhesion and the cytoskeleton. *EMBO Journal* **18**, 578-85.

Rifes, P., Carvalho, L., Lopes, C., Andrade, R. P., Rodrigues, G., Palmeirim, I. and Thorsteinsdóttir, S. (2007). Redefining the role of ectoderm in somitogenesis: a player in the formation of the fibronectin matrix of presomitic mesoderm. *Development* **134**, 3155-65.

Rifes, P. and Thorsteinsdóttir, S. (2012). Extracellular matrix assembly and 3D organization during paraxial mesoderm development in the chick embryo. *Developmental Biology* **368**, 370-81.

Ruoslahti, E. (1996). RGD and other recognition sequences for integrins. *Annual Review of Cell and Developmental Biology* **12**, 697-715.

Saga, Y. (2007). Segmental border is defined by the key transcription factor Mesp2, by means of the suppression of Notch activity. *Developmental Dynamics* **236**, 1450-5.

Saga, Y. (2012). The mechanism of somite formation in mice. *Current Opinion in Genetics and Development* **22**, 331-8.

Saga, Y., Hata, N., Kobayashi, S., Magnuson, T., Seldin, M. F. and Taketo, M. M. (1996). MesP1: a novel basic helix-loop-helix protein expressed in the nascent mesodermal cells during mouse gastrulation. *Development* **122**, 2769-78.

Saga, Y., Hata, N., Koseki, H. and Taketo, M. M. (1997). Mesp2: a novel mouse gene expressed in the presegmented mesoderm and essential for segmentation initiation. *Genes & Development* **11**, 1827-39.

Saga, Y. and Takeda, H. (2001). The making of the somite: molecular events in vertebrate segmentation. *Nature Reviews: Genetics* **2**, 835-45.

Sasaki, N., Kiso, M., Kitagawa, M. and Saga, Y. (2011). The repression of Notch signaling occurs via the destabilization of mastermind-like 1 by Mesp2 and is essential for somitogenesis. *Development* **138**, 55-64.

Sato, Y. and Takahashi, Y. (2005). A novel signal induces a segmentation fissure by acting in a ventral-to-dorsal direction in the presomitic mesoderm. *Developmental Biology* **282**, 183-91.

Sawada, A., Shinya, M., Jiang, Y. J., Kawakami, A., Kuroiwa, A. and Takeda, H. (2001). Fgf/MAPK signalling is a crucial positional cue in somite boundary formation. *Development* **128**, 4873-80.

Schwartz, M. A. and DeSimone, D. W. (2008). Cell adhesion receptors in mechanotransduction. *Current Opinion in Cell Biology* **20**, 551-6.

Schwarzbauer, J. E. (1991). Identification of the fibronectin sequences required for assembly of a fibrillar matrix. *Journal of Cell Biology* **113**, 1463-73.

Schwarzbauer, J. E. and DeSimone, D. W. (2011). Fibronectins, their fibrillogenesis, and in vivo functions. *Cold Spring Harbor Perspectives in Biology* **3**.

Singh, P., Carraher, C. and Schwarzbauer, J. E. (2010). Assembly of fibronectin extracellular matrix. *Annual Review of Cell and Developmental Biology* **26**, 397-419.

Straight, A. F., Cheung, A., Limouze, J., Chen, I., Westwood, N. J., Sellers, J. R. and Mitchison, T. J. (2003). Dissecting temporal and spatial control of cytokinesis with a myosin II Inhibitor. *Science* **299**, 1743-7.

Takahashi, S., Leiss, M., Moser, M., Ohashi, T., Kitao, T., Heckmann, D., Pfeifer, A., Kessler, H., Takagi, J., Erickson, H. P. et al. (2007). The RGD motif in fibronectin is essential for development but dispensable for fibril assembly. *Journal of Cell Biology* **178**, 167-78.

Takahashi, Y., Koizumi, K., Takagi, A., Kitajima, S., Inoue, T., Koseki, H. and Saga, Y. (2000). Mesp2 initiates somite segmentation through the Notch signalling pathway. *Nature Genetics* **25**, 390-6.

Takahashi, Y. and Sato, Y. (2008). Somitogenesis as a model to study the formation of morphological boundaries and cell epithelialization. *Development Growth & Differentiation* **50 Suppl 1**, S149-55.

Tanaka, M. and Tickle, C. (2004). Tbx18 and boundary formation in chick somite and wing development. *Developmental Biology* **268**, 470-80.

Vicente-Manzanares, M., Ma, X., Adelstein, R. S. and Horwitz, A. R. (2009). Non-muscle myosin II takes centre stage in cell adhesion and migration. *Nature Reviews: Molecular Cell Biology* **10**, 778-90.

Wei, L., Roberts, W., Wang, L., Yamada, M., Zhang, S., Zhao, Z., Rivkees, S. A., Schwartz, R. J. and Imanaka-Yoshida, K. (2001). Rho kinases play an obligatory role in vertebrate embryonic organogenesis. *Development* **128**, 2953-62.

Yamada, K. M. and Kennedy, D. W. (1984). Dualistic nature of adhesive protein function: fibronectin and its biologically active peptide fragments can autoinhibit fibronectin function. *Journal of Cell Biology* **99**, 29-36.

Yang, J. T., Rayburn, H. and Hynes, R. O. (1993). Embryonic mesodermal defects in alpha 5 integrin-deficient mice. *Development* **119**, 1093-105.

Yarrow, J. C., Totsukawa, G., Charras, G. T. and Mitchison, T. J. (2005). Screening for cell migration inhibitors via automated microscopy reveals a Rho-kinase inhibitor. *Chemistry & Biology* **12**, 385-95.

Yasuhiko, Y., Haraguchi, S., Kitajima, S., Takahashi, Y., Kanno, J. and Saga, Y. (2006). Tbx6-mediated Notch signaling controls somite-specific Mesp2 expression. *Proceedings of the National Academy of Sciences of the United States of America* **103**, 3651-6.

Yu, W., Shewan, A. M., Brakeman, P., Eastburn, D. J., Datta, A., Bryant, D. M., Fan, Q. W., Weiss, W. A., Zegers, M. M. and Mostov, K. E. (2008). Involvement of RhoA, ROCK I and myosin II in inverted orientation of epithelial polarity. *EMBO Reports* **9**, 923-9.

Supplementary material

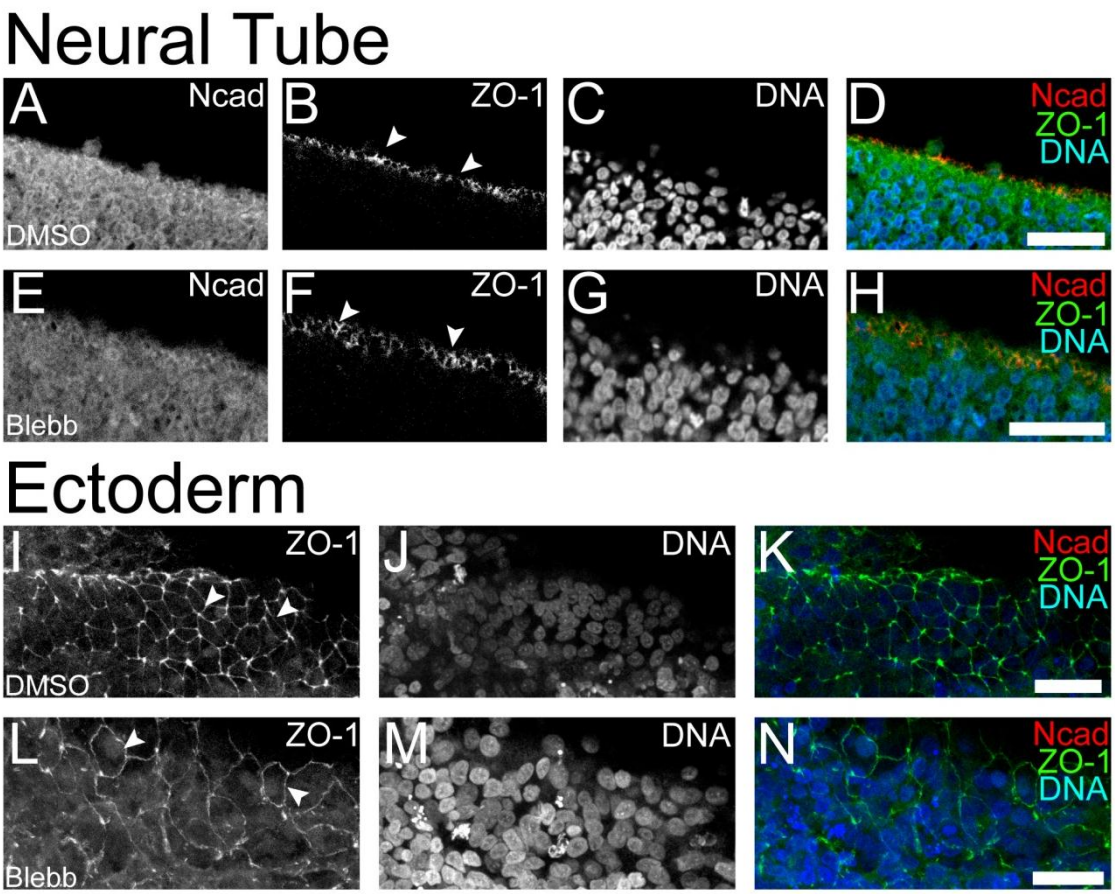

Supplementary Figure S1. ***Absence of significant effect of NMMII inhibition with blebbistatin on neural tube and ectoderm*** . Explants cultured in the presence of DMSO vehicle (A-D and I-K) showed strong apically located ZO-1 labeling (B, I) both in the neural tube (A-D) and in the overlying ectoderm (I-K). In the presence of blebbistatin (E-H, L-N), ZO-1 labeling was also restricted to the apical end of neural tube cells (F) and in the ectoderm (L). Dorsal view of the ectoderm clearly depicts the ZO-1-rich apical adhesion belt characteristic of epithelial cells in both DMSO treated (arrowheads in I) and blebbistatin treated explants (arrowheads in L). Interestingly, inhibition of cell derived tension by blebbistatin appeared to result in wider ectoderm cells (compare K and N). Neural tube images are single optical confocal slices of cultured explants, as described in text. Ectoderm images result from 10-12 µm z-projections of optical confocal slices, necessary to obtain the adhesion belts which are not in a single place due to the explants normal surface irregularities. Blebb: Blebbistatin; Ncad: N-cadherin; DNA: ToPro-3 nuclei staining. Arrowheads point ZO-1 labeling. Scale bars represent 20 µm.

Chapter 6

Discussion

Important note

During the course of the writing of this thesis, I realized that an unexpected contaminant in the 70 kDa amino-terminal fibronectin fragment has had a pleiotropic effect in the respective experiments. The product used, from a commercial source, had a high salt and glucose content (clarified after direct contact with the company) that may have altered the osmolarity of the medium. As a result, the observations produced by the use of the 70kDa fragment were magnified by the osmotic alteration.

I have decided to maintain in this thesis the chapters were the fragment was used (chapters 2 and 3), because of the following reasons.

First, the importance of the 70kDa amino terminal fibronectin fragment in fibronectin assembly is an established, undisputed point for fibronectin assembly (for reviews see McDonald, 1988; Potts and Campbell, 1996; Magnusson and Mosher, 1998; Schwarzbauer and Sechler, 1999; Pankov and Yamada, 2002; Wierzbicka-Patynowski and Schwarzbauer, 2003; Mao and Schwarzbauer, 2005a; Cho and Mosher, 2006; Schwarzbauer and DeSimone, 2011 and finally Singh et al., 2010, for a major, recent and high reputation review).

Second, the dominant-negative effect on fibronectin matrix assembly by the presence of excess 70kDa fragment was described with the original discovery of this domain (McKeown-Longo and Mosher, 1985), and since then, this technique has been exhaustively used for the inhibition of fibronectin matrix assembly (see references above).

Third, the effect of the excess 70kDa on fibronectin assembly not only has been extensively studied for isolated cells, plated on a flat rigid substrate, but also in a multicellular, 3D, malleable contexts (e.g. Robinson et al., 2004; Mao and Schwarzbauer, 2005b; Salmenpera et al., 2008; Zhou et al., 2008; Stratman et al., 2009; Sabari et al., 2011). Moreover, some of these reports used a 70kDa fragment from the same commercial source and in similar concentrations to what was used in this thesis, (Salmenpera et al., 2008; Zhou et al., 2008; Stratman et al., 2009; Sabari et al., 2011).

Fourth; in spite of not being presented in any of the publications in this thesis, I determined that the presence of the fragment, in the concentrations used, in the culture medium of embryo explants did not produce any significant alterations in cell proliferation or apoptosis, compared to the control explant cultures preformed at the same time (see Fig.1 and 2 below)

Five: using another approach, more amenable for amphibians (embryo injection with recombinant mRNA), the effect of the 70 kDa fragment also affect fibronectin fibrillogenesis and embryonic morphogenesis (Rozario et al., 2009).

Sixth: in the aftermath of this unfortunate setback, our lab has performed experiments with the 70 kDa fragment after dialysis against medium, and concluded that it does affect somite formation and morphology, albeit in a milder way than observed when it was dissolved directly in medium.

Therefore, I will continue with the discussion based on the observations reported in the previous chapters, and also on the extensive literature on the subject, particularly, the effect of the 70 kDa fragment on fibronectin fibrillogenesis.

I have, however, excluded from this thesis all the unpublished results, observations or conclusions obtained from experiments where the 70 kDa fibronectin fragment was used, either with embryos or cultured cells.

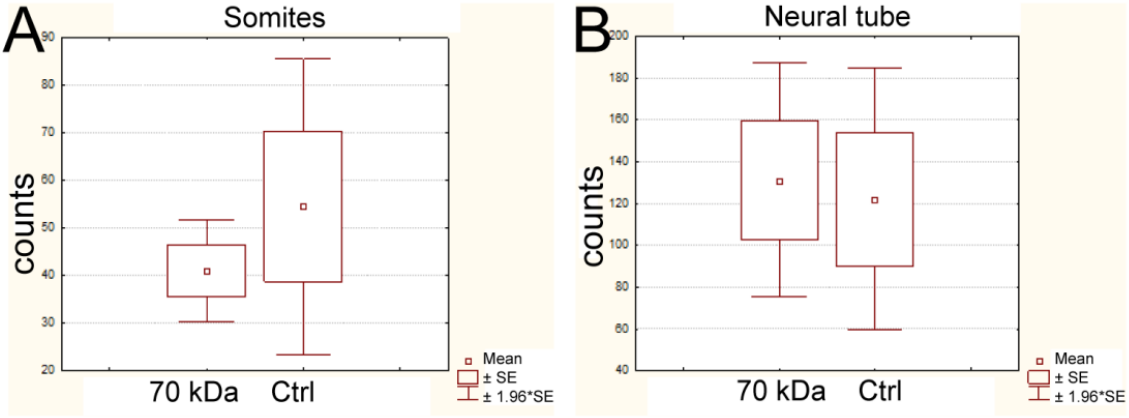

Figure 1. Apoptosis in chicken embryo explants exposed to 70 kDa fibronectin fragment. Box and Whisker plots for the average count of apoptotic nuclei in somites (A) and neural tubes (B) in control (n=4) and 70 kDa-treated (n=4) chicken embryo explants. I found no significant difference between the control and 70 kDa-treated explants, either in the paraxial mesoderm (p=0.45) and in the neural tube (p=0.83). A paraxial mesoderm portion (S0 at the beginning of culture) was selected from each explant, as well as the somite-length portion of the adjacent neural tube. Using the ROI manager in ImageJ, the apoptotic nuclei were scored using ToPro3 labeling. A paired T-test was performed using STATISTICA 6 (StatSoft) on the obtained scores. For more details on explants and labeling, see chapter 3 (Martins et al., 2009).

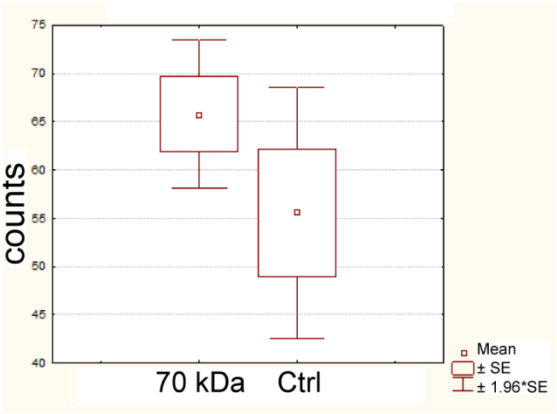

Figure 2. Proliferation in chicken embryo explants exposed to 70 kDa fibronectin fragment. Box and Whisker plot for the average number of mitotic nuclei per 100µm of paraxial mesoderm in control (n=4) and 70 kDa-treated (n=4) chicken embryo explants. I found no significant difference between the control and the 70 kDa-treated explants (p=0.23). Mitotic nuclei were labeled using an anti-phospho-histone 3 antibody (Milipore, ref. 05-806, clone 3H10, 1:200), visualized on a confocal microscope in whole mounts, and z-stacks were imported into Amira (Visage Imaging Inc.) software. The paraxial mesoderm was manual segmented in 3D, the paraxial mesoderm phospho-histone 3 staining was analyzed in 3D and identified as separate volumes. The phospho-histone 3 positive nuclei were automatically scored by the software, and the length of the segmented paraxial mesoderm was measured. The total number of mitotic nuclei (circa 300 per paraxial mesoderm) was divided by the length of each paraxial mesoderm. A paired T-test was performed on the obtained scores using STATISTICA 6 (StatSoft). For more details on explants, labeling, image acquisition and 3D analysis see chapter 3 (Martins et al., 2009).

References

Cho, J. and Mosher, D. F. (2006). Role of fibronectin assembly in platelet thrombus formation. *Journal of Thrombosis and Haemostasis* **4**, 1461-9.

Magnusson, M. K. and Mosher, D. F. (1998). Fibronectin: structure, assembly, and cardiovascular implications. *Arteriosclerosis, Thrombosis, and Vascular Biology* **18**, 1363-70.

Mao, Y. and Schwarzbauer, J. E. (2005a). Fibronectin fibrillogenesis, a cell-mediated matrix assembly process. *Matrix Biology* **24**, 389-99.

Mao, Y. and Schwarzbauer, J. E. (2005b). Stimulatory effects of a three-dimensional microenvironment on cell-mediated fibronectin fibrillogenesis. *Journal of Cell Science* **118**, 4427-36.

Martins, G. G., Rifes, P., Amândio, R., Rodrigues, G., Palmeirim, I. and Thorsteinsdóttir, S. (2009). Dynamic 3D cell rearrangements guided by a fibronectin matrix underlie somitogenesis. *PLoS One* **4**, e7429.

McDonald, J. A. (1988). Extracellular matrix assembly. *Annual Review of Cell Biology* **4**, 183-207.

McKeown-Longo, P. J. and Mosher, D. F. (1985). Interaction of the 70,000-mol-wt amino-terminal fragment of fibronectin with the matrix-assembly receptor of fibroblasts. *Journal of Cell Biology* **100**, 364-74.

Pankov, R. and Yamada, K. M. (2002). Fibronectin at a glance. *Journal of Cell Science* **115**, 3861-3.

Potts, J. R. and Campbell, I. D. (1996). Structure and function of fibronectin modules. *Matrix Biology* **15**, 313-20.

Robinson, E. E., Foty, R. A. and Corbett, S. A. (2004). Fibronectin matrix assembly regulates alpha5beta1-mediated cell cohesion. *Molecular Biology of the Cell* **15**, 973-81.

Rozario, T., Dzamba, B., Weber, G. F., Davidson, L. A. and DeSimone, D. W. (2009). The physical state of fibronectin matrix differentially regulates morphogenetic movements in vivo. *Developmental Biology* **327**, 386-98.

Sabari, J., Lax, D., Connors, D., Brotman, I., Mindrebo, E., Butler, C., Entersz, I., Jia, D. and Foty, R. A. (2011). Fibronectin matrix assembly suppresses dispersal of glioblastoma cells. *PLoS One* **6**, e24810.

Salmenpera, P., Kankuri, E., Bizik, J., Siren, V., Virtanen, I., Takahashi, S., Leiss, M., Fassler, R. and Vaheri, A. (2008). Formation and activation of fibroblast spheroids depend on fibronectin-integrin interaction. *Experimental Cell Research* **314**, 3444-52.

Schwarzbauer, J. E. and DeSimone, D. W. (2011). Fibronectins, their fibrillogenesis, and in vivo functions. *Cold Spring Harbor Perspectives in Biology* **3,** a005041.

Schwarzbauer, J. E. and Sechler, J. L. (1999). Fibronectin fibrillogenesis: a paradigm for extracellular matrix assembly. *Current Opinion in Cell Biology* **11**, 622-7.

Singh, P., Carraher, C. and Schwarzbauer, J. E. (2010). Assembly of fibronectin extracellular matrix. *Annual Review of Cell and Developmental Biology* **26**, 397-419.

Stratman, A. N., Malotte, K. M., Mahan, R. D., Davis, M. J. and Davis, G. E. (2009). Pericyte recruitment during vasculogenic tube assembly stimulates endothelial basement membrane matrix formation. *Blood* **114**, 5091-101.

Wierzbicka-Patynowski, I. and Schwarzbauer, J. E. (2003). The ins and outs of fibronectin matrix assembly. *Journal of Cell Science* **116**, 3269-76.

Zhou, X., Rowe, R. G., Hiraoka, N., George, J. P., Wirtz, D., Mosher, D. F., Virtanen, I., Chernousov, M. A. and Weiss, S. J. (2008). Fibronectin fibrillogenesis regulates three-dimensional neovessel formation. *Genes & Development* **22**, 1231-43.

Discussion

The serial repetition of elements, metamerism, is a striking form of body organization, evident throughout the animal kingdom, and even in plants (see (Richmond and Oates, 2012). The results presented in this thesis attempt to shed some light onto the morphological formation of somites, the most conspicuous segmented structures of the vertebrate embryo, which give rise to the distinctive feature from which the name of this subphylum is derived.

This thesis addresses the interaction between cells and their surrounding matrix during the formation of the individual somite segment, contributing to the notion that developmental programs are executed through a continuous, reciprocal interaction with the microenvironment surrounding the cell or a group of cells (see (Nelson and Bissell, 2006).

6.1. ECM assembly and organization is part of the developmental program of the paraxial mesoderm

It is a commonly accepted notion that paraxial mesoderm cells travelling along the PSM experience parallel or opposing morphogen gradients. These mRNA decay or source-sink morphogen gradients translate the maturation process of the PSM, leading to its progressive maturation, culminating in somite formation at its rostral end (see (Aulehla and Pourquié, 2010).

The results presented in this thesis show that the ECM microenvironment also gradually changes along the paraxial mesoderm, in parallel with the undergoing morphological transformations. In Chapter 2 and 4 we present evidence that fibronectin is assembled into an increasingly more fibrillar matrix around the PSM, concomitantly with PSM maturation, which culminates in its support of the somite detachment event.

Here, the new supramolecular perspective on ECM assembly in a 3D in vivo embryonic tissue brought by this thesis will be confronted with the existing observations obtained in classical cell culture or other *in vivo* models. Furthermore, based on Chapter

4 and 5, the possible signals emanating from this matrix gradient will be discussed, while a more integrative view on somite morphogenesis will be proposed in section 6.2, below.

6.1.1. Fibronectin assembly in vivo

Since its discovery, fibronectin has attained a preponderant and ubiquitous position in the biology of cells and tissues; not only is it detectable in most embryonic and adult tissues, but it is also almost omnipresent in *in vitro* cell culture conditions, both as a solid coating substrate and as a component of the liquid medium (from serum). However, we are still far from fully comprehending how cells assemble and perceive their surrounding fibronectin matrix (Singh et al., 2010) particularly in complex *in vivo* contexts (Schwarzbauer and DeSimone, 2011). Although it has been known for some time that fibronectin assembly is seriously hampered on a pliable substrate, resembling soft tissue *in vivo* (Halliday and Tomasek, 1995), and is enhanced in a simulated 3D environment *in vitro* (Mao and Schwarzbauer, 2005b), the bulk of the work on fibronectin matrix assembly has been performed on standard 2D plastic/glass substrates. Therefore, fibronectin matrix assembly *in vivo* may not follow the dynamics described for *in vitro* conditions.

The analyses of the fibronectin matrix surrounding the paraxial mesoderm presented in this thesis, particularly the detailed 3D approach used in Chapter 4, offers one of the first glimpses of the rapid fibronectin matrix assembly in a complex, 3D, *in vivo* tissue. Results from Chapter 2 show a strong mRNA expression of *Fn1* in the ectoderm with some expression also detected in the caudal PSM. These mRNA data agree with the protein localization results from Chapter 2 and 4 which clearly show the compact form of secreted fibronectin, proposed as the **first step** in fibronectin assembly (Peters and Mosher, 1987, reviewed in Mao and Schwarzbauer, 2005a; Singh et al., 2010; Wierzbicka-Patynowski and Schwarzbauer, 2003, see Figure 1), associated with the *Fn1*-expressing ectoderm. Compact fibronectin labeling is also found within the caudal, recently formed PSM, along with few short fibrils, interspersed with the mesenchymal cells.

The formation of short fibronectin fibrils located at the periphery of individual cells characterizes plated cells (Bae et al., 2004; McDonald et al., 1987; Ohashi et al., 2002), and cells in early zebrafish and amphibian embryos (Davidson et al., 2008; Dzamba et al., 2009; Latimer and Jessen, 2010). This peripheral arrangement of fibrils connecting adjacent cells has been proposed to represent a **second step** in fibronectin assembly (Dzamba et al., 2009). According to the proposed assembly model for *Xenopus* blastocoel roof cells, cell-cell adhesions serve as a fulcrum for the force-dependent extension of fibronectin molecules between two adjacent cells (Dzamba et al., 2009), much like between cells in culture (Bae et al., 2004; Baneyx et al., 2002) and between cells and their substrate (Ohashi et al., 2002).

We did not observe such an arrangement of short fibrils bridging adjacent cells on the PSM surface in our 3D analysis in Chapter 4. Much like within the amphibian mesoderm (Davidson et al., 2004), we see a few short fibrils intermingled among the mesenchymal cells within the PSM. However, the bulk of the fibronectin matrix of the PSM is located at its surface and is organized in a wide net of long thin fibrils cast around the PSM. This arrangement is readily observed already at caudal, “young” positions, thus being in agreement with the proposed stimulatory effect of a 3D architecture on fibronectin fibrillogenesis (Mao and Schwarzbauer, 2005b). Though the cellular tug-of-war extension of fibronectin fibrils may occur whenever two cells share a fibronectin dimer, we hypothesize that the pattern of peripheral fibronectin fibrils bridging two adjacent cells as described in the blastocoel roof cell model of fibronectin assembly, is exclusive to tissue surfaces composed of large, relatively immotile and aligned cells, such as those of early zebrafish (Latimer and Jessen, 2010) and *Xenopus* embryos (Davidson et al., 2008; Dzamba et al., 2009), or trophectoderm cells of mouse blastocyst (Thorsteinsdóttir, 1992). Our observations, combined with those of others (Czirok et al., 2004; Czirok et al., 2006), thus lead us to conclude that at the surface of mesenchymal tissues composed of small motile cells, such as the chicken embryo PSM (Bénazéraf et al., 2010; Delfini et al., 2005), Chapter 3), globular fibronectin is rapidly assembled directly to what can been called the **final pattern** of fibronectin assembly, namely the formation of long fibrils, spanning several cell lengths (Chapter 4). In addition, the mechanical particularities of tissue interfaces may underline the prevalence of fibronectin assembly

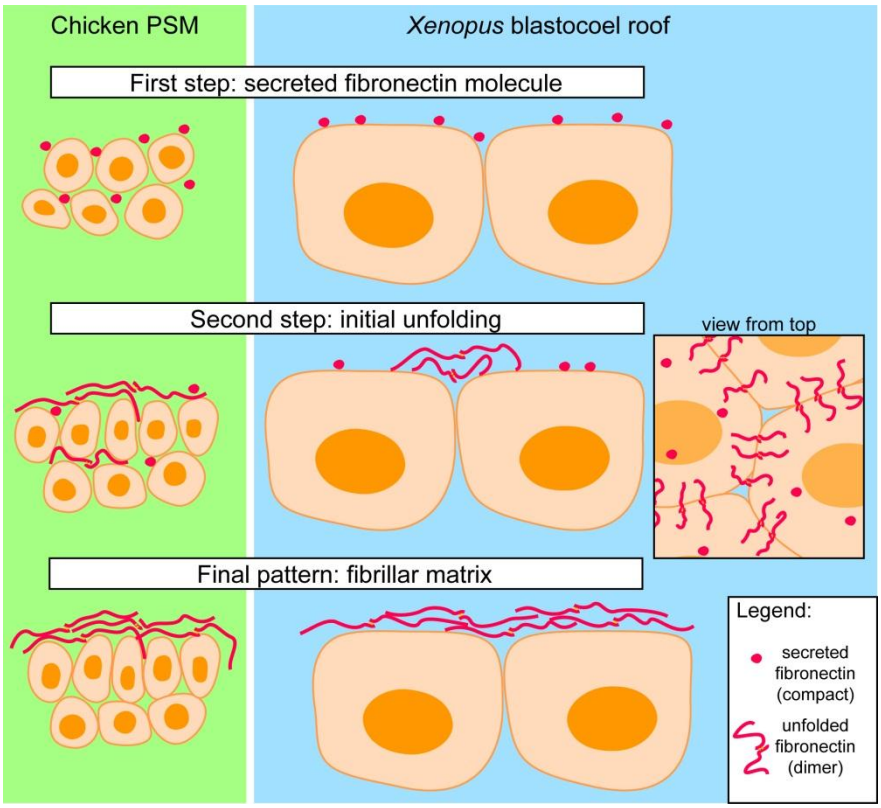

Figure 1. Fibronectin assembly model in tissues in vivo. The first depiction of a fibronectin matrix is the punctate or globular form of the secreted molecule, associated with the surface of cells, either in mesenchymal tissue composed of small cells, such as in the chicken PSM (light-green panel on the left), or at the surface of tissues composed of large immotile cells, such as the blastocoel roof of amphibian embryos (light-blue panel on the right). The second step of fibronectin matrix assembly, the initial elongation of the fibronectin molecule, is notably visible in large cells as radially oriented peripheral fibrils extended between neighboring cells, crossing their interface. Fibronectin elongation is rapidly achieved between the numerous small cells composing the mesenchymal PSM, assembling long fibrils at the surface, while few short fibrils populate the interstitial space. Note that this "step" is not as identifiable as the peripheral fibrils in large cells (see view from the top), but rather depicts an intermediate state where the globular and the long fibrils spanning several cells co-exist. With the continuous supply and assembly of new fibronectin molecules, a dense fibrillar fibronectin matrix preferentially covers the outer tissue surface. The size proportion between chicken PSM cells and *Xenopus* cells is approximate, based on observations presented in this thesis (Chapter 5) and in the literature (Davidson et al., 2008; Dzamba et al., 2009).

at the free-surface of the PSM (discussed in section 6.2.2 ahead). In any case, this thesis validates that *in vivo* fibronectin matrix assembly may follow different dynamics of assembly depending on the nature of the tissue that assembles it. Further studies addressing fibronectin assembly in *in vivo* systems are however required to fully understand how this process proceeds and varies *in vivo*.

In addition to contributing to the understanding of fibronectin matrix assembly *in vivo*, the results of this thesis reveal that ECM assembly can be considered a particular

form of tissue interaction during embryogenesis. The ectoderm overlying the paraxial mesoderm is a known source of paracrine factors (such as Wnts), particularly important for the differentiation programs after somite formation (see Bothe et al., 2007; Christ et al., 2007). In Chapter 2 we show that the ectoderm and the PSM have a source/assembler relationship with regard to fibronectin matrix assembly. This phenomenon parallels the ECM contribution from the myoepithelial cells surrounding the luminal cells during the morphogenesis of the mammary gland (see Gudjonsson et al., 2005). Our observations thus further broaden the concept of the cell/tissue microenviroment. The results presented in this thesis alert to the fact that instructive signals between tissues are not limited to paracrine factors (see Nelson and Bissell, 2006), as ECM molecules can be secreted by one tissue but assembled and utilized by neighboring ones.

6.1.2. Laminin matrix assembly in vivo

The results presented in Chapter 4 are among the first detailed depictions of laminin matrix deposition at the surface of an *in vivo* 3D tissue, in the form of individual patches coalescing during paraxial mesoderm development. Given the apparent 2D structure of the flat basal lamina, the full 3D approach was pivotal in this assessment. Our results raised two important questions: (1) is the patchwork aspect of the laminin matrix a widespread basement membrane format during the development of epithelia, whether they are transient or not; and (2) how do PSM cells perceive the co-availability of (at least) two major ECM components, fibronectin and laminin?

A comprehensive answer to the first question requires a wider survey on the pattern of laminin matrix assembly during the epithelializing process of other tissues, using a similar 3D approach. The results from Chapter 4 indicate that the patchwork laminin matrix is not essential for the initial epithelialization process of the PSM. However, this patchwork laminin basement membrane plays a role and is sufficient to sustain the epithelial character of the dermomyotome (also see Deries et al., 2012) and limit the de-epithelialization process of the sclerotome. Therefore, we find reasonable that a discontinuous laminin lining may well be a widespread feature of the morphogenesis of epithelial tissues.

Regarding the second question, basic information on the presence and function of different ECM components during an embryonic event is scarce. Research on post-embryonic development of the mouse mammary gland has headed the field, thoroughly illustrating the importance of ECM components and respective remodeling during morphogenesis and differentiation (see Fata et al., 2004). However, the dynamics of the ECM and its components during earlier embryonic development has not deserved much attention, and few reports assess more than one ECM component. For example, fibronectin and laminin, and respective receptors, are present during mouse myogenesis (Bajanca et al., 2004; Cachaço et al., 2005), although cell-laminin interaction appear to be preponderant in the regulation of the myogenic program (Bajanca et al., 2006). In zebrafish embryos, these two ECM components are also present in the myotendinous junctions, the remnant of the intersomitic boundary, to which muscle fibers anchor (Snow and Henry, 2009). Fibronectin is essential for the correct attachment and delineation of myogenic cells within the segment (Snow et al., 2008b), although it becomes selectively excluded in the junction of fast twitching muscle fibers (Snow and Henry, 2009), which require a laminin-based anchoring point (Snow et al., 2008a).

The observations reported in this thesis indicate that fibronectin, but not laminin, is essential for the somite epithelialization process. However, laminin is strongly expressed in the presomitic mesoderm of mouse embryos (Anderson et al., 2009; Copp et al., 2011). We speculate that laminin deposition at a more cell-proximal location than the pre-existing fibronectin matrix reflects the transition from the fibronectin-preponderant stage during somite epithelialization, to the laminin-prominent stage of epithelial somite development. Likewise, fibronectin is essential for zebrafish somitic boundary maintenance (Jülich et al., 2005; Koshida et al., 2005; Snow et al., 2008b), acting as a key tissue separator during embryonic growth (see (Dahmann et al., 2011), while laminin interactions regulate subsequent muscle development (Dolez et al., 2011; Snow et al., 2008a). On the other hand, the importance of the dense laminin patchwork covering the ventral, de-epithelialized sclerotome remains elusive, and further investigation in older embryonic stages is required. The laminin matrix may be part of the segment separator machinery, maintaining the consecutive caudal and rostral

sclerotome populations separate until the sclerotomes resegment and the chondrogenic derivatives develop (see Huang et al., 2000).

6.1.3. Signaling from the matrix: what cells perceive from the ECM

Time-lapsed observations (Davidson et al., 2008) together with the high resolution 3D analyses of the fibronectin matrix reported in Chapter 4 reveal extensive remodeling of fibrils and an increase in their thickness and density. Although no obvious cueing property of the ECM can be extrapolated from these observations, cells perceive the modifications in the matrix and alter their behavior accordingly, performing massive cellular rearrangements: somite formation (Chapter 2 and 3) or oriented cell division and epiboly (Dzamba et al., 2009; Rozario et al., 2009). Therefore rather than just the presence/absence of fibronectin, other qualitative traits on the nature of the fibronectin matrix are relevant and necessary for somite formation (Chaper 2 and 4).

However, the identification and evaluation of qualitative traits of the ECM is far from being consensual or straight forward. In Chapter 5 we provide evidence that cell tension is essential for the epithelialization process during the formation of a new somite. Results from Chapters 2 and 3 strongly implicate the surrounding fibronectin matrix as the tension provider in the PSM. Thus these results are in line with the recent awareness on the importance of cell tension in all aspects of the cells life (Engler et al., 2006, see Buxboim et al., 2010; Eyckmans et al., 2011; Hoffman et al., 2011; Mammoto and Ingber, 2010). The tensional state of the ECM, fore fronted by collagen gel-based studies (Elsdale and Bard, 1972), has deserved increased attention, by relating the gel rigidity to malignant phenotypes (e.g. Levental et al., 2009; Paszek et al., 2005, see Egeblad et al., 2010). Hampered by the fact that fibronectin matrices are assembled in a cell-dependent manner, *in vitro* 3D fibronectin-rich matrices (see Cukierman et al., 2001) are not yet commonly used in the study of tension. Nevertheless, fibronectin is quite a "mechanical" molecule. Tension-dependent extension of the highly folded tertiary structure of the numerous fibronectin type III modules (Potts and Campbell, 1996) is essential for matrix assembly (Baneyx et al., 2002; Smith et al., 2007, see Singh et al., 2010). These type III modules also endow enormous extensibility and force bearing properties to fibronectin fibrils (Klotzsch et al., 2009). Therefore, as tensioned

fibronectin adhesions prompt the catch-bond linkage by the integrin receptor and the respective intracellular signaling (Friedland et al., 2009), it is not surprising that mature fibronectin matrices elicit an increased rigidity response from the cells (Antia et al., 2008). Studies using fibroblasts in artificially stiffened 3D fibronectin-rich matrices have not been very informative (Engler et al., 2009; Kubow et al., 2009), but endothelial cells grown in 3D require extensive fibronectin matrix assembly for tensional support during neovascularization (Zhou et al., 2008). Therefore, it is reasonable to propose that the increasingly fibrillar fibronectin matrix surrounding the rostral PSM, characterized in Chapter 4, may be perceived as an increasingly more rigid support by the peripheral PSM cells, and which exerts the tension necessary to promote somitogenesis (Chapter 5).

6.2. A mature fibronectin matrix is an essential multi-task player during the morphogenesis of the somite segment

The most established and prominent evidence of the importance of fibronectin in somitogenesis came from the observation that *Fn1*-/- mouse embryos lack all somites (George et al., 1993). These embryos form paraxial mesoderm (Georges-Labouesse et al., 1996), expressing *Mox1* (Candia et al., 1992) and *Notch1* (Bettenhausen et al., 1995), but somite formation fails completely (George et al., 1993). Together with *FAK*-null embryos (Furuta et al., 1995; Ilic et al., 1995), *Fn1*-null embryos are the only single-gene knock-out mouse embryos lacking all somites. *FAK*-null embryos show sparse and punctate fibronectin labeling (Ilic et al., 2004), indicating assembly defects, although no information regarding the formation of paraxial mesoderm is available (Furuta et al., 1995; Ilic et al., 1995; Ilic et al., 2004). The work presented in this thesis validates the absolute requirement for fibronectin during somitogenesis in an avian model, in line with the observations in the remaining vertebrate model systems, therefore further advocating fibronectin-associated cues as universal players in the formation of the somitic segments in the whole vertebrate taxa.

The work presented in this thesis clarified that the fibronectin matrix surrounding the PSM is the necessary factor for somite formation to occur in isolated PSMs, as neither *Paraxis* (Chapter 2) nor *Meso1* expression (Chapter 5) can drive somite

formation on their own. In mouse embryos, these two bHLH transcription factors are critical for somitic cleft formation (Saga et al., 1997) and somite epithelialization (Burgess et al., 1996). However no target genes for Paraxis have been found and only one relevant target of Mesp2 has been identified, namely *EphA4* (Nakajima et al., 2006, see also Wilson-Rawls et al., 2004). Moreover, Paraxis and Mesp2 neither interact in *in vitro* assays nor do they influence each other's expression (Takahashi et al., 2007) thus failing to throw light on how these two transcription factors promote somite morphogenesis in mouse embryos. Here we will attempt to integrate our observations on the role of the fibronectin matrix surrounding the PSM with recent data from other model systems and propose a working model on how different molecular pathways may collaborate to bring about somite morphogenesis.

6.2.1. Fibronectin on the edge: the polarizing co-partner during somite cleft formation

In chicken embryos, the ectopic over-expression of *Meso1* upregulates *EphA4* expression in PSM cells, and these PSM cells, when microsurgically implanted into a host PSM, induce an ectopic boundary immediately rostral to the graft (Watanabe et al., 2009). Counter-intuitively, but in line with the results presented in Chapter 3, it is the rostral border cells that drive cleft formation, in an ephrinB2 response to the Meso1/EphA4 over-expressing graft (Watanabe et al., 2009). However, the authors show that the ephrinB2 downstream signal is dependent on the activity of Cdc42 (Watanabe et al., 2009), which was previously shown to dictate the mesenchymal *versus* epithelial fate of PSM cells (Nakaya et al., 2004). Thus, the authors suggested the existence of co-adjuvant of the ephrin action (Watanabe et al., 2009; Watanabe and Takahashi, 2010), in line with an earlier proposal put forth for zebrafish somitogenesis (Barrios et al., 2003). Interestingly, the ectopic boundaries generated around ephrinB2-overexpressing cell clusters in the mosaic paraxial mesoderm of zebrafish embryos (Barrios et al., 2003; Durbin et al., 2000) results in integrin clustering and fibronectin matrix assembly at the interface (Jülich et al., 2009), although no direct interaction between integrins and ephrins was reported (Lackner et al., 2013).

The results presented in this thesis indicate that integrin-mediated fibronectin signaling may be the missing Cdc42-suppressing partner in the Eph-ephrin-reverse signaling-mediated cleft formation. Although the ephrin reverse signaling is poorly understood (see Pasquale, 2005; Pasquale, 2010 and references therein), a basal ECM/integrin-mediated cue is a known trigger for the establishment of epithelial cell polarity, which involves the transfer of Cdc42 activity to the apical side of the cell, a step which is essential for apical surface identity (Bryant and Mostov, 2008; Martin-Belmonte and Mostov, 2008; Papusheva and Heisenberg, 2010; Sacharidou et al., 2012).

Therefore, it is reasonable to assume that an adequate fibronectin, integrin-mediated tensioned signal can lead to downregulation of Cdc42 activity on the basal side of the peripheral cells of the rostral PSM, allowing the Eph-ephrin "spacer" mechanism to act, thus initiating the somitic cleft. The rapid invasion of the cleft by fibronectin fibrils (Chapter 4) may ensure the propagation of the basal downregulation of Cdc42 activity to other border cells, extending the cleft and completing the formation of the full intersomitic boundary (Chapter 3). A similar fibronectin-assembly wedging mechanism for cleft extension has been described during salivary gland branching morphogenesis (Larsen et al., 2006). The accumulation of a fibronectin matrix next to the outer salivary gland cells initiates cleft formation by inducing basal downregulation of cadherins in the future border cells (Larsen et al., 2006; Onodera et al., 2010; Sakai et al., 2003) in a ROCK dependent fashion (Daley et al., 2009), downstream of cell-fibronectin adhesion plaques (Daley et al., 2011). Although somite formation and salivary gland branching morphogenesis are two distinct embryonic events with different cleft initiation mechanisms (Onodera et al., 2010), this thesis illustrates that they share a general force-dependent morphogenetic mechanism regulating the intra and inter-cellular segregation of cell-cell and cell-ECM adhesion complexes (Burute and Thery, 2012; Papusheva and Heisenberg, 2010).

6.2.2. Making a somite, putting the pieces together

Despite the likely implication of the Eph-ephrin signaling in somite boundary formation, the redundancy depicted by the mouse mutants for these genes and the overlapping expression domains of the various members of the family present in the

rostral PSM (see Baker and Antin, 2003) indicates that the EphA4-ephrinB2 duet cannot explain the seamless PSM separation into two neighboring elements. Likewise, despite the clear implication of fibronectin in chicken somitogenesis presented in this thesis, there is no evidence for a region specific, fibronectin-dependent cleft-inducing mechanism in the rostral PSM. Hence, the making of a somite may involve the shared but partially redundant roles between the several players intervening in somite formation. In fact, a balance of several mechanisms could explain how the morphological robustness of the somitic phenotype is ensured.

The dynamic rearrangements of rostral PSM cells presented in Chapter 3 suggest that an orthogonal Eph-ephrin interface is not a requirement for boundary formation. Rather, rapid cell shuffling could ensure the robust discrimination of two neighboring populations of cells undergoing intense Eph-ephrin repulsive action. Moreover, the N-cadherin-based adhesions in the PSM (Chapters 2 and 3) convey further cohesion to the cell populations on either side of the boundary, preventing cells from escaping their cohort (Chapter 3). Thus, under these conditions, plus the increased cell tension at the rostral PSM (Chapter 5) provided by the surrounding fibronectin network (Chapter 4), each newly formed segment is swiftly and neatly segregated upon cleft initiation, despite the continuous cell movements (Chapter 3). Moreover, the surrounding matrix also delivers the adequate polarizing cue for the epithelialization of all the cells that either belong to or move into the peripheral cell layer of the somite (Chapters 2 and 3). Additionally, the free surface created by the Eph-ephrin spacing ensures increased tension on the border cells and their retraction (see (Amack and Manning, 2012), further aiding fibronectin fibrillogenesis, and the gap can thus be filled with fibronectin fibrils (Chapter 4). The convergent action of all players results in the establishment of a clear boundary and the epithelialization of the somitic segment, conveniently insulated by a fibronectin matrix ensuring that the non-lineage boundary between segments is maintained during development (see Dahmann et al., 2011). Interestingly, rostro-caudal somite patterning may play an extra, supportive role in somite boundary maintenance, as *Tbx18* overexpression can induce ectopic boundaries, in an unknown, Eph-ephrin-independent fashion (Tanaka and Tickle, 2004; Watanabe et al., 2009).

6.3. Incresead ECM tension at the rostral PSM: tuning the tempo for determination?

The work present in Chapter 5 indicates that a tensional cue, probably downstream of integrin signaling, may be involved in the establishment of the determined domain of the rostral PSM. Here I will refer recent advances and views on the temporal/spatial regulation of somitogenesis and attempt to integrate them with the results obtained in this thesis.

The current view argues that the opposing FGF/Wnt and RA gradients generate a hypothetical signaling threshold, the determination front, establishing in the PSM, the frontier between the caudal, undetermined region and the rostral, determined PSM, committed to form somitic segments with rostro-caudal polarity (Aulehla and Pourquié, 2010; Oates et al., 2012; Pourquié, 2011). The axial level at which *Mesp2* is expressed in the form of a stripe has been proposed to be the first marker of rostral PSM identity in the mouse embryo, and this notion also applies for *Mesp2*-homolog genes in other vertebrate model systems (Hitachi et al., 2008; Sawada et al., 2001 see Oates et al., 2012; Pourquié, 2011; Saga, 2012).

The results reported in this thesis (Chapters 2 and 5) are not consistent with this concept, but rather agree with earlier studies (Dubrulle et al., 2001) which place the determination front in the chick embryo slightly further caudally, caudal to the stripes of *Meso1* expression. Furthermore, several other observations in this model system (Palmeirim et al., 1997; Resende et al., 2010) indicate that the determination front is localized at S-IV, thus caudal to *Meso1* expression. Therefore, at least in the chicken embryo, *Meso1* is only expressed after cells have crossed the determination front. However, two general questions still remain: 1) how do PSM cells interpret the hypothetical gradient threshold, establishing the spatial landmark (the determination front), and 2) how is the striped expression of *Meso1* initiated?

Regarding the second question, extensive work in the mouse model has shown that Notch signaling can positively regulate Tbx6-dependent *Mesp2* expression, which in turn induces the expression of its own repressor, thus confining *Mesp2* to a stripe

(Morimoto et al., 2007; Oginuma et al., 2008; Takahashi et al., 2010; Yasuhiko et al., 2006). However, since Notch signaling and Tbx6 mRNA and protein are present throughout the PSM, it remains unclear why *Mesp2* expression is restricted to the rostral PSM (see (Saga, 2012). This brings us back to the first question: how are the gradients integrated to give rise to a precise spatial output?

The results presented in Chapter 5 indicate that, in the presence of tension inhibitors, the location of the *Meso1* stripe is more rostral than in controls. This means that the overall reduction of cell-tension extends the undetermined PSM region more rostrally. Assuming that the increased fibrillar density of fibronectin matrix brings about increased matrix rigidity, then it can be proposed that another new gradient, namely a rostro-caudal tension gradient, runs along the PSM, opposite the FGF/Wnt concentration gradient. Further experiments using other markers are of course essential to investigate whether the effect of the tension inhibitors is restricted to *Meso1* expression or whether they also influence the expression of other genes in the PSM. Nevertheless, our data bring forth the tantalizing possibility that PSM cells interpret the FGF/Wnt gradient in accordance with the tensional state of their microenvironment. According to this hypothesis, an integrin-sensed feedback on the ECM tensional state along the PSM would serve as a balancing check-point for PSM cells to move forward in their developmental program when the microenvironment settings (i.e. ECM rigidity and paracrine environment) are such that normal somite formation can be ensured (Figure 2).

Recent evidence from mouse embryos indicate that, unlike the proposed Fgf8 gradient, the downstream ERK signals oscillate in a bi-phasic manner in the non-determined PSM, where the low pERK phase allows a Notch signaling activation of *Mesp2* at the rostral end of the non-determined PSM, (Niwa et al., 2011). As integrin-associated signaling has been extensively shown to act directly or indirectly on the MAPK/ERK pathway (Ramos, 2008; Streuli and Akhtar, 2009), we speculate that an integrin signal may aid in the integration of the ERK signal in the rostral PSM. In agreement with this hypothesis, overexpression of Fgf8 and MKK1 (Delfini et al., 2005), Snail2, an Fgf8 target (Dale et al., 2006), and the forced depletion of the β1 integrin in

chicken PSM cells (Rallis et al., 2010), all abolish *Meso1* expression. Though a detailed evaluation on the tensional influence over signaling pathways is still in its infancy, it is clear that integrin-mediated mechanosensitivity underlies a broad range of cell fate decisions (Engler et al., 2006, see Mammoto et al., 2012). Results from this thesis suggest that PSM maturity may be one of those.

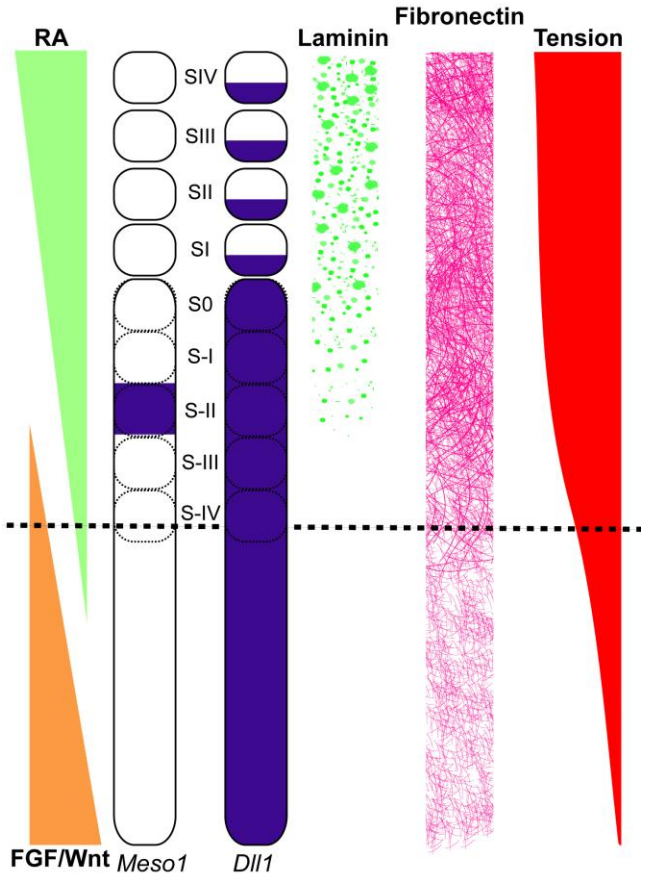

Figure 2. Integration of the proposed ECM gradients with the morphogen gradient paradigm in the chicken embryo. In parallel to the opposing FGF/Wnt and RA gradients, the PSM cells experience a rostral increase in fibronectin matrix complexity (in magenta), corresponding to an increased cell tension (red). The incorporation of this latter gradient further aids in the establishment of the determination front (dashed line) preluding *Meso1* expression (left paraxial mesoderm), which underlies somite RC polarity (such as *Dll1*, on the right paraxial mesoderm). A patchy laminin matrix (in green) appears insipiently in the rostral PSM, but becomes increasingly dense on the surface of the epithelial somite once it is formed.

6.4. Final considerations

The work presented in this thesis emphasizes the importance of cell-ECM interactions during development and morphogenesis, showing that it is an imperative contributor to the intricate regulation of cell behavior. Unlike genetic regulation, contained within the “cell unit”, the very extracellular nature of the ECM is a major hurdle for the comprehension of cell-ECM interactions, as the producing, assembling, or user cells may not be the same, like we show in Chapter 2. Moreover, the multifactorial aspect of the ECM, such as composition, assembly state, degradation, dimensionality, or

mechanical properties, further complicates our comprehension of the cell/tissue-specific response to a given ECM. As emphasized throughout this thesis, fibronectin, a molecule which has been implicated in the attachment, mobility and dispersal of cells, is unmistakably also essential for the assembly of a spherical epithelial tissue, the somite.

Much still escapes our comprehension in the study of embryonic development. This is not surprising as a cell's interaction with its milieu, including other cells or the ECM, has been superbly perfected since the "first" multicellular organism arose. Fortunately, embryo development reminds us that whatever cells do, they perform it with admirable flawlessness, and, if we identify the few key cues that initiate the whole process, we can make cells do it all over again (Eiraku et al., 2011).

6.5. References

Amack, J. D. and Manning, M. L. (2012). Knowing the boundaries: extending the differential adhesion hypothesis in embryonic cell sorting. *Science* **338**, 212-5.

Anderson, C., Thorsteinsdóttir, S. and Borycki, A. G. (2009). Sonic hedgehog-dependent synthesis of laminin α1 controls basement membrane assembly in the myotome. *Development* **136**, 3495-504.

Antia, M., Baneyx, G., Kubow, K. E. and Vogel, V. (2008). Fibronectin in aging extracellular matrix fibrils is progressively unfolded by cells and elicits an enhanced rigidity response. *Faraday Discussions* **139**, 229-420.

Aulehla, A. and Pourquié, O. (2010). Signaling gradients during paraxial mesoderm development. *Cold Spring Harbor Perspectives in Biology* **2**, a000869.

Bae, E., Sakai, T. and Mosher, D. F. (2004). Assembly of exogenous fibronectin by fibronectin-null cells is dependent on the adhesive substrate. *Journal of Biological Chemistry* **279**, 35749-59.

Bajanca, F., Luz, M., Duxson, M. J. and Thorsteinsdóttir, S. (2004). Integrins in the mouse myotome: developmental changes and differences between the epaxial and hypaxial lineage. *Developmental Dynamics* **231**, 402-15.

Bajanca, F., Luz, M., Raymond, K., Martins, G. G., Sonnenberg, A., Tajbakhsh, S., Buckingham, M. and Thorsteinsdóttir, S. (2006). Integrin alpha6beta1-laminin interactions regulate early myotome formation in the mouse embryo. *Development* **133**, 1635-44.

Baker, R. K. and Antin, P. B. (2003). Ephs and ephrins during early stages of chick embryogenesis. *Developmental Dynamics* **228**, 128-42.

Baneyx, G., Baugh, L. and Vogel, V. (2002). Fibronectin extension and unfolding within cell matrix fibrils controlled by cytoskeletal tension. *Proceedings of the National Academy of Sciences of the United States of America* **99**, 5139-43.

Barrios, A., Poole, R. J., Durbin, L., Brennan, C., Holder, N. and Wilson, S. W. (2003). Eph/Ephrin signaling regulates the mesenchymal-to-epithelial transition of the paraxial mesoderm during somite morphogenesis. *Current Biology* **13**, 1571-82.

Bénazéraf, B., Francois, P., Baker, R. E., Denans, N., Little, C. D. and Pourquié, O. (2010). A random cell motility gradient downstream of FGF controls elongation of an amniote embryo. *Nature* **466**, 248-52.

Bettenhausen, B., Hrabě de Angelis, M., Simon, D., Guenet, J. L. and Gossler, A. (1995). Transient and restricted expression during mouse embryogenesis of Dll1, a murine gene closely related to *Drosophila* Delta. *Development* **121**, 2407-18.

Bothe, I., Ahmed, M. U., Winterbottom, F. L., von Scheven, G. and Dietrich, S. (2007). Extrinsic versus intrinsic cues in avian paraxial mesoderm patterning and differentiation. *Developmental Dynamics* **236**, 2397-409.

Bryant, D. M. and Mostov, K. E. (2008). From cells to organs: building polarized tissue. *Nature Reviews: Molecular Cell Biology* **9**, 887-901.

Burgess, R., Rawls, A., Brown, D., Bradley, A. and Olson, E. N. (1996). Requirement of the paraxis gene for somite formation and musculoskeletal patterning. *Nature* **384**, 570-3.

Burute, M. and Thery, M. (2012). Spatial segregation between cell-cell and cell-matrix adhesions. *Current Opinion in Cell Biology* **24**, 628-36.

Buxboim, A., Ivanovska, I. L. and Discher, D. E. (2010). Matrix elasticity, cytoskeletal forces and physics of the nucleus: how deeply do cells 'feel' outside and in? *Journal of Cell Science* **123**, 297-308.

Cachaço, A. S., Pereira, C. S., Pardal, R. G., Bajanca, F. and Thorsteinsdóttir, S. (2005). Integrin repertoire on myogenic cells changes during the course of primary myogenesis in the mouse. *Developmental Dynamics* **232**, 1069-78.

Candia, A. F., Hu, J., Crosby, J., Lalley, P. A., Noden, D., Nadeau, J. H. and Wright, C. V. (1992). Mox-1 and Mox-2 define a novel homeobox gene subfamily and are differentially expressed during early mesodermal patterning in mouse embryos. *Development* **116**, 1123-36.

Christ, B., Huang, R. and Scaal, M. (2007). Amniote somite derivatives. *Developmental Dynamics* **236**, 2382-96.

Copp, A. J., Carvalho, R., Wallace, A., Sorokin, L., Sasaki, T., Greene, N. D. and Ybot-Gonzalez, P. (2011). Regional differences in the expression of laminin isoforms during mouse neural tube development. *Matrix Biology* **30**, 301-9.

Cukierman, E., Pankov, R., Stevens, D. R. and Yamada, K. M. (2001). Taking cell-matrix adhesions to the third dimension. *Science* **294**, 1708-12.

Czirok, A., Rongish, B. J. and Little, C. D. (2004). Extracellular matrix dynamics during vertebrate axis formation. *Developmental Biology* **268**, 111-22.

Czirok, A., Zamir, E. A., Filla, M. B., Little, C. D. and Rongish, B. J. (2006). Extracellular matrix macroassembly dynamics in early vertebrate embryos. *Current Topics in Developmental Biology* **73**, 237-58.

Dahmann, C., Oates, A. C. and Brand, M. (2011). Boundary formation and maintenance in tissue development. *Nature Reviews: Genetics* **12**, 43-55.

Dale, J. K., Malapert, P., Chal, J., Vilhais-Neto, G., Maroto, M., Johnson, T., Jayasinghe, S., Trainor, P., Herrmann, B. and Pourquié, O. (2006). Oscillations of the snail genes in the presomitic

mesoderm coordinate segmental patterning and morphogenesis in vertebrate somitogenesis. *Developmental Cell* **10**, 355-66.

Daley, W. P., Gulfo, K. M., Sequeira, S. J. and Larsen, M. (2009). Identification of a mechanochemical checkpoint and negative feedback loop regulating branching morphogenesis. *Developmental Biology* **336**, 169-82.

Daley, W. P., Kohn, J. M. and Larsen, M. (2011). A focal adhesion protein-based mechanochemical checkpoint regulates cleft progression during branching morphogenesis. *Developmental Dynamics* **240**, 2069-83.

Davidson, L. A., Dzamba, B. D., Keller, R. and Desimone, D. W. (2008). Live imaging of cell protrusive activity, and extracellular matrix assembly and remodeling during morphogenesis in the frog, *Xenopus* laevis. *Developmental Dynamics* **237**, 2684-92.

Davidson, L. A., Keller, R. and DeSimone, D. W. (2004). Assembly and remodeling of the fibrillar fibronectin extracellular matrix during gastrulation and neurulation in *Xenopus* laevis. *Developmental Dynamics* **231**, 888-95.

Delfini, M. C., Dubrulle, J., Malapert, P., Chal, J. and Pourquié, O. (2005). Control of the segmentation process by graded MAPK/ERK activation in the chick embryo. *Proceedings of the National Academy of Sciences of the United States of America* **102**, 11343-8.

Deries, M., Gonçalves, A. B., Vaz, R., Martins, G. G., Rodrigues, G. and Thorsteinsdóttir, S. (2012). Extracellular matrix remodeling accompanies axial muscle development and morphogenesis in the mouse. *Developmental Dynamics* **241**, 350-364.

Dolez, M., Nicolas, J. F. and Hirsinger, E. (2011). Laminins, via heparan sulfate proteoglycans, participate in zebrafish myotome morphogenesis by modulating the pattern of Bmp responsiveness. *Development* **138**, 97-106.

Dubrulle, J., McGrew, M. J. and Pourquié, O. (2001). FGF signaling controls somite boundary position and regulates segmentation clock control of spatiotemporal Hox gene activation. *Cell* **106**, 219-32.

Durbin, L., Sordino, P., Barrios, A., Gering, M., Thisse, C., Thisse, B., Brennan, C., Green, A., Wilson, S. and Holder, N. (2000). Anteroposterior patterning is required within segments for somite boundary formation in developing zebrafish. *Development* **127**, 1703-13.

Dzamba, B. J., Jakab, K. R., Marsden, M., Schwartz, M. A. and DeSimone, D. W. (2009). Cadherin adhesion, tissue tension, and noncanonical Wnt signaling regulate fibronectin matrix organization. *Developmental Cell* **16**, 421-32.

Egeblad, M., Rasch, M. G. and Weaver, V. M. (2010). Dynamic interplay between the collagen scaffold and tumor evolution. *Current Opinion in Cell Biology* **22**, 697-706.

Eiraku, M., Takata, N., Ishibashi, H., Kawada, M., Sakakura, E., Okuda, S., Sekiguchi, K., Adachi, T. and Sasai, Y. (2011). Self-organizing optic-cup morphogenesis in three-dimensional culture. *Nature* **472**, 51-6.

Elsdale, T. and Bard, J. (1972). Collagen substrata for studies on cell behavior. *Journal of Cell Biology* **54**, 626-37.

Engler, A. J., Chan, M., Boettiger, D. and Schwarzbauer, J. E. (2009). A novel mode of cell detachment from fibrillar fibronectin matrix under shear. *Journal of Cell Science* **122**, 1647-53.

Engler, A. J., Sen, S., Sweeney, H. L. and Discher, D. E. (2006). Matrix elasticity directs stem cell lineage specification. *Cell* **126**, 677-89.

Eyckmans, J., Boudou, T., Yu, X. and Chen, C. S. (2011). A hitchhiker's guide to mechanobiology. *Developmental Cell* **21**, 35-47.

Fata, J. E., Werb, Z. and Bissell, M. J. (2004). Regulation of mammary gland branching morphogenesis by the extracellular matrix and its remodeling enzymes. *Breast Cancer Research* **6**, 1-11.

Friedland, J. C., Lee, M. H. and Boettiger, D. (2009). Mechanically activated integrin switch controls $\alpha 5\beta 1$ function. *Science* **323**, 642-4.

Furuta, Y., Ilic, D., Kanazawa, S., Takeda, N., Yamamoto, T. and Aizawa, S. (1995). Mesodermal defect in late phase of gastrulation by a targeted mutation of focal adhesion kinase, FAK. *Oncogene* **11**, 1989-95.

George, E. L., Georges-Labouesse, E. N., Patel-King, R. S., Rayburn, H. and Hynes, R. O. (1993). Defects in mesoderm, neural tube and vascular development in mouse embryos lacking fibronectin. *Development* **119**, 1079-91.

Georges-Labouesse, E. N., George, E. L., Rayburn, H. and Hynes, R. O. (1996). Mesodermal development in mouse embryos mutant for fibronectin. *Developmental Dynamics* **207**, 145-56.

Gudjonsson, T., Adriance, M. C., Sternlicht, M. D., Petersen, O. W. and Bissell, M. J. (2005). Myoepithelial cells: their origin and function in breast morphogenesis and neoplasia. *Journal of Mammary Gland Biology and Neoplasia* **10**, 261-72.

Halliday, N. L. and Tomasek, J. J. (1995). Mechanical properties of the extracellular matrix influence fibronectin fibril assembly in vitro. *Experimental Cell Research* **217**, 109-17.

Hitachi, K., Kondow, A., Danno, H., Inui, M., Uchiyama, H. and Asashima, M. (2008). Tbx6, Thylacine1, and E47 synergistically activate bowline expression in *Xenopus* somitogenesis. *Developmental Biology* **313**, 816-28.

Hoffman, B. D., Grashoff, C. and Schwartz, M. A. (2011). Dynamic molecular processes mediate cellular mechanotransduction. *Nature* **475**, 316-23.

Huang, R., Zhi, Q., Brand-Saberi, B. and Christ, B. (2000). New experimental evidence for somite resegmentation. *Anatomy and Embryology (Berl)* **202**, 195-200.

Ilic, D., Furuta, Y., Kanazawa, S., Takeda, N., Sobue, K., Nakatsuji, N., Nomura, S., Fujimoto, J., Okada, M. and Yamamoto, T. (1995). Reduced cell motility and enhanced focal adhesion contact formation in cells from FAK-deficient mice. *Nature* **377**, 539-44.

Ilic, D., Kovacic, B., Johkura, K., Schlaepfer, D. D., Tomasevic, N., Han, Q., Kim, J. B., Howerton, K., Baumbusch, C., Ogiwara, N. et al. (2004). FAK promotes organization of fibronectin matrix and fibrillar adhesions. *Journal of Cell Science* **117**, 177-87.

Jülich, D., Geisler, R., Consortium, T. S. and Holley, S. A. (2005). Integrinalpha5 and delta/notch signaling have complementary spatiotemporal requirements during zebrafish somitogenesis. *Developmental Cell* **8**, 575-86.

Jülich, D., Mould, A. P., Koper, E. and Holley, S. A. (2009). Control of extracellular matrix assembly along tissue boundaries via Integrin and Eph/Ephrin signaling. *Development* **136**, 2913-21.

Klotzsch, E., Smith, M. L., Kubow, K. E., Muntwyler, S., Little, W. C., Beyeler, F., Gourdon, D., Nelson, B. J. and Vogel, V. (2009). Fibronectin forms the most extensible biological fibers displaying switchable force-exposed cryptic binding sites. *Proceedings of the National Academy of Sciences of the United States of America* **106**, 18267-72.

Koshida, S., Kishimoto, Y., Ustumi, H., Shimizu, T., Furutani-Seiki, M., Kondoh, H. and Takada, S. (2005). Integrinalpha5-dependent fibronectin accumulation for maintenance of somite boundaries in zebrafish embryos. *Developmental Cell* **8**, 587-98.

Kubow, K. E., Klotzsch, E., Smith, M. L., Gourdon, D., Little, W. C. and Vogel, V. (2009). Crosslinking of cell-derived 3D scaffolds up-regulates the stretching and unfolding of new extracellular matrix assembled by reseeded cells. *Integrative Biology* **1**, 635-48.

Lackner, S., Schwendinger-Schreck, J., Julich, D. and Holley, S. A. (2013). Segmental Assembly of Fibronectin Matrix Requires rap1b and integrin α5. *Developmental Dynamics* **242**, 122-31.

Larsen, M., Wei, C. and Yamada, K. M. (2006). Cell and fibronectin dynamics during branching morphogenesis. *Journal of Cell Science* **119**, 3376-84.

Latimer, A. and Jessen, J. R. (2010). Extracellular matrix assembly and organization during zebrafish gastrulation. *Matrix Biology* **29**, 89-96.

Levental, K. R., Yu, H., Kass, L., Lakins, J. N., Egeblad, M., Erler, J. T., Fong, S. F., Csiszar, K., Giaccia, A., Weninger, W. et al. (2009). Matrix crosslinking forces tumor progression by enhancing integrin signaling. *Cell* **139**, 891-906.

Mammoto, A., Mammoto, T. and Ingber, D. E. (2012). Mechanosensitive mechanisms in transcriptional regulation. *Journal of Cell Science* **125**, 3061-73.

Mammoto, T. and Ingber, D. E. (2010). Mechanical control of tissue and organ development. *Development* **137**, 1407-20.

Mao, Y. and Schwarzbauer, J. E. (2005a). Fibronectin fibrillogenesis, a cell-mediated matrix assembly process. *Matrix Biology* **24**, 389-99.

Mao, Y. and Schwarzbauer, J. E. (2005b). Stimulatory effects of a three-dimensional microenvironment on cell-mediated fibronectin fibrillogenesis. *Journal of Cell Science* **118**, 4427-36.

Martin-Belmonte, F. and Mostov, K. (2008). Regulation of cell polarity during epithelial morphogenesis. *Current Opinion in Cell Biology* **20**, 227-34.

McDonald, J. A., Quade, B. J., Broekelmann, T. J., LaChance, R., Forsman, K., Hasegawa, E. and Akiyama, S. (1987). Fibronectin's cell-adhesive domain and an amino-terminal matrix assembly domain participate in its assembly into fibroblast pericellular matrix. *Journal of Biological Chemistry* **262**, 2957-67.

Morimoto, M., Sasaki, N., Oginuma, M., Kiso, M., Igarashi, K., Aizaki, K., Kanno, J. and Saga, Y. (2007). The negative regulation of Mesp2 by mouse Ripply2 is required to establish the rostro-caudal patterning within a somite. *Development* **134**, 1561-9.

Nakajima, Y., Morimoto, M., Takahashi, Y., Koseki, H. and Saga, Y. (2006). Identification of Epha4 enhancer required for segmental expression and the regulation by Mesp2. *Development* **133**, 2517-25.

Nakaya, Y., Kuroda, S., Katagiri, Y. T., Kaibuchi, K. and Takahashi, Y. (2004). Mesenchymal-epithelial transition during somitic segmentation is regulated by differential roles of Cdc42 and Rac1. *Developmental Cell* **7**, 425-38.

Nelson, C. M. and Bissell, M. J. (2006). Of extracellular matrix, scaffolds, and signaling: tissue architecture regulates development, homeostasis, and cancer. *Annual Review of Cell and Developmental Biology* **22**, 287-309.

Niwa, Y., Shimojo, H., Isomura, A., Gonzalez, A., Miyachi, H. and Kageyama, R. (2011). Different types of oscillations in Notch and Fgf signaling regulate the spatiotemporal periodicity of somitogenesis. *Genes & Development* **25**, 1115-20.

Oates, A. C., Morelli, L. G. and Ares, S. (2012). Patterning embryos with oscillations: structure, function and dynamics of the vertebrate segmentation clock. *Development* **139**, 625-39.

Oginuma, M., Niwa, Y., Chapman, D. L. and Saga, Y. (2008). Mesp2 and Tbx6 cooperatively create periodic patterns coupled with the clock machinery during mouse somitogenesis. *Development* **135**, 2555-62.

Ohashi, T., Kiehart, D. P. and Erickson, H. P. (2002). Dual labeling of the fibronectin matrix and actin cytoskeleton with green fluorescent protein variants. *Journal of Cell Science* **115**, 1221-9.

Onodera, T., Sakai, T., Hsu, J. C., Matsumoto, K., Chiorini, J. A. and Yamada, K. M. (2010). Btbd7 regulates epithelial cell dynamics and branching morphogenesis. *Science* **329**, 562-5.

Palmeirim, I., Henrique, D., Ish-Horowicz, D. and Pourquié, O. (1997). Avian hairy gene expression identifies a molecular clock linked to vertebrate segmentation and somitogenesis. *Cell* **91**, 639-48.

Papusheva, E. and Heisenberg, C. P. (2010). Spatial organization of adhesion: force-dependent regulation and function in tissue morphogenesis. *EMBO Journal* **29**, 2753-68.

Pasquale, E. B. (2005). Eph receptor signalling casts a wide net on cell behaviour. *Nature Reviews: Molecular Cell Biology* **6**, 462-75.

Pasquale, E. B. (2010). Eph receptors and ephrins in cancer: bidirectional signalling and beyond. *Nature Reviews: Cancer* **10**, 165-80.

Paszek, M. J., Zahir, N., Johnson, K. R., Lakins, J. N., Rozenberg, G. I., Gefen, A., Reinhart-King, C. A., Margulies, S. S., Dembo, M., Boettiger, D. et al. (2005). Tensional homeostasis and the malignant phenotype. *Cancer Cell* **8**, 241-54.

Peters, D. M. and Mosher, D. F. (1987). Localization of cell surface sites involved in fibronectin fibrillogenesis. *Journal of Cell Biology* **104**, 121-30.

Potts, J. R. and Campbell, I. D. (1996). Structure and function of fibronectin modules. *Matrix Biology* **15**, 313-20.

Pourquié, O. (2011). Vertebrate segmentation: from cyclic gene networks to scoliosis. *Cell* **145**, 650-63.

Rallis, C., Pinchin, S. M. and Ish-Horowicz, D. (2010). Cell-autonomous integrin control of Wnt and Notch signalling during somitogenesis. *Development* **137**, 3591-601.

Ramos, J. W. (2008). The regulation of extracellular signal-regulated kinase (ERK) in mammalian cells. *International Journal of Biochemistry & Cell Biology* **40**, 2707-19.

Resende, T. P., Ferreira, M., Teillet, M. A., Tavares, A. T., Andrade, R. P. and Palmeirim, I. (2010). Sonic hedgehog in temporal control of somite formation. *Proceedings of the National Academy of Sciences of the United States of America* **107**, 12907-12.

Richmond, D. L. and Oates, A. C. (2012). The segmentation clock: inherited trait or universal design principle? *Current Opinion in Genetics and Development* **22**, 600-6.

Rozario, T., Dzamba, B., Weber, G. F., Davidson, L. A. and DeSimone, D. W. (2009). The physical state of fibronectin matrix differentially regulates morphogenetic movements in vivo. *Developmental Biology* **327**, 386-98.

Sacharidou, A., Stratman, A. N. and Davis, G. E. (2012). Molecular mechanisms controlling vascular lumen formation in three-dimensional extracellular matrices. *Cells Tissues Organs* **195**, 122-43.

Saga, Y. (2012). The mechanism of somite formation in mice. *Current Opinion in Genetics and Development* **22**, 331-8.

Saga, Y., Hata, N., Koseki, H. and Taketo, M. M. (1997). Mesp2: a novel mouse gene expressed in the presegmented mesoderm and essential for segmentation initiation. *Genes & Development* **11**, 1827-39.

Sakai, T., Larsen, M. and Yamada, K. M. (2003). Fibronectin requirement in branching morphogenesis. *Nature* **423**, 876-81.

Sawada, A., Shinya, M., Jiang, Y. J., Kawakami, A., Kuroiwa, A. and Takeda, H. (2001). Fgf/MAPK signalling is a crucial positional cue in somite boundary formation. *Development* **128**, 4873-80.

Schwarzbauer, J. E. and DeSimone, D. W. (2011). Fibronectins, their fibrillogenesis, and in vivo functions. *Cold Spring Harbor Perspectives in Biology* **3**.

Singh, P., Carraher, C. and Schwarzbauer, J. E. (2010). Assembly of fibronectin extracellular matrix. *Annual Review of Cell and Developmental Biology* **26**, 397-419.

Smith, M. L., Gourdon, D., Little, W. C., Kubow, K. E., Eguiluz, R. A., Luna-Morris, S. and Vogel, V. (2007). Force-induced unfolding of fibronectin in the extracellular matrix of living cells. *PLoS Biology* **5**, e268.

Snow, C. J., Goody, M., Kelly, M. W., Oster, E. C., Jones, R., Khalil, A. and Henry, C. A. (2008a). Time-lapse analysis and mathematical characterization elucidate novel mechanisms underlying muscle morphogenesis. *PLoS Genetics* **4**, e1000219.

Snow, C. J. and Henry, C. A. (2009). Dynamic formation of microenvironments at the myotendinous junction correlates with muscle fiber morphogenesis in zebrafish. *Gene Expression Patterns* **9**, 37-42.

Snow, C. J., Peterson, M. T., Khalil, A. and Henry, C. A. (2008b). Muscle development is disrupted in zebrafish embryos deficient for fibronectin. *Developmental Dynamics* **237**, 2542-53.

Streuli, C. H. and Akhtar, N. (2009). Signal co-operation between integrins and other receptor systems. *Biochemical Journal* **418**, 491-506.

Takahashi, J., Ohbayashi, A., Oginuma, M., Saito, D., Mochizuki, A., Saga, Y. and Takada, S. (2010). Analysis of Ripply1/2-deficient mouse embryos reveals a mechanism underlying the rostro-caudal patterning within a somite. *Developmental Biology* **342**, 134-45.

Takahashi, Y., Takagi, A., Hiraoka, S., Koseki, H., Kanno, J., Rawls, A. and Saga, Y. (2007). Transcription factors Mesp2 and Paraxis have critical roles in axial musculoskeletal formation. *Developmental Dynamics* **236**, 1484-94.

Tanaka, M. and Tickle, C. (2004). Tbx18 and boundary formation in chick somite and wing development. *Developmental Biology* **268**, 470-80.

Thorsteinsdóttir, S. (1992). Basement membrane and fibronectin matrix are distinct entities in the developing mouse blastocyst. *Anatomical Record* **232**, 141-9.

Watanabe, T., Sato, Y., Saito, D., Tadokoro, R. and Takahashi, Y. (2009). EphrinB2 coordinates the formation of a morphological boundary and cell epithelialization during somite segmentation. *Proceedings of the National Academy of Sciences of the United States of America* **106**, 7467-72.

Watanabe, T. and Takahashi, Y. (2010). Tissue morphogenesis coupled with cell shape changes. *Current Opinion in Genetics and Development* **20**, 443-7.

Wierzbicka-Patynowski, I. and Schwarzbauer, J. E. (2003). The ins and outs of fibronectin matrix assembly. *Journal of Cell Science* **116**, 3269-76.

Wilson-Rawls, J., Rhee, J. M. and Rawls, A. (2004). Paraxis is a basic helix-loop-helix protein that positively regulates transcription through binding to specific E-box elements. *Journal of Biological Chemistry* **279**, 37685-92.

Yasuhiko, Y., Haraguchi, S., Kitajima, S., Takahashi, Y., Kanno, J. and Saga, Y. (2006). Tbx6-mediated Notch signaling controls somite-specific Mesp2 expression. *Proceedings of the National Academy of Sciences of the United States of America* **103**, 3651-6.

Zhou, X., Rowe, R. G., Hiraoka, N., George, J. P., Wirtz, D., Mosher, D. F., Virtanen, I., Chernousov, M. A. and Weiss, S. J. (2008). Fibronectin fibrillogenesis regulates three-dimensional neovessel formation. *Genes & Development* **22**, 1231-43.